Stem Cells International

Application of Stem Cells in Bone and Cartilage Regeneration

Lead Guest Editor: Zengwu Shao
Guest Editors: Zhi-Yong Zhang, Lijie G. Zhang, Kelvin Yeung, James Triffitt, and Jaimo Ahn

Application of Stem Cells in Bone and Cartilage Regeneration

Stem Cells International

Application of Stem Cells in Bone and Cartilage Regeneration

Lead Guest Editor: Zengwu Shao
Guest Editors: Zhi-Yong Zhang, Lijie G. Zhang, Kelvin Yeung, James Triffitt, and Jaimo Ahn

Editorial Board

Contents

Hindawi
Stem Cells International
Volume 2019, Article ID 1201927, 17 pages
https://doi.org/10.1155/2019/1201927

Research Article

Characterization and Optimization of the Seeding Process of Adipose Stem Cells on the Polycaprolactone Scaffolds

Agata Kurzyk,[1] **Barbara Ostrowska**,[2] **Wojciech Święszkowski**,[2] **and Zygmunt Pojda**[1]

[1]*Department of Regenerative Medicine, Maria Sklodowska Curie Institute-Oncology Center, Roentgena 5, 02-781 Warsaw, Poland*
[2]*Materials Design Division, Faculty of Material Science and Engineering, Warsaw University of Technology, Woloska 141, 02-507 Warsaw, Poland*

Correspondence should be addressed to Agata Kurzyk; akurzyk@coi.pl

Received 25 May 2018; Revised 24 August 2018; Accepted 26 September 2018; Published 20 February 2019

Guest Editor: Zengwu Shao

The purpose of the current study was to evaluate the usefulness of adipose-derived stem cells (ASCs) for bone injury therapy. Lipoaspirates were collected from the abdomen regions of 17 healthy female donors (mean age 49 ± 6 years) using Coleman technique or Body-jet liposuction. In the present study, the primary objective was the *in vitro* characteristics of human ASCs. The secondary objective was the optimization of the cell seeding process on 3D-printed scaffolds using polycaprolactone (PCL) or polycaprolactone covered with tricalcium phosphate (PCL + 5% TCP). Biological evaluation of human ASC showed high efficiency of isolation obtaining a satisfying amount of homogeneous cell populations. Results suggest that ASCs can be cultured *in vitro* for a long time without impairing their proliferative capacity. Growth kinetics shows that the highest number of cells can be achieved in passage 5 and after the 16^{th} passage; there is a significant decrease of cell numbers and their proliferative potential. The percentage of colony forming units from the adipose stem cells is $8\% \pm 0.63\%$ ($p < 0.05$). It was observed that the accumulation of calcium phosphate in the cells *in vitro*, marked with Alizarin Red S, was increased along with the next passage. Analysis of key parameters critically related to the cell seeding process shows that volume of cell suspension and propagation time greatly improve the efficiency of seeding both in PCL and PCL + 5% TCP scaffolds. The cell seeding efficiency did differ significantly between scaffold materials and cell seeding methods ($p < 0.001$). Increased seeding efficiency was observed when using the saturation of cell suspension into scaffolds with additional incubation. Alkaline phosphatase level production in PCL + 5% TCP scaffold was better than in PCL-only scaffold. The study results can be used for the optimization of the seeding process and quantification methods determining the successful implementation of the preclinical model study in the future tissue engineering strategies.

1. Introduction

Regenerating or replacing bone defects is an important research field in tissue engineering. Current methods for surgical treatment of fractures and bone defects primarily use metal implants, and autologous and allogeneic bone grafts still represent the gold standard for bone repair. Development of new treatments is mainly focused on the tissue engineering strategies that include stem cells, bioactive signals, and appropriate scaffold support. Mesenchymal stem cells derived from adipose tissue are promising cell source for bone lesion repair [1]. This is important for the optimization of methods aimed at isolation, characterization, expansion, and evaluation of differentiation potential [2]. These parameters ensure the quality of stem cells and the safety of their use. Harvesting procedure, tissue site, age, obesity, and related-chronic diseases may influence cell yields from adipose tissue. ASCs can be isolated from adipose tissue during previous surgical resection or liposuction [2]. Several approaches for ASC isolation have been reported [3, 4], but data comparing the efficacy of various methods are still not available; therefore, no standardized method exists. The protocol described in 2001 by Zuk et al. is still considered as the most widely used method for ASC isolation, based on digestion with collagenase [5]. There are conflicting reports on the effect of donor age on adipose human mesenchymal stem

cells [6–8]. By contrast with bone marrow-derived MSCs, the number of ASCs in adipose tissue does not decrease with age [7, 8] even if their clonogenic and proliferative potential gradually declines. Numerous studies have reported that ASCs isolated from old individuals have reduced function and adipogenic potential compared to ASCs from young subjects [9–11]. The growth rate of ASCs has been reported also to be higher in younger patients (25–30 years old) than in older patients [12]. Nevertheless, adipose tissue displays a significant heterogeneity in terms of stem cell yield, proliferation, and differentiation capacity. Therefore, the primary objective of the present study is aimed at characterizing ASCs from the abdomen regions of 17 healthy female donors (mean age 49 ± 6 years) in order to investigate yield of cell number of stromal vascular fraction (SVF), proliferation, and potential of osteogenic differentiation and for possible evaluation of the usefulness of adipose stem cells (ASC) passage 3 for the construction of polymer-cell scaffolds.

Optimization of cell seeding on polymer scaffolds is essential for the successful *in vitro* cultivation of functional tissue constructs [1]. General seeding requirements for 3D scaffolds include high yield, to maximize the utilization of donor cells; high kinetic rate, to minimize the time in suspension culture for anchorage-dependent and shear-sensitive cells; spatially uniform distribution of attached cells, to provide a basis for uniform tissue regeneration; and high initial construct cellularity, to enhance the rate of tissue development. Additional seeding requirements may depend on cell type and tissue engineering application. The applied seeding technique therefore needs to be simple and easy to use, repeatable, and time-efficient [13]. Besides the individual effect, there is many crucial factors exert on the seeding process and also their interactions play a major role in determining outcome parameters [14–16]. It has been shown that changes in the scaffold porosity significantly affect the mesenchymal stem cell seeding efficiency in 3D-engineered bone scaffolds. In addition, many researches have shown that the initial seeding density did not significantly affect cell seeding efficiency, but the seeding time and the volume of seeding. The biological mechanisms responsible for the regenerative potential of stem cells are still not fully understood.

However, still little is known how to effectively optimize the seeding of scaffolds for bone regeneration. Thus, there is still a need for a simple effective way of improving cell seeding efficiency on scaffolds. Therefore, the secondary objective of this work was to select parameters that can play a key role in effectively seeding ASCs into polycaprolactone scaffolds. Our results may also provide information how seeding method selection affects cell distribution and how modification of scaffolds may influence the seeding efficiency.

2. Materials and Methods

2.1. Experimental Design. Adipose tissue was collected from raw human lipoaspirates according to Coleman technique or Body-jet liposuction. Lipoaspirates were obtained from the abdomen regions of 17 healthy female donors. The age range of the patients was 40–59 years (mean age 49 ± 6 years). All patients consented written forms for the use of the material (lipoaspirate) for the tests, in accordance with the standards of the International Ethical Committee.

2.2. Isolation and Culture of ASCs. Briefly, raw lipoaspirates were washed extensively with sterile phosphate-buffered saline (PBS) (Gibco®, Life Technologies, USA) to eliminate contaminating debris and red blood cells. Washed aspirates were treated with 0.075% collagenase (*Clostridium histolyticum*; type I; Sigma-Aldrich, St. Louis, MO, USA) in PBS for 60 min at 37°C with gentle agitation. The collagenase was inactivated with 10% fetal bovine serum (FBS, Gibco®, USA), and the infranatant centrifuged ($400 \times$g, 10 min, 23°C) until phase separation. To filter out larger tissue particles, the stromal vascular fraction (SVF) pellet was resuspended and passed through a 100 μm filter placed atop a new 50 ml centrifuge tube to facilitate gravitational separation. The filtrate was centrifuged at $400 \times$g for 10 min to obtain a high-density SVF pellet containing ASCs, which was then cultured in tissue-culture-treated culture dishes in a medium comprising an equal volume of low-glucose Dulbecco's modified Eagle's medium (DMEM, Gibco®, USA) and fetal bovine serum (FBS) and incubated in a humidified atmosphere at 37°C and 5% CO_2. Media were replaced twice per week, and cells were passaged on approaching 80–90% confluence, using 0.25% trypsin-EDTA solution (Invitrogen, USA). Routine tests were performed before ASC preparation and after preparation, including sterility control (BACTEC, BacT/Alert, Becton Dickinson, blood agar, Columbia agar, and BHI agar), cell enumeration (Bürker chamber), and viability analysis (fluorescence microscopy, acridine orange plus ethidium bromide staining).

2.3. Flow Cytometric Analyses of ASC Surface Markers. ASCs in passage 3 were harvested, enumerated, and incubated for 20 min with the following specific fluorescent conjugated antibodies including anti-CD29-PE, anti-CD34-PE, anti-CD45-FITC, anti-CD73PE, anti-CD90-PE, anti-CD105-PE, anti-CXCR-4-PE, and lin1-PerCP (anti-CD3-FITC, anti-CD14-FITC, anti-CD16-FITC, anti-CD19-FITC, anti-CD20-FITC, and anti-CD56-FITC). Control staining with directly labeled, isotype matched monoclonal antibodies was included in all fluorescence-activated cell sorting (FACS) experiment control (γ-PE, γ-PerCP, and γ-PE CD105) (BD, USA). Flow cytometry was performed using a Calibur flow cytometer (BD, USA) and CellQuest Pro software (BD, USA). Data are represented as mean values (M) ± standard deviation of the mean (SD) for 17 individual donors.

2.4. Morphology and Multilineage Differentiation Potential of hASCs. The potential of ASC to differentiate into osteoblasts and adipocytes was confirmed in monolayer culture. To induce adipogenic differentiation, cells were cultured in MesenCult™ adipogenic stimulatory supplements (human) (STEMCELL Technologies, Canada) supplemented with MesenCult® MSC basal medium (STEMCELL Technologies, Canada). To induce osteogenic differentiation, we used MesenCult™ osteogenic stimulatory supplements (human) (STEMCELL Technologies, Canada) in the osteogenic medium containing 10^{-4} M dexamethasone (STEMCELL

Technologies, Canada), 1 M β-glycerophosphate (STEMCELL Technologies, Canada), and 10 mg/ml ascorbic acid (STEMCELL Technologies, Canada). Media from both cultures were replaced every 3 d for 21 d in total. The differentiation potential for adipogenesis and the formation of intracellular lipid droplets were assessed by Oil Red O staining after fixation in 10% formalin. The differentiation potential for osteogenesis was assessed by Alizarin Red S (ARS) staining after fixation in 10% formalin. To induce chondrogenic differentiation, we used a chondrogenic medium (LONZA, Switzerland). For histological analysis, pellets were embedded in paraffin and sectioned. Chondrogenic differentiation was assessed by Masson trichrome staining. Morphology and differentiation potential of ASCs are represented for one individual donor from three independent donors.

2.5. Growth Kinetics. To investigate the growth pattern of ASCs, SVF cells were seeded at a density $1–2 \times 10^6$ cells/T25. The cells were grown in DMEM containing 10% FBS at 37°C, 5% CO_2, and 95% humidity. After approaching 80% confluence, the cells were passaged. After primary culture, the passaged cells were plated on a T25 culture bottle at a density 0.3×10^6 cells/T25 and their reproductive rate was recorded. After each passage, culture media were replenished every 3 days until the end of experiment. Cells were then trypsinized and enumerated. Cells were passaged; after which, they were unable to undergo further cell division.

2.6. Clonogenic Potential. The SVF cells isolated from human lipoaspirates were evaluated for their clonogenic ability by using colony-forming (CFU-F) assay. The cells were seeded at a low density (40 cells/cm^2) and cultured in DMEM containing 10% FBS for 6–7 days. Colonies were stained with Giemsa stain, and those comprising >50 cells were enumerated manually using a light microscope. The colony potential was compared by calculating the percentage of cell-forming colonies/number of cells seeded × 100. Clonogenic potential is a representative for 6 individual donors.

2.7. Scaffold Manufacturing. Poly(ε-caprolactone) scaffolds with custom geometry and controlled internal architecture were developed using fused deposition modeling at Faculty of Materials Science and Engineering, Warsaw University of Technology. A composite comprising PCL Mn 80.000 (Sigma-Aldrich) and β-TCP (Progentix, catalog no. P08004C) was used. Cylindrical scaffolds (6 mm diameter and 4 mm height) with three-dimensional orthogonal periodic porous architecture were designed using SOLIDWORKS 3D CAD design software. Layer-by-layer printed microfibrous scaffolds were characterized by the following theoretical parameters: fiber diameter (D1), 330 μm; spacing between fibers in the same layer (D2), 420 μm; layer thickness (D3), 240 μm; layer deposition angle, 0/60/120 the same layer (D2), 420 μm; layer thickness (D3), 240 μm; and layer deposition angle, 0/60/120.

2.8. Sterilization of Scaffolds. Scaffolds (PCL, PCL + 5% TCP) were irradiated at Gamma Chamber 5000 on the dose rate of 8.80 kGy/h in air. The total delivered radiation dose was 25 kGy. Sterilization was performed at the Institute of Chemistry and Nuclear Technology, Warsaw University of Technology. Samples for sterilization were delivered in sealed and sterile containers.

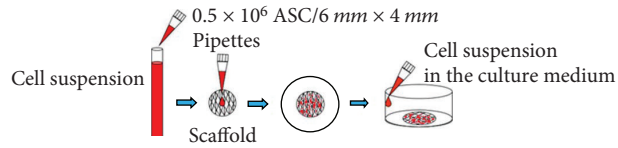

Figure 1: The static method of cell seeding into scaffold. Cell suspension is pipetted directly into the central surface of the scaffold.

2.9. Fixing of Cell-Seeded Scaffolds. Cell-scaffold constructs were fixed in 1.5% glutaraldehyde containing a 0.1 M sodium cacodylate buffer (pH 7.3), rinsed twice with PBS, and left to dry at room temperature.

3. Comparison of Different Strategies for *In Vitro* Seeding of Scaffolds

3.1. Basic Static Cell Seeding Methods. Sterilized scaffolds PCL and PCL + 5% TCP were placed in 24-well tissue culture plates. Culture-expanded human ASCs (passage 3) were suspended in the DMEM medium containing 20% FBS, using 0.5×10^6 cells in three variants of volumes: 50 μl, 35 μl, and 20 μl. The cell suspension was added on the top of each scaffold and pipetted in and out, to enhance even distribution of cells within the scaffolds. The prepared plate was gently transferred to an incubator under conditions of 37°C, 98% humidity, and 5% CO_2 (Figure 1). The medium was changed every three days. Cell-seeded scaffolds were cultured for 21 and 42 days. After this time, cell-seeded scaffolds were fixed and analyzed using a visible light microscope. The process was performed 6 times for each group. To determine cell seeding efficiency, cell numbers in randomly selected scaffolds were determined after 3, 7, and 21 days of incubation using an MTS assay (CellTiter 96® AQueous One Solution Cell Proliferation, Promega, Madison, WI, USA) ($n = 3$). Test MTS was repeated 3 times, from 3 independent donors.

3.2. Saturation of Cell Suspension into Scaffolds Combined with Additional Incubation. Sterilized scaffolds (PCL and PCL + 5% TCP) were placed in 24-well tissue culture plates. Culture-expanded ASCs (passage 3) were suspended in the DMEM medium containing 20% FBS, using 0.5×10^6 cells, in two volumes: (1) 50 μl and (2) 35 μl. At the beginning, half volume of total cell suspension (1) 25 μl from 50 μl and (2) 17.5 μl from 35 μl was added on the top of each scaffold and pipetted in and out, to enhance even distribution of cells within the scaffolds. The prepared plate was gently transferred to an incubator under conditions of 37°C, 98% humidity, and 5% CO_2. After 60 minutes in the incubator, the remainder of volume (1) 25 μl and (2) 17.5 μl was added to the scaffolds, which were subsequently stored in the incubator for 30 minutes. After this time, the scaffolds were placed in different, sterile tissue culture wells, one scaffold per well. Fresh medium (basic medium DMEM with 20% FBS) was added to the cell-seeded scaffolds (Figure 2). The medium was changed every three days. Cell-seeded scaffolds were

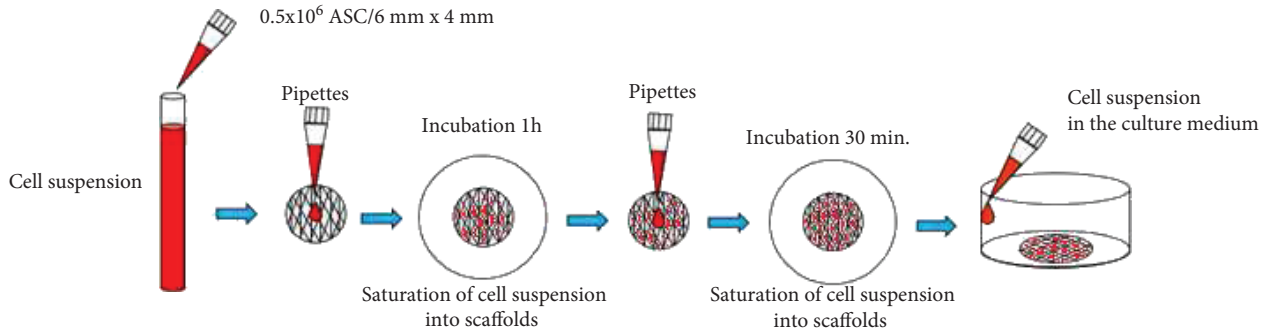

Figure 2: The method of saturation of cell suspension into scaffolds with additional incubation.

cultured for 21 days. After this time, cell-seeded scaffolds were fixed and microscope-analyzed. To determine cell seeding efficiency, cell numbers on randomly selected scaffolds were determined after 3, 7, and 21 days of incubation using and MTS assay (CellTiter 96® AQueous One Solution Cell Proliferation, Promega, Madison, WI, USA). Test MTS was repeated 3 times, from 3 independent donors.

3.3. Optimization of Density of Seeding Cells into Scaffolds. Sterilized scaffolds (PCL and PCL + 5% TCP) were placed in 24-well tissue culture plates. Culture-expanded human ASCs (passage 3) were suspended in the DMEM medium containing 20% FBS, using three densities of cell suspensions: 0.5×10^6, 0.9×10^6, and 1.5×10^6. The medium was changed every three days. Cell-seeded scaffolds were cultured for 3, 7, and 21 days. The process was performed 7 times.

3.4. Response Measurements and Data Analysis. The response measurements are based on the metabolic activity and alkaline phosphatase activity of the cells in the seeded scaffolds. In addition, the cell spatial distribution was also evaluated for the cell seeding on 3D scaffolds.

3.5. Cell Metabolic Activity Analysis. To determine the cell seeding efficiency, cell numbers on some seeded scaffolds were determined after 1, 3, 7, and 21 days of incubation, using the 3-(4.5-dimethylthiazol-2-yl)-5-(3-carboxymethoxyphenyl)-2-(4 sulfophenyl)-2H-tetrazolium (MTS) assay (CellTiter 96® AQueous One Solution Cell Proliferation, Promega, Madison, WI, USA). The MTS assay (CellTiter 96® AQueous One Solution Cell Proliferation Assay, Promega Corporation, Fitchburg, WI, USA) was used to measure the metabolic activity of the cells. Twenty microliters of MTS was added to 100 μl of fresh culture medium per well. The plates were incubated for 4 h at 37°C and 5% CO_2. Thereafter, the optical density was measured spectrophotometrically in 100 μl per well, using a multimode microplate reader (Synergy HT; BioTek, Winooski, VT, USA) at 490 nm. At this point, the MTS assay was performed to determine the total cell numbers for each scaffold, as described above. See MTS standard curve in Supplementary Materials.

3.6. Alkaline Phosphatase Activity Assay. ALP activity of the cells was measured using a Thermo Fisher Scientific PNPP phosphate substrate kit (Pierce, USA); P-nitrophenyl phosphate (pNPP) was used as the phosphatase substrate, which yields a yellow coloration ($\lambda_{max} = 405$ nm) when dephosphorylated by ALP. The activity of this enzyme was monitored on days 7 and 14. First, the medium was aspirated from the wells and 100 μl of pNPP reagent was added to each well with a scaffold sample. Thereafter, the plates were incubated for 30 min at 37°C and 5% CO_2 until sufficient coloration developed, and then, pNPP reagent was transferred into new wells. The reaction was terminated by adding 50 μl of 2 N NaOH to each well. The optical density was recorded using a microplate reader, at 405 nm.

3.7. Evaluation of Cell Growth after Cell Seeding Scaffolds. The prepared scaffold composites were examined by the CKX41 inverted microscope, confocal microscope, and SEM. The morphology and structure of the scaffolds were studied at 42 days following cell seeding using a scanning electron microscope (SEM, SU8000, Hitachi, Tokyo, Japan). The diameters of 50 randomly selected fibers were measured using image analysis software (ImageJ, National Institute of Health, Bethesda, MD, USA). The prepared and fixed cell-seeded scaffolds PCL and PCL + 5% TCP were examined by SEM at Faculty of Materials Science and Engineering, Warsaw University of Technology.

3.8. DAPI Staining Test. Stem cell-seeded scaffolds were fixed with 4% paraformaldehyde at 4°C for 30 min on days 1, 3, and 5 after cell seeding. Then, samples were washed twice with PBS, incubated with 4′, 6-diamidino-2-phenylindole (DAPI) (Sigma Chemical Co., USA) for 30 seconds to label nuclei of the cells, and rinsed twice with PBS. The immunofluorescence images were obtained by using a fluorescence microscope. Experiment was repeated 3 times, from 3 independent donors.

3.9. Statistics. The statistical analysis of the material was carried out using statistical tests of the STATISTICA v. 10 package by StatSoft Polska (comparison of the seeding methods on PCL and PCL + 5% TCP scaffolds) and the statistical program R version 3.4.3 (2017). The Shapiro-Wilk test was performed to assess normality; hypothesis testing was performed using the Benjamini-Hochberg test, and analysis of variance (ANOVA), followed by a Tukey test (for variables with normal distribution) for post hoc analysis or a Kruskal-Wallis test with Dunn's test (nonparametric) for

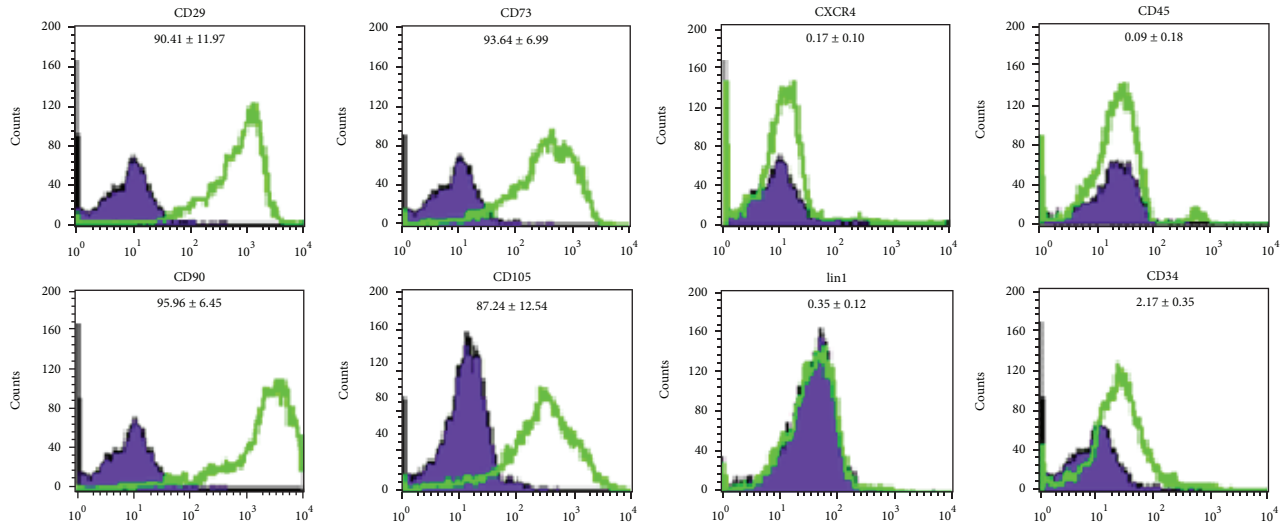

Figure 3: Histograms show results of ASC staining for indicated surface markers from one representative donor, passage 3. Cell counts are indicated on the y-axis and fluorescence intensity on the x-axis. The percentages of ASCs positively stained are indicated in each panel. Violet: isotype controls; green: antigen-specific antibodies.

post hoc analysis, was performed. Variables are presented as mean (M) ± standard deviation of the mean values (SD). A p value less than 0.05 indicated statistical significance, and additional significance was indicated with $^{*}p < 0.05$, $^{**}p < 0.01$, and $^{***}p < 0.001$.

4. Results

4.1. Flow Cytometry. Cultures of ASCs at passage 3 were analyzed for the expression of cell surface markers. ASCs were negative for the hematopoietic lineage marker CD45, on average 0.09% ± 0.18% CD45, 2.17% ± 0.35% CD34, and 0.35% ± 0.12% lin1. ASCs were positive for CD29, CD90, and CD105, on average 90.41% ± 11.97% CD29, 95.96% ± 5.45% CD90, and 87.24% ± 12.54% CD105. Representative histograms show results of ASC staining for indicated surface markers from one representative donor (Figure 3).

4.2. Morphology and Multineage Differentiation Potential of ASCs from Human Lipoaspirate. The shape of the isolated cells was initially round (Figure 4(a)) and became polygonal or spindle-shaped thereafter (ASC cells) (Figures 4(b)–4(d)). Attachment of spindle-shaped cells to tissue culture plastic flask was observed after 5 days of ASC culture (Figure 4(c)). After 7 days, spindle-shaped cells reached above 80% (Figure 4(d)). Morphology of cells changed gradually with passage number. Cells become more flat shape with increasing passage number.

4.3. Proliferation and Growth Kinetics of ASCs. ASCs were obtained from abdomen tissue from 17 female donors over a broad age range (49 ± 6 years). ASCs were successfully obtained from all donors. Yield of SVF cells was average 0.36×10^6 per milliliter of lipoaspirate, viability average 86%. Characterization of donors and number of SVF are presented in Supplementary Materials (Table 1). The growth curve (Figure 5(a)) describes the kinetics of cell proliferation in primary culture (SVF) and the first three secondary cultures (ASC). Differences between individual passages are statistically significant. The maximum ASC proliferation capacity was observed in passages from 2 to 5 ($^{*}p < 0.05$). A significant decrease of cell number and their proliferative potential is occurred after the 6^{th} to 16^{th} passages. Significant differences are also observed between passages 20 and 23 ($^{*}p < 0.05$). Results of average number of ASCs are presented in Supplementary Materials (Table 2). Growth kinetics is represented for 5 individual donors (Figure 5(a), from SVF to passage 3) and for 3 individual donors (Figure 5(b), from SVF to passage 23). Analyzing the propagation time of culture of human ASCs in terms to particular passages, we observed that the time of expansion of SVF cells from primary culture to passage 1 was on average 6 days. Passage 3 was obtained after 15–19 days, and passage 6 was obtained after 60 days (Figure 6(a)). CFU-F assay is a suitable tool for evaluating the proliferation and clonogenic capacity of the SVF expanded in culture. Giemsa staining showed that human SVF cells are able to form colonies from a single progenitor cell. It was observed 8% ± 0.63%. CFU-F colonies at a density of 40 cells/cm^2 were observed as shown in Figure 6(b).

4.4. Multipotency: Osteogenesis, Chondrogenesis, and Adipogenesis. Human ASCs showed ability to differentiate to osteocyte, adipocyte, and chondrocyte. Upon applying adipogenic differentiation, the cells showed accumulated intracellular lipid droplet as revealed by Oil Red O staining (Figure 7). Osteogenic differentiation displayed extracellular calcium precipitates, which were identified by Alizarin Red staining (Figure 8) and chondrogenic differentiation demonstrated by Masson's trichrome staining (Figure 9). Microscopic observation indicates that these cells can differentiate into adipocytes, osteoblast, and chondroblast. Control cultures were added to the experiment using basic culture medium, where there was no cell differentiation

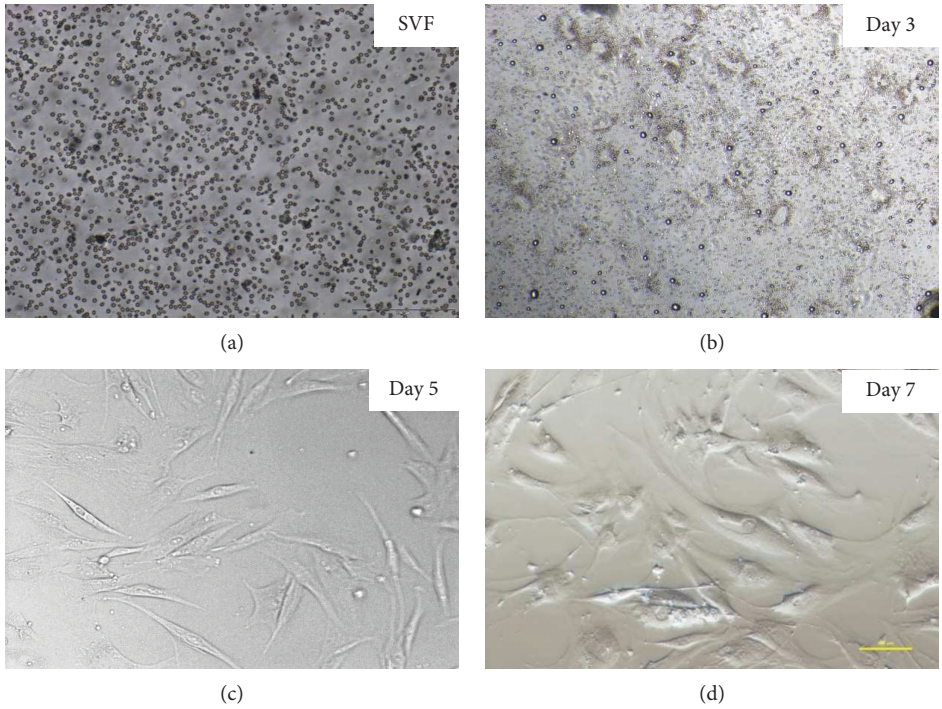

Figure 4: The representative images of human ASCs after fresh isolation, 3, 5, and 7 days of 2D culture. Representative images are shown at 4x magnification. Scale bars represent 100 μm (Olympus CKX41). The representative images are from one donor.

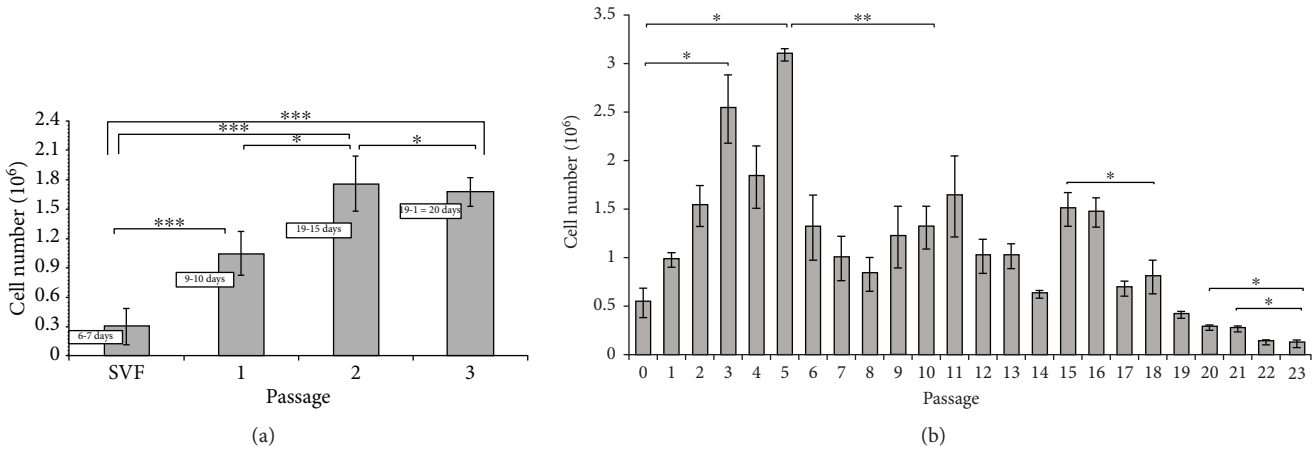

Figure 5: The number of human adipose stem cells obtained in individual passages. (a) From isolation SVF to passage 3. $M \pm$ SD ($n = 5$). (b) From passage 0 to passage 23. $M \pm$ SD ($n = 3$).

(Figures 7(a) and 8(a)). Moreover, it was observed that osteogenic potential increased with increasing passage.

4.5. Effect Volume of Cell Suspension for Efficiency of Seeding. To evaluate the effect of cell seeding and growth on 3D tissue engineering scaffolds which we placed into the well *in vitro*, cell metabolism was analyzed over a three-week period (days 1, 3, 7, and 21). Analysis of the proliferation of human ASCs suspended in the seeding volume of 50 μl and 35 μl showed statistically significant differences after 3 and 21 days of culture into PCL ($^*p < 0.05$) and after day 21 of culture for PCL + 5% TCP scaffold. Results shows that cell seeding efficiency increased when using a seeding volume of 35 μl. We also observed a greater cell activity on the scaffolds on day 21 (Figure 10). Our results may suggest that, except volume cell seeding, also propagation time plays an important role in efficiency of seeding. See raw data in Supplementary Materials (Table 3).

4.6. Comparison of Two Different Strategies for In Vitro Seeding of Human ASC of PCL and PCL + 5% TCP Scaffolds. To compare the effect of two methods to cell seeding PCL and PCL + 5% TCP, cell metabolism was analyzed over a week period (1 and 7 days). Results indicate that ASC cells attached and proliferated on PCL and PCL + 5% TCP scaffolds cultured in a basic medium. We observed

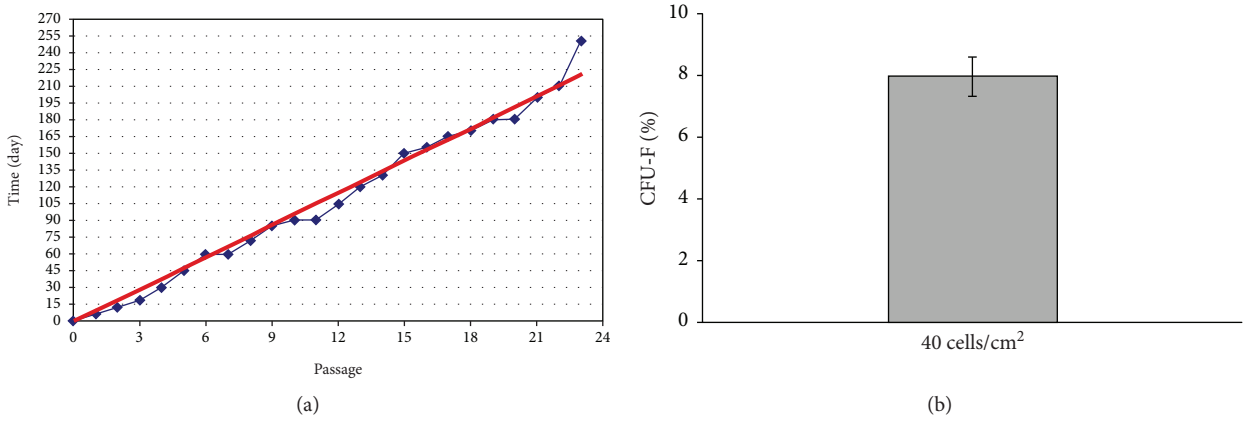

Figure 6: (a) The association between the duration of adipose stem cell cultures and individual passages in cells obtained from human adipose tissue ($n = 5$). (b) Clonal growth test (CFU-F) of stromal vascular fraction cells obtained from human adipose tissue. $M \pm \mathrm{SD}$ ($n = 6$).

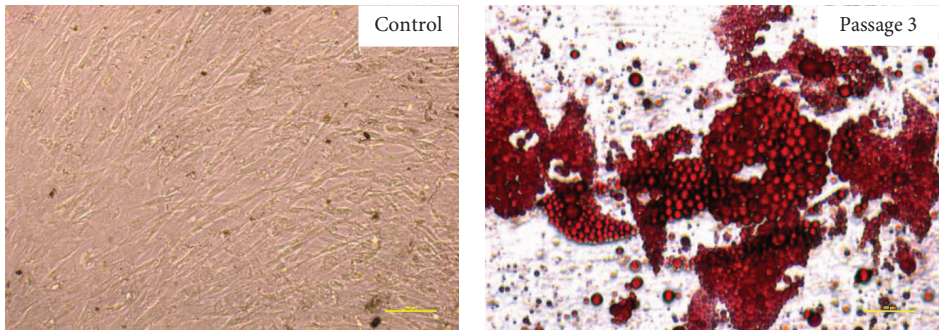

Figure 7: Oil Red O staining of human adipose stem cells after passage 3. (a) Control, undifferentiated adipose stem cells. (b) Adipogenic differentiation. Representative images are shown at 10x magnification. Scale bars represent 100 μm. The representative images are from one independent donor.

significant differences between two methods used ($^{**}p < 0.001$). See raw data in Supplementary Materials (Table 4). Increased seeding efficiency was observed when using the saturation of cell suspension into scaffolds with additional incubation. Basic static cell seeding method did not generate this level of seeding efficiency. Figure 11 contains an assessment of the statistical significance between the method of basic static ASC cell seeding and the method of saturation of cell suspension, respectively. Results implying that the selection of the method of cell seeding can significantly increase seeding efficiency. Data presents a higher level of ASC proliferation into PCL + 5% TCP than PCL scaffold.

4.7. Optimization of Density of Seeding Cells into Scaffolds. The level of metabolic activity measured by the MTS test for human ASCs placed on PCL and PCL + 5% TCP significantly increased in cells after 3, 7, and 21 days of culture using the initial cell number equal to 0.9×10^6 (6 mm × 4 mm of the scaffold area) in comparison with the density of 0.5×10^6 and 1.5×10^6 (Figure 12). A significant decrease in proliferation was observed after 7 days of culture at the initial ASC cell count of 0.5×10^6 for PCL ($^{*}p < 0.05$) and PCL + 5% TCP ($^{***}p < 0.001$) compared to 0.9×10^6 and after 7 days of culture on PCL + 5% TCP for 1.5×10^6 ($p < 0.05$). Interestingly, the differences between the density 0.9×10^6 and 1.5×10^6 were not significant after 21 days of cultivation, while they were observed comparing the densities of 0.5×10^6 and 0.9×10^6 ($^{*}p < 0.05$). Result of analysis is shown in Supplementary Materials (Tables 5 and 6).

4.8. Cellular Distribution. Analysis of images of human ASC cell seeding onto PCL scaffold shows high adhesion capacity (Figures 13(a)–13(c)) and cell migration (Figures 13–18). Both types of scaffolds promote adhesion and proliferation of cells (Figure 15). Microscopic analysis of fibers of scaffolds (Figures 13 and 14) shows that ASCs adhere to scaffold surface and make extensive cell clusters. Cell distribution was homogeneous throughout the scaffold material (Figure 15). DAPI staining was used to evaluate the proliferation rate of adipose stem cells seeded on PCL and PCL + 5% TCP cultured up to 21 days. We observed that seeded ASCs adhere to the surface and migrate into the scaffolds (Figure 16).

SEM images of the PCL and PCL + 5% TCP scaffold surface and cross section were collected at different magnifications. The cells are evenly distributed over its entire porous surface of scaffolds (Figure 17). Also, at the fiber interface,

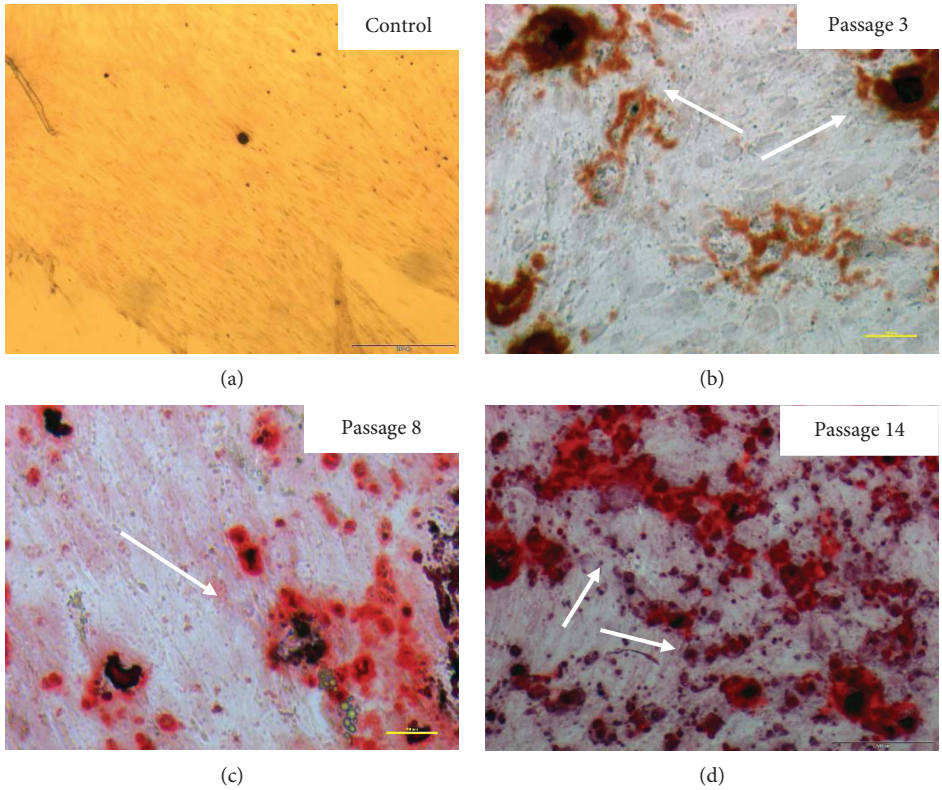

Figure 8: Alizarin Red staining and mineralization assay of human adipose stem cells after 3, 8, and 14 passages. (a) Control, undifferentiated ASCs. (b, c, d) Osteogenic differentiation. Representative images are shown at 10x magnification. Scale bars represent 100 μm. The representative images are from one independent donor. Calcium deposits are indicated with white arrows.

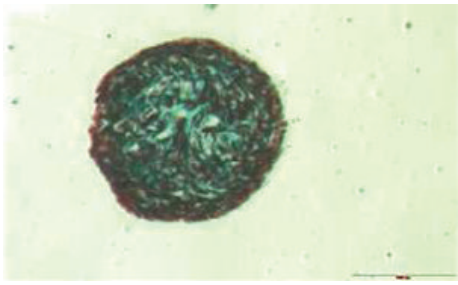

Figure 9: Chondrogenic differentiation of the human adipose stem cells. After 3 weeks of chondrogenic induction, the pellet was observed. Pellets were stained with Masson's trichrome stain. Representative images are shown at 4x magnification. Scale bars: 200 μm. The representative images are from one independent donor.

the cells adhering the scaffold are visible (Figures 17(c), 17(d), and 17(g)). In the proximal part of the scaffold, attached layers of cells were observed (Figures 17(e), 17(f), 17(h), and 17(i)). Likewise, in the distal part, the adherent cell-forming groups cover the surface. The cells are characterized by the presence of many cell convexities (Figures 17(f), 17(g), and 17(i)). In all cases of the tested PCL and PCL + 5% TCP scaffold surfaces, positive ASC cell responses were noted.

4.9. Osteogenic Potential of ASCs into the PCL and PCL Covered with 5% Tricalcium Phosphate. Alizarin Red S staining was employed to observe the calcium deposition in the osteogenic differentiation of ASCs on PCL and PCL + 5% TCP scaffolds for 7 and 14 days postdifferentiation. Alizarin Red-positive nodules formed in ASCs on both scaffolds uniformly (Figures 18(a)–18(c) and 19). Adipogenic differentiation of the cells into PCL and PCL + 5% TCP showed accumulated intracellular lipid droplet as revealed by Oil Red O staining (Figures 18(d)–18(f)).

The osteogenic assay showed that cell-seeded PLC + 5% TCP scaffolds cultured in the osteogenic medium presented significantly greater signal of staining dye and higher alkaline phosphatase level production during the 14-day culture period ($^{**}p < 0.01$), compared with the control medium and PCL scaffold. These results imply that the modification of scaffolds may influence the degree of ASC cell differentiation (Figure 20). See raw data in Supplementary Materials (Table 7).

5. Discussion

In the present study, ASCs were obtained from abdomen tissue from 17 female donors over a broad age range (49 ± 6 years). Analysis indicated that the overall yield of SVF cells was 0.36×10^6 per milliliter of lipoaspirate. Our results are comparable with data published by Suga et al. [17], Millan et al. [18], Markarian et al. [19], Condé-Green et al. [20], and Aronowitz et al. [21]. Nevertheless, there are reports in the literature that indicate a significantly higher number of SVFs obtained from $2–6 \times 10^6$/ml of adipose tissue [22],

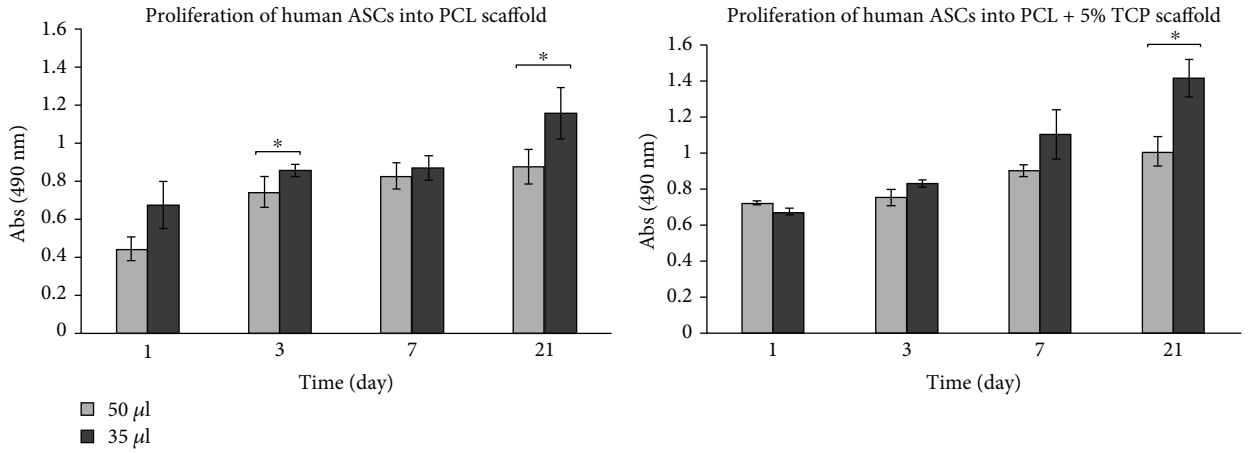

Figure 10: Seeding efficiency of human ASCs into PCL and PCL + 5% TCP scaffolds after 1, 3, 7, and 21 days. All scaffolds were seeded with 0.5×10^6 ASCs, passage 3. Volume of cell suspension: 50 μl and 35 μl ($n = 3$ for each group). Significance: $^{*}p < 0.05$.

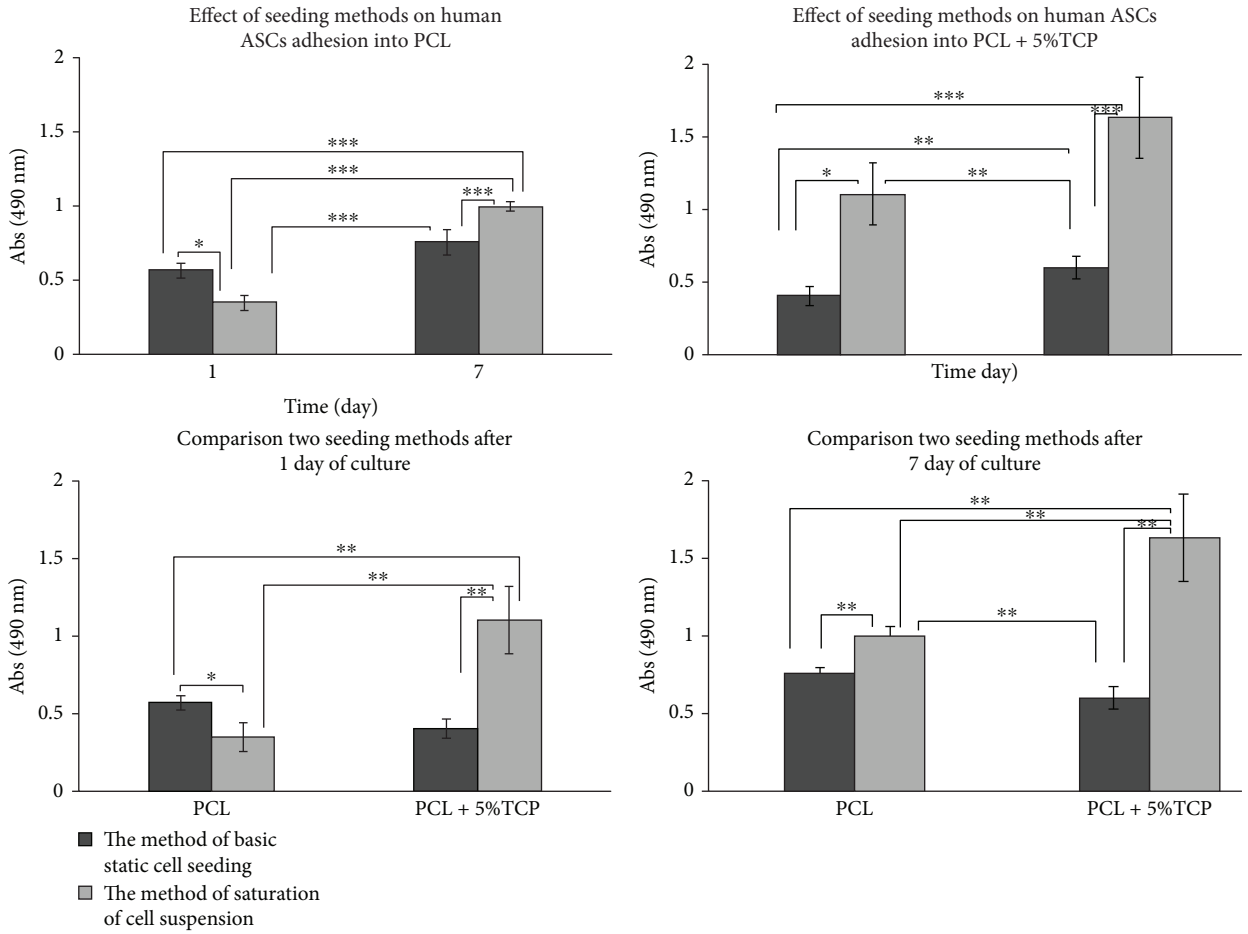

Figure 11: Metabolic activity of the human adipose stem cells measured by MTS assay into PCL and PCL + 5% TCP scaffolds ($n = 3$). Notes: statistical analysis: $^{*}p < 0.05$, $^{**}p < 0.01$, $^{***}p < 0.001$.

but also it is obtained from 0.5×10^4 to 7.95×10^5 per 1 g of adipose tissue [19, 23–25]. The reason for such individual variability of ASCs is not fully understood yet. One of the causes can be lack of standard isolation and culture procedures. As a result, comparison and interpretation of the various scientific researches are restricted. Standardization of these parameters may increase reliability and repeatability of results, but there are also factors affecting the quality of ASC, which cannot be standardized, i.e., age, ethnicity, medical history, and BMI index [5, 23, 26–29].

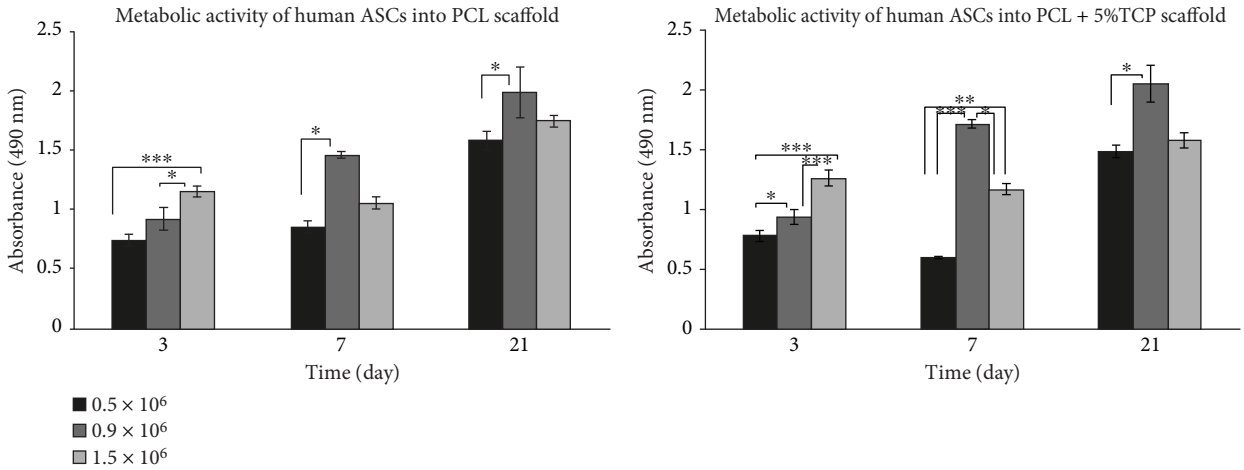

Figure 12: Metabolic activity of the human adipose stem cells measured by MTS assay into PCL and PCL + 5% TCP scaffolds ($n = 3$). Statistical analysis: $^{*}p < 0.05$, $^{**}p < 0.01$, and $^{***}p < 0.001$.

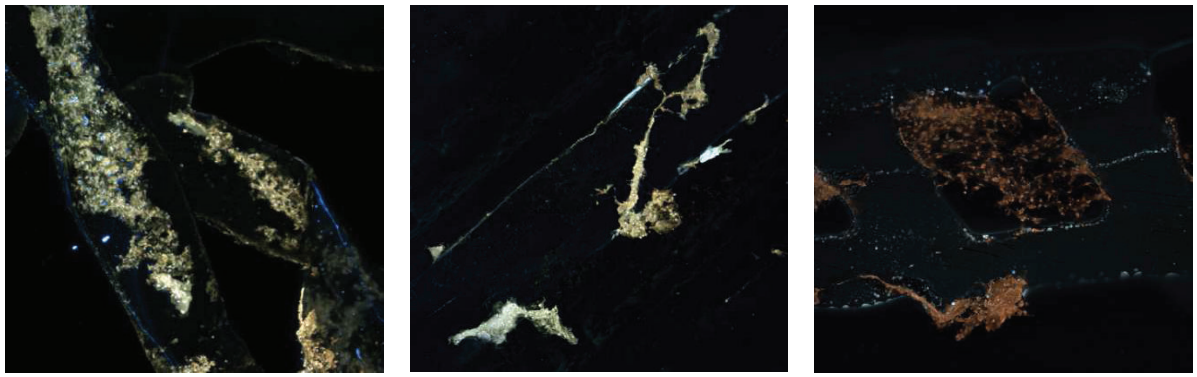

(a) (b) (c)

Figure 13: The representative images of human adipose stem cells, seeding into PCL after 21 days of culture. Seeding density of ASC: 0.9×10^6/scaffold. Representative images are shown at 10x magnification. Scale bars represent 100 μm. Images were taken by using a Nikon Eclipse Ti confocal microscope. Representative images are from one donor.

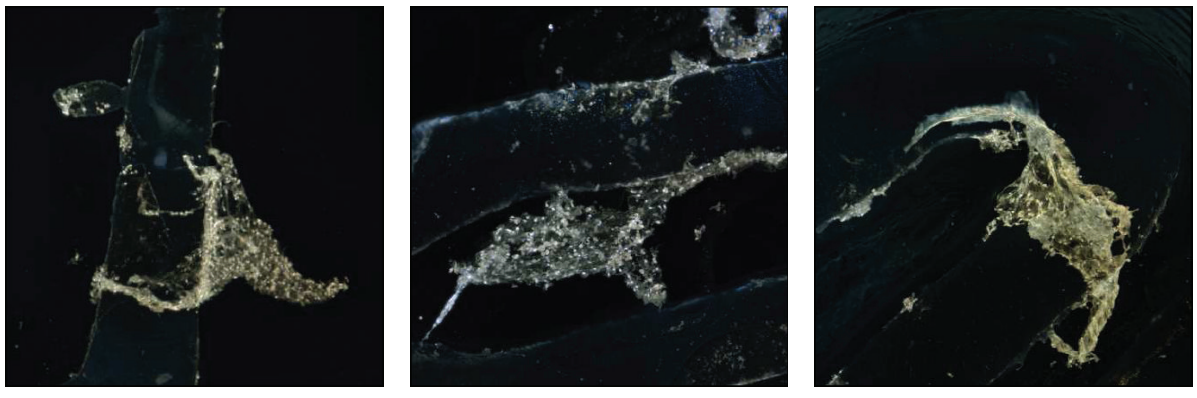

(a) (b) (c)

Figure 14: The representative images of human adipose stem cells seeding into PCL + 5% TCP after 21 days of culture. Seeding density of ASC: 0.9×10^6/scaffold. Representative images are shown at 10x magnification. Scale bars represent 100 μm. Images were taken by using a Nikon Eclipse Ti confocal microscope. Representative images are from one donor.

There are many conflicting reports about the effect of donor's age and the number of cells obtained from adipose tissue. It is believed that cells residing in the elderly are subjected to age-related changes and thus contribute less to tissue rejuvenation [30]. In contrast, some studies reported that donor age does not affect the characteristics,

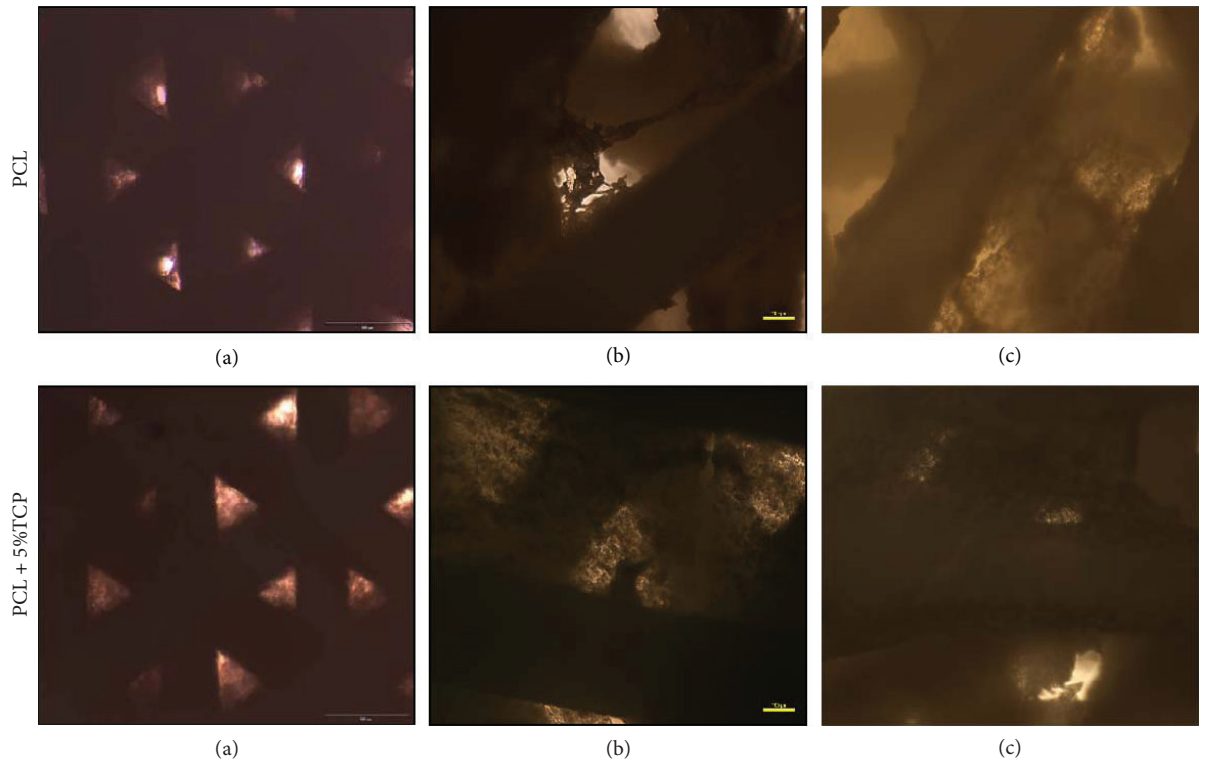

Figure 15: The representative images of human adipose stem cells seeding into PCL and PCL + 5% TCP after 42 days of culture. Seeding density of ASC: 0.9×10^6/scaffold. Representative images are shown at 10x magnification. Scale bars represent 100 μm. Images were taken by using an Olympus CKX41 microscope. (a) Proximal part of seeding scaffolds. (b, c) Distal part of seeding scaffolds. Representative images are from one donor.

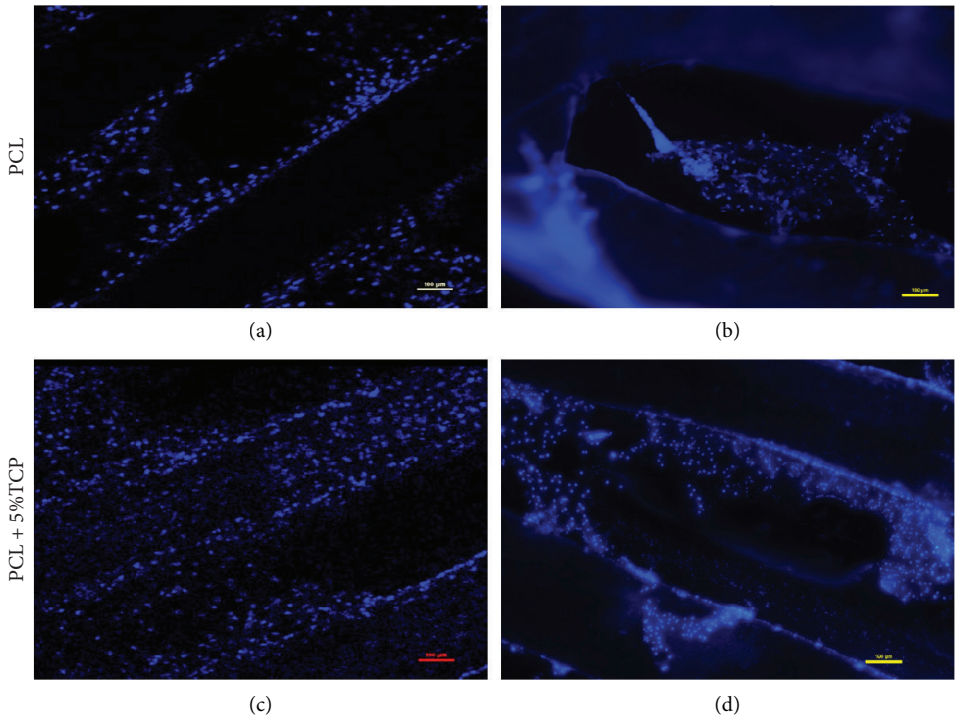

Figure 16: Fluorescence microscope images for DAPI staining (blue nucleus) of human adipose stem cells seeded onto the PCL and PCL + 5% TCP after 21 days of culture. (a, c) Single cell nucleus of ASC. (b, d) Clusters of nucleus inside scaffolds. Seeding density = 0.9×10^6. Representative images are shown at 10x magnification. Scale bars represent 100 μm. Representative images are from one donor.

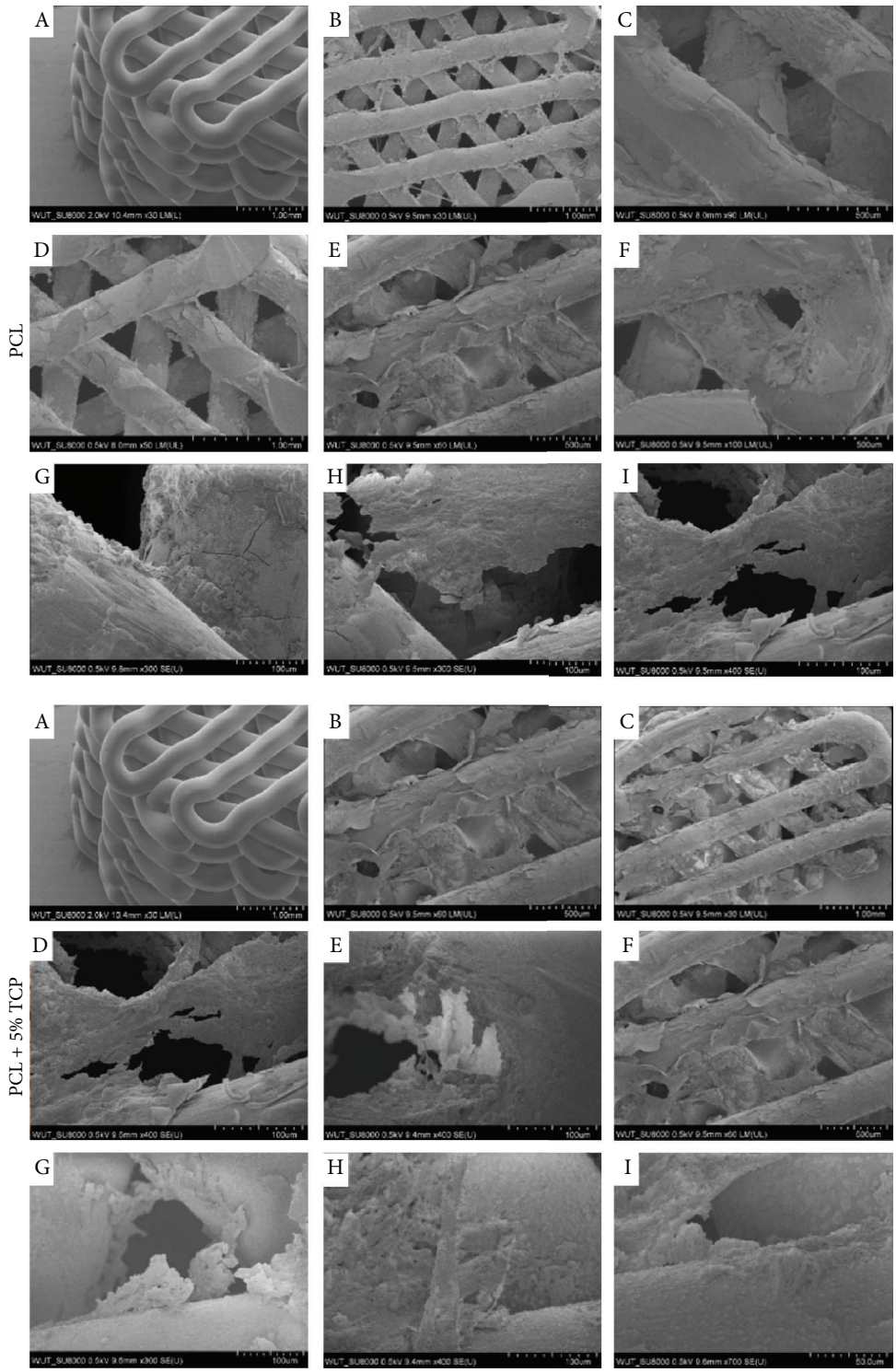

Figure 17: SEM analyses of PCL and PCL + 5% TCP composite after 42 days of ASC culture. Density seeding 0.9×10^6. (a) Control PCL without ASCs. (b, c) Proximal part of scaffolds. (d–i) Distal part of scaffolds. Representative images are from one donor.

proliferation, or osteogenic differentiation potential of ASCs allowing expansion of the use of multipotent mesenchymal stem cell donors [12, 31]. Our results demonstrated no effect of donor age (49 ± 6 years) on the cell expansion and differentiation potential. Discrepancies of many reports may imply from the broad age ranges and the health status of the donors that were studied.

The kinetics of the proliferation of cells obtained from human adipose tissue shows that the highest number of ASCs can be achieved in passage 5 and after passage 16, proliferation is significantly decrease. This may suggest that ASCs can be cultured *in vitro* for a long time without impairing their proliferative capacity [32]. In contrast, some studies have reported decrease of ASC proliferation capacity in

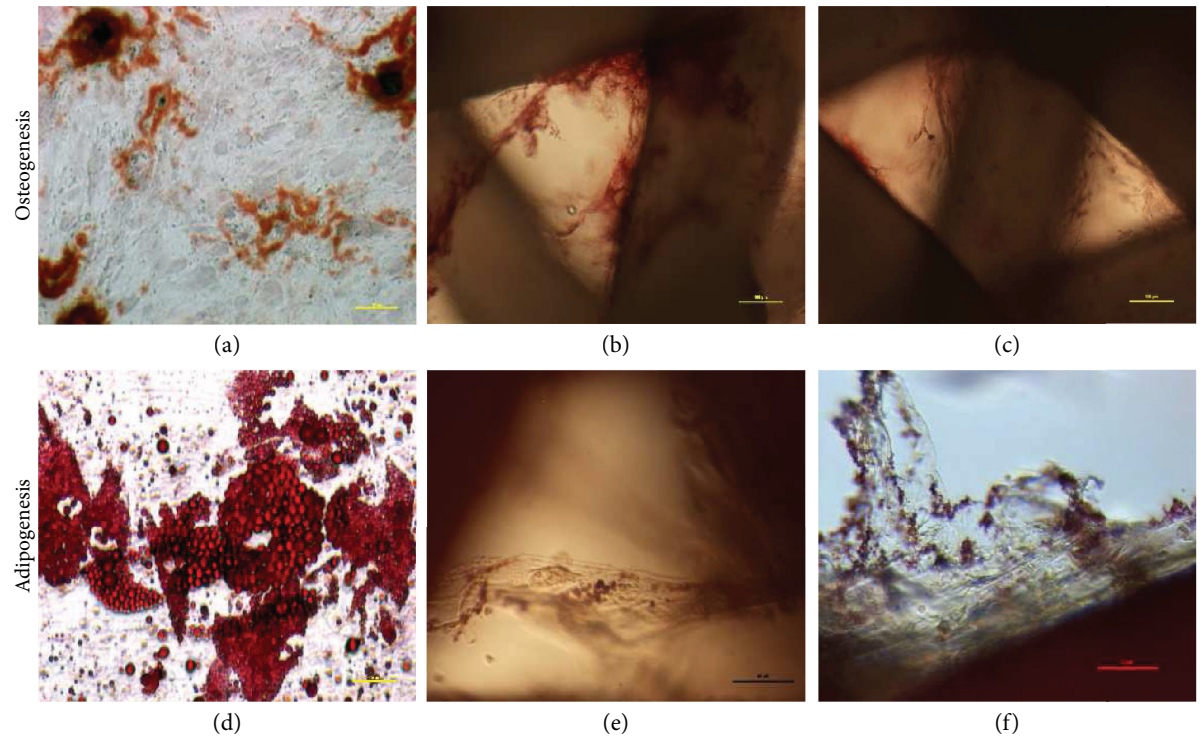

Figure 18: The representative images of human adipose stem cells seeding into PCL and PCL + 5% TCP after 21 days of culture. (a) Osteogenic differentiation of ASCs in 2D culture (density: 0.3×10^6). (b) Osteogenic differentiation (ARS) in PCL scaffold. (c) Osteogenic differentiation in PCL + 5% TCP. (d) Adipogenic differentiation (Oil Red O) of ASCs in 2D culture. (e) Adipogenic differentiation in PCL scaffold. (f) Adipogenic differentiation in PCL + 5% TCP scaffold. Seeding density of ASCs: 0.9×10^6 per scaffold. Representative images are shown at 10x magnification. Scale bars represent 100 μm. Images were taken by using an Olympus CKX41 microscope.

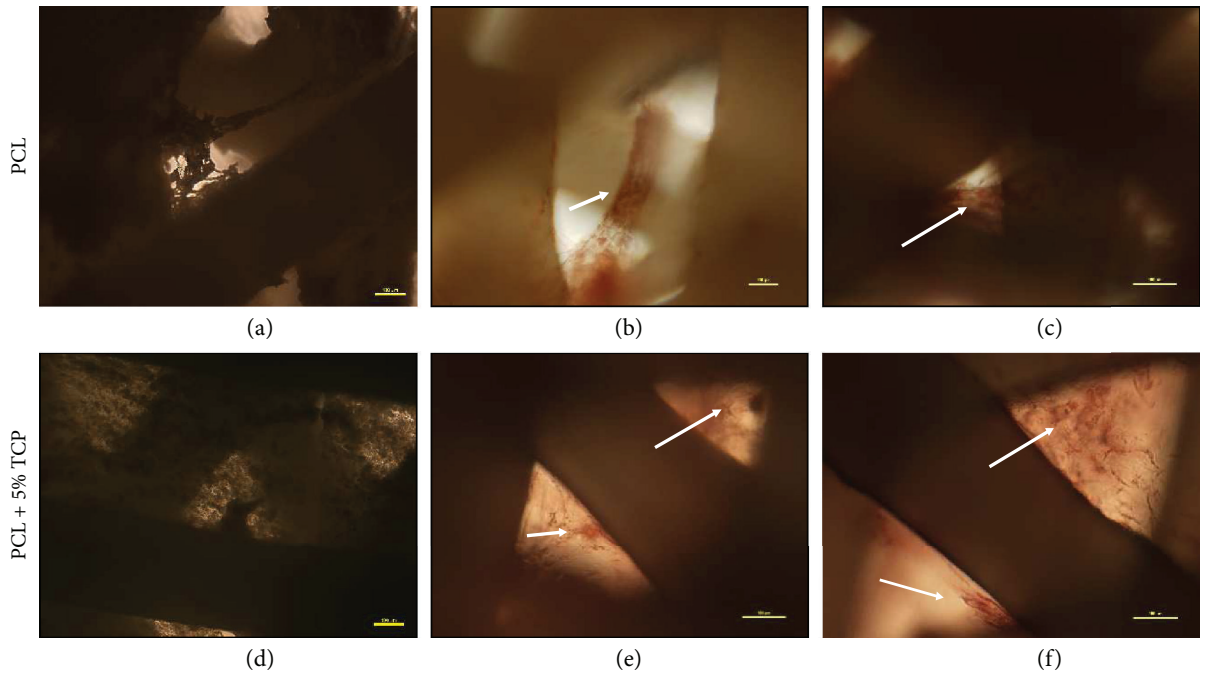

Figure 19: The representative images of human adipose stem cells seeding into PCL and PCL + 5% TCP after 42 days of culture. (a, d) Control, undifferentiated of ASCs. (b, c, e, f) Osteogenic differentiation (ARS). Seeding density of ASC: 0.9×10^6/scaffold. Representative images are shown at 10x magnification. Scale bars represent 100 μm. Images were taken by using an Olympus CKX41 microscope.

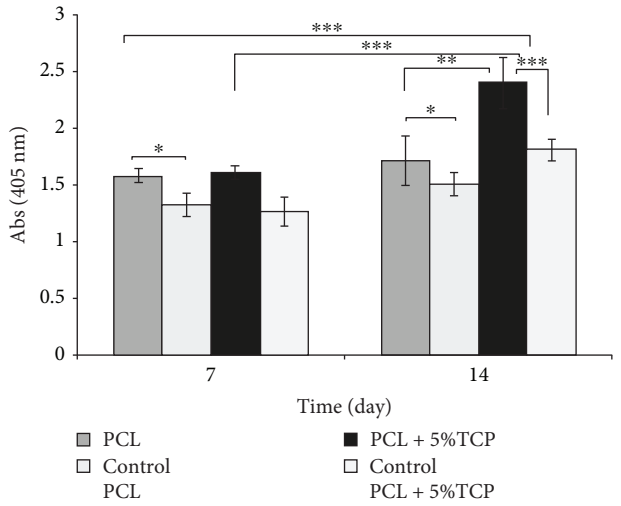

Figure 20: Alkaline phosphate activity of cultured osteoblasts on PCL and PCL + 5% TCP scaffolds after 7 and 14 days. Control: undifferentiated of ASCs. Statistical analysis: $^{*}p < 0.05$, $^{**}p < 0.01$, and $^{***}p < 0.001$.

number of passages [33–36]. On the other hand, we also observed large deviation of the mean results after 5th passage. These differences can be due to a noise measurement or differences depending on the donors. The results obtained thus suggest that age-related changes in ASC number should be taken individually into account whenever these cells are considered for clinical applications. Interestingly, we also observed that the percentage of colony-forming units from ASCs was significantly higher than results demonstrated by Rodriguez et al. [25] or Aronovitz et al. [24] and slightly lower than the results by Güven et al. [37]. Numerous studies have reported that CFU-F may decrease with increasing age of the donor [38]. Therefore, ASCs may require either a larger amount of adipose tissue or a pretreatment strategy to increase proliferation *in vitro* and the clonogenic ability of ASCs.

In our study, we demonstrated that along with the next passage of ASCs, the accumulation of calcium phosphate in cells *in vitro* marked with ARS is increasing. These changes in the ability to differentiate are confirmed by other reports, where ALP levels and the expression of osteogenic genes began to increase with rising passage [39]. Studies have also reported that after intensive passage of human ASC cells, osteogenic differentiation begins to prevail and adipogenic potential disappears [35, 40]. Some reports that osteogenic potential decreases during aging [6, 14, 25, 33, 41] while others demonstrate that human adipose tissues have high osteogenic potential and are most important in response to osteogenic factors [42]. The result we obtained suggests that the use of conditioned cells of older passage may give better effects of osteogenic differentiation than the use of early passage cells in bone regeneration [43–45].

It is well known in fact that surface topography strongly affects implant performance and influences cell adhesion, cell shape, and tissue organization as well as the production of local microenvironment [46, 47]. In the present study, microscopic observations noted that cells can migrate along the whole scaffold and the pore size range used is not a limitation for cell migration. It was observed that the cells on PCL scaffolds are distributed in small amount heterogeneously across the entire area of the scaffold, while on PCL + 5% TCP constitute a compact cell structure inside the scaffold. It was also noted that after 42 days of culture, many cells filled the space between the scaffolding fibers, which additionally suggests that the cells need more time in seeding the scaffold structure.

Seeding of cells on the scaffolds is a critical step in the process for the construction of polymer-cell scaffolds and often determines the quality of tissue engineering products. The criteria for an optimal seeding method assume that cell distribution should be homogeneous on scaffolds, with high efficiency and easy to use with minimal cell damage during the procedure [48]. We observed that the increase in the volume of cell suspension is a significant parameter of the reduction in the efficiency of seeding scaffolds. The highest efficiency of seeding ASCs on scaffolds was obtained with seeding volume of 35 μl and the lowest using 50 μl. Similar results were presented by Zhou et al. [49] and Buckley and O'Kelly [50], who observed a tendency that, depending on the volume of the cell suspension, the efficiency of seeding decreases. Buckley and O'Kelly [50] demonstrated that the maximum yield was obtained using a volume of 25 μl (85.4% ± 4.9%) and the smallest yield using a volume of 50 μl (67.7% ± 2.2%) and 100 μl (43.8% ± 3, 2%).

Comparing methods of seeding scaffolds, we observed the effect of cell aspiration into PCL and PCL + 5% TCP when the method of saturation of cell suspension with additional incubation was used. Literature reports show that aspiration of cell suspension and capillary force is of great importance in the organization of cells and seeding into scaffolds [51]. Therefore, in our presented methods of the seeding process, we used an additional incubation step. This modification contributed to a better cell adhesion onto scaffolds and effective cell migration inside porous. Increased seeding efficiency was observed when using the saturation of cell suspension into scaffolds with additional incubation. Basic static cell seeding method was not generating this level of seeding efficiency. Furthermore, we also observed that the cell seeding efficiency did differ significantly between scaffold materials and cell seeding methods ($^{***}p < 0.001$). These may imply from the increased hydrophilicity of the polymer, as well as from the presence of the calcium phosphate component in the scaffold matrix, which can increase the absorption of proteins [48, 49, 52–54]. These suggest that the architecture and modification of scaffolds may affect cell distribution during seeding, as well as active migration and tissue formation. Furthermore, using the method of saturation of cell suspension increases significantly the cell seeding on PCL + 5% TCP after 7 days of culture.

Obtaining of the optimal density of seeding ASC cells of scaffolds tested is difficult due to the complicated structure of the scaffolds and many interactions between cell scaffolds. The results of these studies suggest that optimal ASC growth on scaffolds was observed at the initial density of 0.9×10^6 to

the surface of scaffold, after 21 days of culture. Interestingly, the differences between the density 0.9×10^6 and 1.5×10^6 were not significant after 21 days of culture and significant between 0.5×10^6 and 0.9×10^6 cell seeding densities ($^*p < 0.05$). Our result are similar with other previous studies and suggest that time can significantly influence the seeding efficiency [55, 56]. On the other hand, the positive effect of using low cell densities for seeding scaffolds was noted by Zhou et al. [49]. In contrast, Tan et al. [57] showed that the higher number of cell seeding increased the adhered cells on the scaffolds. Thevenot et al. [47] noted that when a static method was used, 25% of cell seeding on a scaffold underwent apoptosis after 3 hours of seeding and by a dynamic seeding method, over 50% of cell seeding underwent apoptosis. These observations may imply that the time and method of seeding may be more important than the initial cell density for seeding and the use of a large number of cells does not necessarily mean better adhesion and more efficient seeding. These results confirm with the literature data, in which cell attachment was low on scaffolds on initial seeding (determined at 15%) and, depending on the pore size, could decrease even up to 40% after 4 days of culture and then can gradually increase after 21 days of culture [52].

Evaluation of an osteogenic marker ALP of ASCs revealed that changes in the scaffold structures could influence the degree of cell differentiation. A significant increase in osteogenesis of ASCs on the PCL + 5% TCP scaffold was observed after 14 days of culturing, compared to undifferentiated ASCs cultured in a standard culture medium. The results obtained thus are consistent with those of the previous studies reporting an increase in ALP level activity after 14 days of ASC differentiation on scaffolds [40, 58–60]. In addition, studies have reported that there are reports that show that the addition of tricalcium phosphate may improve the ability of cells to differentiate towards osteogenesis in PCL scaffold [56, 61, 62]. In contrast, there are also studies reported that an admixture of 3–5% TCP or HA does not show yield significant differences in the cell mineralization on scaffolds [59, 63].

6. Conclusions

The conducted experiments show that the tested materials have a positive influence on ASC cell adhesion and proliferation and applied material may play a role as a temporary extracellular matrix. PCL and PCL + 5% TCP are promising cellular platforms for regenerative therapy for further *in vitro* and *in vivo* studies. Porous PCL scaffold with 5% TCP can play an important role in cell migration, adhesion and infusion of nutrients, promoting proliferation, and differentiation of ASC cells for osteogenesis better than PCL. ASC cells adhere to scaffold surfaces; for better seeding efficiency, cells should be cultured for a longer time. From the perspective on the potential use for clinical applications, PCL covered with 5% tricalcium phosphate may contribute to the promotion of bone repair and provide an appropriate model to support the regeneration of new bone for future tissue engineering strategy.

Data Availability

The numeric and graphic data used to support the findings of this study are included within the Supplementary Materials' file.

Conflicts of Interest

All authors state that they have no conflicts of interest.

Acknowledgments

This research was supported by grant from the National Center for Research and Development, Poland (STRATEGMED 1/233224/10/NCBR/2014, project START).

Supplementary Materials

MTS standard curve. Table 1: characterization of donors and number of SVF ($n = 17$). Table 2: growth kinetics of human ASCs. Summary table of average number of human ASCs. $M \pm$ SD ($n = 3$). Table 3: seeding efficiency of human ASCs within PCL and PCL + 5% TCP scaffolds. Summary table of absorbance values measured by the MTS test for seeding hASC into PCL and PCL + 5% TCP. $M \pm$ SD ($n = 3$). Table 4: summary table of absorbance values measured by the MTS test for seeding human ASC into PCL and PCL + 5% TCP. $M \pm$ SD ($n = 6$). Table 5: summary table of absorbance values measured by the MTS test for seeding human ASC into PCL and average number of cells, measured by the standard curve of MTS. $M \pm$ SD ($n = 3$). Table 6: summary table of absorbance values measured by the MTS test for seeding human ASC into PCL + 5% TCP, and average number of cells, measured by the standard curve of MTS. $M \pm$ SD ($n = 3$). Table 7: summary table of absorbance values measured by the ALP test for seeding human ASC into PCL + 5% TCP. $M \pm$ SD ($n = 5$). *(Supplementary Materials)*

References

[1] C. R. M. Black, V. Goriainov, D. Gibbs, J. Kanczler, R. S. Tare, and R. O. C. Oreffo, "Bone tissue engineering," *Current Molecular Biology Reports*, vol. 1, no. 3, pp. 132–140, 2015.

[2] P. Palumbo, F. Lombardi, G. Siragusa, M. Cifone, B. Cinque, and M. Giuliani, "Methods of isolation, characterization and expansion of human adipose-derived stem cells (ASCs): an overview," *International Journal of Molecular Sciences*, vol. 19, no. 7, p. 1897, 2018.

[3] W. U. Hassan, U. Greiser, and W. Wang, "Role of adipose-derived stem cells in wound healing," *Wound Repair and Regeneration*, vol. 22, no. 3, pp. 313–325, 2014.

[4] E. Raposio and N. Bertozzi, "Isolation of ready-to-use adipose-derived stem cell (ASC) pellet for clinical applications and a comparative overview of alternate methods for ASC isolation," *Current Protocols in Stem Cell Biology*, vol. 41, no. 1, pp. 1F.17.1–1F.17.12, 2017.

[5] P. A. Zuk, M. Zhu, H. Mizuno et al., "Multilineage cells from human adipose tissue: implications for cell-based therapies," *Tissue Engineering*, vol. 7, no. 2, pp. 211–228, 2001.

[6] M. S. Choudhery, M. Badowski, A. Muise, J. Pierce, and D. T. Harris, "Donor age negatively impacts adipose

tissue-derived mesenchymal stem cell expansion and differentiation," *Journal of Translational Medicine*, vol. 12, no. 1, p. 8, 2014.

[7] L. d. Girolamo, S. Lopa, E. Arrigoni, M. F. Sartori, F. W. Baruffaldi Preis, and A. T. Brini, "Human adipose-derived stem cells isolated from young and elderly women: their differentiation potential and scaffold interaction during in vitro osteoblastic differentiation," *Cytotherapy*, vol. 11, no. 6, pp. 793–803, 2009.

[8] L. J. Harris, P. Zhang, H. Abdollahi et al., "Availability of adipose-derived stem cells in patients undergoing vascular surgical procedures," *The Journal of Surgical Research*, vol. 163, no. 2, pp. e105–e112, 2010.

[9] G. Caso, M. A. McNurlan, I. Mileva, A. Zemlyak, D. C. Mynarcik, and M. C. Gelato, "Peripheral fat loss and decline in adipogenesis in older humans," *Metabolism*, vol. 62, no. 3, pp. 337–340, 2013.

[10] I. Karagiannides, T. Tchkonia, D. E. Dobson et al., "Altered expression of C/EBP family members results in decreased adipogenesis with aging," *American Journal of Physiology-Regulatory, Integrative and Comparative Physiology*, vol. 280, no. 6, pp. R1772–R1780, 2001.

[11] T. Tchkonia, D. E. Morbeck, T. von Zglinicki et al., "Fat tissue, aging, and cellular senescence," *Aging Cell*, vol. 9, no. 5, pp. 667–684, 2010.

[12] B. M. Schipper, K. G. Marra, W. Zhang, A. D. Donnenberg, and J. P. Rubin, "Regional anatomic and age effects on cell function of human adipose-derived stem cells," *Annals of Plastic Surgery*, vol. 60, no. 5, pp. 538–544, 2008.

[13] S. Ciuffi, R. Zonefrati, and M. L. Brandi, "Adipose stem cells for bone tissue repair," *Clinical Cases in Mineral and Bone Metabolism*, vol. 14, no. 2, pp. 217–226, 2017.

[14] Y. Chen, V. Bloemen, S. Impens, M. Moesen, F. P. Luyten, and J. Schrooten, "Characterization and optimization of cell seeding in scaffolds by factorial design: quality by design approach for skeletal tissue engineering," *Tissue Engineering. Part C, Methods*, vol. 17, no. 12, pp. 1211–1221, 2011.

[15] A. M. Leferink, W. J. Hendrikson, J. Rouwkema, M. Karperien, C. A. van Blitterswijk, and L. Moroni, "Increased cell seeding efficiency in bioplotted three-dimensional PEOT/PBT scaffolds," *Journal of Tissue Engineering and Regenerative Medicine*, vol. 10, no. 8, pp. 679–689, 2016.

[16] L. Ghasemi-Mobarakeh, M. P. Prabhakaran, L. Tian, E. Shamirzaei-Jeshvaghani, L. Dehghani, and S. Ramakrishna, "Structural properties of scaffolds: crucial parameters towards stem cells differentiation," *World Journal of Stem Cells*, vol. 7, no. 4, pp. 728–744, 2015.

[17] H. Suga, H. Eto, N. Aoi et al., "Adipose tissue remodeling under ischemia: death of adipocytes and activation of stem/-progenitor cells," *Plastic and Reconstructive Surgery*, vol. 126, no. 6, pp. 1911–1923, 2010.

[18] A. Millan, T. Landerholm, and J. R. Chapman, "Comparison between collagenase adipose digestion and stromal cell mechanical dissociation for mesenchymal stem cell separation," *McNair Scholars Journal*, vol. 15, pp. 86–101, 2014.

[19] C. F. Markarian, G. Z. Frey, M. D. Silveira et al., "Isolation of adipose-derived stem cells: a comparison among different methods," *Biotechnology Letters*, vol. 36, no. 4, pp. 693–702, 2014.

[20] A. Condé-Green, R. L. Rodriguez, S. Slezak, D. P. Singh, N. H. Goldberg, and J. McLenithan, "Enzymatic digestion and mechanical processing of aspirated adipose tissue," *Plastic and Reconstructive Surgery*, vol. 134, no. 4S-1, p. 54, 2014.

[21] J. A. Aronowitz, R. A. Lockhart, and C. S. Hakakian, "Mechanical versus enzymatic isolation of stromal vascular fraction cells from adipose tissue," *SpringerPlus*, vol. 4, no. 1, p. 713, 2015.

[22] K. Yoshimura, T. Shigeura, D. Matsumoto et al., "Characterization of freshly isolated and cultured cells derived from the fatty and fluid portions of liposuction aspirates," *Journal of Cellular Physiology*, vol. 208, no. 1, pp. 64–76, 2006.

[23] P. C. Baer and H. Geiger, "Adipose-derived mesenchymal stromal/stem cells: tissue localization, characterization, and heterogeneity," *Stem Cells International*, vol. 2012, Article ID 812693, 11 pages, 2012.

[24] J. A. Aronowitz, R. A. Lockhart, C. S. Hakakian, and Z. E. Birnbaum, "Adipose stromal vascular fraction isolation: a head-to-head comparison of 4 cell separation systems #2," *Annals of Plastic Surgery*, vol. 77, no. 3, pp. 354–362, 2016.

[25] J. Rodriguez, A. S. Pratta, N. Abbassi et al., "Evaluation of three devices for the isolation of the stromal vascular fraction from adipose tissue and for ASC culture: a comparative study," *Stem Cells International*, vol. 2017, Article ID 9289213, 14 pages, 2017.

[26] L. E. Kokai, D. O. Traktuev, L. Zhang et al., "Adipose stem cell function maintained with age: an intra-subject study of long-term cryopreserved cells," *Aesthetic Surgery Journal*, vol. 37, no. 4, pp. 453–463, 2016.

[27] D. Dufrane, "Impact of age on human adipose stem cells for bone tissue engineering," *Cell Transplantation*, vol. 26, no. 9, pp. 1496–1504, 2017.

[28] C. Siciliano, M. Ibrahim, G. Scafetta et al., "Optimization of the isolation and expansion method of human mediastinal-adipose tissue derived mesenchymal stem cells with virally inactivated GMP-grade platelet lysate," *Cytotechnology*, vol. 67, no. 1, pp. 165–174, 2015.

[29] S.-Y. Liu, Y.-B. He, S.-Y. Deng, W.-T. Zhu, S.-Y. Xu, and G.-X. Ni, "Exercise affects biological characteristics of mesenchymal stromal cells derived from bone marrow and adipose tissue," *International Orthopaedics*, vol. 41, no. 6, pp. 1199–1209, 2017.

[30] S. Dimmeler and A. Leri, "Aging and disease as modifiers of efficacy of cell therapy," *Circulation Research*, vol. 102, no. 11, pp. 1319–1330, 2008.

[31] T. Khan, E. S. Muise, P. Iyengar et al., "Metabolic dysregulation and adipose tissue fibrosis: role of collagen VI," *Molecular and Cellular Biology*, vol. 29, no. 6, pp. 1575–1591, 2009.

[32] I. Christodoulou, F. N. Kolisis, D. Papaevangeliou, and V. Zoumpourlis, "Comparative evaluation of human mesenchymal stem cells of fetal (Wharton's jelly) and adult (adipose tissue) origin during prolonged *in vitro* expansion: considerations for cytotherapy," *Stem Cells International*, vol. 2013, Article ID 246134, 12 pages, 2013.

[33] M. Zhu, E. Kohan, J. Bradley, M. Hedrick, P. Benhaim, and P. Zuk, "The effect of age on osteogenic, adipogenic and proliferative potential of female adipose-derived stem cells," *Journal of Tissue Engineering and Regenerative Medicine*, vol. 3, no. 4, pp. 290–301, 2009.

[34] M. E. Danoviz, V. Bassaneze, J. S. Nakamuta et al., "Adipose tissue-derived stem cells from humans and mice differ in proliferative capacity and genome stability in long-term cultures," *Stem Cells and Development*, vol. 20, no. 4, pp. 661–670, 2011.

[35] M. E. Wall, S. H. Bernacki, and E. G. Loboa, "Effects of serial passaging on the adipogenic and osteogenic differentiation potential of adipose-derived human mesenchymal stem cells," *Tissue Engineering*, vol. 13, no. 6, pp. 1291–1298, 2007.

[36] W. Shu, Y. T. Shu, C. Y. Dai, and Q. Z. Zhen, "Comparing the biological characteristics of adipose tissue-derived stem cells of different persons," *Journal of Cellular Biochemistry*, vol. 113, no. 6, pp. 2020–2026, 2012.

[37] S. Güven, M. Karagianni, M. Schwalbe et al., "Validation of an automated procedure to isolate human adipose tissue-derived cells by using the Sepax technology," *Tissue Engineering. Part C, Methods*, vol. 18, no. 8, pp. 575–582, 2012.

[38] H. T. Chen, M. J. Lee, C. H. Chen et al., "Proliferation and differentiation potential of human adipose-derived mesenchymal stem cells isolated from elderly patients with osteoporotic fractures," *Journal of Cellular and Molecular Medicine*, vol. 16, no. 3, pp. 582–592, 2012.

[39] F. Hu, X. Wang, G. Liang et al., "Effects of epidermal growth factor and basic fibroblast growth factor on the proliferation and osteogenic and neural differentiation of adipose-derived stem cells," *Cellular Reprogramming*, vol. 15, no. 3, pp. 224–232, 2013.

[40] Y. Zhu, T. Liu, K. Song, X. Fan, X. Ma, and Z. Cui, "Adipose--derived stem cell: a better stem cell than BMSC," *Cell Biochemistry and Function*, vol. 26, no. 6, pp. 664–675, 2008.

[41] K. Kornicka, K. Marycz, K. A. Tomaszewski, M. Marędziak, and A. Śmieszek, "The effect of age on osteogenic and adipogenic differentiation potential of human adipose derived stromal stem cells (hASCs) and the impact of stress factors in the course of the differentiation process," *Oxidative Medicine and Cellular Longevity*, vol. 2015, Article ID 309169, 20 pages, 2015.

[42] M. Panek, I. Marijanovic, and A. Ivkovic, "Stem cells in bone regeneration," *Periodicum biologorum*, vol. 117, no. 1, pp. 177–184, 2015.

[43] K. Kwist, W. C. Bridges, and K. J. L. Burg, "The effect of cell passage number on osteogenic and adipogenic characteristics of D1 cells," *Cytotechnology*, vol. 68, no. 4, pp. 1661–1667, 2016.

[44] X. Z. Yan, W. Yang, F. Yang, M. Kersten-Niessen, J. A. Jansen, and S. K. Both, "Effects of continuous passaging on mineralization of MC3T3-E1 cells with improved osteogenic culture protocol," *Tissue Engineering. Part C, Methods*, vol. 20, no. 3, pp. 198–204, 2014.

[45] J. D. Kretlow, Y.-Q. Jin, W. Liu et al., "Donor age and cell passage affects differentiation potential of murine bone marrow-derived stem cells," *BMC Cell Biology*, vol. 9, no. 1, p. 60, 2008.

[46] M. Mashhadikhan, M. Soleimani, K. Parivar, and P. Yaghmaei, "ADSCs on PLLA/PCL hybrid nanoscaffold and gelatin modification: cytocompatibility and mechanical properties," *Avicenna Journal of Medical Biotechnology*, vol. 7, no. 1, pp. 32–38, 2015.

[47] P. Thevenot, A. Nair, J. Dey, J. Yang, and L. Tang, "Method to analyze three-dimensional cell distribution and infiltration in degradable scaffolds," *Tissue Engineering. Part C, Methods*, vol. 14, no. 4, pp. 319–331, 2008.

[48] A. T. Buizer, A. G. Veldhuizen, S. K. Bulstra, and R. Kuijer, "Static versus vacuum cell seeding on high and low porosity ceramic scaffolds," *Journal of Biomaterials Applications*, vol. 29, no. 1, pp. 3–13, 2013.

[49] Y. F. Zhou, V. Sae-Lim, A. M. Chou, D. W. Hutmacher, and T. M. Lim, "Does seeding density affect *in vitro* mineral nodules formation in novel composite scaffolds?," *Journal of Biomedical Materials Research*, vol. 78A, no. 1, pp. 183–193, 2006.

[50] C. T. Buckley and K. U. O'Kelly, "Maintaining cell depth viability: on the efficacy of a trimodal scaffold pore architecture and dynamic rotational culturing," *Journal of Materials Science. Materials in Medicine*, vol. 21, no. 5, pp. 1731–1738, 2010.

[51] H. Bai, D. Wang, B. Delattre et al., "Biomimetic gradient scaffold from ice-templating for self-seeding of cells with capillary effect," *Acta Biomaterialia*, vol. 20, pp. 113–119, 2015.

[52] C. S. Moura, C. L. d. Silva, P. J. Bártolo, and F. C. Ferreira, "Combination of 3D extruded-based poly (ε-caprolactone) scaffolds with mesenchymal stem/stromal cells: strategy optimization," *Procedia Engineering*, vol. 110, pp. 122–127, 2015.

[53] Y.-M. Lee, Y.-J. Seol, Y.-T. Lim et al., "Tissue-engineered growth of bone by marrow cell transplantation using porous calcium metaphosphate matrices," *Journal of Biomedial Materials Research*, vol. 54, no. 2, pp. 216–223, 2001.

[54] Z. Tang, X. Li, Y. Tan, H. Fan, and X. Zhang, "The material and biological characteristics of osteoinductive calcium phosphate ceramics," *Regenerative Biomaterials*, vol. 5, no. 1, pp. 43–59, 2018.

[55] M. Wiedmann-al-Ahmad, R. Gutwald, G. Lauer, U. Hübner, and R. Schmelzeisen, "How to optimize seeding and culturing of human osteoblast-like cells on various biomaterials," *Biomaterials*, vol. 23, no. 16, pp. 3319–3328, 2002.

[56] P. Gao, H. Zhang, Y. Liu et al., "Beta-tricalcium phosphate granules improve osteogenesis *in vitro* and establish innovative osteo-regenerators for bone tissue engineering *in vivo*," *Scientific Reports*, vol. 6, no. 1, article 23367, 2016.

[57] L. Tan, Y. Ren, and R. Kuijer, "A 1-min method for homogenous cell seeding in porous scaffolds," *Journal of Biomaterials Applications*, vol. 26, no. 7, pp. 877–889, 2010.

[58] M. Chen, D. Q. S. le, J. Kjems, C. Bünger, and H. Lysdahl, "Improvement of distribution and osteogenic differentiation of human mesenchymal stem cells by hyaluronic acid and β-tricalcium phosphate-coated polymeric scaffold *in vitro*," *BioResearch Open Access*, vol. 4, no. 1, pp. 363–373, 2015.

[59] S. Rumiński, B. Ostrowska, J. Jaroszewicz et al., "Three-dimensional printed poly-caprolactone-based scaffolds provide an advantageous environment for osteogenic differentiation of human adipose-derived stem cells," *Journal of Tissue Engineering and Regenerative Medicine*, vol. 12, no. 1, pp. e473–e485, 2018.

[60] A. Ergun, X. Yu, A. Valdevit, A. Ritter, and D. M. Kalyon, "Radially and axially graded multizonal bone graft substitutes targeting critical-sized bone defects from polycaprolactone/-hydroxyapatite/tricalcium phosphate," *Tissue Engineering. Part A*, vol. 18, no. 23-24, pp. 2426–2436, 2012.

[61] F. Causa, P. A. Netti, L. Ambrosio et al., "Poly-ϵ-caprolactone/hydroxyapatite composites for bone regeneration: in vitro characterization and human osteoblast response," *Journal of Biomedical Materials Research Part A*, vol. 76A, no. 1, pp. 151–162, 2006.

[62] Y. M. Shin, J.-S. Park, S. I. Jeong et al., "Promotion of human mesenchymal stem cell differentiation on bioresorbable polycaprolactone/biphasic calcium phosphate composite scaffolds for bone tissue engineering," *Biotechnology and Bioprocess Engineering*, vol. 19, no. 2, pp. 341–349, 2014.

[63] A. Polini, D. Pisignano, M. Parodi, R. Quarto, and S. Scaglione, "Osteoinduction of human mesenchymal stem cells by bioactive composite scaffolds without supplemental osteogenic growth factors," *PLoS One*, vol. 6, no. 10, article e26211, 2011.

Hindawi
Stem Cells International
Volume 2019, Article ID 8914569, 13 pages
https://doi.org/10.1155/2019/8914569

Review Article

Multiscale Stem Cell Technologies for Osteonecrosis of the Femoral Head

Yi Wang,[1,2] Xibo Ma,[2,3] Wei Chai,[1] and Jie Tian[2,3]

[1]*Department of Orthopedics, Chinese PLA General Hospital, Beijing 100853, China*
[2]*CAS Key Laboratory of Molecular Imaging, Institute of Automation, Chinese Academy of Sciences, Beijing 100190, China*
[3]*The University of Chinese Academy of Sciences, Beijing 100049, China*

Correspondence should be addressed to Wei Chai; chaiwei301@163.com and Jie Tian; tian@ieee.org

Received 25 May 2018; Revised 21 October 2018; Accepted 14 November 2018; Published 8 January 2019

Guest Editor: Zengwu Shao

The last couple of decades have seen brilliant progress in stem cell therapies, including native, genetically modified, and engineered stem cells, for osteonecrosis of the femoral head (ONFH). In vitro studies evaluate the effect of endogenous or exogenous factor or gene regulation on osteogenic phenotype maintenance and/or differentiation towards osteogenic lineage. The preclinical and clinical outcomes accelerate the clinical translation. Bone marrow mesenchymal stem cells and adipose-derived stem cells have demonstrated better effects in the treatment of femoral head necrosis. Various materials have been used widely in the ONFH treatment in both preclinical and clinical trials. In a word, in vivo and multiscale efforts are expected to overcome obstacles in the approaches for treating ONFH and provide clinical relevance and commercial strategies in the future. Therefore, we will discuss the above aspects in this paper and present our opinions.

1. Introduction

Osteonecrosis of the femoral head (ONFH) is a debilitating skeletal disorder leading to loss of hip joint function which brings a heavy financial burden to healthcare system worldwide [1, 2]. The repair processes following osteonecrosis include the differentiation of preexisting mesenchymal stem cells (MSC) (the latest research shows that osteocytes are differentiated from skeletal stem cells (SSC) [3]) into osteoblasts, bone matrix secretion, and mineralization. The rate of bone generation is less than that of bone resorption, which will lead to a natural repair failure in the necrotic zone of the femoral head [4]. As a strategy to manage ONFH in the early stage, conservative treatments (e.g., physical therapy or pharmacotherapy) have questionable efficiency in current clinical practice [5–9]. For patients in the end stage of ONFH, total hip arthroplasty (THA) remains an inevitable choice as the clinical gold standard. However, THA has its disadvantages including the limited longevity of implants [10] and complications of surgical intervention (e.g., infection, revision, and dislocation) [11–13]. These disadvantages have triggered a growing expectation for research on femoral head regeneration.

Stem cells have characteristics of proliferation and differentiation. These properties make stem cell technology stand out in the field of femoral head regeneration. In recent years, stem cell science has overcome many obstacles in ONFH treatments by using multiscale stem cell technologies [14]. Multiscale stem cell technology refers to the spatial scales of different stem cells alone or with material stem cells for treatment. In this review, we cover multiscale stem cell technologies to treat ONFH (Figure 1). We briefly review the changes affecting repair abilities of MSC in the osteonecrosis area and five main microRNAs about osteogenesis. We also discuss multiscale stem cell technologies to introduce new therapeutic strategies for ONFH therapies. The multiscale stem cell technologies cover micron-sized stem cell suspensions, tens to hundreds of micron-sized stem cell carriers, and millimeter-scale stem cell scaffolds. We also outline promising stem cell materials for bone regeneration in other fields

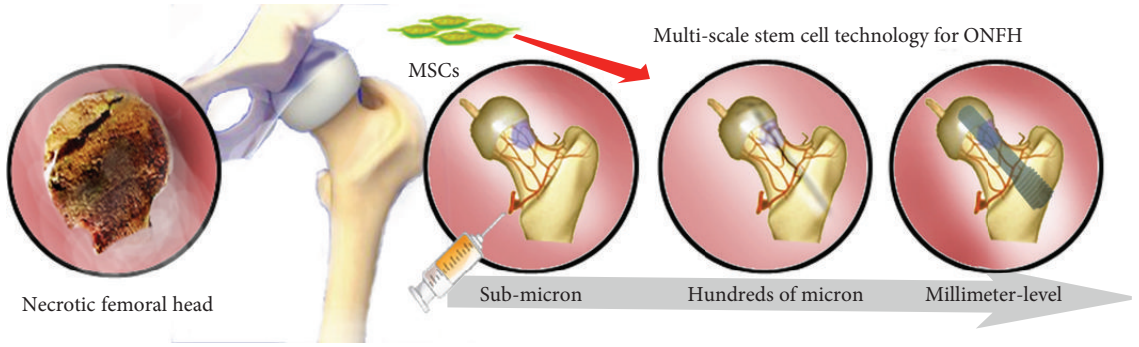

Figure 1: Multiscale stem cell technologies for ONFH therapies.

and analyze their reference to this field. Finally, we discuss the future trends of multiscale stem cell technology for treatment of ONFH.

Mesenchymal stem cells can regenerate the necrotic area of the femoral head by multiscale stem cell technologies. The stem cells are delivered to the necrosis zone by injecting suspension into the lateral artery of the circumflex (submicron), by load on carriers via core decompression (hundreds of microns), and by load on scaffolds via implantation (millimeter-level).

2. Changes in Microenvironment and MicroRNAs

The pathophysiology of ONFH remains unclear, although many attempts have been made to establish theoretical models [15]. Several recognized risk factors of ONFH have been studied at the cellular or molecular biology level in recent years including traumatic factors (e.g., femoral neck/head fracture, dislocation of the hip, and femur skull slip) and nontraumatic factors (e.g., glucocorticoids, alcohol abuse, sickle cell disease, and lipid disorders) [16].

MSC extracted from necrotic trabeculae present decreased proliferation and osteogenesis [17]. However, the components around MSC have different effects on their activities (Figure 2(a)). The trabecular structure from the necrotic area promotes MSC proliferation but inhibits ossification [18], while the surrounding demineralized matrix can promote MSC ossification [19]. The colony-forming ability of endothelial progenitor cells in peripheral blood vessels decreases, and the ability to secrete the vascular endothelial growth factor (VEGF) also decreases which will result in no blood supply in the necrotic area and necrosis aggravation [20]. Lipotoxicity is a major factor of steroid-induced necrosis of the femoral head. Increased levels of palmitate and oleate lead to the dysregulation of stearoyl-coenzyme A desaturase 1/carnitine palmitoyl transferase 1 as well as increased expression of interleukin-6 and interleukin-8 (IL-6 and IL-8) which promote adipogenesis and inhibit osteogenesis [21]. The hepatocyte growth factor (HGF) promotes osteogenesis by activating the PI3K/AKT pathway and inhibiting the WNT pathway [22].

In addition, changes in microRNA (miR) expression of MSC in necrotic areas also play important roles in the progression of ONFH (Figure 2(b)). miR-708 is significantly upregulated in MSC from patients with steroid-induced ONFH. Targeting miR-708 enhances osteogenesis and inhibits adipogenesis of MSC, while knockdown of miR-708 avoids the inhibition of osteogenesis of glucocorticoids [23]. miR-210 demethylation promotes miR-210 expression and increases endothelial cell viability and differentiation for angiogenesis [24]. Overexpression of miR-548d-5p enhances the expression of osteocalcin and Runx2 (osteogenic transcription factor) and alkaline phosphatase (ALP). Thus, it can be a marker for osteoblast differentiation. Peroxisome proliferator-activated receptor gamma (PPARγ) has been identified as a target for miR-548d-5p [25]. Downregulation of HOTAIR (HOX transcript antisense RNA), a long noncoding RNA, increases miR-17-5p levels and inhibits Smad7 expression. Knockout of HOTAIR promotes the expression of COL1A1, Runx2, and ALP [26, 27]. Both PPARγ and gremlin 1 (GREM1) are the direct targets of miRNA-27a, and the knockdowns of them also enhance the osteogenesis of MSC [28]. MicroRNA activation or silence may be an effective method for the osteogenesis recovery of stem cells. However, the biosecurity still requires significant experimental evidence. Changes in or around stem cells can affect cytoactivity, and hence the therapeutic effects will be unstable. Therefore, the supplementary cells with healthy states are prerequisites for stem cell therapies.

3. Multiscale Stem Cell Technologies for ONFH Therapies

Over the past two decades, lots of efforts for femoral head regeneration have been made on cell-based repair in ONFH treatments. A variety of MSC have been used to regenerate the necrotic bone tissue with angiogenesis, including bone marrow mesenchymal stem cells (BMSC) [29], adipose-derived mesenchymal stem cells (ADSC) [30], synovial-derived mesenchymal stem cells (SDMSC) [31], dental-pulp stem cells (DPSC) [32], blood-derived mesenchymal stem cells (BDMSC) [33], and umbilical cord-derived mesenchymal stem cells (UCDMSC) [34]. However, the clinical translations of these methods are mainly limited by the following: (1) the method of cell implantations alone is only effective for patients in the early stage of ONFH [35]; (2) there is lack of safe, robust in vivo stem cell tracing techniques [36, 37]; (3) potential risks of heterotopic ossification [38] or tumorigenesis still exist [39]; and (4) the volume of

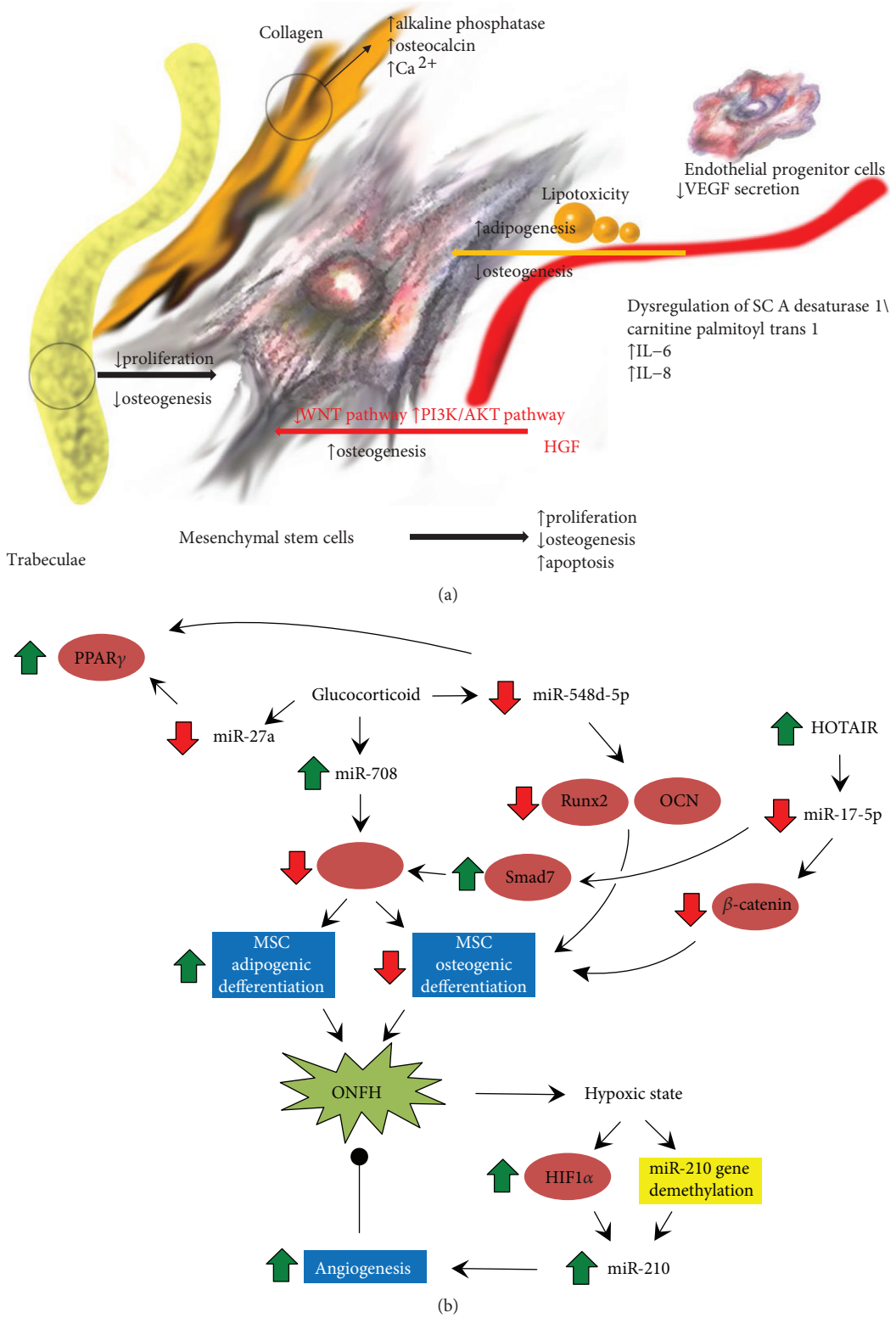

Figure 2: (a) Changes in proliferation and osteogenesis of stem cells in the area of osteonecrosis. (b) Five specific micro-RNAs play functional roles in femoral head necrosis. Figure adapted from ref. [103], John Wiley & Sons Publishers Ltd.

tissue available to extract stem cells is limited. In addition, the stem cell implantation approach will influence the therapeutic and adverse effects of ONFH.

Stem cells alone cannot work well in the advanced stage of ONFH. Carriers or scaffolds loaded with stem cells can provide mechanical support while delivering stem

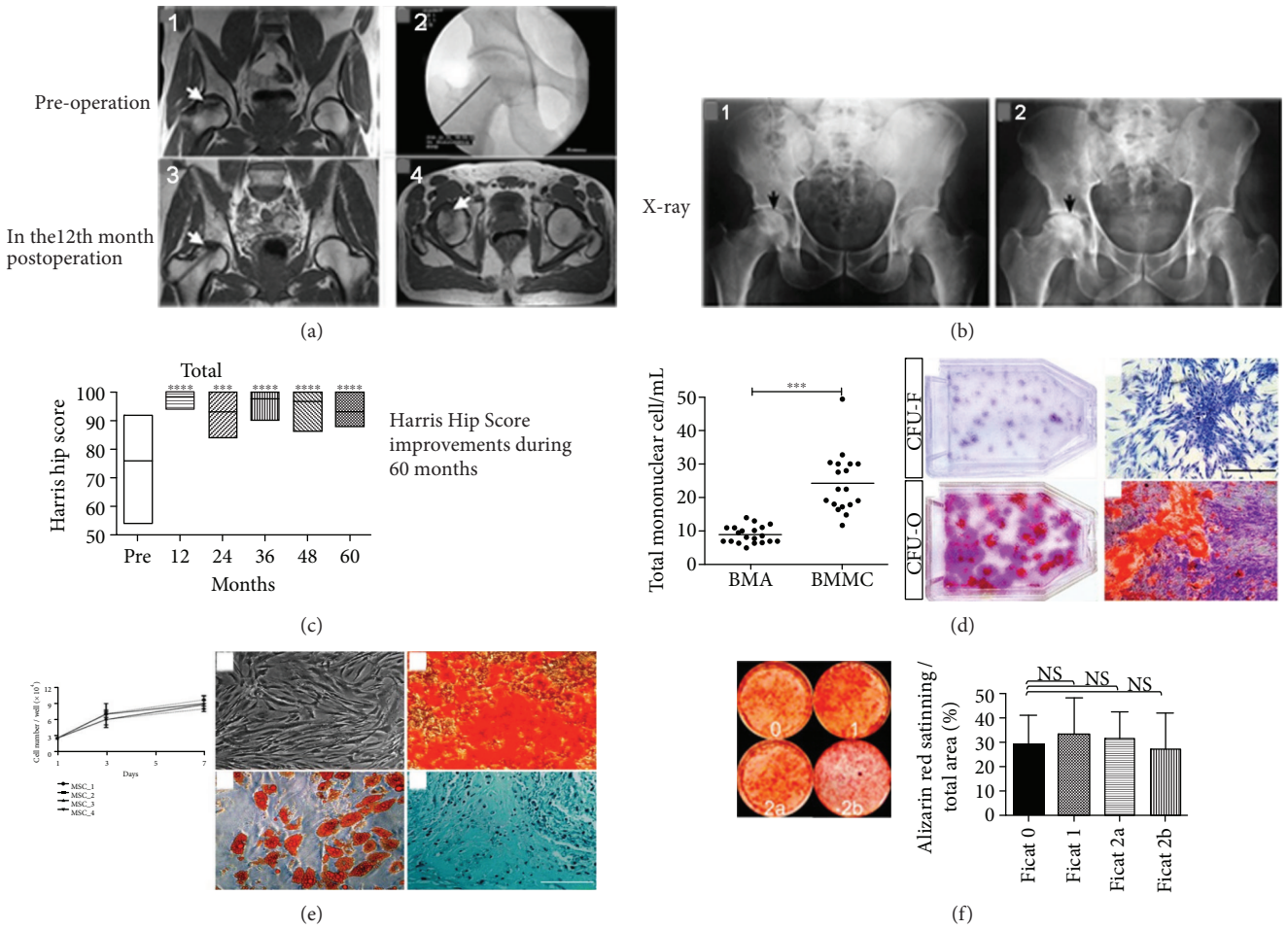

Figure 3: (a, 1) MRI T1-weighted (white arrow) suggests femoral head necrosis; (a, 2) X-ray guided minimally invasive decompression and implantation of MSC; (a, 3-4) MRI T1-weighted (12 months post-operation) shows femoral head edema decreased in the coronal plane (a, 3) and the axial plane (a, 4). (b, 1) Preoperative pelvic X-ray shows the necrosis zone; (b, 2) pelvic X-ray (60 months post-operation) shows the bone sclerosis band in the femoral head. (c) Harris Hip Score improvement with MSC therapy. (d) Concentrated MSC are of fibrogenic differentiation and osteogenic colony forming ability. (e) The proliferated MSC are of good differentiation potential of the three lineages. (f) The osteogenesis of MSC does not decline. Figure adapted from ref. [35].

cells to the necrosis zone. Better outcomes may be achieved by those methods.

Notably, the lack of control of cells following transplantation is another crucial issue in the biological-environmental field. One theory is that the implanted stem cells form new bones at the transplant site [40]. Another argument is that most of the stem cells do not differentiate into new osteoblasts, but play a regulation role by paracrine effects [41, 42]. Thus, the stem cell therapeutic process is expected to be monitored and the developments of cell tracing have skyrocketed in recent years. However, the large animal in vivo tracings are still limited by tracer properties (e.g., limited penetration depth of fluorescent dye, low sensitivity response of magnetic probe, or high biotoxicity). Safe, robust, and effective tracers are still underdeveloped [43, 44].

The risk of heterotopic ossification and tumor formation may be related to the choice of stem cell populations or subpopulations [45, 46]. Shimono et al. believed that mesenchymal stem cells with inhibited nuclear retinoic acid receptor-γ did not undergo heterotopic ossification [46]; the risk of tumor formation might be also reduced by selecting stem cell subpopulations without tumorigenicity [47, 48]. Therefore, the right choice of the subpopulation of stem cells may avoid these adverse effects.

The number of stem cells can influence the therapeutic effect [49]. The ability of stem cell proliferation can be enhanced by in vitro pretreatment [50], including transgene [51], drugs [52], and proliferation *in vitro* [53].

Compared to intravascular infusion [54, 55], the method of in situ cell suspension implantation via core decompression (CD) can overcome obstacles of insufficient cell number due to cell redistribution. CD can also remove the necrotic tissue which is bad for osteogenesis. All in all, CD appears to be more reliable in increasing cell seeding density without the redistribution in blood. Therefore, in situ injection or transplantation of therapeutic cells can significantly improve the therapeutic efficacy (Figure 3).

In the remainder of this section, we will discuss how multiscale stem cell technology addresses the four major limitations and the delivery of stem cells.

3.1. Cell-Based Therapy Strategy. The selection of cell population initializes the stem cell therapy. Proper pretreatments can effectively improve survivability, proliferation ability, and/or osteogenic capability of MSC.

3.1.1. Bone Marrow Stem Cells and Pretreatments. BMSC are the most common cell seeds in the treatment for ONFH. Many studies demonstrate the factors that influence osteogenic differentiation of BMSC to different degrees (e.g., growth factors, hormones, and small molecule drugs). HGF influences BMSC in a dose-dependent manner. The osteogenic differentiation of BMSC is promoted at a low concentration (20 ng/mL), by upregulated c-Met, p27, Runx2, and osterix, while BMSC are proliferated at a high concentration of HGF (100 ng/mL) by the overactivated ERK1/2 signaling pathway [29]. The granulocyte colony-stimulating factor and stem cell factor (G-CSF/SCF) promote the osteogenesis of BMSC and inhibit the caspase-3-dependent apoptosis [56]. P-glycoprotein (P-gp) alone or induced by icariin can alleviate oxidative stress of BMSC and promote osteogenesis [50, 57]. Lithium chloride (LiCl) promotes the osteogenesis of BMSC by inhibition on adipogenesis. The expression of PPARγ and fatty acid-binding protein 4 (Fabp4) presents antiadipogenic effects associated with upregulated β-catenin and downregulated phosphorylated GSK-3β at the Tyr-216 site [58]. The decreased VEGF-D expression may have disastrous consequences for vascularization, while VEGF-A or B expresses at a normal level in ONFH patients [59]. Vitamin E shows protective effects against apoptosis by downregulating caspase-3 expression and upregulating Bcl-2 expression [52]. Vitamin K2 antagonizes steroids and promotes bone formation and bone morphogenetic protein (BMP) expression [60].

The osteogenic potential of BMSC can be enhanced when transfected into the *Homo sapiens* forkhead box C2 (Foxc2) gene via lentivirus [61]. In view of the effects of HGF on proliferation and differentiation of BMSC [29], BMSC transfected by the HGF gene appear to be a promising candidate for ONFH treatment [62]. BMSC can be endowed with the secretion of VEGF following the delivery of the VEGF 165 gene into cells by Lipofectamine. Thus, BMSC have the dual ability to promote osteogenesis and angiogenesis [51]. Based on this idea, BMSC infected by adeno-associated virus loaded with the VEGF 165 gene, BMP-7 gene, and internal ribosome entry site present enhanced osteogenesis and angiogenesis [63–66]. The specific siRNA can silence PPARγ. The siRNA adenovirus vector can efficiently inhibit BMSC adipogenic differentiation induced by steroid, and BMSC retain their osteogenic potential by targeting PPARγ [67].

3.1.2. Preclinical and Clinical Trials. Intra-arterial or intravenous infusion of stem cells was declared as a safe and curative method for the ONFH [68]. Tong and his fellows performed the femoral circumflex arterial perfusion of autologous BMSC in canine models of ONFH established by the liquid nitrogen freezing method. The results showed that this strategy promoted vascular repair and angiogenesis, while VEGF mRNA and microvessel density (MVD) were significantly higher than the uninjected group. It is worth noting that the volume and cell number of the injected stem cell suspension are easily available (1 mL of the BMSC suspension contains 107 cells/mL) [69]. Cells cultured in two dishes of 60 mm diameter can reach the culture purpose. They subsequently reported a five-year follow-up clinical trial [68]. Their result showed that the femoral head collapse rate of patients in the Ficat I-II stage was low (3 of 68 hips failed, 4.41%), but that in Ficat III was high (3 of 10 hips failed, 30%). They believed that this method was a safe and effective minimally invasive treatment strategy for patients with early ONFH [68, 70].

Li et al. investigated the natural homing ability of BMSC in the necrosis of the femoral head via peripheral vein injection. The migration directions of fluorescently labeled BMSC are observed on the ONFH model of nude mice and rabbits, but the migration mechanism still requires further studies [54]. The therapeutic effect of this method is explored in rabbit ONFH models. The femoral head cut in the longitudinal direction shows that the ONFH necrotic area remained undeveloped in the BMSC group, while the control group shows a large amount of necrotic bone. X-ray and CT results show that there was no significant change in the BMSC group, while the trabecular bone fracture and articular surface collapse occurred in the control group. Masson staining indicates that the cartilage surface of the BMSC group is not significantly exfoliated, and the necrotic area is replaced by new bone, while the control group formed a large amount of fibrous connective tissue. Osteopontin (OPN) and core binding factor 1 (Cbfa1) in the BMSC group were higher than those in the control group. They believed that bone regeneration was initiated by at least two processes after BMSC transplantation: (a) the local secretion of cytokines or growth factors to promote angiogenesis and (b) BMSC directly generating new bone [55].

CD can provide channels for in situ implantation of stem cells, and hypoxic pretreatment is a simple and feasible MSC pretreatment method. Fan et al. [71] investigated that BMSC isolated from the ONFH rabbit anterior superior iliac spine were cultured at 20% and 2% oxygen concentrations, respectively. The two groups of BMSC were evaluated after BMSC were implanted into the femoral head of rabbits via CD. The apoptotic rate, cell viability, growth factor secretion, and capillary-like structure formation of BMSC at 2% oxygen concentration were as good as those of the normal BMSC and better than those at the 20% oxygen concentration. Ciapetti et al. [72] extracted BMSC from the anterior superior iliac spine of ONFH patients and cultured BMSC at 2% and 21% oxygen concentrations. The results show that the colony forming ability of BMSC exposed to hypoxia is enhanced, with increased expressions of bone-related genes (ALP, type I collagen, and osteocalcin) and normal mineralization, compared with those cultured at 21% oxygen concentration. However, there is an opposite opinion that CD with or without stem cells will not affect the therapy efficacy of ONFH according to the analysis of many preclinical and clinical trials [73].

BMSC pretreatments with the factors above are safe, although repeated treatment is not available. However, the effects are considered to be relatively mild. Meanwhile,

genetically modified cells stand out with strong and lasting interventions.

3.1.3. Adipose-Derived Stem Cells and Pretreatments. The disadvantages of BMSC cannot be ignored (e.g., low stem cell yield, painful extraction procedure, and surgery complications). ADSC have attracted attention from researchers due to their high yield. ADSC induced to osteogenic differentiation can enhance osteogenesis and promote vascularization in rabbit ONFH models [74]. W9 (a peptide) can block nuclear factor-κB ligand- (RANKL-) RANK signaling and enhance ADSC osteogenesis even under no osteogenic conditions [30]. VEGF 165 gene-modified ADSC also promote osteogenesis and angiogenesis [75] as well as VEGF 165-gene modified BMSC.

3.1.4. Preclinical and Clinical Trials. Abudusaimi et al. [76] implanted the ADSC into the tunnel via the CD in the rabbit ONFH models. CT of the ADSC group shows an increase in trabecular bone volume and density in the necrotic area. Immunohistochemistry results showed high osteocalcin in the ADSC group. Pak [77] reported a clinical trial of 2 cases via CD with ADSC. Clinical results show improvements in their pain visual analogue scale score, physical therapy tests, and Harris Hip Score. T1-weighted MRI shows that signal changes are consistent with medullary bone regeneration.

3.1.5. Other Stem Cells and Preclinical and Clinical Trials. The synovial fluid mesenchymal stem cells loaded on alginate beads have the potential of osteogenesis and differentiation. These implanted beads can help increase bone density and preserve the shape of the femoral head in rabbit ONFH models [31]. DPSC are considered to be safe cell seeds. The bone tissue restoration of DPSC therapy via CD in ovine ONFH models is better than that in heterologous MSC therapy when assessed by histological assessments [32]. Allogeneic peripheral blood-derived mesenchymal stem cells will upregulate BMP-2 expression and downregulate PPARγ expression in the osteonecrosis zone. Human umbilical cord-derived MSC therapy achieved good clinical outcomes in the treatment for ONFH by femoral artery injection according to the report of Chen et al. [34]. They used the oxygen delivery index (ODI) as a prognostic indicator for ONFH and provided the calculation method (ODI = hematocrit/SBV = $100H/1.4175 + 5.878H - 12.98H2 + 31.964H3$, where H stands for the volume fraction of erythrocytes and SBV stands for systolic blood viscosity). The indicator can be used to evaluate the oxygen transport status of the necrotic area and contribute to the ONFH assessment system to some extent. Aarvold et al. proposed the concept of SSC, although SSC was not confirmed at that time [78]. The location of SSC in the MSC differentiation pedigree was not known until Chan et al.'s [3] research on identification and characterization of SSC. Exosomes secreted by induced pluripotent stem cell-derived mesenchymal stem cells (IPSC) can reduce bone loss in the necrotic area and increase angiogenesis by activation of the PI3K/Akt signaling pathway on endothelial cells [79]. Cai et al. isolated and cultured autologous bone marrow mononuclear cells (BM-MNC) and allogeneic UCDMSC and injected mixed cell suspension by femoral artery angiography. This method presents an infusion time course of 30 minutes and a liquid volume of 90-130 mL, but no cell number. Treatment results showed that this method had a certain therapeutic effect but could not reverse the stage of ONFH patients [80].

In summary, stem cells alone with cytokines or genetic engineering techniques have not revolutionized the status of ONFH treatment. The focus is then shifted to the carriers and scaffolds.

The carriers and support scaffolds with stem cells should be manufactured with properties of osseointegration, biodegradation, and bony replacement. Lots of efforts have been made for improvements on the three properties above. We will describe the applications of carriers and scaffolds in ONFH therapies and assess their performance in the following sections (Figure 4).

3.2. Stem Cells on Carriers to the Necrosis Area of ONFH. Some natural properties of carriers are preserved (e.g., the microstructure that facilitates stem cell attachment, the support strength of natural trabecular bone, and the elastic modulus prone to bone growth) following the extraction and processing, including the demineralized bone matrix (DBM) [19, 81, 82], bisphosphonate carriers [83], xenograft bone substitute [84], bone-marrow buffy coat (BBC) [85], fibrin glue [86], and small intestine submucosa (SIS) matrix. These carriers have low immunogenicity and high histocompatibility.

BMSC modified with the BMP-2 gene and basic fibroblast growth factor (bFGF) gene loaded on DBM can repair the femoral head necrotic zone in canine models, resulting in the production of a large number of new bone, the regeneration of high-density new blood vessels, and the increase in compression and bending strength [82]. Stem cells via CD have also been widely used in clinical trials. CD and MSC implants with bisphosphonate carriers probably delayed the progression of femoral head collapse in a clinical trial of 8 cases [83]. In a long-term follow-up clinical trial of 38 patients with early ONFH, 33 patients are cured in clinical outcomes and imaging manifestations through implants (autologous MSC, xenograft bone substitute, and recombinant morphogenetic proteins) via CD [84]. BBC implantation via CD can effectively prevent progress of ONFH, relieve pain, and improve joint movements for patients assessed by the Lequesne Index and Western Ontario and McMaster Universities Arthritis Index (ClinicalTrials.gov identifier NCT01613612, registered 13 December 2011) [85]. Tabatabaee et al. [87] declared that BMSC implants via CD were only effective in the early stage of ONFH. MSC mixed with medical fibrin glue were delivered to the avascular necrosis area of the femoral head, which was performed by Wen et al. [86], and they achieved good outcomes. In a HGF transgenic cell research, the results show that the therapeutic effect of the HGF-gene transgenic MSC group was superior to that of the HGF-gene transgenic fibroblast group. This phenomenon suggests that the mechanism of MSC treatment for ONFH is more inclined to MSC osteogenic theory. Song et al. [88] implanted cancellous bone,

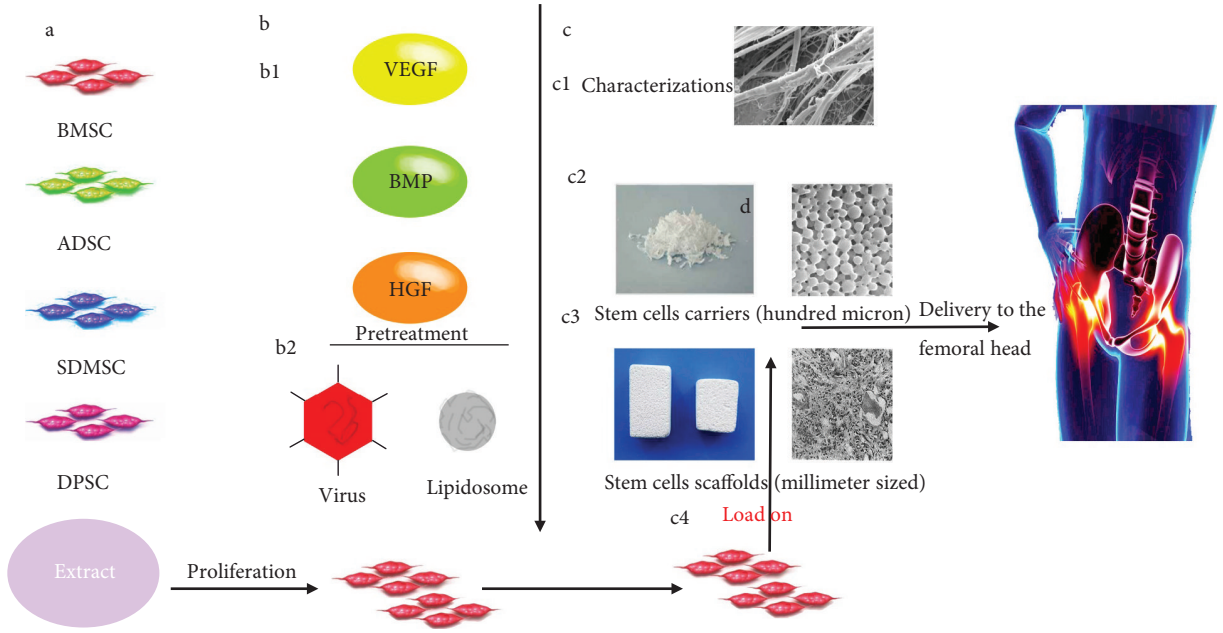

Figure 4: Schematic diagram of the manufacture and applications of stem cell carriers or scaffolds. (a) Stem cell population selection, extraction, and proliferation. (b) Stem cell pretreatment: (b1) the pretreatment of stem cells induced by cytokines and (b2) the pretreatment of transgenic stem cells. (c) Stem cells loaded on carriers or scaffolds: (c1) material characterization, (c2) stem cell carriers (hundred microns), (c3) stem cell scaffolds (millimeter-sized), and (c4) the pretreated stem cells loaded onto the carrier or scaffold. (d) Delivery of the stem cells loaded onto the carrier or scaffold to the femoral head necrosis area.

SIS, and BDMSC into the osteonecrosis area. Bone formation and angiogenesis of SIS and BDMSC are stronger than those of other combinations of interventions in the rabbit ONFH models. Better yet, this strategy has demonstrated no inflammatory cell infiltration.

In the advanced ONFH, stem cells without support scaffolds may not accomplish the treatment task. Thus, the support scaffolds appear to be particularly necessary.

3.3. Stem Cell Scaffolds Supporting the Femoral Head. Synthetic scaffolds are developed with spatial structure and mechanical support for ONFH therapies. Materials have been processed into scaffolds for ONFH therapies, including polylactide-co-glycolide acid (PLGA) biomimetic synthetic scaffolds [89], polylactide-co-glycolide acid and calcium phosphate (PLGA-CPC) microsphere [90] or scaffolds [91], porous tantalum rod implants [92, 93], strontium-doped calcium polyphosphate (SSCPP) [94], β-tricalcium phosphate (β-TCP) [95], and biphasic calcium phosphate (BCP) ceramic scaffolds [96].

Tantalum rods and BCP ceramic scaffolds are considered to be promising for clinical translation, owing to their good properties (e.g., high ultimate strength and Young's modulus, good osseointegration, optimal porosity, appropriate pore size, and material surface chemistry).

Mao et al. [97] injected peripheral blood stem cells (PBSC) into patients' medial circumflex femoral arteries and implanted porous tantalum (Figure 5(a)) into patients' femoral head in their clinical trial (36 months of follow-up). This method provides biomechanical support and is a safe and feasible choice for patients with early- and intermediate-stage ONFH, although 3 cases required THA (48 cases in total). Meanwhile, Zhao et al. implanted porous tantalum rods with BMSC into patients' femoral head necrotic zone for the end stage of ONFH, and 5 cases failed (31 cases in total) [92, 97].

The BCP ceramic scaffolds are manufactured based on the reconstructed bone trabecula data model of microcomputed tomography images (Figure 5(b)). Peng et al. implanted the scaffolds into the necrotic area of the femoral head in dog ONFH models. The results show that the osseointegration and new bone formation of scaffolds loaded with BMSC are significantly higher than those without BMSC. Higher-strength and compressive moduli have been tested out at the repair site in the BCP and BMSC groups [96].

Kang et al. [94] doped strontium into the calcium polyphosphate (CPP) scaffolds, as strontium can inhibit bone resorption [98, 99]. Autologous BM-MNC loading on this scaffold is implanted into the necrotic zone via CD in rabbit ONFH models. The levels of VEGF expression and osteogenesis are higher than those in the CPP group and bone grafting group. Better yet, its mechanical strength is not impaired following the implantation of the femoral head.

Tomoki Aoyama and his fellows [95] implanted autologous MSC mixed with β-TCP granules (OSferion; Olympus Terumo Biomaterials Co., Tokyo, Japan) into patients' femoral head necrotic zone via CD in a clinical trial (UMIN Clinical Trials Registry, UMIN000001601). Some young patients with extensive necrotic lesions with pain achieved symptom relief.

Zhang et al. [90] developed a novel calcium phosphate composite (CPC) scaffold, which was loaded on microspheres (BMP and VEGF loaded on poly-lactic-co-glycolic acid microspheres) and BMSC. The scaffold has excellent characteristics, including the porosity (62%), interconnected

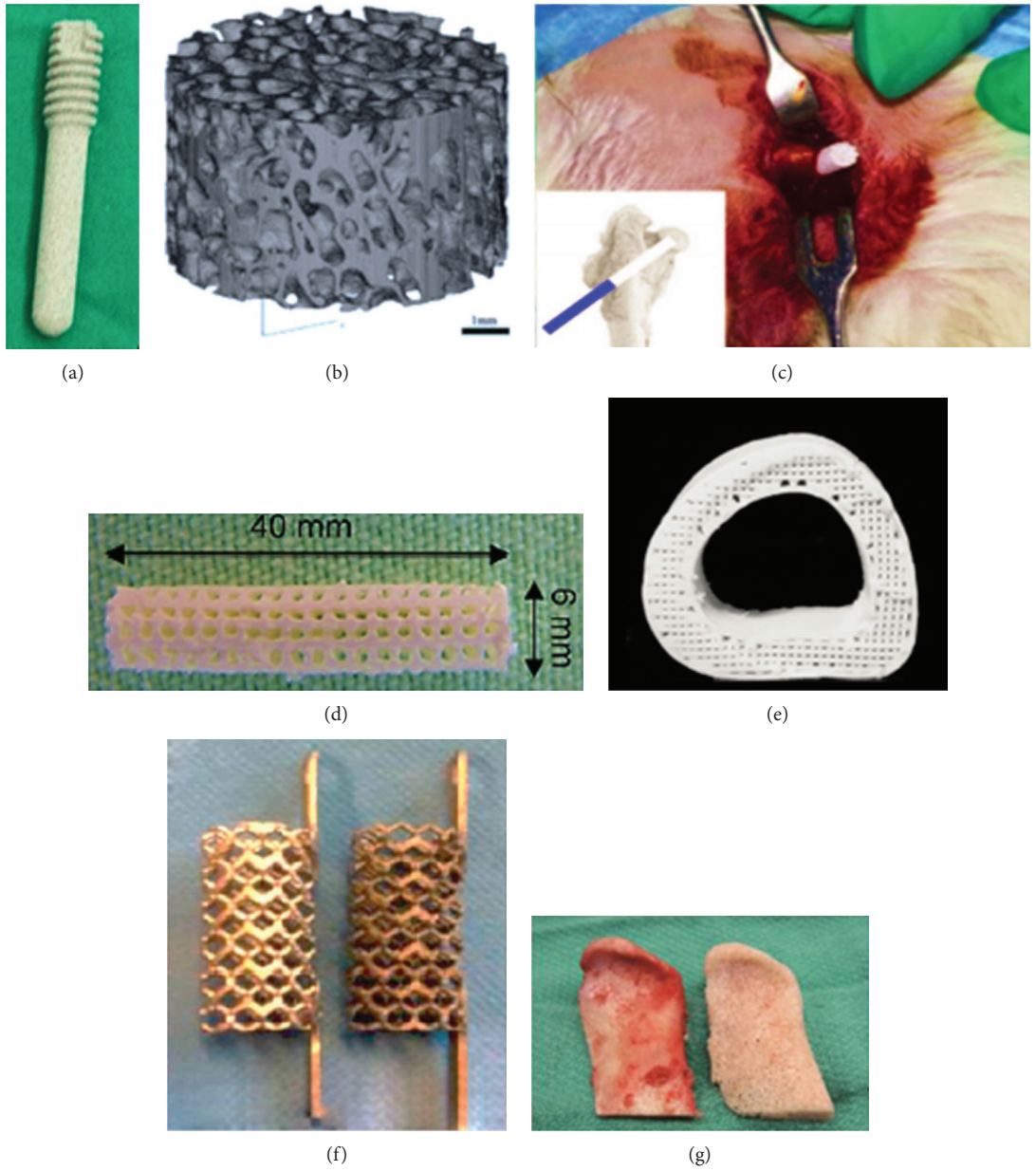

(a) (b) (c) (d) (e) (f) (g)

Figure 5: Stem cell scaffolds for ONFH treatment and other promising designs of stem cell scaffold designs. (a) The porous tantalum metal rod for supporting the necrosis of the femoral head. (b) The bone ceramic scaffold with similar dimensions as cancellous bone trabeculae (bar = 1 mm). Figure adapted from ref. [96], John Wiley & Sons Publishers Ltd. (c) The CPC scaffold loaded on microspheres (BMP and VEGF loaded on PLGA microspheres) and BMSC in the operation. Figure adapted from ref. [90], Elsevier Publishers Ltd. (d) 3D-printing PLGA/tricalcium scaffold with the polylactic acid-co-glycolic acid/tricalcium phosphate. Figure adapted from ref. [91], Elsevier Publishers Ltd. (e) Hyperelastic bone fabricated via 3D printing and liquid inks consisted of hydroxyapatite and polycaprolactone or PLGA. Figure adapted from ref. [100], The American Association for the Advancement of Science Publishers Ltd. (f) Low-elastic modulus titanium alloy 3D-printed mesh scaffold (more conducive to bone growth). Figure adapted from ref. [101], The American Association for the Advancement of Science Publishers Ltd. (g) Tissue engineered anatomical autologous bone scaffold used for facial reconstruction in high fidelity. Figure adapted from ref. [102], The American Association for the Advancement of Science Publishers Ltd.

porous structures, pore sizes (219 μm), and compressive strength (6.60 MPa). These characteristics are similar to the physiological trabecular bone and indicate the good biocompatibility and osteogenesis and angiogenesis of the scaffold (Figure 5(c)).

Qin et al. [91] developed a 3D-printed scaffold with polylactic acid-co-glycolic acid/tricalcium phosphate. This scaffold is loaded with icariin and implanted into the necrotic zone via CD in both quadruped and biped animal models (Figure 5(d)). The radiographic results, gait assessments, and finite element analyses show that this scaffold can reduce the incidence of collapse, promote new bone formation, and improve hip function recovery.

Although the current scaffolds exhibit a certain therapeutic effect, their structures and properties have not been deeply optimized to the level of competence. The

achievement of exact therapy efficacy for ONFH remains a challenge. The development of superior MSC scaffolds is a future goal in this field.

4. Conclusions and Challenges

This review outlined the emerging developments, strengths, and weaknesses of multiscale stem cell technology for ONFH from the perspective of clinicians and material developers, all of which offer significant opportunities to advance this field. We show that multiscale stem cell technology has great potential to delay ONFH progress and for bone regeneration.

Stem cell technology is rapidly evolving, and a large number of transgenic MSC for achieving specific function have been studied. The five microRNAs mentioned in Section 2 may be promising targets for improving stem cell activities. More attention should be paid to the genetic safety of stem cell subpopulations and transgenes. Strong expression of a specific factor may overly affect other normal tissues. The effects of small molecule drugs on the proliferation and differentiation of stem cells had been confirmed. However, the therapeutic cells used for ONFH are rarely investigated in this aspect. Small molecule drugs can be metabolized. Small molecule drugs appear more controllable for stem cell pretreatment and may be an alternative research direction for stem cell pretreatment for ONFH therapies in the future.

The field is rapidly evolving and has been steadily published in a variety of *in vitro* or *in vivo* animal studies or even clinical trials. However, successful goals of ONFH permanent cure via multiscale stem cell technologies are still difficult to achieve. ONFH is likely to be caused by multiple factors (e.g., ischemia, cell death, and bone resorption). The designs of carriers and scaffolds required considerations for these factors. We may draw on some design ideas from other promising methods of bone and joint regeneration materials. Besides the choice of the material types of scaffolds, the proportion of each component is a top priority in optimization. Optimizing the proportion of each component can balance the support strength and elastic modulus of the material. For example, a good bone replacement scaffold was produced by 3D printing with a surface structure suitable for stem cell growth and a good modulus for osseointegration [100] (Figure 5(e), hyperplastic "bone" designed and manufactured by Jakus et al.). In addition to the proportion of each component, we should pay more attention to the influence of the design structures of the scaffolds, thus reducing the heterogeneity on bone and joint regeneration [101] (Figure 5(f); Pobloth et al. believed that a soft titanium alloy stent grid bracket is more prone to bone growth).

The recent manufacture of tissue engineered autografts with low absorbance and high fidelity has shown very promising results in creating a new functional ball-mortar joint [102] (Figure 5(g); anatomical grafts for facial reconstruction developed by Bhumiratana et al.) Therefore, tissue engineering methods will catch our eyes in the future. The advantages of diverse technologies (3D printing technology, high-precision stereo computer numerical control engraving and stem cell technology, etc.) may be extracted and combined into a multiscale stem cell technology for tissue engineering of femoral head grafts or even the entire femoral head. Effective blood flow recanalization and bone replacement are also keys to ONFH treatment, so the establishment of the blood vessels' access to the necrotic area may result in better clinical outcomes. These design philosophies will be adopted by multiscale stem cell technologies for ONFH.

Last but not least, in order to accelerate breakthroughs in this area, funding for stem cell technology for ONFH treatment should be substantially increased. Compared to other hip treatment techniques (e.g., metal or ceramic prosthesis techniques), the femoral head necrosis stem cell technology lagged behind in breadth and depth. Its slow progress also reflects (at least in part) insufficiency in government/fund and investor investment. However, in the past few years, more funding opportunities have been created in the field of stem cell technology for ONFH treatment which has also become part of our review. We believe that multiscale stem cell technologies will revolutionize the current ONFH therapies in the foreseeable future.

Conflicts of Interest

The authors have no conflicts of interests to declare.

Authors' Contributions

Yi Wang and Xibo Ma contributed equally to this work.

Acknowledgments

Thanks are due to Jerry Yongqiang Chen for the English writing revision. This work was supported by the National Key Research Program of China under Grants 2016YFA0100900 and 2016YFA0100902; the National Natural Science Foundation of China under Grants 81772320, 81227901, 815270805, 61231004, 81471739, 81472594, and 81770781; the Key Research Program of the Chinese Academy of Sciences under Grant KGZD-EW-T03; the Scientific Research and Equipment Development Project of Chinese Academy of Sciences under Grant YZ201457; and the Beijing Natural Science Foundation (No. 7174314).

References

[1] W. L. Grayson, B. A. Bunnell, E. Martin, T. Frazier, B. P. Hung, and J. M. Gimble, "Stromal cells and stem cells in clinical bone regeneration," *Nature Reviews Endocrinology*, vol. 11, no. 3, pp. 140–150, 2015.

[2] C. G. Zalavras and J. R. Lieberman, "Osteonecrosis of the femoral head: evaluation and treatment," *The Journal of the American Academy of Orthopaedic Surgeons*, vol. 22, no. 7, pp. 455–464, 2014.

[3] C. K. F. Chan, G. S. Gulati, R. Sinha et al., "Identification of the human skeletal stem cell," *Cell*, vol. 175, no. 1, pp. 43–56.e21, 2018.

[4] P. Hernigou, M. Trousselier, F. Roubineau et al., "Stem cell therapy for the treatment of hip osteonecrosis: a 30-year review of progress," *Clinics in Orthopedic Surgery*, vol. 8, no. 1, pp. 1–8, 2016.

[5] L. Zhai, N. Sun, B. Zhang et al., "Effects of focused extracorporeal shock waves on bone marrow mesenchymal stem cells in patients with avascular necrosis of the femoral head," *Ultrasound in Medicine & Biology*, vol. 42, no. 3, pp. 753–762, 2016.

[6] S. G. Yan, L. Y. Huang, and X. Z. Cai, "Low-intensity pulsed ultrasound: a potential non-invasive therapy for femoral head osteonecrosis," *Medical Hypotheses*, vol. 76, no. 1, pp. 4–7, 2011.

[7] S. A. Lozano-Calderon, M. W. Colman, K. A. Raskin, F. J. Hornicek, and M. Gebhardt, "Use of bisphosphonates in orthopedic surgery: pearls and pitfalls," *The Orthopedic Clinics of North America*, vol. 45, no. 3, pp. 403–416, 2014.

[8] R. Klumpp and C. Trevisan, "Aseptic osteonecrosis of the hip in the adult: current evidence on conservative treatment," *Clinical Cases in Mineral and Bone Metabolism*, vol. 12, Supplement 1, pp. 39–42, 2015.

[9] F. A. Petrigliano and J. R. Lieberman, "Osteonecrosis of the hip: novel approaches to evaluation and treatment," *Clinical Orthopaedics and Related Research*, vol. 465, pp. 53–62, 2007.

[10] N. T. Dion, C. Bragdon, O. Muratoglu, and A. A. Freiberg, "Durability of highly cross-linked polyethylene in total hip and total knee arthroplasty," *Orthopedic Clinics of North America*, vol. 46, no. 3, pp. 321–327, 2015.

[11] A. J. Smith, P. Dieppe, P. W. Howard, and A. W. Blom, "Failure rates of metal-on-metal hip resurfacings: analysis of data from the National Joint Registry for England and Wales," *Lancet*, vol. 380, no. 9855, pp. 1759–1766, 2012.

[12] J. L. Del Pozo and R. Patel, "Infection associated with prosthetic joints," *New England Journal of Medicine*, vol. 361, no. 8, pp. 787–794, 2009.

[13] B. Ravi, D. Pincus, D. Wasserstein et al., "Association of overlapping surgery with increased risk for complications following hip surgery: a population-based, matched cohort study," *JAMA Internal Medicine*, vol. 178, no. 1, pp. 75–83, 2018.

[14] L. Rackwitz, L. Eden, S. Reppenhagen et al., "Stem cell- and growth factor-based regenerative therapies for avascular necrosis of the femoral head," *Stem Cell Research & Therapy*, vol. 3, no. 1, p. 7, 2012.

[15] J. M. Aldridge 3rd and J. R. Urbaniak, "Avascular necrosis of the femoral head: etiology, pathophysiology, classification, and current treatment guidelines," *American Journal of Orthopedics*, vol. 33, no. 7, pp. 327–332, 2004.

[16] M. T. Houdek, C. C. Wyles, J. R. Martin, and R. J. Sierra, "Stem cell treatment for avascular necrosis of the femoral head: current perspectives," *Stem Cells and Cloning: Advances and Applications*, vol. 7, pp. 65–70, 2014.

[17] M. T. Houdek, C. C. Wyles, B. D. Packard, A. Terzic, A. Behfar, and R. J. Sierra, "Decreased osteogenic activity of mesenchymal stem cells in patients with corticosteroid-induced osteonecrosis of the femoral head," *The Journal of Arthroplasty*, vol. 31, no. 4, pp. 893–898, 2016.

[18] M. Wang, Q. Liao, B. Zhou, Z. Q. Qiu, and L. M. Cheng, "Preliminary study of influence of bone tissue from osteonecrosis of femoral head on the proliferation and differentiation of canine bone marrow mesenchymal stem cells," *Zhonghua Yi Xue Za Zhi*, vol. 93, no. 11, pp. 856–859, 2013.

[19] B. Zhang, M. Y. Liu, and J. H. Zhao, "Osteoinductive activity of demineralized bone matrix and deprotenized bone derived from human avascular necrotic femoral head," *Chinese Journal of Traumatology*, vol. 12, no. 6, pp. 379–383, 2009.

[20] C. Chen, S. Yang, Y. Feng et al., "Impairment of two types of circulating endothelial progenitor cells in patients with glucocorticoid-induced avascular osteonecrosis of the femoral head," *Joint, Bone, Spine*, vol. 80, no. 1, pp. 70–76, 2013.

[21] C. Gillet, A. Dalla Valle, N. Gaspard et al., "Osteonecrosis of the femoral head: lipotoxicity exacerbation in MSC and modifications of the bone marrow fluid," *Endocrinology*, vol. 158, no. 3, pp. 490–502, 2017.

[22] Q. Wen, S. Zhang, X. Du et al., "The multiplicity of infection-dependent effects of recombinant adenovirus carrying HGF gene on the proliferation and osteogenic differentiation of human bone marrow mesenchymal stem cells," *International Journal of Molecular Sciences*, vol. 19, no. 3, 2018.

[23] C. Hao, S. Yang, W. Xu et al., "MiR-708 promotes steroid-induced osteonecrosis of femoral head, suppresses osteogenic differentiation by targeting SMAD3," *Scientific Reports*, vol. 6, no. 1, article 22599, 2016.

[24] H. F. Yuan, V. R. Christina, C. A. Guo, Y. W. Chu, R. H. Liu, and Z. Q. Yan, "Involvement of microRNA-210 demethylation in steroid-associated osteonecrosis of the femoral head," *Scientific Reports*, vol. 6, no. 1, article 20046, 2016.

[25] J. Sun, Y. Wang, Y. Li, and G. Zhao, "Downregulation of PPARγ by miR-548d-5p suppresses the adipogenic differentiation of human bone marrow mesenchymal stem cells and enhances their osteogenic potential," *Journal of Translational Medicine*, vol. 12, no. 1, p. 168, 2014.

[26] J. Jia, X. Feng, W. Xu et al., "MiR-17-5p modulates osteoblastic differentiation and cell proliferation by targeting SMAD7 in non-traumatic osteonecrosis," *Experimental & Molecular Medicine*, vol. 46, no. 7, article e107, 2014.

[27] J. Hu, Z. Wang, Y. Shan, Y. Pan, J. Ma, and L. Jia, "Long non-coding RNA HOTAIR promotes osteoarthritis progression via miR-17-5p/FUT2/β-catenin axis," *Cell Death & Disease*, vol. 9, no. 7, p. 711, 2018.

[28] C. Gu, Y. Xu, S. Zhang et al., "miR-27a attenuates adipogenesis and promotes osteogenesis in steroid-induced rat BMSCs by targeting PPARγ and GREM1," *Scientific Reports*, vol. 6, no. 1, article 38491, 2016.

[29] Q. Wen, L. Zhou, C. Zhou, M. Zhou, W. Luo, and L. Ma, "Change in hepatocyte growth factor concentration promote mesenchymal stem cell-mediated osteogenic regeneration," *Journal of Cellular and Molecular Medicine*, vol. 16, no. 6, pp. 1260–1273, 2012.

[30] Y. Otsuki, M. Ii, K. Moriwaki, M. Okada, K. Ueda, and M. Asahi, "W9 peptide enhanced osteogenic differentiation of human adipose-derived stem cells," *Biochemical and Biophysical Research Communications*, vol. 495, no. 1, pp. 904–910, 2018.

[31] Y. P. Chen, W. C. Chen, K. C. Wang, and C. H. Chen, "Effectiveness of synovial fluid mesenchymal stem cells embedded in alginate beads for treatment of steroid-induced avascular necrosis of the femoral head," *Journal of Orthopaedic Science*, vol. 19, no. 4, pp. 657–666, 2014.

[32] M. L. T. Feitosa, L. Fadel, P. C. B. Beltrão-Braga et al., "Successful transplant of mesenchymal stem cells in induced osteonecrosis of the ovine femoral head: preliminary results," *Acta Cirúrgica Brasileira*, vol. 25, no. 5, pp. 416–422, 2010.

[33] Q. Fu, N. N. Tang, Q. Zhang et al., "Preclinical study of cell therapy for osteonecrosis of the femoral head with allogenic peripheral blood-derived mesenchymal stem cells," *Yonsei Medical Journal*, vol. 57, no. 4, pp. 1006–1015, 2016.

[34] C. Chen, Z. Qu, X. Yin et al., "Efficacy of umbilical cord-derived mesenchymal stem cell-based therapy for osteonecrosis of the femoral head: a three-year follow-up study," *Molecular Medicine Reports*, vol. 14, no. 5, pp. 4209–4215, 2016.

[35] G. C. Daltro, V. Fortuna, E. S. de Souza et al., "Efficacy of autologous stem cell-based therapy for osteonecrosis of the femoral head in sickle cell disease: a five-year follow-up study," *Stem Cell Research & Therapy*, vol. 6, no. 1, p. 110, 2015.

[36] Q. Cui and E. A. Botchwey, "Emerging ideas: treatment of precollapse osteonecrosis using stem cells and growth factors," *Clinical Orthopaedics and Related Research*, vol. 469, no. 9, pp. 2665–9, 2011.

[37] A. Marsh, R. Schiffelers, F. Kuypers et al., "Microparticles as biomarkers of osteonecrosis of the hip in sickle cell disease," *British Journal of Haematology*, vol. 168, no. 1, pp. 135–138, 2015.

[38] J. A. Forsberg, T. A. Davis, E. A. Elster, and J. M. Gimble, "Burned to the bone," *Science Translational Medicine*, vol. 6, no. 255, article 255fs37, 2014.

[39] S. A. Mani, W. Guo, M. J. Liao et al., "The epithelial-mesenchymal transition generates cells with properties of stem cells," *Cell*, vol. 133, no. 4, pp. 704–715, 2008.

[40] H. S. Lee, G. T. Huang, H. Chiang et al., "Multipotential mesenchymal stem cells from femoral bone marrow near the site of osteonecrosis," *Stem Cells*, vol. 21, no. 2, pp. 190–199, 2003.

[41] C. Li, G. Li, M. Liu, T. Zhou, and H. Zhou, "Paracrine effect of inflammatory cytokine-activated bone marrow mesenchymal stem cells and its role in osteoblast function," *Journal of Bioscience and Bioengineering*, vol. 121, no. 2, pp. 213–219, 2016.

[42] A. Haumer, P. E. Bourgine, P. Occhetta, G. Born, R. Tasso, and I. Martin, "Delivery of cellular factors to regulate bone healing," *Advanced Drug Delivery Reviews*, vol. 129, pp. 285–294, 2018.

[43] Y. Liu, Y. Liu, C. Zheng et al., "Ru nanoparticles coated with γ-Fe_2O_3 promoting and monitoring the differentiation of human mesenchymal stem cells via MRI tracking," *Colloids and Surfaces B Biointerfaces*, vol. 170, pp. 701–711, 2018.

[44] J. Santelli, S. Lechevallier, H. Baaziz et al., "Multimodal gadolinium oxysulfide nanoparticles: a versatile contrast agent for mesenchymal stem cell labeling," *Nanoscale*, vol. 10, no. 35, pp. 16775–16786, 2018.

[45] Z. Yin, J. J. Hu, L. Yang et al., "Single-cell analysis reveals a $nestin^+$ tendon stem/progenitor cell population with strong tenogenic potentiality," *Science Advances*, vol. 2, no. 11, article e1600874, 2016.

[46] K. Shimono, W. E. Tung, C. Macolino et al., "Potent inhibition of heterotopic ossification by nuclear retinoic acid receptor-γ agonists," *Nature Medicine*, vol. 17, no. 4, pp. 454–460, 2011.

[47] C. Lu, S. U. Jain, D. Hoelper et al., "Histone H3K36 mutations promote sarcomagenesis through altered histone methylation landscape," *Science*, vol. 352, no. 6287, pp. 844–849, 2016.

[48] X. Lan, D. J. Jörg, F. M. G. Cavalli et al., "Fate mapping of human glioblastoma reveals an invariant stem cell hierarchy," *Nature*, vol. 549, no. 7671, pp. 227–232, 2017.

[49] P. Hernigou and F. Beaujean, "Treatment of osteonecrosis with autologous bone marrow grafting," *Clinical Orthopaedics and Related Research*, vol. 405, pp. 14–23, 2002.

[50] Z. B. Sun, J. W. Wang, H. Xiao et al., "Icariin may benefit the mesenchymal stem cells of patients with steroid-associated osteonecrosis by ABCB1-promoter demethylation: a preliminary study," *Osteoporosis International*, vol. 26, no. 1, pp. 187–197, 2015.

[51] D. Hang, Q. Wang, C. Guo, Z. Chen, and Z. Yan, "Treatment of osteonecrosis of the femoral head with VEGF165 transgenic bone marrow mesenchymal stem cells in mongrel dogs," *Cells Tissues Organs*, vol. 195, no. 6, pp. 495–506, 2012.

[52] Y. B. Jia, D. M. Jiang, Y. Z. Ren, Z. H. Liang, Z. Q. Zhao, and Y. X. Wang, "Inhibitory effects of vitamin E on osteocyte apoptosis and DNA oxidative damage in bone marrow hemopoietic cells at early stage of steroid-induced femoral head necrosis," *Molecular Medicine Reports*, vol. 15, no. 4, pp. 1585–1592, 2017.

[53] J. Leotot, A. Lebouvier, P. Hernigou, P. Bierling, H. Rouard, and N. Chevallier, "Bone-forming capacity and biodistribution of bone marrow-derived stromal cells directly loaded into scaffolds: a novel and easy approach for clinical application of bone regeneration," *Cell Transplantation*, vol. 24, no. 10, pp. 1945–1955, 2015.

[54] Z. H. Li, W. Liao, X. L. Cui et al., "Intravenous transplantation of allogeneic bone marrow mesenchymal stem cells and its directional migration to the necrotic femoral head," *International Journal of Medical Sciences*, vol. 8, no. 1, pp. 74–83, 2011.

[55] Z. Li, W. Liao, Q. Zhao et al., "Angiogenesis and bone regeneration by allogeneic mesenchymal stem cell intravenous transplantation in rabbit model of avascular necrotic femoral head," *The Journal of Surgical Research*, vol. 183, no. 1, pp. 193–203, 2013.

[56] X. Wu, S. Yang, H. Wang et al., "G-CSF/SCF exert beneficial effects via anti-apoptosis in rabbits with steroid-associated osteonecrosis," *Experimental and Molecular Pathology*, vol. 94, no. 1, pp. 247–254, 2013.

[57] N. Han, Z. Li, Z. Cai, Z. Yan, Y. Hua, and C. Xu, "P-glycoprotein overexpression in bone marrow-derived multipotent stromal cells decreases the risk of steroid-induced osteonecrosis in the femoral head," *Journal of Cellular and Molecular Medicine*, vol. 20, no. 11, pp. 2173–2182, 2016.

[58] Z. Yu, L. Fan, J. Li, Z. Ge, X. Dang, and K. Wang, "Lithium chloride attenuates the abnormal osteogenic/adipogenic differentiation of bone marrow-derived mesenchymal stem cells obtained from rats with steroid-related osteonecrosis by activating the β-catenin pathway," *International Journal of Molecular Medicine*, vol. 36, no. 5, pp. 1264–1272, 2015.

[59] F. Mwale, H. Wang, A. J. Johnson, M. A. Mont, and J. Antoniou, "Abnormal vascular endothelial growth factor expression in mesenchymal stem cells from both osteonecrotic and osteoarthritic hips," *Bulletin of the NYU Hospital for Joint Diseases*, vol. 69, Supplement 1, pp. S56–861, 2011.

[60] Y. L. Zhang, J. H. Yin, H. Ding, W. Zhang, C. Q. Zhang, and Y. S. Gao, "Vitamin K2 prevents glucocorticoid-induced osteonecrosis of the femoral head in rats," *International Journal of Biological Sciences*, vol. 12, no. 4, pp. 347–358, 2016.

[61] W. You, K. Wang, D. Duan, C. Wang, L. Fan, and R. Liu, "Construction of lentiviral vector containing Homo sapiens forkhead box C2 gene and its expression in bone marrow mesenchymal stem cells of rabbits," *Zhongguo Xiu Fu Chong Jian Wai Ke Za Zhi*, vol. 27, no. 5, pp. 535–540, 2013.

[62] Q. Wen, D. Jin, C. Y. Zhou, M. Q. Zhou, W. Luo, and L. Ma, "HGF-transgenic MSCs can improve the effects of tissue self-repair in a rabbit model of traumatic osteonecrosis of the femoral head," *PLoS One*, vol. 7, no. 5, article e37503, 2012.

[63] C. Zhang, Q. Ma, H. Qiang, M. Li, X. Dang, and K. Wang, "Study on effect of recombinant adeno-associated virus vector co-expressing human vascular endothelial growth factor 165 and human bone morphogenetic protein 7 genes on bone regeneration and angiopoiesis in vivo," *Zhongguo Xiu Fu Chong Jian Wai Ke Za Zhi*, vol. 24, no. 12, pp. 1449–1454, 2010.

[64] Z. B. Shi and K. Z. Wang, "Effects of recombinant adeno-associated viral vectors on angiopoiesis and osteogenesis in cultured rabbit bone marrow stem cells via co-expressing hVEGF and hBMP genes: a preliminary study in vitro," *Tissue & Cell*, vol. 42, no. 5, pp. 314–321, 2010.

[65] C. Zhang, K. Z. Wang, H. Qiang et al., "Angiopoiesis and bone regeneration via co-expression of the hVEGF and hBMP genes from an adeno-associated viral vector in vitro and in vivo," *Acta Pharmacologica Sinica*, vol. 31, no. 7, pp. 821–830, 2010.

[66] B. Y. Liu and D. W. Zhao, "Treatment for osteonecrosis of femoral head by hVEGF-165 gene modified marrow stromal stem cells under arthroscope," *Zhonghua Yi Xue Za Zhi*, vol. 89, no. 37, pp. 2629–2633, 2009.

[67] Y. Wang, J. Li, M. Liu, G. Zhao, L. Hao, and Y. Li, "Inhibition of peroxisome proliferator-activated receptor-γ in steroid-induced adipogenic differentiation of the bone marrow mesenchymal stem cells of rabbit using small interference RNA," *Chinese Medical Journal*, vol. 127, no. 1, pp. 130–136, 2014.

[68] Q. Mao, H. Jin, F. Liao, L. Xiao, D. Chen, and P. Tong, "The efficacy of targeted intraarterial delivery of concentrated autologous bone marrow containing mononuclear cells in the treatment of osteonecrosis of the femoral head: a five year follow-up study," *Bone*, vol. 57, no. 2, pp. 509–516, 2013.

[69] H. Jin, B. Xia, N. Yu et al., "The effects of autologous bone marrow mesenchymal stem cell arterial perfusion on vascular repair and angiogenesis in osteonecrosis of the femoral head in dogs," *International Orthopaedics*, vol. 36, no. 12, pp. 2589–2596, 2012.

[70] P. J. Tong, F. S. Ye, S. X. Zhang, J. Li, and L. Xin-Qi, "Treatment of non-traumatic femoral head avascular necrosis by perfusion of bone marrow stromal stem cells through optional artery," *Zhongguo Gu Shang*, vol. 27, no. 7, pp. 565–569, 2014.

[71] L. Fan, C. Zhang, Z. Yu, Z. Shi, X. Dang, and K. Wang, "Transplantation of hypoxia preconditioned bone marrow mesenchymal stem cells enhances angiogenesis and osteogenesis in rabbit femoral head osteonecrosis," *Bone*, vol. 81, pp. 544–553, 2015.

[72] G. Ciapetti, D. Granchi, C. Fotia et al., "Effects of hypoxia on osteogenic differentiation of mesenchymal stromal cells used as a cell therapy for avascular necrosis of the femoral head," *Cytotherapy*, vol. 18, no. 9, pp. 1087–1099, 2016.

[73] Y. W. Lim, Y. S. Kim, J. W. Lee, and S. Y. Kwon, "Stem cell implantation for osteonecrosis of the femoral head," *Experimental & Molecular Medicine*, vol. 45, no. 11, article e61, 2013.

[74] A. Aimaiti, Y. Saiwulaiti, M. Saiyiti, Y. H. Wang, L. Cui, and A. Yusufu, "Therapeutic effect of osteogenically induced adipose derived stem cells on vascular deprivation-induced osteonecrosis of the femoral head in rabbits," *Chinese Journal of Traumatology*, vol. 14, no. 4, pp. 215–220, 2011.

[75] H. J. Wang, B. Cai, X. Y. Zhao et al., "Repairing diabetic rats with bone defect by VEGF165 gene modified adipose-derived stem cells," *Zhongguo Gu Shang*, vol. 30, no. 6, 6, pp. 545–551, 2017.

[76] A. Abudusaimi, Y. Aihemaitijiang, Y. H. Wang, L. Cui, S. Maimaitiming, and M. Abulikemu, "Adipose-derived stem cells enhance bone regeneration in vascular necrosis of the femoral head in the rabbit," *The Journal of International Medical Research*, vol. 39, no. 5, pp. 1852–1860, 2011.

[77] J. Pak, "Autologous adipose tissue-derived stem cells induce persistent bone-like tissue in osteonecrotic femoral heads," *Pain Physician*, vol. 15, no. 1, pp. 75–85, 2012.

[78] A. Aarvold, J. O. Smith, E. R. Tayton et al., "A tissue engineering strategy for the treatment of avascular necrosis of the femoral head," *The Surgeon*, vol. 11, no. 6, pp. 319–325, 2013.

[79] X. Liu, Q. Li, X. Niu et al., "Exosomes secreted from human-induced pluripotent stem cell-derived mesenchymal stem cells prevent osteonecrosis of the femoral head by promoting angiogenesis," *International Journal of Biological Sciences*, vol. 13, no. 2, pp. 232–244, 2017.

[80] J. Cai, Z. Wu, L. Huang et al., "Cotransplantation of bone marrow mononuclear cells and umbilical cord mesenchymal stem cells in avascular necrosis of the femoral head," *Transplantation Proceedings*, vol. 46, no. 1, pp. 151–155, 2014.

[81] R. Velez, A. Hernández-Fernández, M. Caminal et al., "Treatment of femoral head osteonecrosis with advanced cell therapy in sheep," *Archives of Orthopaedic and Trauma Surgery*, vol. 132, no. 11, pp. 1611–1618, 2012.

[82] W. X. Peng and L. Wang, "Adenovirus-mediated expression of BMP-2 and BFGF in bone marrow mesenchymal stem cells combined with demineralized bone matrix for repair of femoral head osteonecrosis in beagle dogs," *Cellular Physiology and Biochemistry*, vol. 43, no. 4, pp. 1648–1662, 2017.

[83] A. L. Gianakos, J. Moya-Angeler, S. Duggal et al., "The efficacy of bisphosphonates with core decompression and mesenchymal stem cells compared with bisphosphonates alone in the treatment of osteonecrosis of the hip: a retrospective study," *HSS Journal*, vol. 12, no. 2, pp. 137–144, 2016.

[84] G. M. Calori, E. Mazza, M. Colombo, S. Mazzola, G. V. Mineo, and P. V. Giannoudis, "Treatment of AVN using the induction chamber technique and a biological-based approach: indications and clinical results," *Injury*, vol. 45, no. 2, pp. 369–373, 2014.

[85] Y. Ma, T. Wang, J. Liao et al., "Efficacy of autologous bone marrow buffy coat grafting combined with core decompression in patients with avascular necrosis of femoral head: a prospective, double-blinded, randomized, controlled study," *Stem Cell Research & Therapy*, vol. 5, no. 5, p. 115, 2014.

[86] Q. Wen, C. Zhou, W. Luo, M. Zhou, and L. Ma, "Pro-osteogenic effects of fibrin glue in treatment of avascular necrosis of the femoral head *in vivo* by hepatocyte growth factor-transgenic mesenchymal stem cells," *Journal of Translational Medicine*, vol. 12, no. 1, p. 114, 2014.

[87] R. M. Tabatabaee, S. Saberi, J. Parvizi, S. M. J. Mortazavi, and M. Farzan, "Combining concentrated autologous bone marrow stem cells injection with core decompression improves outcome for patients with early-stage osteonecrosis of the femoral head: a comparative study," *The Journal of Arthroplasty*, vol. 30, no. 9, pp. 11–15, 2015.

[88] H. J. Song, B. S. Lan, B. Cheng et al., "Treatment of early avascular necrosis of femoral head by small intestinal submucosal matrix with peripheral blood stem cells," *Transplantation Proceedings*, vol. 43, no. 5, pp. 2027–2032, 2011.

[89] H. Liao, Z. Zhong, Z. Liu, L. Li, Z. Ling, and X. Zou, "Bone mesenchymal stem cells co-expressing VEGF and BMP-6 genes to combat avascular necrosis of the femoral head," *Experimental and Therapeutic Medicine*, vol. 15, no. 1, pp. 954–962, 2018.

[90] H. X. Zhang, X. P. Zhang, G. Y. Xiao et al., "In vitro and in vivo evaluation of calcium phosphate composite scaffolds containing BMP-VEGF loaded PLGA microspheres for the treatment of avascular necrosis of the femoral head," *Materials Science & Engineering. C, Materials for Biological Applications*, vol. 60, pp. 298–307, 2016.

[91] L. Qin, D. Yao, L. Zheng et al., "Phytomolecule icaritin incorporated PLGA/TCP scaffold for steroid-associated osteonecrosis: proof-of-concept for prevention of hip joint collapse in bipedal emus and mechanistic study in quadrupedal rabbits," *Biomaterials*, vol. 59, pp. 125–143, 2015.

[92] D. Zhao, B. Liu, B. Wang et al., "Autologous bone marrow mesenchymal stem cells associated with tantalum rod implantation and vascularized iliac grafting for the treatment of end-stage osteonecrosis of the femoral head," *BioMed Research International*, vol. 2015, Article ID 240506, 9 pages, 2015.

[93] M. Xu and D. Peng, "Mesenchymal stem cells cultured on tantalum used in early-stage avascular necrosis of the femoral head," *Medical Hypotheses*, vol. 76, no. 2, pp. 199-200, 2011.

[94] P. Kang, X. Xie, Z. Tan et al., "Repairing defect and preventing collapse of femoral head in a steroid-induced osteonecrotic of femoral head animal model using strontium-doped calcium polyphosphate combined BM-MNCs," *Journal of Materials Science: Materials in Medicine*, vol. 26, no. 2, p. 80, 2015.

[95] T. Aoyama, K. Goto, R. Kakinoki et al., "An exploratory clinical trial for idiopathic osteonecrosis of femoral head by cultured autologous multipotent mesenchymal stromal cells augmented with vascularized bone grafts," *Tissue Engineering. Part B, Reviews*, vol. 20, no. 4, pp. 233–242, 2014.

[96] J. Peng, C. Wen, A. Wang et al., "Micro-CT-based bone ceramic scaffolding and its performance after seeding with mesenchymal stem cells for repair of load-bearing bone defect in canine femoral head," *Journal of Biomedical Materials Research. Part B, Applied Biomaterials*, vol. 96B, no. 2, pp. 316–325, 2011.

[97] Q. Mao, W. Wang, T. Xu et al., "Combination treatment of biomechanical support and targeted intra-arterial infusion of peripheral blood stem cells mobilized by granulocyte-colony stimulating factor for the osteonecrosis of the femoral head: a randomized controlled clinical trial," *Journal of Bone and Mineral Research*, vol. 30, no. 4, pp. 647–656, 2015.

[98] Y. Li, J. Li, S. Zhu et al., "Effects of strontium on proliferation and differentiation of rat bone marrow mesenchymal stem cells," *Biochemical and Biophysical Research Communications*, vol. 418, no. 4, pp. 725–730, 2012.

[99] Y. W. Chen, T. Feng, G. Q. Shi et al., "Interaction of endothelial cells with biodegradable strontium-doped calcium polyphosphate for bone tissue engineering," *Applied Surface Science*, vol. 255, no. 2, pp. 331–335, 2008.

[100] A. E. Jakus, A. L. Rutz, S. W. Jordan et al., "Hyperelastic "bone": a highly versatile, growth factor-free, osteoregenerative, scalable, and surgically friendly biomaterial," *Science Translational Medicine*, vol. 8, no. 358, p. 358ra127, 2016.

[101] A. M. Pobloth, S. Checa, H. Razi et al., "Mechanobiologically optimized 3D titanium-mesh scaffolds enhance bone regeneration in critical segmental defects in sheep," *Science Translational Medicine*, vol. 10, no. 423, p. eaam8828, 2018.

[102] S. Bhumiratana, J. C. Bernhard, D. M. Alfi et al., "Tissue-engineered autologous grafts for facial bone reconstruction," *Science Translational Medicine*, vol. 8, no. 343, article 343ra83, 2016.

[103] Z. Li, B. Yang, X. Weng, G. Tse, M. T. V. Chan, and W. K. K. Wu, "Emerging roles of microRNAs in osteonecrosis of the femoral head," *Cell Proliferation*, vol. 51, no. 1, 2018.

Hindawi
Stem Cells International
Volume 2018, Article ID 7412304, 11 pages
https://doi.org/10.1155/2018/7412304

Review Article

Intervertebral Disc-Derived Stem/Progenitor Cells as a Promising Cell Source for Intervertebral Disc Regeneration

Binwu Hu,[1] Ruijun He,[1] Kaige Ma,[1] Zhe Wang,[1] Min Cui,[1] Hongzhi Hu,[1] Saroj Rai,[1,2] Baichuan Wang,[1] and Zengwu Shao[1]

[1]*Department of Orthopaedics, Union Hospital, Tongji Medical College, Huazhong University of Science and Technology, Wuhan 430022, China*
[2]*National Trauma Center, National Academy of Medical Sciences, Kathmandu, Nepal*

Correspondence should be addressed to Baichuan Wang; wangbaichuan-112@163.com and Zengwu Shao; szwpro@163.com

Received 24 May 2018; Revised 18 October 2018; Accepted 5 November 2018; Published 18 December 2018

Academic Editor: Frederic Deschaseaux

Intervertebral disc (IVD) degeneration is considered to be the primary reason for low back pain. Despite remarkable improvements in both pharmacological and surgical management of IVD degeneration (IVDD), therapeutic effects are still unsatisfactory. It is because of the fact that these therapies are mainly focused on alleviating the symptoms rather than treating the underlying cause or restoring the structure and biomechanical function of the IVD. Accumulating evidence has revealed that the endogenous stem/progenitor cells exist in the IVD, and these cells might be a promising cell source in the regeneration of degenerated IVD. However, the biological characteristics and potential application of IVD-derived stem/progenitor cells (IVDSCs) have yet to be investigated in detail. In this review, the authors aim to perform a review to systematically discuss (1) the isolation, surface markers, classification, and biological characteristics of IVDSCs; (2) the aging- and degeneration-related changes of IVDSCs and the influences of IVD microenvironment on IVDSCs; and (3) the potential for IVDSCs to promote regeneration of degenerated IVD. The authors believe that this review exclusively address the current understanding of IVDSCs and provide a novel approach for the IVD regeneration.

1. Introduction

Low back pain (LBP) is one of the most common musculoskeletal disorders causing a tremendous socioeconomic burden to the patients due to lost productivity and increasing health care costs [1–3]. Although numerous and complex causes are involved in the pathogenesis of LBP, the intervertebral disc (IVD) degeneration appears to be the foremost cause [4, 5]. However, established treatments of IVD degeneration (IVDD), including medical and surgical treatments, are mainly focused on alleviating the symptoms rather than treating the underlying cause or restoring the structure and biomechanical function of the IVD [6–8].

The loss of disc cell viability and functionality plays a critical role in disturbing disc homeostasis, which reduces biosynthesis of extracellular matrix (ECM) components and triggers the IVDD [9, 10]. Therefore, cell-based therapy and regenerative medicine aiming at restraining or even reverting the loss of disc cell number and function have attracted much attention in the field of IVD regeneration [11]. Currently, a number of therapeutic modalities, such as growth factor supply, gene therapy and the delivery of functional cells, have been developed in order to rescue the disc cells [12–15]. Of these, the delivery of functional cells is, possibly, a promising therapeutic strategy. Many different kinds of functional cells from different areas of the body, i.e., nucleus pulposus cells (NPCs), bone marrow mesenchymal stem cells (BMSCs), adipose stem cells (ASCs), muscle-derived stem cells, synovial stem cells, induced pluripotent stem cells, olfactory neural stem cells, hematopoietic stem cells, and embryonic stem cells, can be successfully transplanted into the IVD with a hope to repair or regenerate the IVD [16]. Owing to wide availability and multilineage differentiation potential, the stem cells (SCs) have been extensively used and have shown

a promising result in animal models and clinical trials [17, 18]. However, some obstacles are always hindering the further application of SCs in disc regeneration. These problems include puncture injury during SC extraction from the tissues and formation of osteophytes in the degenerated disc due to the leakage of SCs [19, 20]. Moreover, the microenvironment of IVD is characterized by excessive mechanical loading, high osmolarity, limited nutrition, acidic pH, and low oxygen tension [21–23]. Such microenvironment might impair the viability, proliferation, and ECM biosynthesis abilities of transplanted SCs leading to a limited repair potential [21–23]. Thus, it is desperately necessary to identify novel cell sources for IVD regeneration.

Many tissues have been identified to contain adult tissue-specific SCs, also known as endogenous SCs [24–26]. These endogenous SCs are capable of balancing the homeostasis of the tissues by regulating their own proliferation and differentiation. Therefore, endogenous stem/progenitor cells are regarded as a promising cell source for regenerating tissues because of the potential of overcoming the obstacles related to cell transplantation [24]. The IVD is the largest avascular structure in the body, which has been previously thought to have a little or poor self-repair capacity in adult mammals [27]. Nevertheless, many previous studies have indicated that the resident SCs exist both in normal and degenerated IVD and are referred to as IVD-derived stem/progenitor cells (IVDSCs) [28–31]. These cells can be isolated from different compartments of IVD, including nucleus pulposus (NP), annulus fibrosus (AF), and cartilage endplate (CEP) and can express most of the phenotype markers that define MSCs [29, 32–36]. Furthermore, it is also proven that there exists SC niche (SCN) within the IVD, which is confined around the perichondrium region adjacent to the epiphyseal plate (EP) and outer zone of the AF [6, 27]. Thus, promoting self-repair via mobilizing the endogenous SCs might be a prospective approach for stem cell-based therapy and the IVD regeneration. However, as a novel cell subset in IVD, our knowledge about IVDSCs remains largely limited.

Therefore, authors aim to perform a review to systematically discuss (1) the isolation, surface markers, classification, and biological characteristics of IVDSCs; (2) the aging- and degeneration-related changes of IVDSCs and the influences of IVD microenvironment on IVDSCs; and (3) the potential for IVDSCs to promote regeneration of degenerated IVDSCs. The authors believe that this review exclusively addresses the current understanding of IVDSCs and provides a novel approach for the IVD regeneration.

2. Identification of IVDSCs

In 2007, Risbud et al. identified a cluster of cells in human degenerated IVD that express the surface markers of SCs and could perform adipogenic, osteogenic, and chondrogenic differentiation [28]. Similarly, other studies also detected the cells presenting similar characteristics in all components of human IVD including the AF, NP, CEP, and putative SCN [6, 30, 32, 36]. These cells could be classified into MSCs according to the criteria established by the International Society for Cellular Therapy (ISCT) (for example, the plastic-adherent growth; the expression of CD105, CD73, and CD90 and the lack of expression of CD45, CD34, CD14 or CD11b, CD79alpha or CD19, and HLA-DR surface molecules; and multilineage differentiation ability *in vitro*) [30, 32, 37, 38]. From these reports, we can conclude that the endogenous SCs, also called IVDSCs, definitely exist within IVD. It has been isolated, not only from the human being but also from many other species including murine, rhesus macaque, porcine, and rabbit [6, 31, 39–42].

3. Classification of IVDSCs

The normal IVD is composed of three distinct components: the central gelatinous NP, the outer AF, and the upper and lower CEP [43]. Based on the different anatomical regions of IVD, the IVDSCs are usually divided into three subsets, which are referred to as NP-derived stem cells (NPSCs), AF-derived stem cells (AFSCs), and CEP-derived stem cells (CESCs), respectively [28, 30, 36, 38]. Recently, some researchers propose the existence of SCN, a dynamic microenvironment consisting of the ECM and neighboring cells with the ability to regulate local SCs, within IVD [20, 27, 44]. Through a series of *in vivo* labeling procedures, the SCN is recognized as the perichondrium region adjacent to the EP and outer zone of the AF (Figure 1) [6, 20, 27]. Moreover, cells extracted from the SCN also meet the criteria defining MSCs [20]. Therefore, SCN-derived stem cells (SCNSCs) might be another classification of the IVDSCs [37].

However, classifying the IVDSCs into absolutely different four groups might not be completely reasonable when taking the sources of IVDSCs into account. Many researches have demonstrated that the SCs in SCN could migrate into the AF, NP, and CEP along certain routes [27, 44]. Our previous experiments also confirmed that the SCs in SCN could migrate into the inner part of IVD during the process of compression-induced IVD degeneration. Furthermore, results from Xiong et al. illustrated that the CESCs could migrate from CEP to NP tissue, and the migration could be inhibited by macrophage migration inhibitory factor [45]. In addition, the SCs might be infiltrated from growing vessels during disc degeneration, and adjacent bone marrow might also be the source in IVD [14, 46]. Despite the location of SCs in the different region, the SCNSCs, AFSCs, NPSCs, and CESCs possibly contain a proportion of cells having the same origin and biological characteristics. Hence, the SCs distributed in different anatomical regions of IVD are both independent and relevant. In Figure 1, we displayed the hypothetical distribution of IVDSCs according to different anatomic regions.

4. Isolation of IVDSCs

To date, many techniques have been developed to isolate stem/progenitor cells from different parts of the IVD. Generally speaking, most extraction methods are designed based on the distinct characteristics of SCs such as rapid proliferation rate, colony formation capacity, and unique surface markers [31, 38, 47, 48].

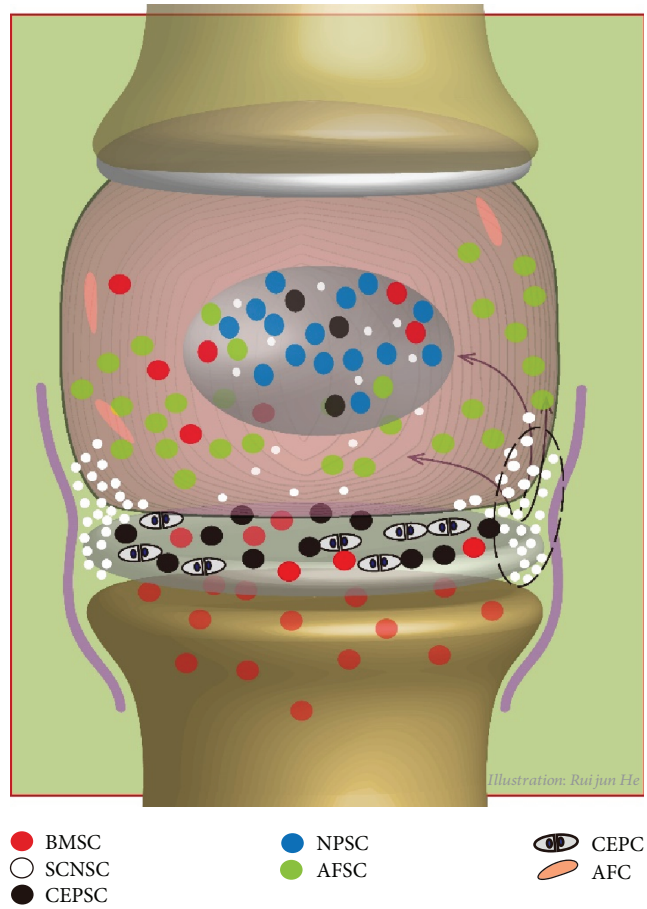

Figure 1: Schematic overview of the location of different kinds of IVDSCs. The stem cells located in IVD and the adjacent vertebras are indicated with dots. Elliptical broken line indicates the area of stem cell niche. The arrows indicate the possible migration pathways of SCNSCs. BMSC: bone marrow-derived stem cells; SCNSC: stem cell niche-derived stem cells; CESC: cartilage end plate-derived stem cells; NPSC: nucleus pulposus-derived stem cells; AFSC: annulus fibrosus-derived stem cells; CEPC: cartilage end plate cells. AFC: annulus fibrosus cells.

The SCs are characterized by their self-renew and rapid-proliferation capacity, which make them superior to other cells located in IVD in plastic-adherent and proliferation speed. Based on the above theory, differential adhesion method was developed to successfully isolate cells meeting the criteria of MSCs [47, 49, 50]. The main step of this method is to discard culture medium together with suspension cells and fragments when cell suspensions are seeded about 24 h later, and the remaining adherent cells are regarded as SCs without any further isolation [49]. Using this method, researchers have successfully isolated NPSCs from human and other species [11, 39, 47, 50, 51].

Colony formation is another important property of SCs. The cells with stem/progenitor cell characteristics survive at 50 cells/cm^2, while other types of cells die due to loss of cell-cell contacts or undergo dissolution because of the low proliferation velocity [52]. Thus, colony formation assay might be another way to separate IVDSCs. Using this method, also named as limiting dilution method, Liu et al. extracted AFSCs from rabbit AF tissue, and they found an initial seeding density of 200 cells/cm^2 to be optimal for the formation of colonies [33]. Similarly, rat NPSCs were also successfully isolated using this method [48]. For this method, the cell seeding density is the most critical because inappropriate cell density would cause the difficulty of colony formation or the failure of the SC extraction.

Some special culture medium is also utilized to isolate the IVDSCs. Agarose suspension culture is a chondrocyte selective culture system, in which chondrocytes are the only cell type to survive apart from tumor cells [48]. Employing the agarose culture system, the NPSC, AFSC, and CESC were all successfully isolated [32, 36, 38, 45, 53]. Methylcellulose semisolid medium, a culture system established to identify tissue-specific stem/progenitor cells from various organs, is also applied to extract the IVDSCs, and the NPSCs had been extracted through this method [31, 54]. In addition, some researchers including our group successfully extracted IVDSCs by using standard MSC expansion medium [55, 56].

Except for the above methods, the explant culture technique and fluorescence-activated cell sorter (FACS) cell sorting have also been developed to isolate IVDSCs [23, 31]. And some researchers even isolated IVDSCs directly by cell culture without any special treatment [30, 43, 57]. Besides that, some important points must be taken into consideration during the isolation of IVDSCs. Firstly, the blood cells must be thoroughly removed to avoid the

Table 1: Surface markers of IVDSCs.

Species	Cell type	Positive markers	Negative markers	References
Human	NPSC	CD73, CD90, and CD105	CD34, CD45	[47]
Human	NPSC	CD73, CD90, and CD105	CD34, CD45, and HLA-DR	[43, 55]
Rat	NPSC	CD44, CD90, and CD105	CD34, CD45	[50]
Human	NPSC	CD29, CD44, and CD105	CD14, CD34, CD45, and HLA-DR	[34]
Human	NPSC	Tie2,GD2, Flt1, and CD271	CD24	[31]
Mini pig	NPSC	CD29, CD90, and CD44	—	[42]
Rat	NPSC	CD73, CD90, and CD105	CD34, CD45	[40]
Human	NPSC	CD29, CD44, CD73, CD90, and CD105	CD29, CD44, CD73, CD90, and CD105	[23]
Human	NPSC	CD90, CD73, CD105, CD106, and CD166	CD14, CD19, CD24, CD34, CD45, and HLA-DR,	[29]
Human	NPSC	CD24, CD73, CD90, and CD105	CD29, CD45	[58]
Rhesus macaque	NPSC	CD44, CD90, CD146, CD166, and HLA-DR	CD90, CD271	[39]
Human	AFSC, NPSC	CD49a, CD63, CD73, CD90, CD105, CD166, p75 NTR, and CD133/1	CD34	[28]
Rhesus macaque	AFSC	CD44, CD90, CD146, CD166, and HLA-DR	CD29, CD106, and CD271	[39]
Human	AFSC	CD29, CD49e, CD51, CD73, CD90, CD105, CD166, CD184, nestin, and neuron-specific enolase	CD31, CD34, CD45, CD106, CD117, and CD133	[35]
Human	AFSC, NPSC, and CESC	CD73, CD90, and CD105	CD19, CD34, CD45, and HLA-DR	[38]
Human	CESC	CD73, CD90, and CD105	CD14, CD19, CD34, CD45, and HLA-DR	[45, 59, 60]
Human	CESC	CD73, CD90, CD105, and Stro-1	CD14, CD19, CD34, CD45, and HLA-DR	[36]
Human	CESC	CD44, CD73, CD90, CD105, CD133, CD166, and Stro-1	CD14. CD19, CD34, CD45, and HLA-DR	[32]
Rat	SCNSC	CD29, CD90, and CD44	CD19, CD34, CD45, and CD11b	[20]
Human	IVDSC	CD90, CD105, and Stro-1	—	[61]

contamination of SCs. Then, when isolating IVDSCs from human samples, the age and degeneration grade of patients must be taken into account, which might influence the quantity and quality of the IVDSCs [31]. So, the technique such as FACS cell sorting should be carried out to purify the IVDSCs meticulously.

5. Surface Marker of IVDSCs

The currently identified surface markers for IVDSCs are shown in Table 1. However, Sakai et al. demonstrated that some surface markers exist both in NP cells and NPSCs [31]. Thus, we must realize that the cells expressing these markers are not necessarily the IVDSCs. Therefore, it is quite exigent to explore the distinct surface markers of IVDSCs. From another aspect, the expression of surface markers is associated with functional status of the IVDSCs. For example, CD105 is related to cell migration, and the expression of Tie2 and GD2 indicates the differentiation of NPSCs [31, 32]. Additionally, the IVDSCs can express neural stem cell-associated surface markers. Some researchers have proven that AFSCs could perform neurogenesis differentiation and NPSCs could differentiate into Schwann-like cells [35, 54].

6. Biological Characteristics of IVDSCs

The biological characteristics of IVDSCs (given that the concept of SCNSCs is not received so far, we only discuss the NPSCs, AFSCs, and CESCs in this chapter) have been comprehensively explored. It has been displayed that all three kinds of IVDSCs share almost the same morphology and immunophenotype [30, 32, 34, 35, 38]. For proliferation capacity, Liang et al. demonstrated that NPSCs and AFSCs had stronger cell proliferation capacity than that of CESCs [30]. At the same time, results from Wang et al. exhibited that there was no significant difference in proliferation ability among NPSCs, AFSCs, and CESCs [38]. Additionally, for multilineage differentiation ability, Liang et al. concluded that the expression of different lineage differentiation-related genes of AFSCs was stronger than that of NPSCs and CESCs [30]. Wang et al. comprehensively compared the pluripotency of IVDSCs. They found that the osteogenic and chondrogenic capacities to be superior in CESCs

followed by AFSCs and NPSCs; similarly, the adipogenic capacity to be superior in NPSCs followed by CESCs and AFSCs. However, when cultured in alginate bead, the CESCs consistently showed superior chondrogenic potential when comparing with rest of the cell types [38]. It seems that IVDSCs isolated from different anatomical regions have different biological characteristics. This phenomenon might be ascribed to the special microenvironment of different IVD components [38]. Furthermore, for the discrepancy in biological properties of IVDSCs among the studies, we speculate that this might be associated with different isolation technique, passaging, and culture protocols [38].

The IVDSCs also contain some special features that are different from other SCs. The CESCs are reported to have better osteogenic and chondrogenic ability as compared to BMSCs, while the NPSCs that were isolated from degenerated NP tissue showed much lower adipogenic differentiation ability [29, 32]. Wu et al. demonstrated that compared to umbilical cord mesenchymal stem cells (UCMSCs), NPSCs isolated from degenerated IVD displayed impaired proliferation capability and differentiation potential [23]. Furthermore, when cultured in a disc mimicking microenvironment, the NPSCs are more resistant to hypoxic and acidic pH microenvironment as compared to ASCs, making NPSCs preferable cell sources for IVD regeneration [11, 51].

7. The Aging- and Degeneration-Related Changes of IVDSCs

It is a proven fact that the disc cells undergo a series of biologic changes as they become old and degenerated. These changes include alternation of cell type in NP, decrease in number of viable cells, and increase in cell senescence [9]. Similarly, aging and degeneration also alter the quantity and quality of IVDSCs. With the progression of aging and degeneration, the number of cells expressing stem/progenitor cell markers in IVD tissues decreases markedly, indicating the exhaustion of IVDSCs [31, 41]. In Zhao et al.'s report, the aged NPSCs demonstrated deteriorative capacities of proliferation, colony forming, and multilineage differentiation but had more senescent features [40]. For degeneration-related changes, previous studies have shown that the NPSCs derived from degenerated NP have impaired ability in colony formation, chemotactic migration, proliferation, and have less expression of stem cell markers and stemness genes [42, 43]. In addition, these NPSCs exhibit notably inferior chondrogenic differentiation ability [42]. Owing to these aging- and degeneration-related changes, the failure of endogenous repair of IVD is inevitable. Thus, preventing or even reverting the changes incurred by aging or degeneration will be of great necessity in recovering or promoting the endogenous repair of IVD.

The DNA damage, telomere shortening, oxidative stress, and disturbance of the intracellular homeostasis contribute to the initiation of IVDD by causing cell senescence and programmed cell death [62–65]. With aging and degeneration, the degradation of misfolded proteins and clearance of toxic cellular waste products are constrained, making it difficult to maintain the homeostasis and resulting in a presenescence state [66, 67]. When the presenescence SCs are in quiescence, their intrinsic homeostasis can still be maintained [68]. However, once the presenescence SCs is activated to exert the endogenous repair function, it is difficult to maintain normal physiological activities and then die [69]. Therefore, repair capability of these subhealthy SCs can be restored by restoration of the cellular homeostasis, where autophagy may play a significant role. Sousa-Victor et al. reversed senescence and restored the regenerative properties of old muscle satellite cells in an injury model by promoting autophagy [69]. Sousa-Victor et al. reported that rapamycin, an agonist of autophagy, had antisenescence effects on AFSCs but inhibited the differentiation of AFSCs under multilineage induction, thus maintaining the stemness [69]. However, appropriate differentiation of SCs is also vital to IVD regeneration. So, precise regulation of the autophagy is required in order to keep the SCs in the right direction towards tissue repair.

8. The Influences of IVD Microenvironment on IVDSCs

The SCs are enclosed in a tissue-specific microenvironment that significantly influences their biological and metabolic vitality. The special microenvironment of the IVD is characterized by low oxygen tension, excessive stress or strain, hypertonicity, low pH, and poor nutrient supply, which present challenges to the survival and the function of implanted or endogenous SCs [70].

One overriding characteristic of disc cells is that they are resided under conditions of hypoxia due to the lack of blood supply. Under hypoxia, the NPSCs exhibit better cell proliferation ability than ASCs, and its chondrogenic capacity is enhanced when compared to normoxic environment [51]. For CESCs, hypoxic precondition might weaken the differentiation in osteogenic induction, indicating the antimineralization effect of hypoxia [60]. Thus, physiological hypoxia may be beneficial to exert normal physiological functions of IVDSCs. However, during the process of degeneration, blood vessels might invade into IVD through the fissures, which might increase the oxygen levels and disrupt the physiological hypoxic microenvironment of the IVDSCs [71, 72]. Therefore, restoring the hypoxic microenvironment may favor IVDSC-based endogenous repair of IVD.

In addition to hypoxia, excessive mechanical loading is another crucial microenvironmental factor. The disc-specific biomechanical features have been shown to exert a wide range of impacts on the biological functions of IVDSCs. *In vitro* studies have demonstrated that cyclic tensile stress would induce apoptosis of CESCs via the BNIP3/Bcl-2 pathway, whereas static compression stress would induce mitochondrial apoptosis in NPSCs [56, 59]. Besides the induction of cell death, stress stimuli are also essential for the normal function of SCs [73–75]. For example, it has been proven that the proportion of ECM components synthesized by AFSCs changes with fluid shear stress [76]. These results indicate the double-edged sword effects of mechanical loading. Therefore, further studies should

focus on exploring various methods to protect IVDSCs from excessive mechanical loading-induced cell death and dysfunction. In the meanwhile, the biomimetic matrix would also be produced by optimizing mechanical stimulation for i*n vitro* cultured IVDSCs.

Moreover, hypertonicity, low pH, and poor nutrient supply are also important microenvironmental factors and are detrimental for implanted or endogenous SCs. The osmotic pressure of healthy NP, AF, and CEP (450~550 mOsm/L) is distinctly higher than the normal blood (280~320 mOsm/L) [77]. Nevertheless, the SC-related researches taking high osmolarities into consideration are still scarce. Tao et al. pioneered the investigation regarding the influence of osmotic pressure on IVDSCs [49]. They found that high osmolarity could decrease the viability, proliferation, and expression levels of SOX-9, aggrecan, and collagen II in NPSCs [49]. Regarding the influences of low pH, Han et al. compared ASCs with NPSCs which were cultured in an acidic environment [11]. They found NPSCs to be less inhibited in proliferation and cell viability [11]. Liu et al. further illuminated that in NPSCs, the acid-sensing ion channel (ASIC) plays an important role in acid-induced apoptosis and the downregulation in stem cell-related genes and ECM synthesis [55]. Furthermore, it was also demonstrated that the nutrition deficiency could cause mitochondrial translocation of BNIP3 in CESCs, leading to caspase-dependent apoptosis [78].

9. The Influences of ECM on IVDSCs

With the degeneration of IVD, the cell clustering and cell death make it more difficult to maintain the balance between anabolism and catabolism of ECM and further aggravate the tissue dysfunction [79, 80]. When investigating the IVDSCs *in vitro*, importance of ECM in the original tissue is often ignored. However, the cell-matrix interactions are essential in modulating not only the morphology and phenotype but also the function of SCs, and that has been successfully demonstrated in NP tissue [81, 82]. Perlecan, the common component of many SCNs, is found to be produced by progenitor cells located in this region [83–85]. In addition, it plays a positive role in chondrogenic differentiation of the mesenchymal progenitor cells in IVD [86, 87]. The changes in mechanical strength of the ECM in degenerated discs may be transmitted to the cell membrane and activate the IVDSCs via perlecan or other components of SCN [88, 89]. Moreover, the Piezo1 ion channel exists in human NP cells and underlies mechanical force-induced apoptosis via mediating the mitochondrial dysfunction and endoplasmic reticulum stress [90]. Similar mechanosensitive ion channels that function between ECM and cells are continued to be discovered. Nevertheless, whether there are other mechanisms in the modulation of stem cells' fate, and how the IVDSCs react with the alternation in mechanics, requires further studies.

Tissue engineering relies on suitable seed cells and scaffold materials. The biomechanical properties of scaffold materials affect the function of IVDSCs and determine the efficiency of IVD regeneration [91–94]. The natural molecules that make up the ECM of the IVD are a good choice of scaffold material. The laminin that exists in normal NP tissue, but is absent in degenerated NP tissue, attracts the attention of researchers [95–97]. Nerurkar et al. have presented a novel strategy using anisotropic nanofibrous laminates seeded with MSCs to replicate the form and function of the AF [98]. In addition, *in vitro* influences of laminins on the proliferation and chondrogenesis of SCs have also been demonstrated [99, 100]. Moreover, the SCs also produce laminins which in turn enhance the regeneration ability [101, 102]. Another important component of ECM in IVD is collagen II, which promote the differentiation of SCs, especially the chondrogenic differentiation in a concentration-dependent manner [103]. When cultured in a high concentration of collagen II, the ASCs express a high level of collagen II, aggrecan, SOX9, and low levels of collagen I, which is associated with cross-talk mechanisms between MAPK/ERK and Smad3 pathways [103, 104]. The small leucine-rich proteoglycans (SLRPs) are reported to be the key molecules in modulating the physiological and pathological process of SCs by binding to collagens, growth factors, and other matrix components in the niche of tendon [105] and articular cartilage [106], as well as IVD [107]. The SLRPs might act as a unique niche component regulating the activities of IVDSCs through hypoxia-inducible factor (HIF), thus allowing the survival of these cells under low oxygen tension [39]. In conclusion, the components of the ECM in IVD play a significant role in activation, self-renew, and differentiation of IVDSCs. However, the positive effects of these natural molecules on promoting IVD regeneration rely on optimistic space and time, which remains to be further elucidated [82, 108, 109].

10. The Potential of IVDSCs for IVD Regeneration

Endogenous neural stem cells react to stroke and spinal cord injury by generating a significant number of new neural cells [110]. In the brain, neural stem/progenitor cells might play a supportive role in the cortex to promote neuronal survival and glial cell expansion after traumatic brain injury [111]. Even more encouraging, using a surgical method preserving the endogenous lens epithelial stem/progenitor cells, Lin et al. successfully achieved the regeneration of functional lens in rabbits and macaques, as well as in human infants with cataracts [112]. Thus, motivating the IVDSCs to promote endogenous repair of IVD seems to be a prospective method for IVD regeneration. It has been proven that SCNSCs migrate toward and into IVD tissue following the intercellular space direction of the lamellae [44]. Huang et al. also proposed that stimulating endogenous SCs with simvastatin might retard the progression of IVDD [113]. Chen et al. further proved that transplantation of NPSCs has superior regenerative efficacy than transplantation of NP cells for treating IVDD in rabbit models [47]. However, current researches about the regenerative potential of IVDSCs are still scarce. Additionally, some endogenous factors might inhibit the migration of IVDSCs. For example, Xiong et al. have demonstrated that macrophage migration inhibitory factor secreted by NP cells could inhibit the migration of

CESCs [45]. Therefore, further studies are desperately needed to explore the approaches of promoting the endogenous repair of IVD.

11. Conclusion

The IVD itself has endogenous stem/progenitor cells, which satisfy the criteria defining the MSCs. Compared to other SCs, the IVDSCs might be an excellent cell source for IVD regeneration due to the following advantages: (1) the IVDSCs are generally extracted from surgical specimens derived from patients with disc herniation. Thus, IVDSCs are more accessible and could avoid the damage caused by isolating other kinds of SCs, such as BMSCs. (2) IVDSCs are superior to other SCs in tolerating the harsh microenvironment of IVD.

However, there are some limitations in understanding of IVDSCs. First, current researches about IVDSCs are scarce. Therefore, we only have limited knowledge about the biological characteristics of IVDSCs. Then, surface markers of IVDSCs are still controversial and more specific markers are needed to identify IVDSCs *in vivo* and *in vitro*. Furthermore, how to isolate purer IVDSCs simply and economically is still waiting for exploration. Finally, how to protect IVDSCs from aging, degeneration, and harsh microenvironment is not fully elucidated. In conclusion, the IVDSCs might play a pivotal role in the regeneration of IVD, but more studies are necessary.

Conflicts of Interest

The authors declare that they have no competing interests.

Authors' Contributions

Binwu Hu and Ruijun He contributed equally to this work.

Acknowledgments

This study was supported by grant 2016YFC1100100 from The National Key Research and Development Program of China, grant 81501916 from the National Natural Science Foundation of China, grant 91649204 from the Major Research Plan of National Natural Science Foundation of China, and grant 30872610 from the National Natural Science Foundation of China.

References

[1] A. Maetzel and L. Li, "The economic burden of low back pain: a review of studies published between 1996 and 2001," *Best Practice & Research Clinical Rheumatology*, vol. 16, no. 1, pp. 23–30, 2002.

[2] X. Luo, R. Pietrobon, S. X Sun, G. G. Liu, and L. Hey, "Estimates and patterns of direct health care expenditures among individuals with back pain in the United States," *Spine*, vol. 29, no. 1, pp. 79–86, 2004.

[3] W. F. Stewart, J. A. Ricci, E. Chee, D. Morganstein, and R. Lipton, "Lost productive time and cost due to common pain conditions in the US workforce," *JAMA*, vol. 290, no. 18, pp. 2443–2454, 2003.

[4] M. C. Battié, T. Videman, E. Levalahti, K. Gill, and J. Kaprio, "Heritability of low back pain and the role of disc degeneration," *Pain*, vol. 131, no. 3, pp. 272–280, 2007.

[5] S. Chen, X. Lv, B. Hu et al., "RIPK1/RIPK3/MLKL-mediated necroptosis contributes to compression-induced rat nucleus pulposus cells death," *Apoptosis*, vol. 22, no. 5, pp. 626–638, 2017.

[6] H. B. Henriksson, M. Thornemo, C. Karlsson et al., "Identification of cell proliferation zones, progenitor cells and a potential stem cell niche in the intervertebral disc region: a study in four species," *Spine*, vol. 34, no. 21, pp. 2278–2287, 2009.

[7] J. P. G. Urban and S. Roberts, "Degeneration of the intervertebral disc," *Arthritis Research & Therapy*, vol. 5, no. 3, pp. 120–130, 2003.

[8] A. A. Hegewald, J. Ringe, M. Sittinger, and C. Thome, "Regenerative treatment strategies in spinal surgery," *Frontiers in Bioscience*, vol. 13, no. 13, pp. 1507–1525, 2008.

[9] C. Q. Zhao, L. M. Wang, L. S. Jiang, and L. Y. Dai, "The cell biology of intervertebral disc aging and degeneration," *Ageing Research Reviews*, vol. 6, no. 3, pp. 247–261, 2007.

[10] Y. T. Wang, X. T. Wu, and F. Wang, "Regeneration potential and mechanism of bone marrow mesenchymal stem cell transplantation for treating intervertebral disc degeneration," *Journal of Orthopaedic Science*, vol. 15, no. 6, pp. 707–719, 2010.

[11] B. Han, H.-c. Wang, H. Li et al., "Nucleus pulposus mesenchymal stem cells in acidic conditions mimicking degenerative intervertebral discs give better performance than adipose tissue-derived mesenchymal stem cells," *Cells Tissues Organs*, vol. 199, no. 5-6, pp. 342–352, 2015.

[12] D. Sakai and S. Grad, "Advancing the cellular and molecular therapy for intervertebral disc disease," *Advanced Drug Delivery Reviews*, vol. 84, pp. 159–171, 2015.

[13] S. Z. Wang, Y. F. Rui, Q. Tan, and C. Wang, "Enhancing intervertebral disc repair and regeneration through biology: platelet-rich plasma as an alternative strategy," *Arthritis Research & Therapy*, vol. 15, no. 5, p. 220, 2013.

[14] F. Wang, R. Shi, F. Cai, Y. T. Wang, and X. T. Wu, "Stem cell approaches to intervertebral disc regeneration: obstacles from the disc microenvironment," *Stem Cells and Development*, vol. 24, no. 21, pp. 2479–2495, 2015.

[15] C. H. Evans and J. Huard, "Gene therapy approaches to regenerating the musculoskeletal system," *Nature Reviews Rheumatology*, vol. 11, no. 4, pp. 234–242, 2015.

[16] G. Vadalà, F. Russo, L. Ambrosio, M. Loppini, and V. Denaro, "Stem cells sources for intervertebral disc regeneration," *World Journal of Stem Cells*, vol. 8, no. 5, pp. 185–201, 2016.

[17] D. Sakai, J. Mochida, Y. Yamamoto et al., "Transplantation of mesenchymal stem cells embedded in Atelocollagen® gel to the intervertebral disc: a potential therapeutic model for disc degeneration," *Biomaterials*, vol. 24, no. 20, pp. 3531–3541, 2003.

[18] L. Orozco, R. Soler, C. Morera, M. Alberca, A. Sánchez, and J. García-Sancho, "Intervertebral disc repair by autologous mesenchymal bone marrow cells: a pilot study," *Transplantation*, vol. 92, no. 7, pp. 822–828, 2011.

[19] G. Vadalà, G. Sowa, M. Hubert, L. G. Gilbertson, V. Denaro, and J. D. Kang, "Mesenchymal stem cells injection in degenerated intervertebral disc: cell leakage may induce osteophyte

formation," *Journal of Tissue Engineering and Regenerative Medicine*, vol. 6, no. 5, pp. 348–355, 2012.

[20] R. Shi, F. Wang, X. Hong et al., "The presence of stem cells in potential stem cell niches of the intervertebral disc region: an in vitro study on rats," *European Spine Journal*, vol. 24, no. 11, pp. 2411–2424, 2015.

[21] W. E. B. Johnson, S. Stephan, and S. Roberts, "The influence of serum, glucose and oxygen on intervertebral disc cell growth in vitro: implications for degenerative disc disease," *Arthritis Research & Therapy*, vol. 10, no. 2, article R46, 2008.

[22] W. M. Erwin, D. Islam, E. Eftekarpour, R. D. Inman, M. Z. Karim, and M. G. Fehlings, "Intervertebral disc-derived stem cells: implications for regenerative medicine and neural repair," *Spine*, vol. 38, no. 3, pp. 211–216, 2013.

[23] H. Wu, X. Zeng, J. Yu et al., "Comparison of nucleus pulposus stem/progenitor cells isolated from degenerated intervertebral discs with umbilical cord derived mesenchymal stem cells," *Experimental Cell Research*, vol. 361, no. 2, pp. 324–332, 2017.

[24] C. H. Lee, F. Y. Lee, S. Tarafder et al., "Harnessing endogenous stem/progenitor cells for tendon regeneration," *The Journal of Clinical Investigation*, vol. 125, no. 7, pp. 2690–2701, 2015.

[25] H. Yin, F. Price, and M. A. Rudnicki, "Satellite cells and the muscle stem cell niche," *Physiological Reviews*, vol. 93, no. 1, pp. 23–67, 2013.

[26] R. Williams, I. M. Khan, K. Richardson et al., "Identification and clonal characterisation of a progenitor cell subpopulation in normal human articular cartilage," *PLoS One*, vol. 5, no. 10, article e13246, 2010.

[27] H. B. Henriksson, E. Svala, E. Skioldebrand, A. Lindahl, and H. Brisby, "Support of concept that migrating progenitor cells from stem cell niches contribute to normal regeneration of the adult mammal intervertebral disc: a descriptive study in the New Zealand white rabbit," *Spine*, vol. 37, no. 9, pp. 722–732, 2012.

[28] M. V. Risbud, A. Guttapalli, T. T. Tsai et al., "Evidence for skeletal progenitor cells in the degenerate human intervertebral disc," *Spine*, vol. 32, no. 23, pp. 2537–2544, 2007.

[29] J. F. Blanco, I. F. Graciani, F. M. Sanchez-Guijo et al., "Isolation and characterization of mesenchymal stromal cells from human degenerated nucleus pulposus: comparison with bone marrow mesenchymal stromal cells from the same subjects," *Spine*, vol. 35, no. 26, pp. 2259–2265, 2010.

[30] L. Liang, X. Li, D. Li et al., "The characteristics of stem cells in human degenerative intervertebral disc," *Medicine*, vol. 96, no. 25, article e7178, 2017.

[31] D. Sakai, Y. Nakamura, T. Nakai et al., "Exhaustion of nucleus pulposus progenitor cells with ageing and degeneration of the intervertebral disc," *Nature Communications*, vol. 3, no. 1, p. 1264, 2012.

[32] L. T. Liu, B. Huang, C. Q. Li, Y. Zhuang, J. Wang, and Y. Zhou, "Characteristics of stem cells derived from the degenerated human intervertebral disc cartilage endplate," *PLoS One*, vol. 6, no. 10, article e26285, 2011.

[33] C. Liu, Q. Guo, J. Li et al., "Identification of rabbit annulus fibrosus-derived stem cells," *PLoS One*, vol. 9, no. 9, article e108239, 2014.

[34] Q. Shen, L. Zhang, B. Chai, and X. Ma, "Isolation and characterization of mesenchymal stem-like cells from human nucleus pulposus tissue," *Science China Life Sciences*, vol. 58, no. 5, pp. 509–511, 2015.

[35] G. Feng, X. Yang, H. Shang et al., "Multipotential differentiation of human anulus fibrosus cells: an in vitro study," *The Journal of Bone and Joint Surgery-American Volume*, vol. 92, no. 3, pp. 675–685, 2010.

[36] B. Huang, L. T. Liu, C. Q. Li et al., "Study to determine the presence of progenitor cells in the degenerated human cartilage endplates," *European Spine Journal*, vol. 21, no. 4, pp. 613–622, 2012.

[37] M. Dominici, K. le Blanc, I. Mueller et al., "Minimal criteria for defining multipotent mesenchymal stromal cells. The International Society for Cellular Therapy position statement," *Cytotherapy*, vol. 8, no. 4, pp. 315–317, 2006.

[38] H. Wang, Y. Zhou, T.-W. Chu et al., "Distinguishing characteristics of stem cells derived from different anatomical regions of human degenerated intervertebral discs," *European Spine Journal*, vol. 25, no. 9, pp. 2691–2704, 2016.

[39] S. Huang, V. Y. L. Leung, D. Long et al., "Coupling of small leucine-rich proteoglycans to hypoxic survival of a progenitor cell-like subpopulation in r*hesus macaque* intervertebral disc," *Biomaterials*, vol. 34, no. 28, pp. 6548–6558, 2013.

[40] Y. Zhao, Z. Jia, S. Huang et al., "Age-related changes in nucleus pulposus mesenchymal stem cells: an in vitro study in rats," *Stem Cells International*, vol. 2017, Article ID 6761572, 13 pages, 2017.

[41] M. Yasen, Q. Fei, W. C. Hutton et al., "Changes of number of cells expressing proliferation and progenitor cell markers with age in rabbit intervertebral discs," *Acta Biochimica et Biophysica Sinica*, vol. 45, no. 5, pp. 368–376, 2013.

[42] O. Mizrahi, D. Sheyn, W. Tawackoli et al., "Nucleus pulposus degeneration alters properties of resident progenitor cells," *The Spine Journal*, vol. 13, no. 7, pp. 803–814, 2013.

[43] Z. Jia, P. Yang, Y. Wu et al., "Comparison of biological characteristics of nucleus pulposus mesenchymal stem cells derived from non-degenerative and degenerative human nucleus pulposus," *Experimental and Therapeutic Medicine*, vol. 13, no. 6, pp. 3574–3580, 2017.

[44] H. Henriksson, A. Lindahl, E. Skioldebrand et al., "Similar cellular migration patterns from niches in intervertebral disc and in knee-joint regions detected by in situ labeling: an experimental study in the New Zealand white rabbit," *Stem Cell Research & Therapy*, vol. 4, no. 5, p. 104, 2013.

[45] C. J. Xiong, B. Huang, Y. Zhou et al., "Macrophage migration inhibitory factor inhibits the migration of cartilage end plate-derived stem cells by reacting with CD74," *PLoS One*, vol. 7, no. 8, article e43984, 2012.

[46] P. Lama, C. L. le Maitre, I. J. Harding, P. Dolan, and M. A. Adams, "Nerves and blood vessels in degenerated intervertebral discs are confined to physically disrupted tissue," *Journal of Anatomy*, vol. 233, no. 1, pp. 86–97, 2018.

[47] X. Chen, L. Zhu, G. Wu, Z. Liang, L. Yang, and Z. Du, "A comparison between nucleus pulposus-derived stem cell transplantation and nucleus pulposus cell transplantation for the treatment of intervertebral disc degeneration in a rabbit model," *International Journal of Surgery*, vol. 28, pp. 77–82, 2016.

[48] L. Lin, Z. Jia, Y. Zhao et al., "Use of limiting dilution method for isolation of nucleus pulposus mesenchymal stem/progenitor cells and effects of plating density on

biological characteristics and plasticity," *BioMed Research International*, vol. 2017, Article ID 9765843, 16 pages, 2017.

[49] Y. Q. Tao, C. Z. Liang, H. Li et al., "Potential of co-culture of nucleus pulposus mesenchymal stem cells and nucleus pulposus cells in hyperosmotic microenvironment for intervertebral disc regeneration," *Cell Biology International*, vol. 37, no. 8, pp. 826–834, 2013.

[50] Y. Tao, X. Zhou, C. Liang et al., "TGF-β3 and IGF-1 synergy ameliorates nucleus pulposus mesenchymal stem cell differentiation towards the nucleus pulposus cell type through MAPK/ERK signaling," *Growth Factors*, vol. 33, no. 5-6, pp. 326–336, 2015.

[51] H. Li, Y. Tao, C. Liang et al., "Influence of hypoxia in the intervertebral disc on the biological behaviors of rat adipose- and nucleus pulposus-derived mesenchymal stem cells," *Cells, Tissues, Organs*, vol. 198, no. 4, pp. 266–277, 2013.

[52] I. Sekiya, B. L. Larson, J. R. Smith, R. Pochampally, J.-G. Cui, and D. J. Prockop, "Expansion of human adult stem cells from bone marrow stroma: conditions that maximize the yields of early progenitors and evaluate their quality," *Stem Cells*, vol. 20, no. 6, pp. 530–541, 2002.

[53] C. Feng, Y. Zhang, M. Yang, B. Huang, and Y. Zhou, "Collagen-derived N-acetylated proline-glycine-proline in intervertebral discs modulates CXCR1/2 expression and activation in cartilage endplate stem cells to induce migration and differentiation toward a pro-inflammatory phenotype," *Stem Cells*, vol. 33, no. 12, pp. 3558–3568, 2015.

[54] T. Ishii, D. Sakai, J. Schol, T. Nakai, K. Suyama, and M. Watanabe, "Sciatic nerve regeneration by transplantation of in vitro differentiated nucleus pulposus progenitor cells," *Regenerative Medicine*, vol. 12, no. 4, pp. 365–376, 2017.

[55] J. Liu, H. Tao, H. Wang et al., "Biological behavior of human nucleus pulposus mesenchymal stem cells in response to changes in the acidic environment during intervertebral disc degeneration," *Stem Cells and Development*, vol. 26, no. 12, pp. 901–911, 2017.

[56] Z. Li, S. Chen, K. Ma et al., "CsA attenuates compression-induced nucleus pulposus mesenchymal stem cells apoptosis via alleviating mitochondrial dysfunction and oxidative stress," *Life Sciences*, vol. 205, pp. 26–37, 2018.

[57] Y. Navaro, N. Bleich-Kimelman, L. Hazanov et al., "Matrix stiffness determines the fate of nucleus pulposus–derived stem cells," *Biomaterials*, vol. 49, pp. 68–76, 2015.

[58] L. Qi, R. Wang, Q. Shi, M. Yuan, M. Jin, and D. Li, "Umbilical cord mesenchymal stem cell conditioned medium restored the expression of collagen II and aggrecan in nucleus pulposus mesenchymal stem cells exposed to high glucose," *Journal of Bone and Mineral Metabolism*, 2018.

[59] C. Yuan, L. Pu, Z. He, and J. Wang, "BNIP3/Bcl-2-mediated apoptosis induced by cyclic tensile stretch in human cartilage endplate-derived stem cells," *Experimental and Therapeutic Medicine*, vol. 15, no. 1, pp. 235–241, 2018.

[60] Y. Yao, Q. Deng, W. Song et al., "MIF plays a key role in regulating tissue-specific chondro-osteogenic differentiation fate of human cartilage endplate stem cells under hypoxia," *Stem Cell Reports*, vol. 7, no. 2, pp. 249–262, 2016.

[61] H. Brisby, N. Papadimitriou, C. Brantsing, P. Bergh, A. Lindahl, and H. Barreto Henriksson, "The presence of local mesenchymal progenitor cells in human degenerated intervertebral discs and possibilities to influence these in vitro: a descriptive study in humans," *Stem Cells and Development*, vol. 22, no. 5, pp. 804–814, 2013.

[62] H. E. Gruber, J. A. Ingram, H. J. Norton, and E. N. Hanley Jr., "Senescence in cells of the aging and degenerating intervertebral disc: immunolocalization of senescence-associated β-galactosidase in human and sand rat discs," *Spine*, vol. 32, no. 3, pp. 321–327, 2007.

[63] S. Roberts, E. H. Evans, D. Kletsas, D. C. Jaffray, and S. M. Eisenstein, "Senescence in human intervertebral discs," *European Spine Journal*, vol. 15, no. S3, pp. 312–316, 2006.

[64] G. Hou, H. Lu, M. Chen, H. Yao, and H. Zhao, "Oxidative stress participates in age-related changes in rat lumbar intervertebral discs," *Archives of Gerontology and Geriatrics*, vol. 59, no. 3, pp. 665–669, 2014.

[65] L. A. Nasto, K. Ngo, A. S. Leme et al., "Investigating the role of DNA damage in tobacco smoking-induced spine degeneration," *The Spine Journal*, vol. 14, no. 3, pp. 416–423, 2014.

[66] J. V. Chakkalakal, K. M. Jones, M. A. Basson, and A. S. Brack, "The aged niche disrupts muscle stem cell quiescence," *Nature*, vol. 490, no. 7420, pp. 355–360, 2012.

[67] M. Komatsu, S. Waguri, T. Chiba et al., "Loss of autophagy in the central nervous system causes neurodegeneration in mice," *Nature*, vol. 441, no. 7095, pp. 880–884, 2006.

[68] A. M. Cuervo, E. Bergamini, U. T. Brunk, W. Dröge, M. Ffrench, and A. Terman, "Autophagy and aging: the importance of maintaining "clean" cells," *Autophagy*, vol. 1, no. 3, pp. 131–140, 2005.

[69] P. Sousa-Victor, S. Gutarra, L. García-Prat et al., "Geriatric muscle stem cells switch reversible quiescence into senescence," *Nature*, vol. 506, no. 7488, pp. 316–321, 2014.

[70] D. Sakai and G. B. J. Andersson, "Stem cell therapy for intervertebral disc regeneration: obstacles and solutions," *Nature Reviews Rheumatology*, vol. 11, no. 4, pp. 243–256, 2015.

[71] A. G. Nerlich, R. Schaaf, B. Wälchli, and N. Boos, "Temporospatial distribution of blood vessels in human lumbar intervertebral discs," *European Spine Journal*, vol. 16, no. 4, pp. 547–555, 2007.

[72] A. J. Freemont, A. Watkins, C. le Maitre et al., "Nerve growth factor expression and innervation of the painful intervertebral disc," *The Journal of Pathology*, vol. 197, no. 3, pp. 286–292, 2002.

[73] Y. Li, J. Zhou, X. Yang, Y. Jiang, and J. Gui, "Intermittent hydrostatic pressure maintains and enhances the chondrogenic differentiation of cartilage progenitor cells cultivated in alginate beads," *Development, Growth & Differentiation*, vol. 58, no. 2, pp. 180–193, 2016.

[74] M.-S. Hosseini, M. Tafazzoli-Shadpour, N. Haghighipour, N. Aghdami, and A. Goodarzi, "The synergistic effects of shear stress and cyclic hydrostatic pressure modulate chondrogenic induction of human mesenchymal stem cells," *The International Journal of Artificial Organs*, vol. 38, no. 10, pp. 557–564, 2015.

[75] Y. H. Zhao, X. Lv, Y. L. Liu et al., "Hydrostatic pressure promotes the proliferation and osteogenic/chondrogenic differentiation of mesenchymal stem cells: the roles of RhoA and Rac1," *Stem Cell Research*, vol. 14, no. 3, pp. 283–296, 2015.

[76] P. H. Chou, S. T. Wang, M. H. Yen, C. L. Liu, M. C. Chang, and O. K. S. Lee, "Fluid-induced, shear stress-regulated extracellular matrix and matrix metalloproteinase genes expression on human annulus fibrosus cells," *Stem Cell Research & Therapy*, vol. 7, no. 1, p. 34, 2016.

[77] C. Neidlinger-Wilke, A. Mietsch, C. Rinkler, H.-J. Wilke, A. Ignatius, and J. Urban, "Interactions of environmental conditions and mechanical loads have influence on matrix turnover by nucleus pulposus cells," *Journal of Orthopaedic Research*, vol. 30, no. 1, pp. 112–121, 2012.

[78] Z. He, L. Pu, C. Yuan, M. Jia, and J. Wang, "Nutrition deficiency promotes apoptosis of cartilage endplate stem cells in a caspase-independent manner partially through upregulating BNIP3," *Acta Biochimica et Biophysica Sinica*, vol. 49, no. 1, pp. 25–32, 2017.

[79] C. K. Kepler, R. K. Ponnappan, C. A. Tannoury, M. V. Risbud, and D. G. Anderson, "The molecular basis of intervertebral disc degeneration," *The Spine Journal*, vol. 13, no. 3, pp. 318–330, 2013.

[80] C. Feng, H. Liu, M. Yang, Y. Zhang, B. Huang, and Y. Zhou, "Disc cell senescence in intervertebral disc degeneration: causes and molecular pathways," *Cell Cycle*, vol. 15, no. 13, pp. 1674–1684, 2016.

[81] A. Rastogi, P. Thakore, A. Leung et al., "Environmental regulation of notochordal gene expression in nucleus pulposus cells," *Journal of Cellular Physiology*, vol. 220, no. 3, pp. 698–705, 2009.

[82] F. Guilak, D. M. Cohen, B. T. Estes, J. M. Gimble, W. Liedtke, and C. S. Chen, "Control of stem cell fate by physical interactions with the extracellular matrix," *Cell Stem Cell*, vol. 5, no. 1, pp. 17–26, 2009.

[83] J. Melrose, R. P. Bone, and Joint Research Laboratory, "Perlecan delineates stem cell niches in human foetal hip, knee and elbow cartilage rudiments and has potential roles in the regulation of stem cell differentiation," *Stem Cells Research, Development & Therapy*, vol. 3, no. 1, pp. 1–7, 2016.

[84] U. Schlötzer-Schrehardt, T. Dietrich, K. Saito et al., "Characterization of extracellular matrix components in the limbal epithelial stem cell compartment," *Experimental Eye Research*, vol. 85, no. 6, pp. 845–860, 2007.

[85] S. Brown, A. Matta, M. Erwin et al., "Cell clusters are indicative of stem cell activity in the degenerate intervertebral disc: can their properties be manipulated to improve intrinsic repair of the disc?," *Stem Cells and Development*, vol. 27, no. 3, pp. 147–165, 2018.

[86] S. M. Smith, C. Shu, and J. Melrose, "Comparative immunolocalisation of perlecan with collagen II and aggrecan in human foetal, newborn and adult ovine joint tissues demonstrates perlecan as an early developmental chondrogenic marker," *Histochemistry and Cell Biology*, vol. 134, no. 3, pp. 251–263, 2010.

[87] C. Shu, C. Hughes, S. M. Smith et al., "The ovine newborn and human foetal intervertebral disc contain perlecan and aggrecan variably substituted with native 7D4 CS sulphation motif: spatiotemporal immunolocalisation and co-distribution with Notch-1 in the human foetal disc," *Glycoconjugate Journal*, vol. 30, no. 7, pp. 717–725, 2013.

[88] Y. K. Wang and C. S. Chen, "Cell adhesion and mechanical stimulation in the regulation of mesenchymal stem cell differentiation," *Journal of Cellular and Molecular Medicine*, vol. 17, no. 7, pp. 823–832, 2013.

[89] S. D. Subramony, B. R. Dargis, M. Castillo et al., "The guidance of stem cell differentiation by substrate alignment and mechanical stimulation," *Biomaterials*, vol. 34, no. 8, pp. 1942–1953, 2013.

[90] X. F. Li, P. Leng, Z. Zhang, and H. N. Zhang, "The Piezo1 protein ion channel functions in human nucleus pulposus cell apoptosis by regulating mitochondrial dysfunction and the endoplasmic reticulum stress signal pathway," *Experimental Cell Research*, vol. 358, no. 2, pp. 377–389, 2017.

[91] J. S. Choi and B. A. C. Harley, "The combined influence of substrate elasticity and ligand density on the viability and biophysical properties of hematopoietic stem and progenitor cells," *Biomaterials*, vol. 33, no. 18, pp. 4460–4468, 2012.

[92] D. Seliktar, "Designing cell-compatible hydrogels for biomedical applications," *Science*, vol. 336, no. 6085, pp. 1124–1128, 2012.

[93] A. J. Engler, H. L. Sweeney, D. E. Discher, and J. E. Schwarzbauer, "Extracellular matrix elasticity directs stem cell differentiation," *Journal of Biomechanics*, vol. 7, no. 4, p. 335, 2007.

[94] A. H. Hsieh and J. D. Twomey, "Cellular mechanobiology of the intervertebral disc: new directions and approaches," *Journal of Biomechanics*, vol. 43, no. 1, pp. 137–145, 2010.

[95] Y. Sun, T. L. Wang, W. S. Toh, and M. Pei, "The role of laminins in cartilaginous tissues: from development to regeneration," *European Cells and Materials*, vol. 34, pp. 40–54, 2017.

[96] C. B. Foldager, W. S. Toh, B. B. Christensen, M. Lind, A. H. Gomoll, and M. Spector, "Collagen type IV and laminin expressions during cartilage repair and in late clinically failed repair tissues from human subjects," *Cartilage*, vol. 7, no. 1, pp. 52–61, 2016.

[97] C. B. Foldager, W. S. Toh, A. H. Gomoll, B. R. Olsen, and M. Spector, "Distribution of basement membrane molecules, laminin and collagen type IV, in normal and degenerated cartilage tissues," *Cartilage*, vol. 5, no. 2, pp. 123–132, 2014.

[98] N. L. Nerurkar, B. M. Baker, S. Sen, E. E. Wible, D. M. Elliott, and R. L. Mauck, "Nanofibrous biologic laminates replicate the form and function of the annulus fibrosus," *Nature Materials*, vol. 8, no. 12, pp. 986–992, 2009.

[99] J. Hashimoto, Y. Kariya, and K. Miyazaki, "Regulation of proliferation and chondrogenic differentiation of human mesenchymal stem cells by laminin-5 (laminin-332)," *Stem Cells*, vol. 24, no. 11, pp. 2346–2354, 2006.

[100] W. S. Toh, C. B. Foldager, B. R. Olsen, and M. Spector, "Basement membrane molecule expression attendant to chondrogenesis by nucleus pulposus cells and mesenchymal stem cells," *Journal of Orthopaedic Research*, vol. 31, no. 7, pp. 1136–1143, 2013.

[101] S. Rodin, L. Antonsson, C. Niaudet et al., "Clonal culturing of human embryonic stem cells on laminin-521/E-cadherin matrix in defined and xeno-free environment," *Nature Communications*, vol. 5, no. 1, 2014.

[102] A. Laperle, C. Hsiao, M. Lampe et al., "α-5 laminin synthesized by human pluripotent stem cells promotes self-renewal," *Stem Cell Reports*, vol. 5, no. 2, pp. 195–206, 2015.

[103] Y. Tao, X. Zhou, D. Liu et al., "Proportion of collagen type II in the extracellular matrix promotes the differentiation of human adipose-derived mesenchymal stem cells into nucleus pulposus cells," *BioFactors*, vol. 42, no. 2, pp. 212–223, 2016.

[104] G. Fontana, D. Thomas, E. Collin, and A. Pandit, "Microgel microenvironment primes adipose-derived stem cells towards an NP cells-like phenotype," *Advanced Healthcare Materials*, vol. 3, no. 12, pp. 2012–2022, 2014.

[105] Y. Bi, D. Ehirchiou, T. M. Kilts et al., "Identification of tendon stem/progenitor cells and the role of the extracellular matrix in their niche," *Nature Medicine*, vol. 13, no. 10, pp. 1219–1227, 2007.

[106] H. Kizawa, I. Kou, A. Iida et al., "An aspartic acid repeat polymorphism in asporin inhibits chondrogenesis and increases susceptibility to osteoarthritis," *Nature Genetics*, vol. 37, no. 2, pp. 138–144, 2005.

[107] T. Furukawa, K. Ito, S. Nuka et al., "Absence of biglycan accelerates the degenerative process in mouse intervertebral disc," *Spine*, vol. 34, no. 25, pp. E911–E917, 2009.

[108] M. Yuan, C. W. Yeung, Y. Y. Li et al., "Effects of nucleus pulposus cell-derived acellular matrix on the differentiation of mesenchymal stem cells," *Biomaterials*, vol. 34, no. 16, pp. 3948–3961, 2013.

[109] R. Maidhof, A. Rafiuddin, F. Chowdhury, T. Jacobsen, and N. O. Chahine, "Timing of mesenchymal stem cell delivery impacts the fate and therapeutic potential in intervertebral disc repair," *Journal of Orthopaedic Research*, vol. 35, no. 1, pp. 32–40, 2017.

[110] C.-A. Grégoire, B. L. Goldenstein, E. M. Floriddia, F. Barnabé-Heider, and K. J. L. Fernandes, "Endogenous neural stem cell responses to stroke and spinal cord injury," *Glia*, vol. 63, no. 8, pp. 1469–1482, 2015.

[111] K. J. Dixon, M. H. Theus, C. M. Nelersa et al., "Endogenous neural stem/progenitor cells stabilize the cortical microenvironment after traumatic brain injury," *Journal of Neurotrauma*, vol. 32, no. 11, pp. 753–764, 2015.

[112] H. Lin, H. Ouyang, J. Zhu et al., "Lens regeneration using endogenous stem cells with gain of visual function," *Nature*, vol. 531, no. 7594, pp. 323–328, 2016.

[113] Z. Huang, L. Zhang, X. Feng, T. Chen, and S. Bi, "A new in vivo method to retard progression of intervertebral disc degeneration through stimulation of endogenous stem cells with simvastatin," *Medical Hypotheses*, vol. 101, pp. 65-66, 2017.

Hindawi
Stem Cells International
Volume 2018, Article ID 1481243, 10 pages
https://doi.org/10.1155/2018/1481243

Research Article

Effect of Compression Loading on Human Nucleus Pulposus-Derived Mesenchymal Stem Cells

Hang Liang, Sheng Chen, Donghua Huang, Xiangyu Deng, Kaige Ma, and Zengwu Shao

Department of Orthopaedics, Union Hospital, Tongji Medical College, Huazhong University of Science and Technology, 1277 Jiefang Avenue, Wuhan 430022, China

Correspondence should be addressed to Kaige Ma; makaige225@hust.edu.cn and Zengwu Shao; szwpro@163.com

Received 10 March 2018; Accepted 2 May 2018; Published 8 October 2018

Academic Editor: Andrea Ballini

Purpose. Mechanical loading plays a vital role in the progression of intervertebral disc (IVD) degeneration, but little is known about the effect of compression loading on human nucleus pulposus-derived mesenchymal stem cells (NP-MSCs). Thus, this study is aimed at investigating the effect of compression on the biological behavior of NP-MSCs in vitro. *Methods*. Human NP-MSCs were isolated from patients undergoing lumbar discectomy for IVD degeneration and were identified by immunophenotypes and multilineage differentiation. Then, cells were cultured in the compression apparatus at 1.0 MPa for different times (0 h, 24 h, 36 h, and 48 h). The viability-, differentiation-, and differentiation-related genes (Runx2, APP, and Col2) and colony formation-, migration-, and stem cell-related proteins (Sox2 and Oct4) were evaluated. *Results*. The results showed that the isolated cells fulfilled the criteria of MSC stated by the International Society for Cellular Therapy (ISCT). And our results also indicated that compression loading significantly inhibited cell viability, differentiation, colony formation, and migration. Furthermore, gene expression suggested that compression loading could downregulate the expression of stem cell-related proteins and lead to NP-MSC stemness losses. *Conclusions*. Our results suggested that the biological behavior of NP-MSCs could be inhibited by compression loading and therefore enhanced our understanding on the compression-induced endogenous repair failure of NP-MSCs during IVDD.

1. Introduction

Intervertebral disc (IVD) degeneration is among the most important contributors to low back pain, leading to patient disability and heavy financial burdens globally [1, 2]. Currently, conservative and surgical operations are the main treatments for IVD degeneration. However, these treatments are not long-lasting and effective for the limitation that they cannot reverse the structural and mechanical function of IVD tissues [3]. Stem cell-based therapies have shown an exciting perspective for IVD repair recently [4]. In different animal models of disc degeneration, which are established by annular puncture or nucleus aspiration, transplantation of exogenous mesenchymal stem cells (MSCs) has improved the evaluation scores of radiographs, magnetic resonance images (MRI), and histological analysis [5–7]. In a pilot study [8], ten patients suffering from chronic back pain and positively diagnosed with lumbar disc degeneration were treated by injecting autologous expanded bone marrow MSCs into the nucleus pulposus (NP) area. The results indicated the feasibility, safety, and clinical efficacy of the treatment.

Apart from exogenous stem cell transplantation, endogenous stem cell stimulation and recruitment are also essential ways to repair IVD degeneration and play a key role in endogenous repair [9]. Evidence has been found in latest researches that nucleus pulposus mesenchymal stem cells (NP-MSCs) exist naturally in the IVD [10, 11] and participate in IVD regeneration [9]. The aim of NP-MSC therapy is to make NP-MSCs differentiate into nucleus pulposus-like cells and stimulate disc cells maintaining IVD homeostasis. Although activating the endogenous NP-MSCs could be an attractive strategy for endogenous repair, it is hard to

maintain the number of viable and functional NP-MSCs under an adverse microenvironment in IVD [12]. It was reported that the viability and proliferation rate of NP-MSCs were significantly inhibited under hypoxia [13], and acidic conditions could decrease the extracellular matrix (ECM) synthesis and stem cell-related gene expression of NP-MSCs [14]. Mechanical loadings [15], including compression, shear, torsion, and flexion, are another essential factors that influence the fate of NP-MSCs.

The IVD functions as a shock absorber, and external forces on the spine lead to intense stresses that act on the IVD. From a mechanical point of view, disc cells and progenitor cells embedded in the different areas are exposed to wide ranges of mechanical loadings [16]. Inappropriate or excessive compressive force stimulus applied to intervertebral discs (IVDs) is an important contributing factor in the progress of disc degeneration. We have reported that apoptosis and necroptosis could be induced by compression at a magnitude of 1 MPa in rat NP cells previously [17, 18]. However, to our best knowledge, there have been no studies focusing on the effect of compression loading on human NP-MSCs so far. Therefore, the present study is aimed at exploring the effect of compression on the biological behavior of NP-MSCs in vitro.

2. Methods

2.1. Isolation and Culture of NP-MSCs. NP tissues were donated by five patients undergoing lumbar discectomy for lumbar disc hernia, and the ages of those five patients are 42, 49, 45, 41, and 40, respectively. According to Pfirrmann's MRI (T2WI) Grading Criteria for Disc Degeneration, all the patients were in grade III. All procedures in the present study were approved by the ethics committee of Tongji Medical College of Huazhong University of Science and Technology. NP-MSCs were isolated and cultured as previously described [14]. Briefly, NP tissues were first carefully separated by a dissecting microscope and washed by PBS solution. Secondly, the NP samples were dissected and digested in 0.2% type II collagenase for 12 h at 37°C with 5% CO_2. And then the obtained cells and partially digested tissues were cultured in MSC complete medium (Cyagen, USA) at 37°C in a humidified atmosphere containing 5% CO_2. The media were changed twice a week, and the primary culture was 1 : 3 subcultured when cells reached 80%–90% confluence. NP-MSCs in passage 2 were used in this study.

2.2. Surface Marker Identification of NP-MSCs. The collected cells were washed and resuspended in PBS and incubated with the following monoclonal antibodies according to the recommendations of ISCT [19]: CD105, CD73, CD90, CD34, CD14, CD19, and HLA-DR. After being incubated for 30 min at 37°C, the cells were washed with PBS and then resuspended in 500 μL PBS to adjust the cell concentration at about 10^6/mL. The labeled cells were examined via flow cytometry (BD LSR II, Becton Dickinson) following standard procedures.

2.3. Multilineage Differentiation. To assess the multilineage differentiation potential of NP-MSCs, the osteogenic, adipogenic, and chondrogenic differentiation was induced.

For osteogenic differentiation, NP-MSCs were seeded in six-well plates at 2×10^4 cells/cm^2 in normal medium and incubated in osteogenic differentiation medium (Cyagen, USA) at 60%–70% confluence. The inducing conditional medium was changed twice a week. After differentiating for 14 days, the NP-MSCs were used to extract RNA and stained with the Alizarin Red solution, respectively.

For adipogenic differentiation, NP-MSCs were seeded in six-well plates at 2×10^4 cells/cm^2. When the cells grew up to 100% confluence, the medium was changed to adipogenic differentiation medium A (Cyagen, USA). Three days later, the medium was changed to adipogenic differentiation medium B (Cyagen, USA). After 24 h, the medium was replaced back with medium A. The cycle was repeated for 4 times, and the cells were cultured in medium B for additional 7 days. After differentiating, the NP-MSCs were used to extract RNA and stained with Oil Red O.

For chondrogenic differentiation, NP-MSCs were seeded in six-well plates at 2×10^4 cells/cm^2 in normal medium and incubated in chondrogenic differentiation medium (Cyagen, USA) at 60%–70% confluence. The media were changed every 2 to 3 days. After differentiating for three weeks, the NP-MSCs were used to extract RNA and stained with the Alcian blue.

In addition, to evaluate the effect of compression loading on the multilineage differentiation of NP-MSCs, the cells were cultured in a custom-made compression apparatus for different times (0 h, 24 h, 36 h, and 48 h) at a magnitude of 1 MPa as described previously [17, 20]. And the cells were then digested with 0.25% trypsin and seeded in six-well plates for the induced differentiation above.

2.4. Cell Viability Assay (CCK-8). NP-MSCs were seeded in 96-well plates and cultured in the compression apparatus for different times (0 h, 24 h, 36 h, and 48 h). Cell viability was measured by CCK-8 (Dojindo, Japan) following the manufacturer's protocol. At the appropriate time points, 10 μL CCK-8 solution was added to each well. The plates were then incubated at 37°C with 5% CO_2 for 2 h. The surviving cell counts were determined by absorbance detection at 450 nm with a spectrophotometer (BioTek, USA).

2.5. Colony Formation Assay. To demonstrate the effect of compression loading on the capacity of colony formation, the NP-MSCs were treated with compression for different times (0 h, 24 h, 36 h, and 48 h). Then, the cells were collected and seeded in six-well plates at the density of 200 cells/well. The medium was changed twice a week. After two weeks, the cells were fixed with 4% paraformaldehyde. Fifteen minutes later, the cells were washed with PBS and stained with 0.1% crystal violet for 15 min. The colonies containing more than 100 cells were counted.

2.6. Wound Healing Assay. For the wound healing assay, NP-MSCs were seeded in six-well plates with MSC complete medium. When the cells grew to 100% confluence, the

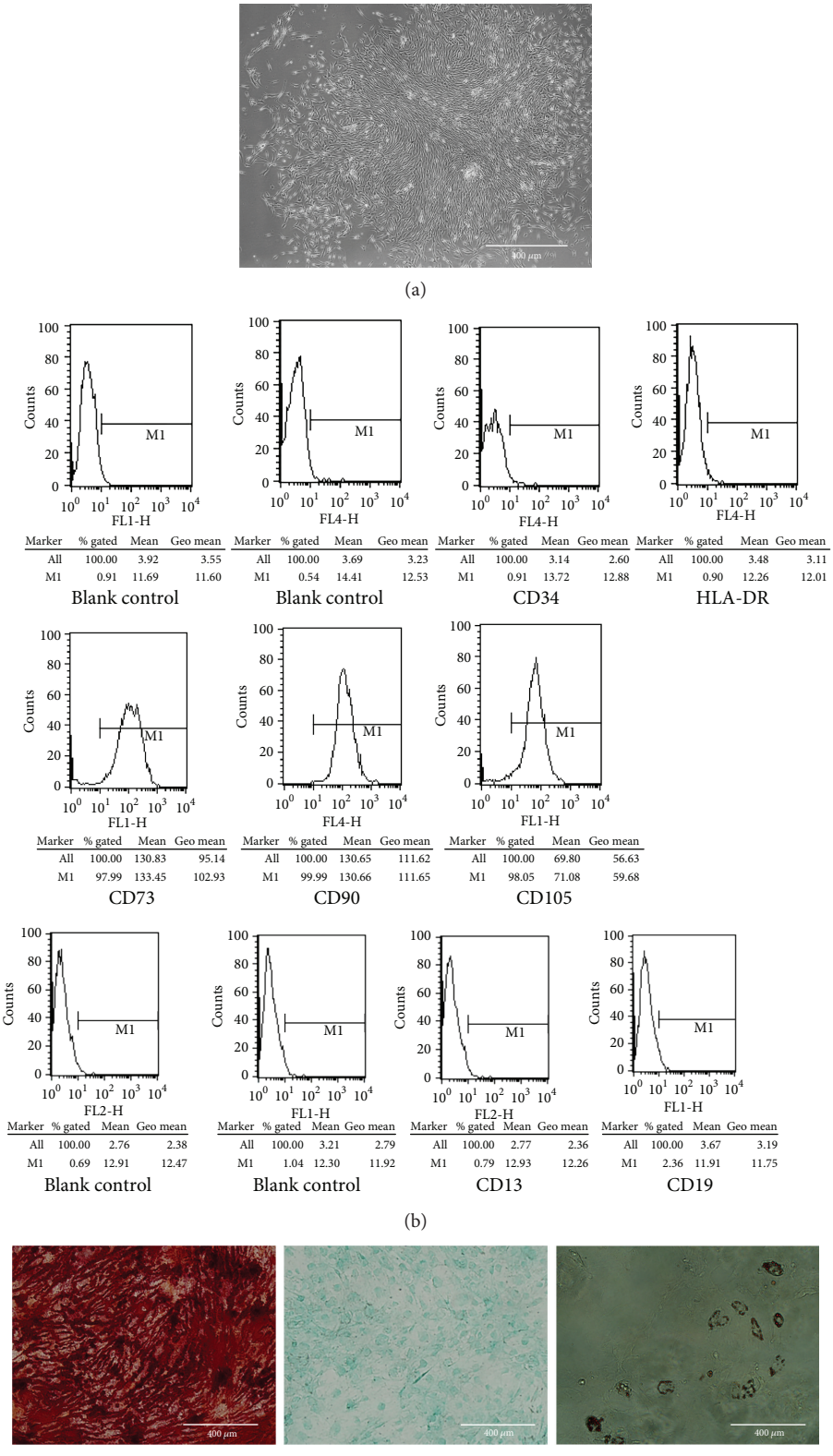

Figure 1: The isolated cells fulfilled the criteria of MSC stated by ISCT. (a) The shape of cells isolated from the degenerated IVDs. (b) The MSC-associated surface markers (CD34, CD14, CD19, HLA-DR, CD73, CD90, and CD105) were analyzed by flow cytometry. (c) The induction of osteogenic, chondrogenic, and adipogenic differentiation of the isolated cells.

wound was created by scraping the monolayer cell with a pipette tip, and the medium was replaced with serum-free DMEM-L. Then, the plates were randomly assigned to the compression group or the control group. The photomicrographs were acquired at different time points (0 h, 24 h, 36 h, and 48 h). The migration areas of wound healing were quantified using ImageJ software.

2.7. Transwell Migration Assay. The 24-well plates with 8 μm pore-size transwell inserts were used to assess the migration abilities of NP-MSCs. The cells were adjusted to a density of 10^5 cells/mL with serum-free DMEM-L, and then 200 μL cell suspension was added into the upper chamber and 600 μL DMEM-L with 10% FBS was added into the lower chamber. Subsequently, the cells were treated with compression for different times (24 h, 36 h, and 48 h), and the cells without compression treatment were used as the control. At the appropriate time points, the nonmigrated NP-MSCs were removed and the migrated cells were fixed and stained with crystal violet. The migrated NP-MSCs were counted in five randomly selected optical fields.

2.8. Quantitative Real-Time Polymerase Chain Reaction (QRT-PCR). Total RNA was extracted from NP-MSCs by TRIzol reagent (Invitrogen, USA); then, the RNA was transcribed into cDNA by a reverse transcription kit (Takara,) following the manufacturer's protocol. After reverse transcription, QRT-PCR was performed with the SYBR Premix Ex Taq II according to the manufacturer's instructions (Takara). The $2^{-\triangle\triangle CT}$ method was used to analyze the data, and the housekeeping gene GAPDH was used to normalize the level of mRNA. Primer sequences were as follows: 5′-GTGGACGAGGCAAGAGTTTCA-3′ (forward) and 5′-GGTGCAGAGTTCAGGGAGGG-3′ (reverse) for RUNX2, 5′-CCCATCCCCACTTTGTGATT-3′ (forward) and 5′-ATTCCGCAGGGCAGCAAC-3′ (reverse) for APP, 5′-AGCATTGCCTATCTGGACGAA-3′ (forward) and 5′-GTACGTGAACCTGCTATTGCC-3′ (reverse) for COL2A1, and 5′-AATCCCATCACCATCTTCCAG-3′ (forward) and 5′-GAGCCCCAGCCTTCTCCAT-3′ (reverse) for GAPDH.

2.9. Western Blot Analysis. NP-MSCs were lysed on ice using standard buffer (Beyotime, China), and total protein was extracted by a protein extraction kit (Beyotime, China). The cell lysate was centrifuged at 12,000 ×g for 10 min at 4°C. After protein transfer, the membranes were blocked by nonfat milk and then incubated overnight at 4°C with a rat polyclonal antibody against cleaved Sox2, Oct4, and GADPH (Abcam, 1 : 3000). After washing several times, the membrane was incubated with secondary antibodies for 1 h at room temperature. Finally, the immunoreactive membranes were visualized via the enhanced chemiluminescence (ECL) method following the manufacturer's instructions (Amersham Biosciences, USA).

2.10. Statistical Analysis. All measurements were performed at least three times. The data were presented as mean ± standard deviation (SD). Student's *t*-tests were used in the analysis of two-group parameters. One-way analysis of variance (ANOVA) test was used in comparisons of multiple sets of data. $p < 0.05$ were considered statistically significant.

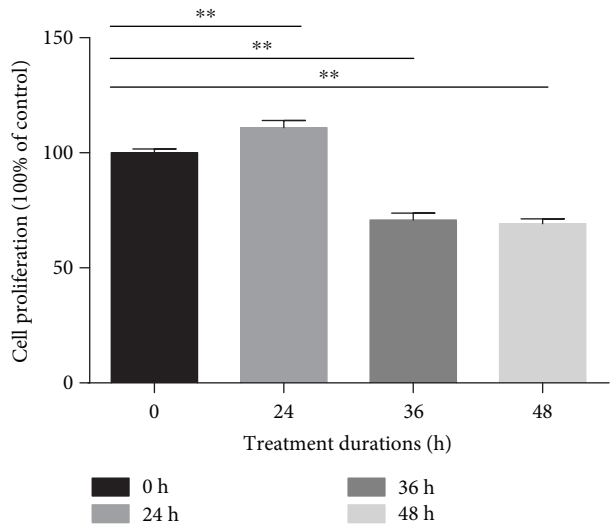

Figure 2: CCK-8 assay showed compression loading inhibiting the viability of NP-MSCs (values are presented as means ± SD, $^{**}p < 0.01$ versus control).

3. Results

3.1. Identification of NP-MSCs. The cells isolated from the degenerated IVDs presented with long spindle-shaped adherent growth and grew in a spiral formation (Figure 1(a)). The MSC-associated surface markers were analyzed by flow cytometry. As shown in Figure 1(b), the isolated cells had high expression levels of markers (CD105, CD73, and CD90) that are normally positive in MSCs and had low expression of markers (CD34, CD14, CD19, and HLA-DR) that are usually negative in MSCs. For osteogenic differentiation, the cells formed highly visible calcium deposits after being induced in osteogenic media for two weeks. In addition, oil droplets were accumulated in the cells and stained with Oil Red O during the adipogenic differentiation. After being induced in chondrogenic media, the cells exhibited strong production of sulfated proteoglycans (Figure 1(c)). The results above showed that the isolated cells fulfilled the criteria of MSC stated by ISCT. Thus, we isolated NP-MSCs, and the cells in passage 2 were used in this study.

3.2. Compression Loading Inhibited the Viability. To evaluate the effect of the compression loading on the viability of NP-MSCs, a CCK-8 assay was performed. As observed in Figure 2, the viability of the NP-MSCs was inhibited by compression and the inhibiting effect was significantly increased as compression time was prolonged except for the time of 24 h, which has shown an increased cell viability. A possible explanation of this phenomenon is that moderate compression may increase the cell viability, but this improvement cannot contribute to the stemness ability of intervertebral disc stem cells (Figure 2, values are presented as means ± SD, $^{*}p < 0.05$ and $^{**}p < 0.01$ versus control).

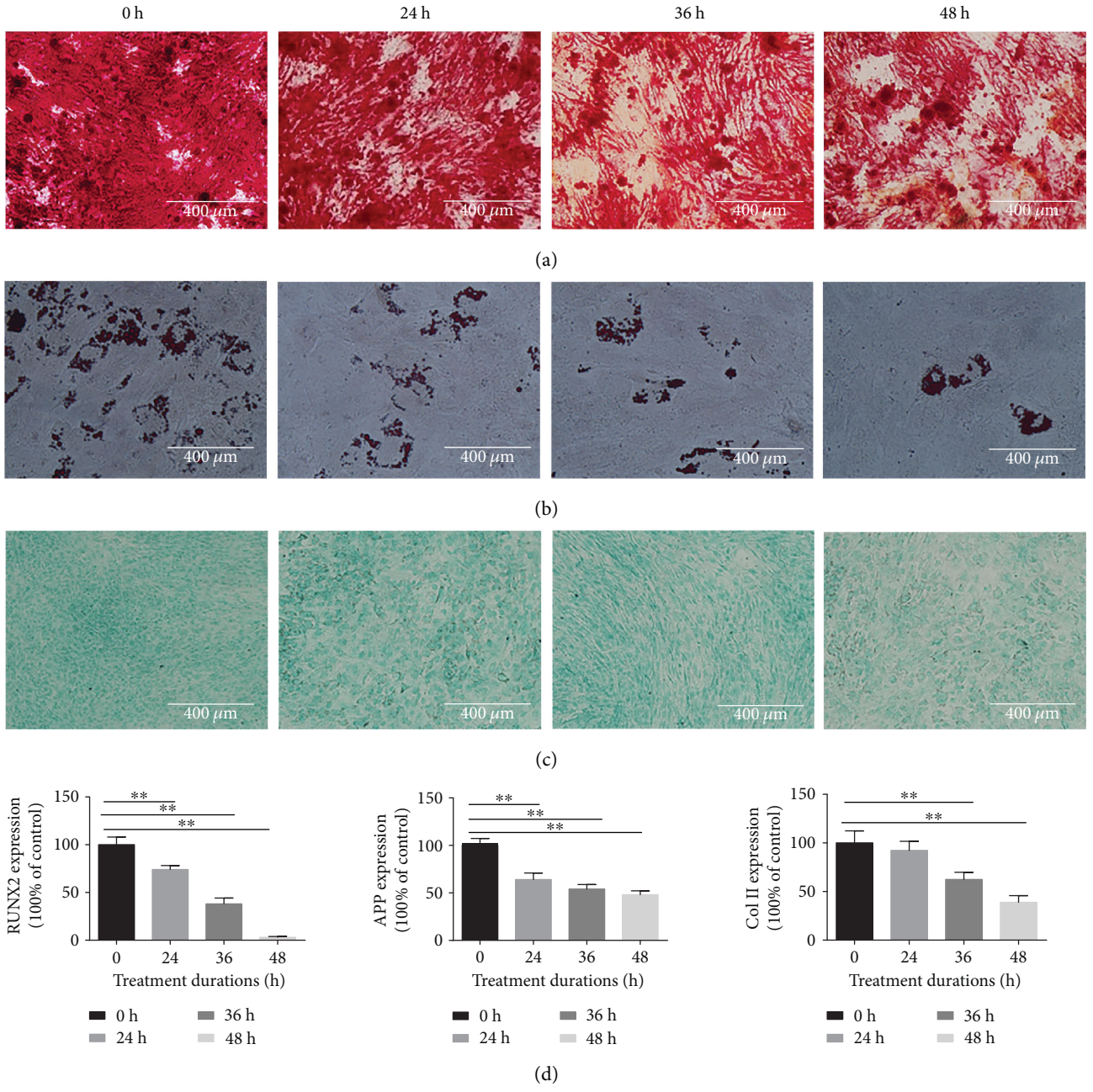

Figure 3: Compression inhibited the multilineage differentiation potential of NP-MSCs. (a) The induction of osteogenic differentiation under the increased compression time from 0 h to 48 h. (b) The induction of adipogenic differentiation under the increased compression time from 0 h to 48 h. (c) The induction of chondrogenic differentiation under the increased compression time from 0 h to 48 h. (d) The expressions of osteogenesis genes (Runx2), adipocyte-specific genes (APP), and chondrocyte-specific genes (Col2) under the increased compression time from 0 h to 48 h (values are presented as means ± SD, $^{**}p < 0.01$ versus control).

3.3. Compression Inhibited the Multilineage Differentiation Potential of NP-MSCs. To determine the effect of the compression loading on the multilineage differentiation potential of NP-MSCs, the osteogenic, adipogenic, and chondrogenic differentiation was induced and the mRNA expressions of Runx2, APP, and Col2 for the osteogenic, adipogenic, and chondrogenic differentiation, respectively, were analyzed. The results showed that the multilineage differentiation was suppressed in accordance with the increased compression time from 0 h to 48 h. For osteogenic differentiation, the mineralized nodules and the expressions of osteogenesis genes (Runx2) significantly decreased in the NP-MSCs with compression treatment (Figures 3(a) and 3(d)). For adipogenic differentiation, the accumulated lipid vacuoles decreased and the expression of adipocyte-specific genes (APP) significantly downregulated (Figures 3(b) and 3(d)). For chondrogenic differentiation, the proteoglycans and the expressions of chondrocyte-specific genes (Col2) obviously decreased (Figures 3(c) and 3(d)). (Figure 3, values are presented as means ± SD, $^{*}p < 0.05$ and $^{**}p < 0.01$ versus control).

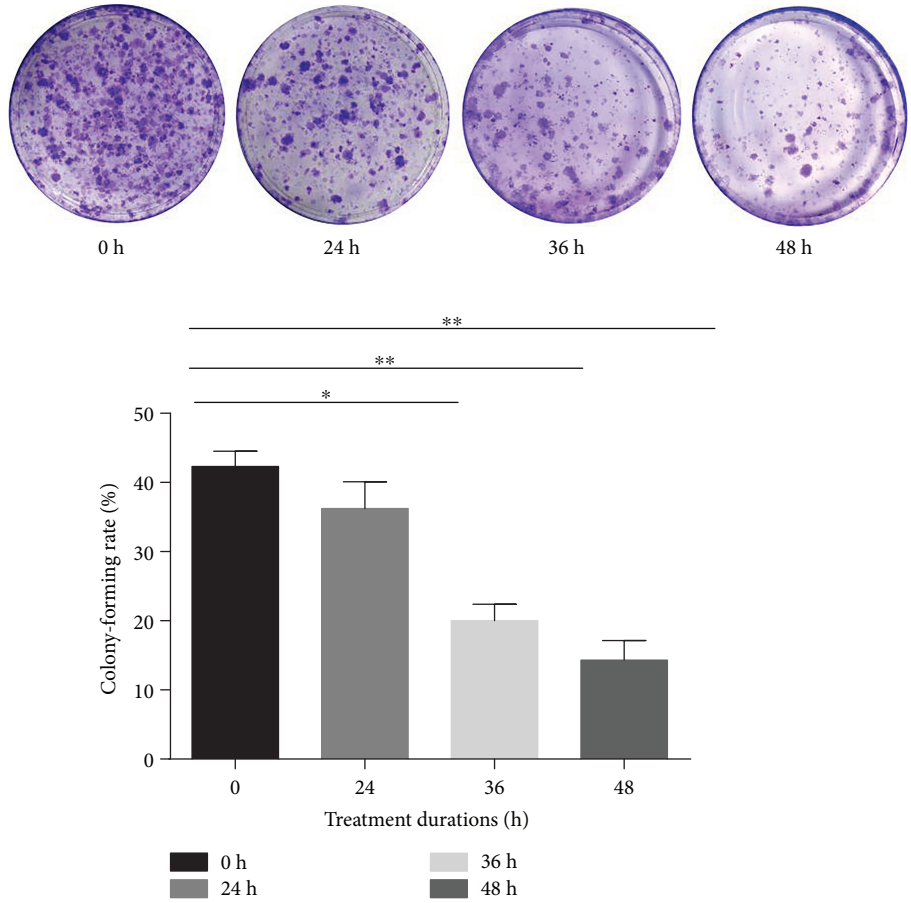

Figure 4: Compression inhibited the capacity of colony formation (values are presented as means ± SD, $^{*}p < 0.05$ and $^{**}p < 0.01$ versus control).

3.4. Compression Inhibited the Capacity of Colony Formation. The colony-forming ability is a vital factor to evaluate the stemness of NP-MSCs. In the control group, the colony-forming rate was 46%. But in the compression group, the results demonstrated that the colony-forming rate was inhibited by 43.33%, 38.27%, 19.4%, and 14.33% compared to the control at different time points from 24 h to 48 h (Figure 4, values are presented as means ± SD, $^{*}p < 0.05$ and $^{**}p < 0.01$ versus control).

3.5. Compression Inhibited the Migration Ability. Nondirectional migration ability and directional migration ability were assessed by wound healing assay and transwell migration assay, respectively. As shown in Figure 5, the migration areas and the migrated NP-MSCs were increased over time. However, the migration areas and the migrated NP-MSCs significantly decreased compared to those at different time points from 24 h to 48 h (Figure 5, values are presented as means ± SD, $^{*}p < 0.05$ and $^{**}p < 0.01$ versus control).

3.6. Compression Decreased the Expression of Stem Cell-Related Genes (Sox2 and Oct4). The genes, including Sox2 and Oct4, were considered the specific genes that maintained the stemness of MSCs. The expression of proteins (Sox2 and Oct4) was significantly decreased. Protein levels of Sox2 and Oct4 from treated cell lysates were analyzed by Western blotting and normalized against GAPDH levels (Figure 6, values are presented as means ± SD, $^{*}p < 0.05$ and $^{**}p < 0.01$ versus control).

4. Discussion

Endogenous stem cell repair for IVD degeneration provides a novel strategy to reverse the structure and mechanical function of IVD tissues, and it has excited a great interest to scientists in the past decade. In 2007, Risbud et al. [21] isolated and identified the skeletal progenitor cells from degenerate human disc in vitro, which could express a series of specific surface markers of MSCs and commit to multilineage differentiation. In 2009, Henriksson et al. [22] applied the labeling technique in vivo and demonstrated the existence of slow-cycling cells and stem cell niche in the IVD region. After that, many groups isolated and identified MSCs from the nucleus pulposus, annulus fibrosus, and cartilage endplate [10, 11, 23–30]. In the present study, the cells isolated from NP had the following characteristics: (1) the cells presented with long spindle-shaped adherent growth and grew in a spiral formation; (2) the cells were positive for CD105, CD73, and CD90 and negative for CD34, CD14, CD19, and HLA-

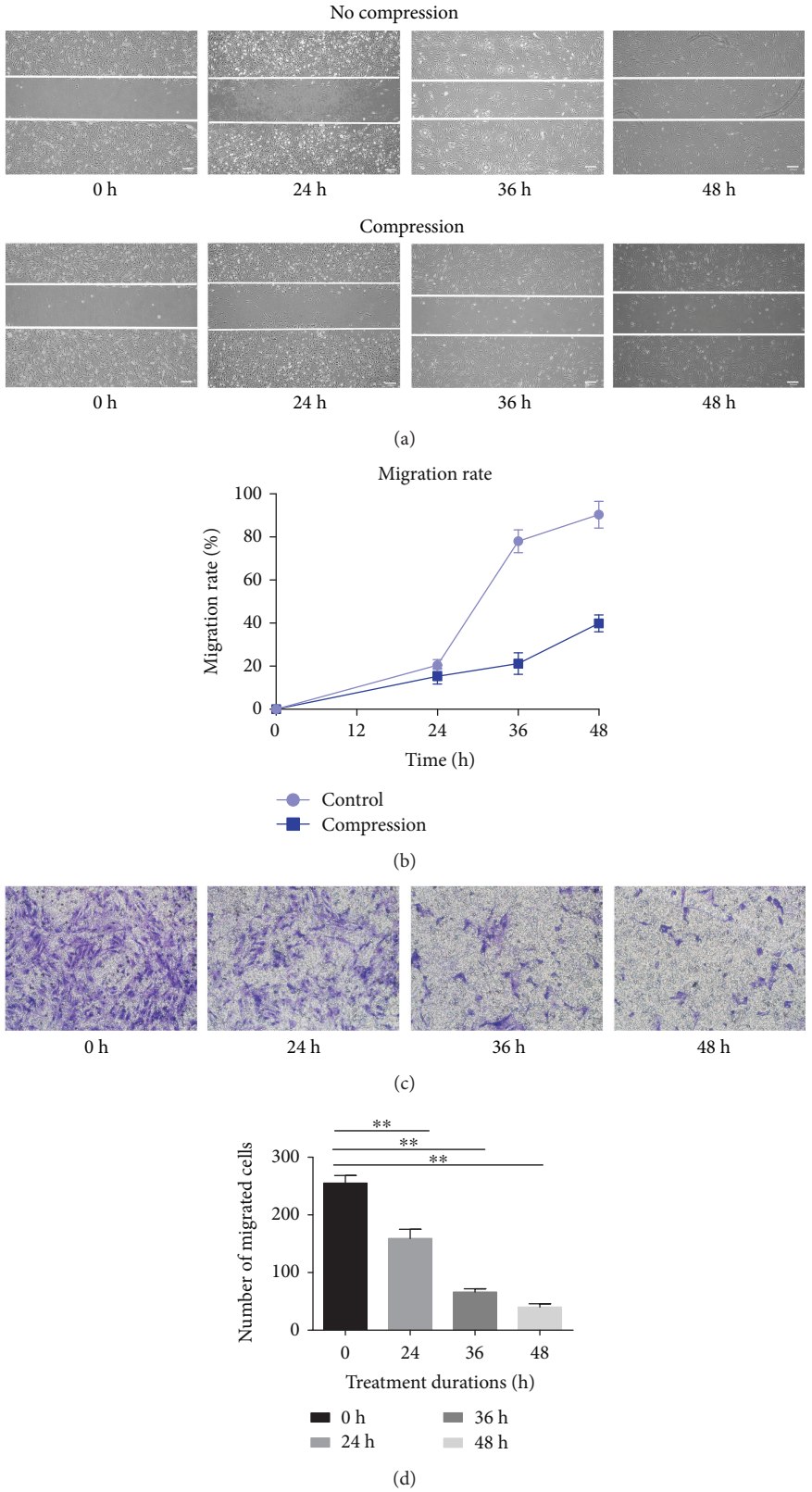

Figure 5: Compression inhibited the migration ability. (a, c) The assessment of nondirectional migration ability by wound healing assay with or without compression from 0 h to 48 h. (b, d) The assessment of directional migration ability by transwell migration assay under compression from 0 h to 48 h (values are presented as mean ± SD, $^{**}p < 0.01$ versus control).

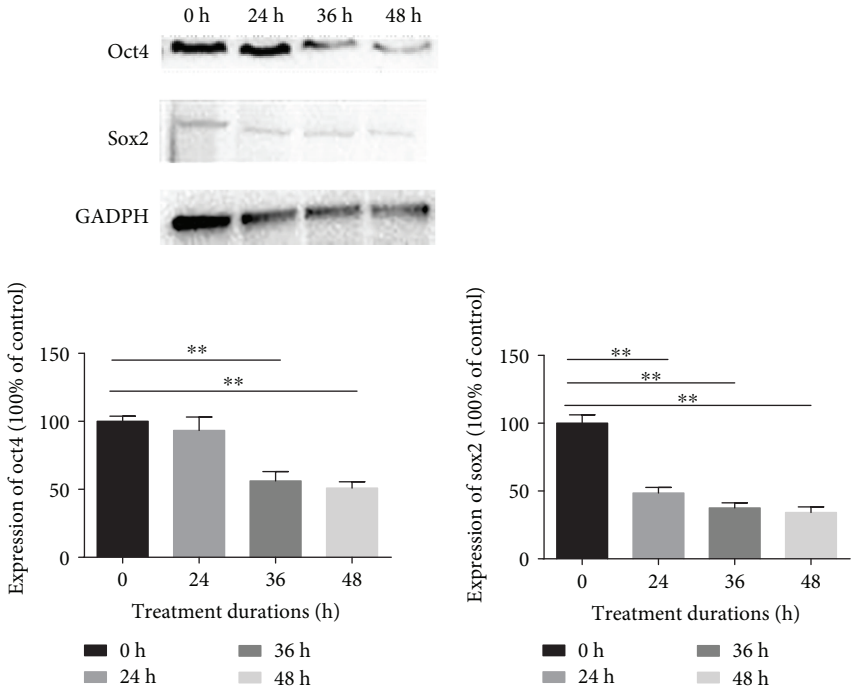

Figure 6: Compression decreased the expression of stem cell-related genes (Sox2 and Oct4). The expression of Sox2 and Oct4 was analyzed by Western blotting and normalized against GAPDH levels (values are presented as mean ± SD, $^{**}p < 0.01$ versus control).

DR; and (3) the cells had the multilineage differentiation potential. These characteristics met the criteria stated by the ISCT for MSC.

In the progress of endogenous tissue regeneration, a single stem cell produces two daughter cells: one maintains the stemness to renew itself while the other differentiates to a specific cell to conduct endogenous repair [31]. In terms of endogenous NP-MSC repair for IVD degeneration, one part of NP-MSCs retains the stem cell identity, and another part of NP-MSCs differentiates into nucleus pulposus-like cells and stimulus disc cells to repair the degenerative disc. Therefore, sustaining the number of viable and functional NP-MSCs is vital for maintaining the IVD homeostasis [9]. However, the IVD is avascular and NP-MSCs in the discs have to bear various stresses, including acidity, hypoxia, nutrient deficiency, and hypertonicity and mechanical loads [12]. Although mechanical stress plays an essential role in the progression of IVD degeneration, there have been no studies reporting the effect of compression loading on human NP-MSCs so far. Thus, the current study applied a custom-made compression apparatus for the first time to study the effect of compression loading on the biological behavior of NP-MSCs in vitro.

The results showed that the viability of the NP-MSCs was inhibited by compression except for the time of 24 h, which has shown an increased cell viability. A possible explanation of this phenomenon is that moderate compression may increase the cell viability, but this improvement cannot contribute to the stemness ability of intervertebral disc stem cells. Stem cells may be a special type of intervertebral disc cells which can react to a short time of compression; however, the differentiation ability, migration ability, and the expression of stem protein have shown a damage when the cells were exposed to the compression of 24 h. We have to say it is interesting and a little strange, but we all know that cell viability cannot be the representative sign of other abilities so this phenomenon needs further research. What is more, the multilineage differentiation potential was also inhibited by compression. But Dai et al. and Kim et al. reported that dynamic compression promoted the proliferation and differentiation of exogenous mesenchymal stem cells [32, 33]. We considered that the conflicting results mainly came from the different modes of compression exerted on cells and the distinct cell types used in the study. In the present study, 1.0 MPa and continuous compression was applied, and NP-MSCs isolated from degenerative NP tissue were used. However, in the study of Dai et al. and Kim et al., lower (17 kPa, 0.2 MPa) and intermittent compression was applied, and viable exogenous MSCs isolated from adipose tissue or bone marrow were used. It was reported that the intradiscal pressure value in a healthy human is around 0.1 MPa in a prone position, 0.5 MPa in a standing position, 1.1 MPa in a flexed position, and even 2.3 MPa in a standing position carrying a weight [15, 34]. Moreover, multiple stress peaks appear under aging and degeneration environment in the IVD [15]. Therefore, our study simulated the effect of excessive compression in degenerative discs on NP-MSCs and emphasized the research of the endogenous repair failure during IVDD.

MSCs can generate colonies when plated at low densities and can also migrate to sites of injury. It has been shown that the colony-forming ability and migration ability are the important biological characteristics of MSCs [35, 36]. The results revealed that compression loading inhibited the

colony-forming ability and migration ability. Stem cell-related genes and proteins (Sox2 and Oct4) also play a vital role in maintaining MSC properties [37, 38]. In keeping with our results above, compression loading suppressed the expression of Sox2 and Oct4. All results in this study suggested that inappropriate or excessive compression loading inhibited the biological behavior of NP-MSCs and might be one of the mechanisms of endogenous repair failure for IVD degeneration. Before the IVD tissue-derived MSCs were isolated, many attentions were concentrated on the fate of disc cells and the repair mainly centered around how to supply the disc cells with exogenous cells, growth factors, or biomaterial [16, 39, 40]. Little is known about endogenous stem cells and endogenous repair. The present study investigated the effect of compression on the biological behavior of NP-MSCs in vitro and tried to enhance our understanding on the endogenous repair failure for IVD degeneration. Moreover, it provided a novel method to repair IVD degeneration by activating the endogenous NP-MSCs.

In conclusion, findings from our study demonstrated that the biological behavior of NP-MSCs could be inhibited by compression loading, and it might be one of the mechanisms of endogenous repair failure for IVD degeneration. Further studies discussing the effect of compression on NP-MSCs in vivo and the underlying specific mechanism may be helpful to understand the endogenous repair failure of NP-MSCs during IVD degeneration.

Abbreviations

NP-MSCs: Nucleus pulposus-derived mesenchymal stem cells
ISCT: International Society for Cellular Therapy
IVD: Intervertebral disc
MSCs: Mesenchymal stem cells
MRI: Magnetic resonance images
NP: Nucleus pulposus
ECM: Extracellular matrix
CCK-8: Cell viability assay
QRT-PCR: Quantitative real-time polymerase chain reaction
SD: Standard deviation
ANOVA: One-way analysis of variance.

Data Availability

The data used to support the findings of this study are available from the corresponding author upon request.

Disclosure

Hang Liang, Sheng Chen, Donghua Huang, and Xiangyu Deng share the first authorship.

Conflicts of Interest

All the authors declare no conflict of interest.

Authors' Contributions

All the authors contribute equally to this paper.

Acknowledgments

The authors want to say thanks to the National Key Research and Development Program of China (Grant no. 2016YFC1100100) and the National Natural Science Foundation of China (Grant nos. 81572203 and 91649204); all the authors want to show their special thanks to their families, as well as for their support and love.

References

[1] K. Luoma, H. Riihimaki, R. Luukkonen, R. Raininko, E. Viikari-Juntura, and A. Lamminen, "Low back pain in relation to lumbar disc degeneration," *Spine*, vol. 25, no. 4, pp. 487–492, 2000.

[2] Y. R. Rampersaud, A. Bidos, C. Fanti, and A. V. Perruccio, "The need for multidimensional stratification of chronic low back pain (LBP)," *Spine*, vol. 42, no. 22, pp. E1318–E1325, 2017.

[3] W. Tong, Z. Lu, L. Qin et al., "Cell therapy for the degenerating intervertebral disc," *Translational Research*, vol. 181, pp. 49–58, 2017.

[4] D. Oehme, T. Goldschlager, P. Ghosh, J. V. Rosenfeld, and G. Jenkin, "Cell-based therapies used to treat lumbar degenerative disc disease: a systematic review of animal studies and human clinical trials," *Stem Cells International*, vol. 2015, Article ID 946031, 16 pages, 2015.

[5] D. Sakai, "Stem cell regeneration of the intervertebral disk," *Orthopedic Clinics of North America*, vol. 42, no. 4, pp. 555–562, 2011.

[6] D. Sakai and S. Grad, "Advancing the cellular and molecular therapy for intervertebral disc disease," *Advanced Drug Delivery Reviews*, vol. 84, pp. 159–171, 2015.

[7] H. Yang, C. Cao, C. Wu et al., "TGF-βl suppresses inflammation in cell therapy for intervertebral disc degeneration," *Scientific Reports*, vol. 5, no. 1, article 13254, 2015.

[8] L. Orozco, R. Soler, C. Morera, M. Alberca, A. Sánchez, and J. García-Sancho, "Intervertebral disc repair by autologous mesenchymal bone marrow cells: a pilot study," *Transplantation*, vol. 92, no. 7, pp. 822–828, 2011.

[9] D. Sakai and G. B. J. Andersson, "Stem cell therapy for intervertebral disc regeneration: obstacles and solutions," *Nature Reviews Rheumatology*, vol. 11, no. 4, pp. 243–256, 2015.

[10] Q. Shen, L. Zhang, B. Chai, and X. Ma, "Isolation and characterization of mesenchymal stem-like cells from human nucleus pulposus tissue," *Science China Life Sciences*, vol. 58, no. 5, pp. 509–511, 2015.

[11] J. F. Blanco, I. F. Graciani, F. M. Sanchez-Guijo et al., "Isolation and characterization of mesenchymal stromal cells from human degenerated nucleus pulposus: comparison with bone marrow mesenchymal stromal cells from the same subjects," *Spine*, vol. 35, no. 26, pp. 2259–2265, 2010.

[12] F. Wang, R. Shi, F. Cai, Y.-T. Wang, and X.-T. Wu, "Stem cell approaches to intervertebral disc regeneration: obstacles from the disc microenvironment," *Stem Cells and Development*, vol. 24, no. 21, pp. 2479–2495, 2015.

[13] H. Li, Y. Tao, C. Liang et al., "Influence of hypoxia in the intervertebral disc on the biological behaviors of rat adipose- and

nucleus pulposus-derived mesenchymal stem cells," *Cells, Tissues, Organs*, vol. 198, no. 4, pp. 266–277, 2013.

[14] J. Liu, H. Tao, H. Wang et al., "Biological behavior of human nucleus pulposus mesenchymal stem cells in response to changes in the acidic environment during intervertebral disc degeneration," *Stem Cells and Development*, vol. 26, no. 12, pp. 901–911, 2017.

[15] C. Neidlinger-Wilke, F. Galbusera, H. Pratsinis et al., "Mechanical loading of the intervertebral disc: from the macroscopic to the cellular level," *European Spine Journal*, vol. 23, no. S3, pp. 333–343, 2014.

[16] R. D. Bowles and L. A. Setton, "Biomaterials for intervertebral disc regeneration and repair," *Biomaterials*, vol. 129, pp. 54–67, 2017.

[17] K.-G. Ma, Z.-W. Shao, S.-H. Yang et al., "Autophagy is activated in compression-induced cell degeneration and is mediated by reactive oxygen species in nucleus pulposus cells exposed to compression," *Osteoarthritis and Cartilage*, vol. 21, no. 12, pp. 2030–2038, 2013.

[18] S. Chen, X. Lv, B. Hu et al., "RIPK1/RIPK3/MLKL-mediated necroptosis contributes to compression-induced rat nucleus pulposus cells death," *Apoptosis*, vol. 22, no. 5, pp. 626–638, 2017.

[19] M. Dominici, K. Le Blanc, I. Mueller et al., "Minimal criteria for defining multipotent mesenchymal stromal cells. The International Society for Cellular Therapy position statement," *Cytotherapy*, vol. 8, no. 4, pp. 315–317, 2006.

[20] F. Ding, Z.-W. Shao, S.-H. Yang, Q. Wu, F. Gao, and L.-M. Xiong, "Role of mitochondrial pathway in compression-induced apoptosis of nucleus pulposus cells," *Apoptosis*, vol. 17, no. 6, pp. 579–590, 2012.

[21] M. V. Risbud, A. Guttapalli, T. T. Tsai et al., "Evidence for skeletal progenitor cells in the degenerate human intervertebral disc," *Spine*, vol. 32, no. 23, pp. 2537–2544, 2007.

[22] H. B. Henriksson, M. Thornemo, C. Karlsson et al., "Identification of cell proliferation zones, progenitor cells and a potential stem cell niche in the intervertebral disc region: a study in four species," *Spine*, vol. 34, no. 21, pp. 2278–2287, 2009.

[23] C. Sang, X. Cao, F. Chen, X. Yang, and Y. Zhang, "Differential characterization of two kinds of stem cells isolated from rabbit nucleus pulposus and annulus fibrosus," *Stem Cells International*, vol. 2016, Article ID 8283257, 14 pages, 2016.

[24] L. T. Liu, B. Huang, C. Q. Li, Y. Zhuang, J. Wang, and Y. Zhou, "Characteristics of stem cells derived from the degenerated human intervertebral disc cartilage endplate," *PLoS One*, vol. 6, no. 10, article e26285, 2011.

[25] C. Liu, Q. Guo, J. Li et al., "Identification of rabbit annulus fibrosus-derived stem cells," *PLoS One*, vol. 9, no. 9, article e108239, 2014.

[26] B. Huang, L.-T. Liu, C.-Q. Li et al., "Study to determine the presence of progenitor cells in the degenerated human cartilage endplates," *European Spine Journal*, vol. 21, no. 4, pp. 613–622, 2012.

[27] H. Wang, Y. Zhou, T.-W. Chu et al., "Distinguishing characteristics of stem cells derived from different anatomical regions of human degenerated intervertebral discs," *European Spine Journal*, vol. 25, no. 9, pp. 2691–2704, 2016.

[28] R. Shi, F. Wang, X. Hong et al., "The presence of stem cells in potential stem cell niches of the intervertebral disc region: an in vitro study on rats," *European Spine Journal*, vol. 24, no. 11, pp. 2411–2424, 2015.

[29] W. M. Erwin, D. Islam, E. Eftekarpour, R. D. Inman, M. Z. Karim, and M. G. Fehlings, "Intervertebral disc-derived stem cells," *Spine*, vol. 38, no. 3, pp. 211–216, 2013.

[30] S. Liu, H. Liang, S. M. Lee, Z. Li, J. Zhang, and Q. Fei, "Isolation and identification of stem cells from degenerated human intervertebral discs and their migration characteristics," *Acta Biochimica et Biophysica Sinica*, vol. 49, no. 2, pp. 101–109, 2016.

[31] H. Clevers, K. M. Loh, and R. Nusse, "An integral program for tissue renewal and regeneration: Wnt signaling and stem cell control," *Science*, vol. 346, no. 6205, article 1248012, 2014.

[32] J. Dai, H. Wang, G. Liu, Z. Xu, F. Li, and H. Fang, "Dynamic compression and co-culture with nucleus pulposus cells promotes proliferation and differentiation of adipose-derived mesenchymal stem cells," *Journal of Biomechanics*, vol. 47, no. 5, pp. 966–972, 2014.

[33] D. H. Kim, S. H. Kim, S. J. Heo et al., "Enhanced differentiation of mesenchymal stem cells into NP-like cells via 3D co-culturing with mechanical stimulation," *Journal of Bioscience and Bioengineering*, vol. 108, no. 1, pp. 63–67, 2009.

[34] H.-J. Wilke, A. Rohlmann, S. Neller, F. Graichen, L. Claes, and G. Bergmann, "ISSLS prize winner: a novel approach to determine trunk muscle forces during flexion and extension: a comparison of data from an *in vitro* experiment and *in vivo* measurements," *Spine*, vol. 28, no. 23, pp. 2585–2593, 2003.

[35] R. Pochampally, "Colony forming unit assays for MSCs," *Methods in Molecular Biology*, vol. 449, pp. 83–91, 2008.

[36] G. Chamberlain, J. Fox, B. Ashton, and J. Middleton, "Concise review: mesenchymal stem cells: their phenotype, differentiation capacity, immunological features, and potential for homing," *Stem Cells*, vol. 25, no. 11, pp. 2739–2749, 2007.

[37] C. C. Tsai, P. F. Su, Y. F. Huang, T. L. Yew, and S. C. Hung, "Oct4 and Nanog directly regulate Dnmt1 to maintain self-renewal and undifferentiated state in mesenchymal stem cells," *Molecular Cell*, vol. 47, no. 2, pp. 169–182, 2012.

[38] R. Feng and J. Wen, "Overview of the roles of Sox2 in stem cell and development," *Biological Chemistry*, vol. 396, no. 8, pp. 883–891, 2015.

[39] P. Colombier, J. Clouet, C. Boyer et al., "TGF-β1 and GDF5 act synergistically to drive the differentiation of human adipose stromal cells toward *nucleus pulposus*-like cells," *Stem Cells*, vol. 34, no. 3, pp. 653–667, 2016.

[40] R. Tsaryk, A. Gloria, T. Russo et al., "Collagen-low molecular weight hyaluronic acid semi-interpenetrating network loaded with gelatin microspheres for cell and growth factor delivery for nucleus pulposus regeneration," *Acta Biomaterialia*, vol. 20, pp. 10–21, 2015.

Hindawi
Stem Cells International
Volume 2018, Article ID 2562105, 9 pages
https://doi.org/10.1155/2018/2562105

Research Article

Icariin Promotes the Migration of BMSCs In Vitro and In Vivo via the MAPK Signaling Pathway

Feng Jiao,[1] **Wang Tang**,[2] **He Huang**,[1] **Zhaofei Zhang**,[1] **Donghua Liu**,[1] **Hongyi Zhang**,[1] **and Hui Ren**[3]

[1]*Guangzhou Hospital of Integrated Traditional and Western Medicine, China*
[2]*Guangzhou University of Chinese Medicine, China*
[3]*The First Affiliated Hospital of Guangzhou University of Traditional Chinese Medicine, China*

Correspondence should be addressed to Feng Jiao; twjiaofeng123@163.com

Received 27 April 2018; Revised 27 June 2018; Accepted 31 July 2018; Published 18 September 2018

Academic Editor: Zengwu Shao

Bone marrow-derived mesenchymal stem cells (BMSCs) are widely used in tissue engineering for regenerative medicine due to their multipotent differentiation potential. However, their poor migration ability limits repair effects. Icariin (ICA), a major component of the Chinese medical herb Herba Epimedii, has been reported to accelerate the proliferation, osteogenic, and chondrogenic differentiation of BMSCs. However, it remains unknown whether ICA can enhance BMSC migration, and the possible underlying mechanisms need to be elucidated. In this study, we found that ICA significantly increased the migration capacity of BMSCs, with an optimal concentration of 1 μmol/L. Moreover, we found that ICA stimulated actin stress fiber formation in BMSCs. Our work revealed that activation of the MAPK signaling pathway was required for ICA-induced migration and actin stress fiber formation. In vivo, ICA promoted the recruitment of BMSCs to the cartilage defect region. Taken together, these results show that ICA promotes BMSC migration in vivo and in vitro by inducing actin stress fiber formation via the MAPK signaling pathway. Thus, combined administration of ICA with BMSCs has great potential in cartilage defect therapy.

1. Introduction

Osteoarthritis (OA), known as degenerative arthritis or joint disease, may lead to the loss of cartilage [1, 2]. Lack of vessels, nerves, and local progenitor cells leads to difficulty in repairing cartilage. With the development of cell therapies, cell-based repair, which includes treatments with chondrocytes and bone marrow-derived mesenchymal stem cells (BMSCs), has recently attracted considerable attention from researchers. Although autologous chondrocyte implantation for the cartilage treatment is a practical solution, the limited sources and dedifferentiation of chondrocytes cultured in vitro restrict its application [3, 4]. In contrast, BMSCs are easy to obtain, have abundant sources, and exhibit strong reproductive activity. BMSCs can be directed to differentiate into many types of cells damaged by disease under certain conditions. Moreover, BMSCs can secrete active components that promote wound healing [5, 6]. However, BMSCs must successfully migrate to the wound to participate in repair processes. The low recruitment of BMSCs to target tissue deters their repair effect [7, 8]. Based on all these characteristics, enhancing the migration ability of BMSCs may be a promising research direction for treating cartilage defects.

Cell-based repair involves migration of stem cells from the sites where they colonize to the wound. The process of migration is regulated by several distinct but interacting signaling pathways. Among these, the mitogen-activated protein kinase (MAPK) signaling pathway has been widely researched [9, 10] and has been confirmed to regulate microtubules and actin filaments; the latter of which can produce pushing (protrusive) forces or pulling (contractile) forces that are particularly important for whole-cell migration [11–13]. These findings provide new directions for the medicine screening.

Herba Epimedii (HEP) is a widely used traditional Chinese herb in the treatment of OA [14]. Icariin (ICA),

the major pharmacologically active component of HEP, was proven to be an efficient accelerator of cartilage tissue engineering. ICA can accelerate the formation of cartilage matrix and chondroid tissue [15, 16]. Moreover, it has been found that ICA exerts multiple effects on BMSCs by activating MAPK signal pathway, including its ability to promote the proliferation and osteogenic, chondrogenic, and adipogenic differentiation [17–19]. Nonetheless, whether ICA has the potential to promote the migration of BMSCs and whether the possible underlying mechanism occurs via the MAPK signaling pathway remain unclear.

In this study, we assessed the effect of ICA on BMSC migration and its underlying mechanisms. In addition, BMSCs were injected via the ear vein of rabbits with knee articular cartilage defects to investigate the effect of ICA on BMSC migration in vivo.

2. Materials and Methods

2.1. Materials. Three-month-old female New Zealand rabbits (2 ± 0.5 kg) were purchased from the Center of Experimental Animals at Guangzhou University of Chinese Medicine. All animals were treated according to the animal guidelines of Guangzhou University of Chinese Medicine. Experimental measurements were carried out in the Laboratory of Orthopaedics and Traumatology of Chinese Medicine of the Lingnan Medical Research Center at Guangzhou University of Chinese Medicine.

2.2. Cell Culture. BMSCs were isolated and cultured from the bone marrow of 3-month-old female New Zealand rabbits. The cells were cultured in alpha minimum essential medium (MEM) containing 10% fetal bovine serum and 1% penicillin-streptomycin in an incubator at 5% CO_2 at 37°C. The culture flask was washed with phosphate-buffered saline (PBS) to remove nonadherent cells after 72 h. When grown to 80–90% confluence, the BMSCs were trypsinized and passaged, and the medium was replaced every 2 days.

To determine whether the isolated BMSCs possess multipotent differentiation ability in vitro, BMSCs at passage 3 were grown in osteogenic medium consisting of alpha MEM containing 10% fetal bovine serum, 1% penicillin-streptomycin, 0.2% ascorbate, 1% β-glycerophosphate, and 0.01% dexamethasone or chondrogenic medium containing 0.01% dexamethasone, 0.3% ascorbate, 1% insulin-transferrin-selenium (ITS) + supplement, 0.1% sodium pyruvate, 0.1% proline, and 1% TGF-β3 for 14 days. The medium was replaced every three days. The cells were then washed with PBS and then fixed with 4% paraformaldehyde for 10 min. Osteogenic cells were stained with alkaline phosphatase and alizarin red. Chondrogenic cells were stained with alcian blue. Photographs were taken using an inverted microscope with a camera.

2.3. Cell Counting Kit-8 (CCK-8) Assay. Cell proliferation was measured using the CCK-8 assay. BMSCs at passage 4 were seeded in 96-well plates at a density of 5×10^3 cells with four replicates for each group. The groups were as follows: 0 μM ICA, 0.01 μM ICA, 0.1 μM ICA, 1 μM ICA, 10 μM ICA, and 100 μM ICA. Cell proliferation was measured at 12, 24, 36, 48, 72, and 76 h after incubation. The CCK-8 solution was changed after the different intervals of incubation. Then, the plates were then incubated at 37°C for an additional 40 min. The optical density was determined at 520 nm using a microplate reader.

2.4. Scratch Wound-Healing Assay. BMSCs at passage 4 were seeded in 6-well plates at a density of 2×10^5 cells per well. When the cells grew to 95% confluence, the medium was aspirated out of the well, and cells were serum-starved for 12 h. A scratch wound was created with a micropipette tip, and the cells were washed twice with PBS to remove cellular debris and floating cells, followed by incubation with vehicle. The control group was treated with culture medium, and the experimental groups were treated with different doses of ICA. The remaining wound area was observed and photographed using an inverted microscope with a camera at 0, 12, and 24 h.

2.5. Transwell Migration Assay. BMSCs were subjected to serum deprivation for 12 h before being cultured on a polycarbonate porous membrane insert with 8 μm pores (Corning Costar, Shanghai, China). The cell density was adjusted to 1×10^6 cells/mL with alpha MEM containing fetal bovine serum. The cells were divided into the following groups: (1) control group (0 μM ICA in both the upper and lower chambers); (2) 0.1 μM ICA group (upper chamber: 0 μM ICA, lower chamber: 0.1 μM ICA); (3) 1 μM ICA group (upper chamber: 0 μM ICA, lower chamber: 1 μM ICA); and (4) 10 μM group (upper chamber: 0 μM ICA, lower chamber: 10 μM ICA). One hundred microliters of cell suspension were added to the upper chamber, and alpha MEM was added to the lower chamber. The cells were allowed to migrate for 24 h; after which, the polycarbonate membrane was removed, fixed with 70% ethanol for 30 min, and stained with 0.1% crystal violet for 30 min. BMSCs were counted under a fluorescence microscope.

2.6. Rhodamine-Phalloidin Staining. BMSCs were grown in 24-well plates with glass coverslips at a density of 100 cells per well. BMSCs in the control group were treated with alpha MEM, while those in the experimental group were incubated with ICA. After treatment, the cells were washed with PBS, fixed with 4% paraformaldehyde for 10 min, washed with PBS, permeabilized with 0.5% Triton X-100 for 5 min, and incubated with 100 nM rhodamine-phalloidin prepared in 1% bovine serum albumin (BSA). Cells were counterstained with Prolong Gold AntiFade Reagent with DAPI for 30 seconds after washing with PBS. Photographs were taken with a confocal laser scanning microscope.

2.7. Western Blotting. After incubation in growth medium or growth medium containing 1 μM ICA for 30, 60, and 120 min, cells were washed three times with cold PBS and suspended in 60 μL of cell lysis buffer containing protease inhibitors (Beyotime, China). The suspension was centrifuged at 15,000 rpm for 20 min at 4°C, and the supernatant was reserved. The concentration of protein in the sample was measured by a BCA protein quantitation kit, and 10%

sodium dodecyl sulfate–polyacrylamide gel electrophoresis (SDS-PAGE) was used to separate aliquots of lysates containing an equal amount of protein (20 μg) followed by transfer onto polyvinylidene fluoride (PVDF) membranes. The membranes were washed with Tris-buffered saline (TBST), blocked for 1 h at room temperature in TBST containing 5% dry milk, and incubated overnight with specific primary antibodies (phospho-p38, phospho-ERK1/2, and phospho-JNK) at 4°C. Next, the membranes were incubated with secondary antibodies for 1 h at room temperature. Blots were visualized using a standard enhanced chemiluminescence system.

2.8. Immunofluorescence Assay. BMSCs at passage 3 were seeded in 12-well culture plates. When the cells grew to 60% confluence, the medium was aspirated from the plates and replaced with 10 μM 5′-bromo-2-deoxyuridine (BrdU) for 48 h. After the media were aspirated, the cells were covered completely with cold 70% ethanol and fixed for 5 min at room temperature. The cells were then blocked with 5% normal goat serum and incubated with BrdU antibody overnight at 4°C. After rinsing three times with PBS for 5 min each, the cells were incubated in fluorochrome-conjugated secondary antibody diluted in Antibody Dilution Buffer for 1 h at room temperature in the dark. In addition, sufficient Prolong Gold AntiFade Reagent with DAPI was applied to cover cells in the 12-well culture plates. Fluorescence microscopy was employed to observe the rate of BrdU labeling.

2.9. Cartilage Defect Model. Fifteen three-month-old healthy female New Zealand white rabbits (2.5 ± 0.3 kg) were randomly divided into the normal control group, BMSC group, and ICA + BMSC group. After anesthesia, the knee joint was exposed, and a full-thickness cylindrical cartilage defect of 4 mm in diameter and 3 mm in depth (reaching the bone marrow exude) was created in the patellar groove using a standard-size stainless steel biopsy punch. In addition, 4×10^5 U penicillin was intramuscularly injected after the operation. Two hours after surgery, rabbits in the experimental group were injected with BMSCs that had been incubated with ICA for 72 h, and rabbits in the BMSC group were injected with BMSCs without ICA pretreatment via the ear vein; the normal control group was injected with PBS. The BMSCs were all labeled with BrdU before injection. The rabbits were housed in separate hutches and allowed to move freely.

2.10. Immunohistochemical Staining of BrdU. The regenerated tissues of all groups were collected 4 weeks after surgery. The sample was fixed in 4% paraformaldehyde for 48 h, decalcified in 10% EDTA for 4 weeks until a needle could impale the tissues, paraffin embedded, and sectioned. After the sections were dewaxed and rehydrated, the slides were submersed in 1× citrate unmasking solution and heated in a microwave until boiling, after which they were maintained for 10 min at a subboiling temperature (95–98°C). After cooling on a bench top for 30 min and three PBS washes for 5 min each, the sections were incubated in 3% hydrogen peroxide for 10 min. The solution was then replaced with BrdU primary antibody for overnight incubation at 4°C. The sections were washed again and incubated with secondary antibody. Then, the sections were washed with PBS and coverslipped. Photographs were taken using an inverted phase contrast microscope. Positively stained BMSCs were quantified in three random areas of each section.

2.11. Statistical Analysis. Statistical analyses were performed using the SPSS 24.0 software. The results were presented as the mean ± standard deviation. Differences among groups were tested by one-way analysis of variance (ANOVA). $P < 0.05$ was considered to indicate a statistically significant difference.

3. Results

3.1. Identification of BMSCs. BMSCs were obtained from rabbits, and their multipotent differentiation ability was detected by osteoplastic and chondrogenic differentiation. BMSCs developed into osteoblasts and chondrocytes after incubation with differentiation solution for 14 days. Osteoplastic cells were detected by alizarin red and alkaline phosphatase, and chondrogenic cells were detected by alcian blue staining. These results showed that many cells remained BMSCs after three generations of subculture (Figure 1).

3.2. Effect of ICA on the Proliferation of BMSCs. To investigate the effect of ICA on BMSC proliferation, we added different doses of ICA and then measured cell proliferation by the CCK-8 assay after 12, 24, 36, 48, 72, and 96 h. As shown in Figure 2, ICA did not noticeably promote BMSC proliferation. There were no statistically significant differences among the groups (Figure 2).

3.3. ICA Accelerates the Migration of BMSCs. The ability of ICA to promote BMSC migration was examined through the wound-healing assay and Transwell migration assay. In the wound-healing assay, many BMSCs in the groups treated with 0.1, 1, and 10 μM ICA but few cells in the control group migrated to the scratch wound at 12 and 24 h after creating the scratch. Among all these groups, the remaining wound area in the group treated with 1 μM ICA was the smallest, and the difference was statistically significant ($P < 0.05$). However, BMSC migration in the 100 μM ICA group was not noticeably promoted compared with that in the control group (Figures 3(a) and 3(b)). As shown in Figure 3(c), the number of cells that migrated to the lower chamber in the 0.1 and 1 μM ICA groups was much higher than that in the control group ($P < 0.05$). Although there was no significant difference in BMSC migration between the 1 μM and 0.1 μM ICA groups, more migrating cells were observed after culture with 1 μM ICA than with 0.1 μM ICA. These results show that 1 μM ICA stimulates BMSC migration.

3.4. ICA Promotes the Migration of BMSCs Probably by Stimulating Actin Stress Fiber Formation. The cytoskeleton is a network of fibers composed of proteins contained within the cytoplasm in all cells of all domains of life, most notably in eukaryotic cells. The cytoskeleton of eukaryotes has three major components: microfilaments, microtubules, and intermediate filaments. By contrast, intermediate

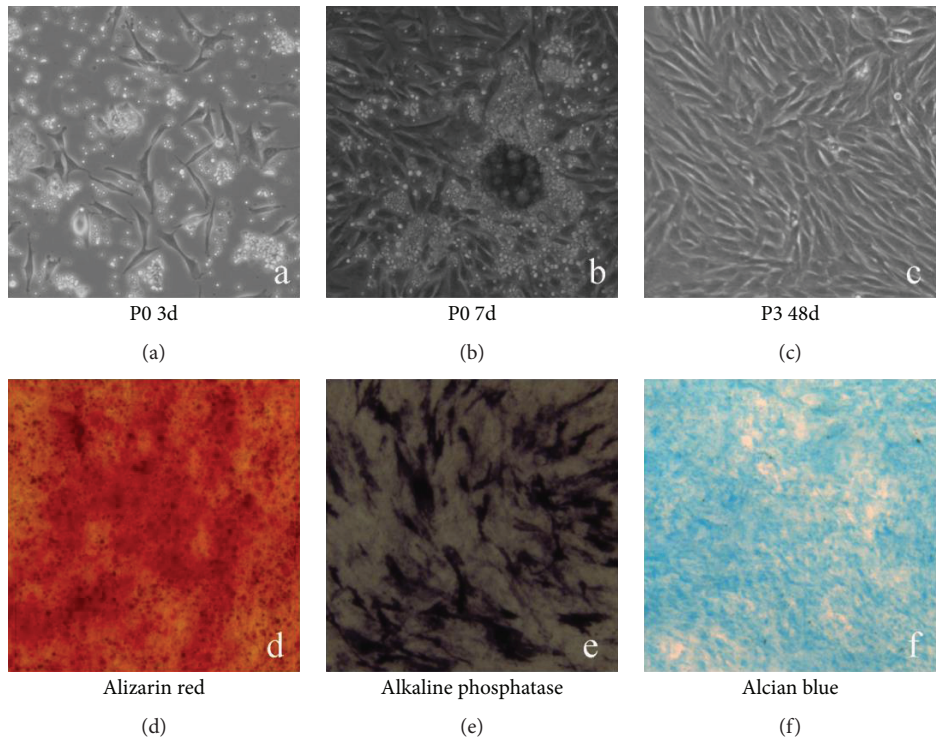

Figure 1: Characteristics of rabbit BMSCs. (a) Few BMSCs grew via static adherence cultured in growth medium in the primary phase. (b) The growth of BMSCs from embryoid body (EB) formation, reaching 80% confluence at day 7. (c) BMSCs at passage 3, reaching confluence 90% after incubation for 48 h. (d) Osteoplastic differentiation revealed by alizarin red staining after 2 weeks. (e) Osteoplastic differentiation revealed by alkaline phosphatase staining after 2 weeks. (f) Chondrogenic differentiation revealed by alcian blue staining after 2 weeks.

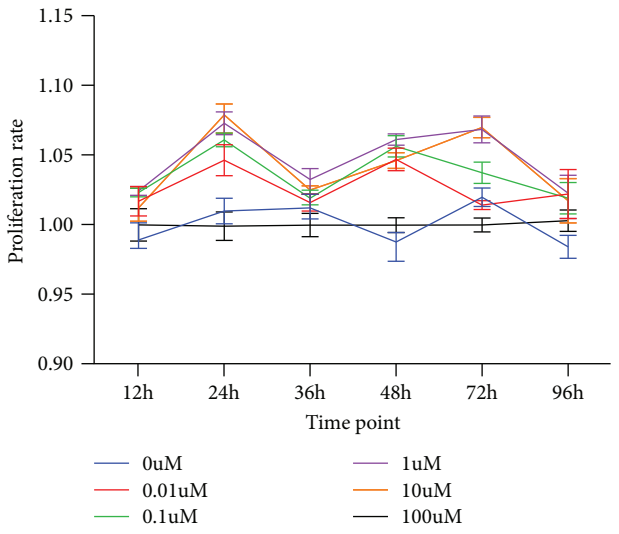

Figure 2: Effect of ICA on the proliferation of BMSCs. BMSCs were treated with various concentrations of ICA (0, 0.01, 0.1, 1, 10, and 100 μM) for 12, 24, 36, 48, 72, and 96 h. The proliferation rate of BMSCs was assessed by the CCK-8 assay.

filaments consist of actin protein, which is the primary force-generating machinery in the cell and can produce pushing forces that can power diverse motility processes. To study the effect of ICA on actin proteins in BMSCs, rhodamine-phalloidin was used to stain actin protein. After ICA treatment (1 μM), the formation of intermediate filaments was apparently increased compared with that in the control group (Figure 3(e)).

3.5. ICA Upregulates Protein Expression of the MAPK Signaling Pathway. There are many signaling pathways involved in BMSC migration, but the MAPK signaling pathway is the most crucial. To examine whether ICA can upregulate the MAPK signaling pathway, cells were treated with ICA (1 μM) for 30, 60, or 120 min, and the expressions of p-P38, extracellular regulated kinase (ERK or p42/p44 MAPK), and jun amino-terminal kinases/stress-activated protein kinase (JNK) were detected by Western blot. We found that p-P38, ERK, and JNK were increased after ICA treatment (Figure 4).

3.6. MAPK Signaling Pathway Participates in the Migration of BMSCs Induced by ICA. To further determine the role of the MAPK signaling pathway in the migration of BMSCs induced by ICA, migration was analysed by a scratch wound-healing assay and rhodamine-phalloidin staining in the presence of the P38-specific inhibitor SB202190, the ERK-specific inhibitor PD98059, or the JNK-specific inhibitor SP600125. As shown in Figure 5(a), in the scratch wound-healing assay, the inhibitor groups exhibited significantly reduced ICA-induced migration of BMSCs. Similar results were also obtained for rhodamine-phalloidin staining. After treatment with ICA in the presence of the three

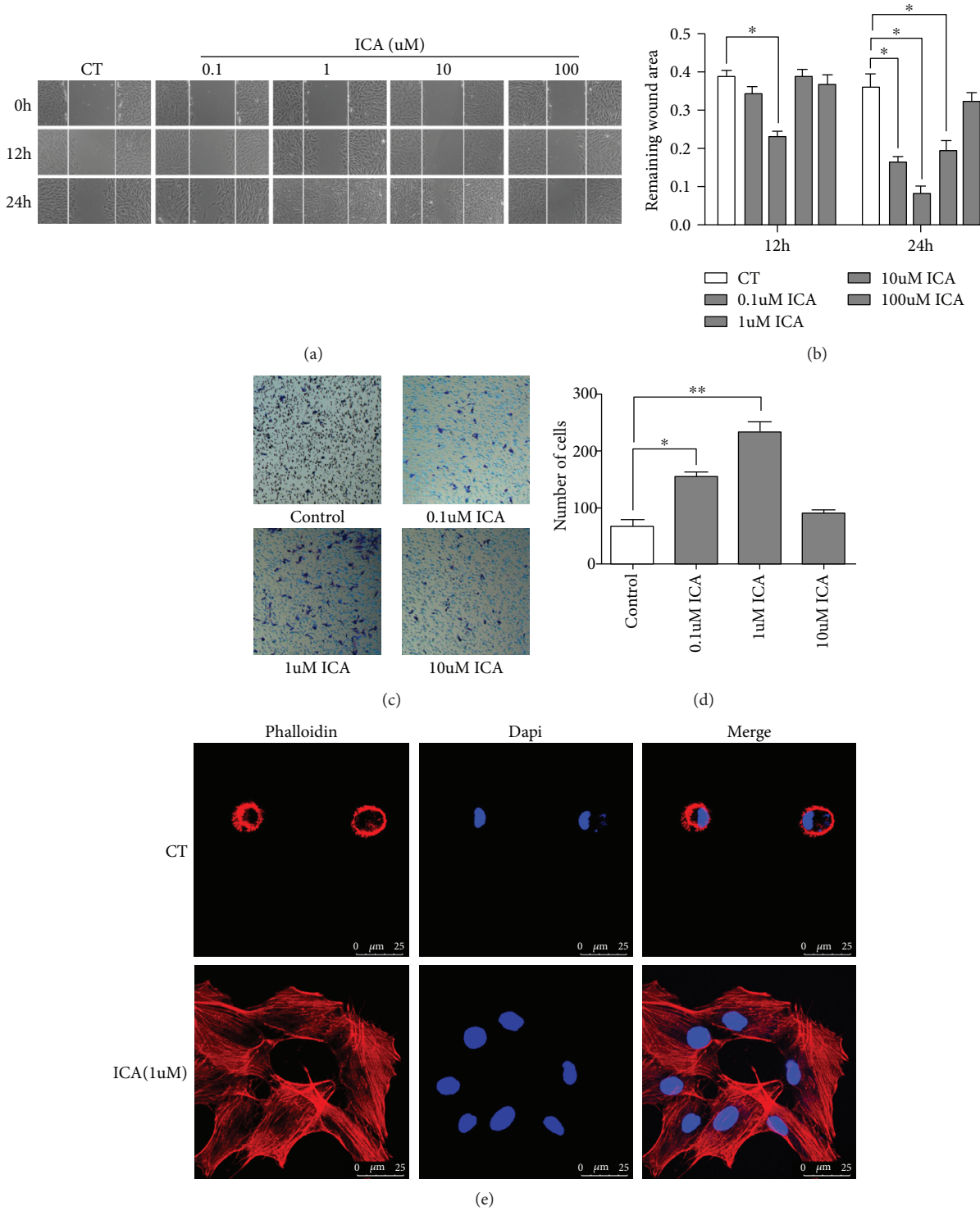

Figure 3: ICA promotes the migration of BMSCs in vitro. (a) Scratch wound-healing assay of BMSCs treated with ICA (0, 0.1, 1, 10, and 100 μM). Phase contrast images were captured after 12 and 24 h. (b) Quantitative analysis of the remaining wound area in Figure 3(a). Three random fields of each group were selected, and the remaining area of wound was measured using Image J. (c) Transwell migration assay of BMSCs treated with ICA (0.1, 1, and 10 μM). The number of BMSCs in the outside bottom chamber was calculated. (d) Quantitative analysis of the migrated cells. The results are shown as the mean value of 5 random fields. (e) ICA stimulated actin stress fiber formation of BMSCs. Data are shown as the mean ± SD of three independent experiments. $^{*}P < 0.05$, $^{**}P < 0.01$ compared with the group control.

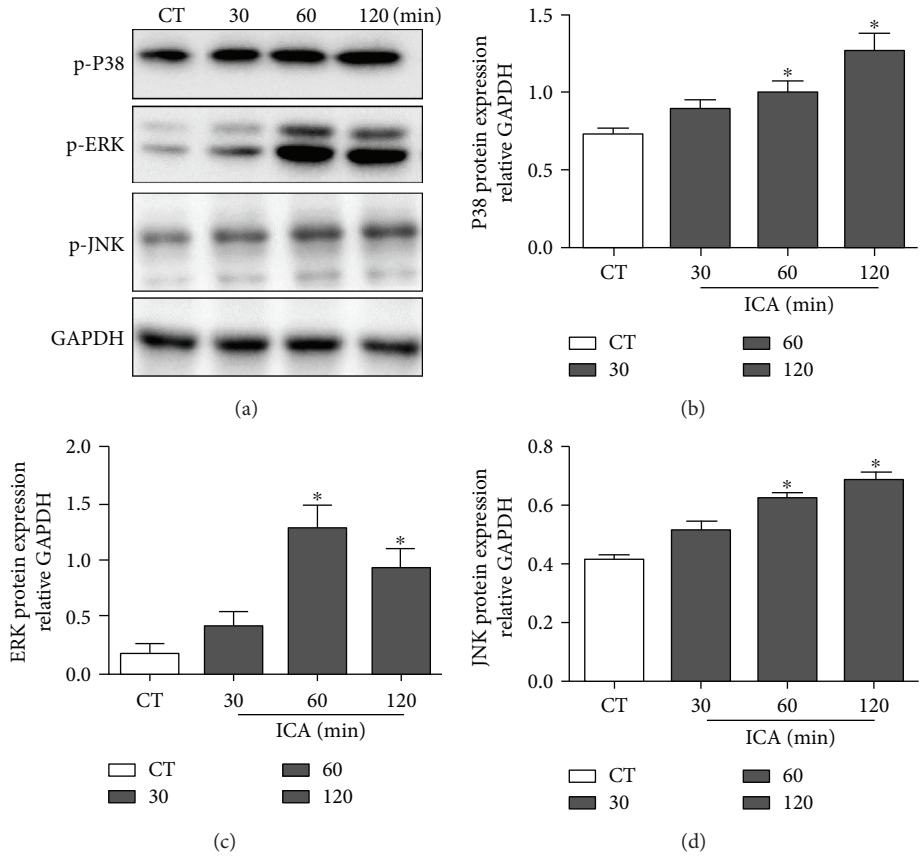

Figure 4: ICA upregulates the protein expression of the MAPK signaling pathway. BMSCs were treated with ICA for 30, 60, and 120 min. Total protein extracts were prepared, and the phosphorylation levels of P38, ERK1/2, and JNK were detected by Western blot. The experiment was repeated at least three times to verify the result. (a) Representative bands of P38, ERK 1/2, and P38. The internal reference was GAPDH. (b, c, d) Densitometric analysis of immunoblotting of phosphorylated-P38, ERK1/2, and JNK compared by one-way ANOVA. Data are shown as the mean ± SD of three independent experiments. $^*P < 0.05$ compared with the group control.

inhibitors, BMSCs had less actin stress fiber formation (Figure 5(b)).

3.7. ICA Improves the Homing Rates of BrdU-Labeled BMSCs. To ensure that most of the BMSCs were labeled by BrdU, an immunofluorescence assay was performed. BMSCs were cultured with 10 μM BrdU for 72 h. Positive cells were labeled with red fluorescence in the nucleus, and the percentage of BrdU-positive cells was 95 ± 2.1% (Figures 6(a) and 6(b)). The $BrdU^+$ cells in the tissues undergoing repair were detected by an immunofluorescence assay at 4 weeks after surgery. As shown in Figure 6(c), there were more BrdU-positive cells in the group that received ICA-treated BMSCs than in the group that received control BMSCs, suggesting that the combination of ICA and BMSCs led to improved migration. Moreover, the distribution of $BrdU^+$ cells in the group that received ICA-treated BMSCs was more extensive and uniform than that in the group that received control BMSCs.

4. Discussion

With the development of cell-based therapies, BMSCs have attracted the attention of researchers for the treatment of OA. As the ideal seed cells for tissue engineering, BMSCs play important roles in the rehabilitation and regeneration of tissue. BMSCs not only have extensive proliferative ability but also retain multilineage mesenchymal differentiation potential [3, 20]. However, the restorative effect of BMSCs is determined by their homing rate, and these cells generally showed limited engraftment upon in vivo implantation due to the hostile microenvironment within the injured tissue [21, 22]. Therefore, increasing the homing rate of BMSCs should improve their therapeutic effects. In the present study, we hypothesized that ICA might promote cell migration. To determine the optimal concentration of ICA for the induction of BMSC migration, concentrations from 0.01 μM to 100 μM were tested in the CCK-8 assay. We found that ICA had no positive effect on BMSC proliferation, which conflicts with other reports [23], most likely due to differences in the species from which the tested cells were obtained. The wound-healing assay and Transwell migration assay showed that 1 μM ICA induced more BMSC migration than other concentrations of ICA. We further showed that ICA promoted the migration of BMSCs probably by stimulating actin stress fiber formation.

Although the underlying mechanism of BMSC migration has not yet been clarified, multiple cell signaling pathways

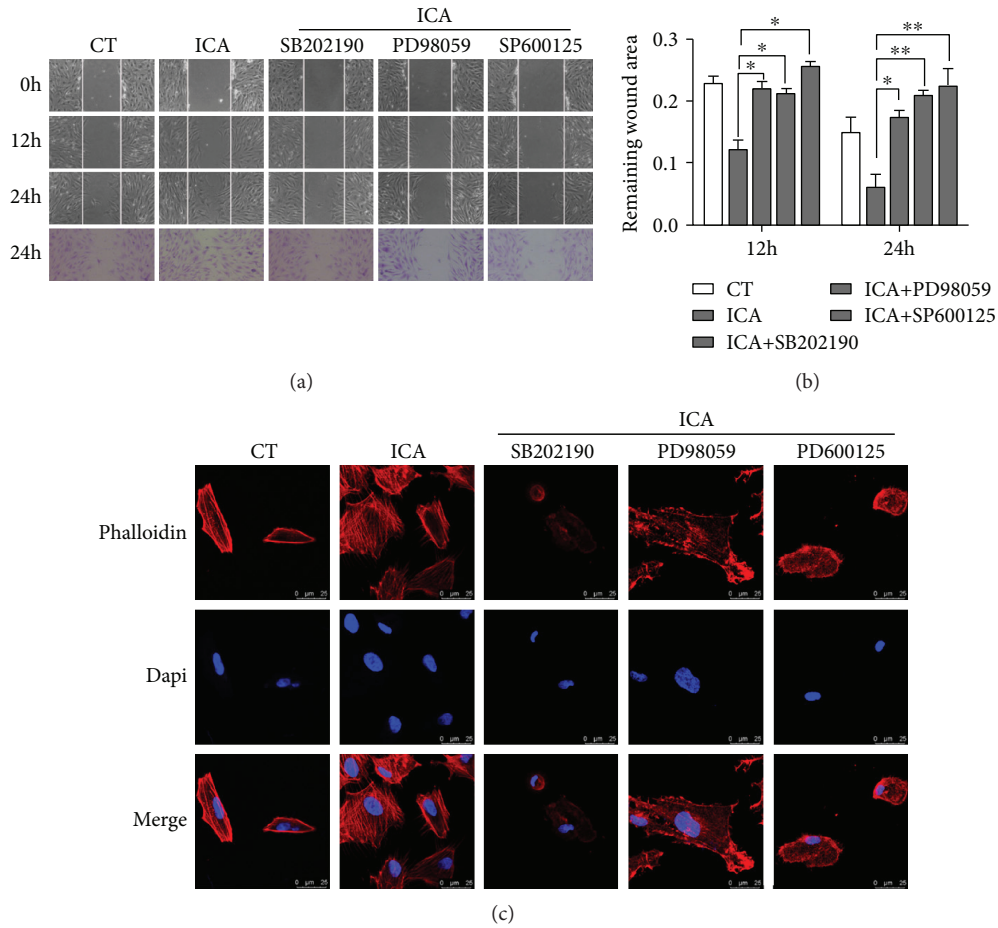

Figure 5: Effect of MAPK inhibitors on the wound-healing assay and rhodamine-phalloidin staining to determine the role of the MAPK signaling pathway in ICA-induced migration. (a) Activation of the MAPK signaling pathway was required for ICA-induced BMSC migration in the scratch wound-healing assay. BMSCs were treated with ICA (1 μM) in the presence of three inhibitors. The wounds were evaluated at 12 and 24 h after scratching. (b) Statistical data analysis of the remaining wound area. (c) ICA induces actin stress fiber formation by upregulating the MAPK signaling pathway. BMSCs were pretreated with the three inhibitors for 1 h. Then, rhodamine-phalloidin staining was performed after treatment with ICA.

have been implicated in the regulation of BMSC migration. The MAPK signaling pathway plays a key role in the process of BMSC migration [24]. The MAPK protein family includes ERK, p38 kinase, and JNK. Extensive evidence has shown that changes in osmotic stress, heat shock, and proinflammatory cytokines can activate the MAPK signaling pathway [10]. When activated, MAPK signaling can enhance myosin light-chain kinase (MLCK) activity, which leads to increased MLC phosphorylation. The phosphorylation of MLC is associated with actin stress fiber formation in the cell body [12]. Our in vitro results suggested that ICA enhanced ERK, p38 kinase, and JNK phosphorylations, and inhibition of them decreased BMSC migration and actin stress fiber formation. These data further verified the complex pleiotropic mechanisms by which BMSC migration is regulated.

To date, many strategies have been developed to improve the homing of BMSCs to the injured site [25–27]. First, BMSCs were genetically engineered to change the genotype of its progeny to improve their homing ability [28]. Second, cytokines were used to induce homing receptor expression in BMSCs to promote their migration [29]. Third, a magnetic system was designed to guide the superparamagnetic iron oxide nanoparticle- (SPION-) labeled cells precisely to the lesion location [30]. However, the safety of the first two methods remains doubtful due to the varying effects [31, 32], and the weakness of the third method is that SPION can cause oxidative damage in tissues. Compared with other strategies, ICA treatment, which by itself was reported to accelerate the formation of cartilage matrix and chondroid tissue, could exert positive effects on BMSCs [19, 23, 33]. In the present study, we successfully labeled the BMSCs with BrdU. The immunofluorescence assay of repairing tissues with the participation of the BrdU-labeled BMSCs showed that ICA could increase the recruitment of BMSCs into the cartilage defect region. Moreover, the distribution of $BrdU^+$ cells in the group that received ICA-treated BMSCs was more extensive and uniform than that in the group that received control BMSCs. This finding demonstrates that ICA-treated BMSCs may become a very promising strategy for the repair of cartilage defects and will increase the possibilities for treatment of other diseases requiring high homing rates.

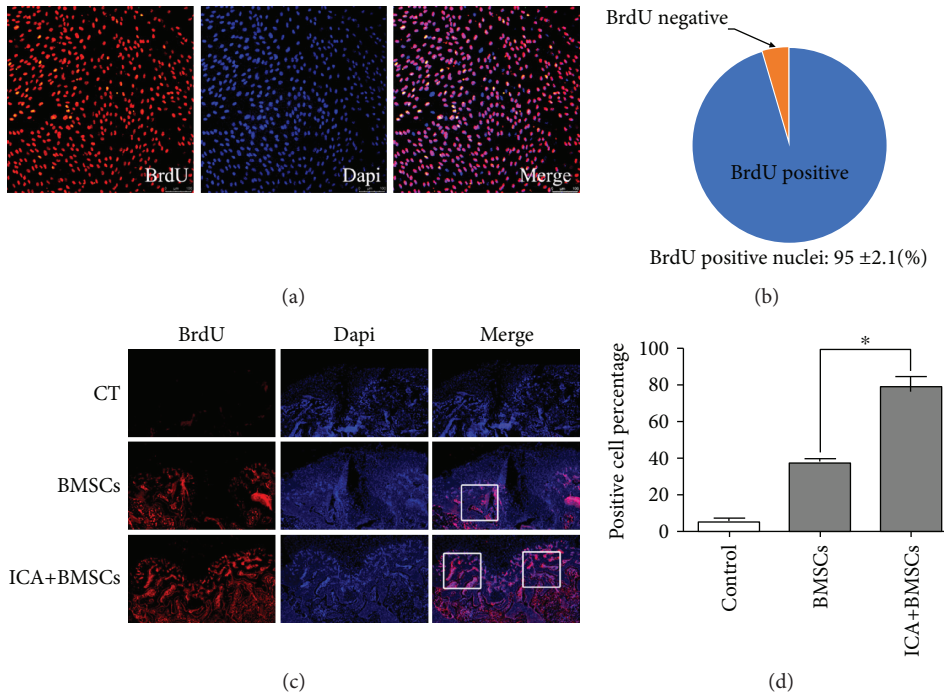

Figure 6: The migration of BrdU-labeled BMSCs in vivo. (a) To observe the migration of BMSCs in vivo, BMSCs were labeled with BrdU. All cells stained with DAPI were shown in blue, while BrdU-positive cells were labeled with red fluorescence. (b) The labeling efficiency of BrdU was 95 ± 2.1%. (c) $BrdU^+$ cells were detected by an immunofluorescence assay at 4 weeks after surgery. The number of BMSCs treated with ICA in the repairing tissue is much greater than that in the group injected with control BMSCs. (d) Statistical data analysis of the positive cell percentage in Figure 6(c). $^*P < 0.05$ compared with the BMSC control.

Although the repairing effect of ICA combined with BMSCs was not detected, the gross appearance showed better results. In future studies, the long-term effects of transplanted ICA-treated BMSCs should be investigated in more detail.

5. Conclusion

In summary, the data reported herein show that ICA promotes BMSC migration in vivo and in vitro. In addition, the mechanism of ICA-induced BMSC migration involves the promotion of actin stress fiber formation via the MAPK signaling pathway. Hence, combined therapy of BMSCs with ICA may confer better results in the treatment of cartilage defects and may be a challenging direction for further study.

Data Availability

The data used to support the findings of this study are available from the corresponding author upon request.

Conflicts of Interest

The authors declare that there is no conflict of interest regarding the publication of this paper.

Acknowledgments

This study was supported by the Traditional Chinese Medicine Bureau of Guangdong Province (no. 20171220).

References

[1] A. M. Lubis and V. K. Lubis, "Adult bone marrow stem cells in cartilage therapy," *Acta Medica Indonesiana*, vol. 44, no. 1, pp. 62–68, 2012.

[2] K. E. Wescoe, R. C. Schugar, C. R. Chu, and B. M. Deasy, "The role of the biochemical and biophysical environment in chondrogenic stem cell differentiation assays and cartilage tissue engineering," *Cell Biochemistry and Biophysics*, vol. 52, no. 2, pp. 85–102, 2008.

[3] J. Gao, J. Q. Yao, and A. I. Caplan, "Stem cells for tissue engineering of articular cartilage," *Proceedings of the Institution of Mechanical Engineers, Part H: Journal of Engineering in Medicine*, vol. 221, no. 5, pp. 441–450, 2007.

[4] M. Mata, L. Milian, M. Oliver et al., "In vivo articular cartilage regeneration using human dental pulp stem cells cultured in an alginate scaffold: a preliminary study," *Stem Cells International*, vol. 2017, Article ID 8309256, 9 pages, 2017.

[5] M. F. Pittenger, A. M. Mackay, S. C. Beck et al., "Multilineage potential of adult human mesenchymal stem cells," *Science*, vol. 284, no. 5411, pp. 143–147, 1999.

[6] H. Nakagawa, S. Akita, M. Fukui, T. Fujii, and K. Akino, "Human mesenchymal stem cells successfully improve skin-substitute wound healing," *British Journal of Dermatology*, vol. 153, no. 1, pp. 29–36, 2005.

[7] E. Chavakis, C. Urbich, and S. Dimmeler, "Homing and engraftment of progenitor cells: a prerequisite for cell therapy," *Journal of Molecular and Cellular Cardiology*, vol. 45, no. 4, pp. 514–522, 2008.

[8] J. M. Karp and G. S. Leng Teo, "Mesenchymal stem cell homing: the devil is in the details," *Cell Stem Cell*, vol. 4, no. 3, pp. 206–216, 2009.

[9] C. Huang, Z. Rajfur, C. Borchers, M. D. Schaller, and K. Jacobson, "JNK phosphorylates paxillin and regulates cell migration," *Nature*, vol. 424, no. 6945, pp. 219–223, 2003.

[10] M. Krishna and H. Narang, "The complexity of mitogen-activated protein kinases (MAPKs) made simple," *Cellular and Molecular Life Sciences*, vol. 65, no. 22, pp. 3525–3544, 2008.

[11] T. Svitkina, "The actin cytoskeleton and actin-based motility," *Cold Spring Harbor Perspectives in Biology*, vol. 10, no. 1, 2018.

[12] K. B. Reddy, S. M. Nabha, and N. Atanaskova, "Role of MAP kinase in tumor progression and invasion," *Cancer Metastasis Reviews*, vol. 22, no. 4, pp. 395–403, 2003.

[13] Y. Shi, Y. Y. Xia, L. Wang, R. Liu, K. S. Khoo, and Z. W. Feng, "Neural cell adhesion molecule modulates mesenchymal stromal cell migration via activation of MAPK/ERK signaling," *Experimental Cell Research*, vol. 318, no. 17, pp. 2257–2267, 2012.

[14] D. Zheng, S. Peng, S. H. Yang et al., "The beneficial effect of icariin on bone is diminished in osteoprotegerin-deficient mice," *Bone*, vol. 51, no. 1, pp. 85–92, 2012.

[15] D. Li, T. Yuan, X. Zhang et al., "Icariin: a potential promoting compound for cartilage tissue engineering," *Osteoarthritis and Cartilage*, vol. 20, no. 12, pp. 1647–1656, 2012.

[16] L. Zhang, X. Zhang, K. F. Li et al., "Icariin promotes extracellular matrix synthesis and gene expression of chondrocytes in vitro," *Phytotherapy Research*, vol. 26, no. 9, pp. 1385–1392, 2012.

[17] S. Zhang, P. Feng, G. Mo et al., "Icariin influences adipogenic differentiation of stem cells affected by osteoblast-osteoclast co-culture and clinical research adipogenic," *Biomedicine & Pharmacotherapy*, vol. 88, pp. 436–442, 2017.

[18] Y. Wu, L. Xia, Y. Zhou, Y. Xu, and X. Jiang, "Icariin induces osteogenic differentiation of bone mesenchymal stem cells in a MAPK-dependent manner," *Cell Proliferation*, vol. 48, no. 3, pp. 375–384, 2015.

[19] Z. C. Wang, H. J. Sun, K. H. Li, C. Fu, and M. Z. Liu, "Icariin promotes directed chondrogenic differentiation of bone marrow mesenchymal stem cells but not hypertrophy in vitro," *Experimental and Therapeutic Medicine*, vol. 8, no. 5, pp. 1528–1534, 2014.

[20] E. L. S. Fong, C. K. Chan, and S. B. Goodman, "Stem cell homing in musculoskeletal injury," *Biomaterials*, vol. 32, no. 2, pp. 395–409, 2011.

[21] C. Toma, W. R. Wagner, S. Bowry, A. Schwartz, and F. Villanueva, "Fate of culture-expanded mesenchymal stem cells in the microvasculature: in vivo observations of cell kinetics," *Circulation Research*, vol. 104, no. 3, pp. 398–402, 2009.

[22] B. M. Gleeson, K. Martin, M. T. Ali et al., "Bone marrow-derived mesenchymal stem cells have innate procoagulant activity and cause microvascular obstruction following intracoronary delivery: amelioration by antithrombin therapy," *Stem Cells*, vol. 33, no. 9, pp. 2726–2737, 2015.

[23] S. Qin, W. Zhou, S. Liu, P. Chen, and H. Wu, "Icariin stimulates the proliferation of rat bone mesenchymal stem cells via ERK and p38 MAPK signaling," *International Journal of Clinical and Experimental Medicine*, vol. 8, no. 5, pp. 7125–7133, 2015.

[24] M. M. Kavurma and L. M. Khachigian, "ERK, JNK, and p38 MAP kinases differentially regulate proliferation and migration of phenotypically distinct smooth muscle cell subtypes," *Journal of Cellular Biochemistry*, vol. 89, no. 2, pp. 289–300, 2003.

[25] B. R. Son, L. A. Marquez-Curtis, M. Kucia et al., "Migration of bone marrow and cord blood mesenchymal stem cells in vitro is regulated by stromal-derived factor-1-CXCR4 and hepatocyte growth factor-c-met axes and involves matrix metalloproteinases," *Stem Cells*, vol. 24, no. 5, pp. 1254–1264, 2006.

[26] A. P. Lykov, Y. V. Nikonorova, N. A. Bondarenko et al., "Proliferation, migration, and production of nitric oxide by bone marrow multipotent mesenchymal stromal cells from Wistar rats in hypoxia and hyperglycemia," *Bulletin of Experimental Biology and Medicine*, vol. 159, no. 4, pp. 443–445, 2015.

[27] S. Bobis-Wozowicz, K. Miekus, E. Wybieralska et al., "Genetically modified adipose tissue–derived mesenchymal stem cells overexpressing CXCR4 display increased motility, invasiveness, and homing to bone marrow of NOD/SCID mice," *Experimental Hematology*, vol. 39, no. 6, pp. 686–696.e4, 2011.

[28] H. Lin, X. Luo, B. Jin, H. Shi, and H. Gong, "The effect of EPO gene overexpression on proliferation and migration of mouse bone marrow-derived mesenchymal stem cells," *Cell Biochemistry and Biophysics*, vol. 71, no. 3, pp. 1365–1372, 2015.

[29] Y. Li, X. Y. Yu, S. G. Lin, X. H. Li, S. Zhang, and Y. H. Song, "Insulin-like growth factor 1 enhances the migratory capacity of mesenchymal stem cells," *Biochemical and Biophysical Research Communications*, vol. 356, no. 3, pp. 780–784, 2007.

[30] D. Tukmachev, O. Lunov, V. Zablotskii et al., "An effective strategy of magnetic stem cell delivery for spinal cord injury therapy," *Nanoscale*, vol. 7, no. 9, pp. 3954–3958, 2015.

[31] A. Saraf and A. Mikos, "Gene delivery strategies for cartilage tissue engineering," *Advanced Drug Delivery Reviews*, vol. 58, no. 4, pp. 592–603, 2006.

[32] F. Buket Basmanav, G. T. Kose, and V. Hasirci, "Sequential growth factor delivery from complexed microspheres for bone tissue engineering," *Biomaterials*, vol. 29, no. 31, pp. 4195–4204, 2008.

[33] Q. Wei, M. C. He, M. H. Chen et al., "Icariin stimulates osteogenic differentiation of rat bone marrow stromal stem cells by increasing TAZ expression," *Biomedicine & Pharmacotherapy*, vol. 91, pp. 581–589, 2017.

Hindawi
Stem Cells International
Volume 2018, Article ID 4258613, 9 pages
https://doi.org/10.1155/2018/4258613

Research Article

Osteogenic Potential of Human Umbilical Cord Mesenchymal Stem Cells on Coralline Hydroxyapatite/Calcium Carbonate Microparticles

A. G. E. Day,[1] W. R. Francis,[1] K. Fu,[2] I. L. Pieper,[1] O. Guy,[3] and Z. Xia[1]

[1]*Institute of Life Science, Swansea University Medical School, Swansea SA2 8PP, UK*
[2]*Department of Orthopaedic Surgery, The First Affiliated Hospital of Hainan Medical College, Hainan, China*
[3]*College of Engineering, Swansea University, Swansea SA2 8PP, UK*

Correspondence should be addressed to K. Fu; fudh168@hotmail.com and Z. Xia; z.xia@swansea.ac.uk

Received 25 March 2018; Accepted 16 May 2018; Published 5 September 2018

Academic Editor: Zhi-Yong Zhang

Coralline hydroxyapatite/calcium carbonate (CHACC) is a biodegradable and osteoconductive bone graft material with promising clinical performance. CHACC has been shown to support proliferation and osteogenic differentiation of human bone marrow mesenchymal stem cells (MSCs) *in vitro* and demonstrated to work as a functional scaffold for bone formation *in vivo*. Umbilical cord matrix is a more accessible and abundant tissue source of MSCs, but its osteogenic capacity in comparison to human bone marrow when cultured on CHACC has not yet been demonstrated. In this study, we assessed the osteogenic differentiation capacity of human MSCs, isolated from bone marrow and umbilical cord matrix and characterised by flow cytometry, when cultured on 200–300 μm CHACC granules. The 3D cultures were characterised by brightfield and scanning electron microscopy (SEM). Osteogenic potential was assessed by immunocytochemistry and qPCR for key markers of bone differentiation (alkaline phosphatase, runx2, type I collagen, and osteocalcin). By day 1, the MSCs had enveloped the surface of the CHACC granules to form organoids, and by day 7, cells had proliferated to bridge nearby organoids. Extracellular matrix deposition and osteogenic differentiation were demonstrated by MSCs from both tissue sources at day 21. However, MSCs from bone marrow demonstrated superior osteogenic differentiation capability compared to those from umbilical cord matrix. In conclusion, it is possible to culture and induce osteogenic differentiation of umbilical cord matrix MSCs on CHACC. Further research is required to optimise the osteogenicity of umbilical cord matrix MSCs to release their full potential as a readily available, accessible, and abundant tissue source for bone tissue engineering.

1. Introduction

Of the diverse range of scaffolds available for use in maxillofacial surgery and dentistry, autografts have been reported to be the "gold standard" with respect to bone grafting procedures [1]. However, harvesting of autografts, usually from the iliac crest, requires surgical intervention, which is associated with additional risks of blood loss, infection, and morbidity, and supply is limited [2, 3]. Other types of grafts include allografts and xenografts, but these can cause an immunological reaction and be rejected by the recipient [3]; so, it is vital to identify suitable alternative materials.

Synthetic biomaterials, such as hydroxyapatite, tricalcium phosphate ceramics and cements, and bioglass, are alternative sources for bone graft substitutes. However, these synthetic biomaterials do not mimic the architecture, porosity, and organic components of the natural bone and are not optimal in regard to biodegradation and host tissue integration or practical to implant or inject. Naturally occurring coral exoskeleton has a porous architecture that is similar to the human trabecular bone [4]. Since its main composition is calcium carbonate, a hydrothermal technique was developed to completely convert the calcium carbonate to be coralline hydroxyapatite (CHA) ceramics for clinical application [5–8].

We have previously reported a coralline hydroxyapatite/calcium carbonate (CHACC) material which shows promising clinical performance when implanted in sizes ranging from 10–100 × 10 × 10 mm^3 [9, 10]. This material not only has properties such as porosity, surface structure, and osteoconductivity of coralline hydroxyapatite (CHA) as previously investigated [5–7] but also improves host tissue integration and can be completely biodegraded during bone remodelling [9]. Herein, we are focusing on smaller-sized CHACC, 200–300 μm particles, with the potential to be injected facilitating administration for maxillofacial and dentistry applications.

To increase the functionality of bone biomaterials by hopefully contributing towards remodelling and host integration, stem cells are commonly added [11]. *In vitro* cellular 3D structures [12] created from stem cells resembling living tissue are known as organoids and have been developed as models for translational medicine [13] and gene therapy [14].

We have previously shown that human bone marrow (BM) mesenchymal stem cells (MSCs) can be cultured on CHACC [9, 10]. Human umbilical cord matrix (UCM) is a relatively new source of MSCs which has several advantages over BM including an abundant supply obtained noninvasively; it does not induce donor site morbidity and avoids ethical restrictions. Moreover, UCM MSCs have a higher proliferation rate, can be expanded further without loss of differentiation potential, and exhibit reduced immunogenicity for clinical use [15]. Osteogenesis of UCM-MSCs has been observed in both monolayer culture systems [16] and 3D culture systems, for example, on a demineralised bone [17] and polycaprolactone tricalcium phosphate [18]. Few studies have compared UCM MSC to BM MSC in 3D culture systems [16, 19].

Therefore, the aim of this study was to (1) confirm that MSCs could adhere to, proliferate on, and undergo osteogenic differentiation on 200–300 μm CHACC particles to form 3D organoids and (2) to evaluate the osteogenic potential of UCM MSCs compared to BM MSCs. MSCs were isolated from BM and UCM and characterised by flow cytometry. CHACC was crushed into 200–300 μm particles onto which MSCs were seeded and cultured in osteogenic differentiation medium. The resulting organoids were characterised by brightfield and scanning electron microscopy, alkaline phosphatase staining, and immunocytochemistry and PCR for key osteogenic markers.

2. Materials and Methods

2.1. Preparation of Human Bone Marrow. This study was approved by the South West Wales Research Ethics Committee (12/WA/0029) and all patients gave informed written consent. Exclusion criteria included preexisting conditions (e.g., connective tissue disease, diabetes, and malignancy) or medication (e.g., steroids and cytotoxic agents). BM aspirates were harvested from the iliac crest of two females (aged 25 and 29 years) and two males (aged 22 and 36 years) undergoing surgery to the pelvic ring or acetabulum using a BM aspiration needle (Mana-Tech Ltd., Burton-on-Trent, UK). Samples were collected in heparinised aspiration needles, transported at room temperature, and processed within 120 min.

Mononuclear cells (MNC) were isolated from the BM aspirate using Histopaque-1077 according to the manufacturer's instructions (Sigma-Aldrich, Poole, UK). Up to 40×10^6 MNCs were seeded into 75 cm^2 tissue culture flasks (CellSTAR, Greiner Bio-One, Stonehouse, UK) in 10 ml Minimum Essential Eagle Alpha Modification media with 10% fetal calf serum (Biosera, Uckfield, UK) and 1% Antibiotic-Antimycotic (100x, Life Technologies, Paisley, UK) and incubated for 7 days at 37°C under 5% CO_2 in air. The media were changed every 3-4 days to remove contaminating nonadherent haematopoietic cells, and the adherent MSCs were cultured until 70% confluent. Cells were detached using Accutase according to the manufacturer's instructions (Sigma-Aldrich) and either propagated at a seeding density of 3×10^5 per 75 cm^2 culture flask or cryopreserved in 10% dimethyl sulfoxide (DMSO) (Sigma-Aldrich) in 90% FBS in liquid nitrogen for future use.

2.2. Preparation of Human Umbilical Cord Matrix. Human umbilical cords and placentas were collected from full-term births after elective caesarean section delivery of four mothers aged 30–35 and processed within 120 min. This study was approved by the South West Wales Research Ethics Committee and all mothers gave informed written consent. Inclusion criteria included mothers aged 18–50 who were at least 37 weeks pregnant. Exclusion criteria included preexisting health conditions (e.g., HIV, hepatitis C, or immunology complications), stillborn babies, or twins. A 3 cm section of the umbilical cord proximal to the placenta was dissected and the vasculature was carefully removed. The remaining matrix was finely diced using a scalpel. The diced tissue was placed in 25 cm^2 flasks with 0.5 ml FBS. After 24 hours, 1 ml Dulbecco's modified Eagle's medium (DMEM, Life Technologies, Paisley, UK) supplemented with 10% FBS and 1% Antibiotic-Antimycotic was added. After 72 hours, an additional 3 ml DMEM was added. Cultures were subsequently fed twice weekly until 70% confluent at which point they were harvested and either propagated or cryopreserved *as above.* Cryopreserved UCM MSCs and BM MSCs were simultaneously used in the experiments for the assessment on CHACC.

2.3. Characterisation by Flow Cytometry. The following antibodies were used to phenotype the cells based on the International Society for Cellular Therapy (ISCT) criteria [20]: CD14-APC-eFluor780 (clone 61D3), CD34-eFluor450 (clone 4H11), CD73-FITC (clone AD2), CD90-APC (clone eBio5E10), CD105-PE (clone SN6) (eBioscience, Hatfield, Ireland, UK), CD19-PE-Cy7 (clone J3-119), and CD45-Krome Orange (clone J.33) (Beckman Coulter, High Wycombe, UK). All antibodies were mouse isotype IgG1, κ. Unstained cells were used as controls. Gating was performed on the forward and side scatter (FSC versus SSC) profile to remove debris and doublets based on scatter. Cells (3×10^5) in 100 μl FACS buffer (Dulbecco's PBS, Life Technologies; 0.2% BSA and 0.05% sodium azide, Sigma-Aldrich) were incubated on ice in the dark for 30 min with predetermined

titrations of antibody. The cells were washed in FACS buffer and resuspended in 200 μl FACS buffer for analysis.

The stained cells were analysed within 2 hours using a BD FACS Aria I flow cytometer with FACS Diva 6.1.3 software (BD Bioscience, Oxford, UK). The instrument was turned on for at least 1 hour prior to each run to allow the lasers to warm up, and Cytometer Setup & Tracking Beads (BD Bioscience) were used to check instrument performance. 10,000 cell events were recorded for each antibody. Voltages were set on unstained samples [21]. The FCS files were analysed in Kaluza 1.2 (Beckman Coulter) and the median fluorescent intensity (MFI) was displayed on logicle (biexponential) axes [22]. To convey information as to the density of events, contour density plots with visualised outliers were chosen as the standard plot [23].

2.4. Preparation of Coralline Hydroxyapatite/Calcium Carbonate Microscaffolds. CHACC (Affiliated Hospital, Hainan Medical College, Haikou, People's Republic of China) was crushed with a mortar and pestle and subsequently sieved through a 300 μm followed by a 200 μm sieve to capture only 200–300 μm particles. The sieved CHACC were then autoclaved for sterilisation. 10 μl of complete organoid medium (α-MEM supplemented with 10% FBS and 1% Antibiotic-Antimycotics), and three CHACC particles were placed into each well of a Terasaki microplate (Greiner Bio-One, Stonehouse, UK) and incubated for 24 hours at 37°C under 5% CO_2 in air.

2.5. Formation and Differentiation of Organoids. 3000 MSCs (P3-5) per 10 μl organoid medium were added to the previously prepared scaffold particles in the Terasaki microplates to produce organoids. The next day, the organoids were transferred to a 100 mm petri dish (Fisher Scientific, Loughborough, UK) and swirled to allow the particles to come into contact with each other, enabling a larger scaffold conglomerate to be created. The organoids were treated with either plain organoid medium (control) or organoid medium supplemented with 100 nM dexamethasone, 10 mM β-glycerol phosphate, and 100 μM 2-phosphate-ascorbic acid to stimulate osteogenic differentiation.

2.6. Characterisation by Microscopy and Live/Dead Assay. The organoids were analysed by brightfield and scanning electron microscopy (SEM). The samples were analysed on days 1, 7, 14, and 21 during differentiation. For SEM, the samples were cut to 1 mm diameter, fixed in 4% glutaraldehyde (Sigma-Aldrich), and then gradually dehydrated through an ethanol series, using sequentially higher concentrations of ethanol (70%, 80%, 90%, 95%, and 100%) for 10 min each. Finally, samples were further dehydrated in 50% hexamethyldisilazane (Sigma-Aldrich) diluted with ethanol for 10 min, followed by full immersion in absolute hexamethyldisilazane, and left to evaporate overnight in a fume cupboard. Control scaffold particles (no cells) were also incubated for 7 days in organoid medium, at 37°C under 5% CO_2 in air, before being fixed and dehydrated. SEM was carried out using a Hitachi S-4800 II SEM with an accelerating voltage of 1 kV at 110x and 5000x. Samples were mounted onto SEM stubs using a double-coated carbon conductive tape (Acros Organics, supplied by Fisher Scientific).

Cell viability was also assessed after 14 and 21 days using Live/Dead assay kit (Life Technologies, Paisley, UK), in which cells were stained with calcein acetoxymethyl (0.1 μg/ml) and propidium iodide (1 μg/ml) and viewed by fluorescence microscopy.

2.7. Assessing Differentiation by Immunocytochemistry. At 21 days differentiation, organoids were washed in PBS and orientated within a large droplet of Bright Cryo-M-Bed embedding compound which was snap frozen on dry ice. 10 μm sections were then cut using a Leica CM1900 and melted onto slides for staining. Slides were fixed in 10% neutral buffered formalin (Sigma-Aldrich), permeabilised in PBS : 0.1% Triton X-100 (Sigma-Aldrich), and incubated in PBS : 0.5% bovine serum albumin (BSA) (Sigma-Aldrich) for 30 min to block nonspecific binding. The organoids were stained with preoptimised concentrations of monoclonal mouse primary antibodies targeting Runx2 (3 μg/ml) (R&D Systems, Abingdon, UK), osteocalcin (10 μg/ml), or polyclonal rabbit primary antibody targeting type I collagen (10 μg/ml) (Abcam, Cambridge, UK) overnight in a humidified environment at +4°C. Unbound primary antibody was removed by washing in PBS and the slides were incubated for 1 hour in the dark at room temperature with a secondary NL557-conjugated anti-mouse or NL493-conjugated anti-rabbit antibody (1 : 200) (R&D Systems). Slides were washed in PBS and stained with 0.1% 4′,6-diamidino-2-phenylindole (DAPI, Life Technologies) for 1 min at room temperature. Each sample was washed in PBS and imaged using a confocal microscope (Zeiss LSM710, Oberkochen, Germany). Negative (no primary antibody) and blank (scaffold without cells) controls were included.

2.8. Alkaline Phosphatase Staining. The slides were fixed in ice cold 70% ethanol (Fisher Scientific) for 10 min after sectioning and washed in PBS, before being immersed in ALP substrate kit (Vector Laboratories, Peterborough, UK) according to the manufacturer's instructions. Slides were stained in 0.1% DAPI (Life Technologies) for 1 min at room temperature to stain nuclei and imaged using a confocal microscope.

2.9. Real-Time PCR Analysis. Key markers of osteogenesis (Runx2, ALP, and type I collagen) were assessed using real-time PCR. 21 days post differentiation, RNA was isolated from the cells using the MasterPure kit (Cambio, Cambridge, UK) according to the manufacturer's instructions. In brief, samples were lysed in 300 μl of tissue and cell lysis solution at 65°C for 30 min. Protein was precipitated out of solution using 150 μl of protein precipitation reagent. After centrifugation, the supernatant was collected and incubated for 1 hour at 37 °C with deoxyribonuclease to remove DNA. This process was then repeated. RNA was collected by precipitation using 2-propanol and centrifugation. 1 μg of RNA was reverse transcribed into cDNA using RETROscript® Kit (Life Technologies) in a reaction volume of 20 μl. Real-time PCR reactions were run at 50°C for 2 min and 95°C for 2 min, as

Table 1: Primer sequences used in real-time PCR.

Gene	Forward primer (5′-3′)	Reverse primer (5′-3′)
Glyceraldehyde-3-phosphate dehydrogenase	TCA TTG ACC TCA ACT ACA TGG T	TCT CGC TCC TGG AAG ATG GTG
RUNX2	CCT AGG CGC ATT TCA GGT GCT T	CTG AGG TGA CTG GCG GGG TGT
Type I collagen	ATG TTC AGC TTT GTG GAC CTC CGG	CGC AGG TGA TTG GTG GGA TGT CT
Alkaline phosphatase	GAC CCT TGA CCC CCA CAA T	GCT CGT ACT GCA TGT CCC CT

an initial denaturation step, followed by 40 cycles at 95°C for 15 secs to denature and 60°C for 30 secs to anneal using SsoFast EvaGreen Supermix and the 2005 MyiQ real-time PCR detection system (Bio-Rad Laboratories, Hemel Hempstead, UK). Amplification of each gene included 10 μl of SsoFast EvaGreen®, 0.6 μl forward primers, 0.6 μl reverse primers, 6.8 μl of nuclease free water, and 2 μl of diluted cDNA (1 : 10 with nuclease-free water). This was followed by a melt curve analysis. The cycle threshold (CT) of amplification for each gene of interest (Table 1) was normalised against the housekeeping gene GAPDH in all samples, and relative gene expression level was determined by the 2^(GAPDH CT-Test CT) method.

2.10. Statistical Analysis. All experiments were repeated at least once until consistent results were obtained. Nonparametric tests were used to analyse statistical data (Statistica Version 6, StatSoft Ltd., UK). All data are expressed as mean ± standard error.

3. Results

3.1. Characterisation by Flow Cytometry. UCM and BM MSC demonstrated the traditional MSC phenotype [20] showing positive expression for CD73, CD90, and CD105 and negative expression for the haematopoietic markers CD14, CD19, CD34, and CD45 (Figure 1).

3.2. Morphology Characterised by Bright Field and Scanning Electron Microscopy. Bright field (Figure 2) and SEM images (Figure 3) were taken on days 1, 7, 14, and 21 of the differentiation process and compared to a control image taken at day 21 with no addition of osteogenic supplement. Bright field images (Figure 2) showed large gaps in between particles devoid of UCM MSCs (Figure 2(A4), white arrow) until day 21. In contrast, BM MSCs (Figure 2(B)) were observed to proliferate and rapidly occupy the spaces between particles as early as day 7 and did not change in appearance after this time point. SEM images (Figure 3) showed over time the surface of the organoids to become smoother due increasing cell density and deposition of extracellular matrix, which bound the CHACC particles together forming a larger conglomerate. Smoother surfaces were exhibited using BM MSCs (Figure 3(B3)) at day 14, whereas UCM MSCs (Figure 3(A4)) did not cover the entire surface until day 21. The addition of osteogenic supplement was not observed to have any significant impact on organoid morphology in relation to the control images at 21 days.

Cell viability was also assessed after 14 and 21 days using Calcein acetoxymethyl (0.1 μg/ml) and propidium iodide (1 μg/ml) and viewed by fluorescence microscopy. Dead cells were barely observed on CHACC using UCM or BM MSCs, which demonstrated that the cell viability was not affected by CHACC microparticles.

3.3. Osteogenesis Characterised by Immunocytochemistry and Alkaline Phosphatase Staining. UCM and BM MSCs were observed throughout the organoid by 21 days of differentiation. Excluding UCM MSCs grown in control α-MEM that did not label for ALP (Figure 4(a), A1), osteogenically induced and noninduced organoids were positive for ALP (Figure 4(a), A2–A4), Runx2 (Figure 4(b), B1–B4), type I collagen, and osteocalcin (Figure 4(c), C1–C4). ALP was active within the MSC's cytoplasm. Runx2 was largely found within the nucleus of MSCs and appeared purple due to blending with the nuclear stain DAPI. Type I collagen and osteocalcin were found within the extracellular matrix on the surface of the organoid.

ALP (Figure 4(a), A5), Runx2 (Figure 4(b), B5), and type I collagen (Figure 4(c), C5) were also assessed by real-time PCR. Osteogenically induced BM MSCs were shown to have significantly more ALP (Figure 4(a), A5) and Runx2 (Figure 4(b), B5) mRNA than osteogenically induced UCM MSCs, relative to the housekeeping gene, GAPDH. However, control BM MSCs were also shown to have significantly more Runx2 mRNA compared to UCM MSC. Nonosteogenically induced UCM MSCs showed high type I collagen mRNA and protein expression but low ALP and Runx2.

4. Discussion

Novel biomaterials for bone regeneration are desired as they do not have inherent disadvantages of autografts (blood loss, infection and morbidity risks, and limited supply). However, they need to match the gold standard of autografts in bone replacement surgery. CHACC has been shown to have excellent properties to function as a bone graft, but it lacks the key component required for autografts: living cells with osteogenic capacity.

In this study, UCM and BM MSCs were incorporated with CHACC microparticles to form organoids and their *in vitro* osteogenic potential was assessed and compared. Human UCM MSCs have been proven to differentiate down the osteogenic lineage and share common surface markers to BM MSCs [15]. CHACC is already used as a bone graft. Therefore, it was expected to provide a 3D structure for UCM and BM MSC attachment, proliferation, and

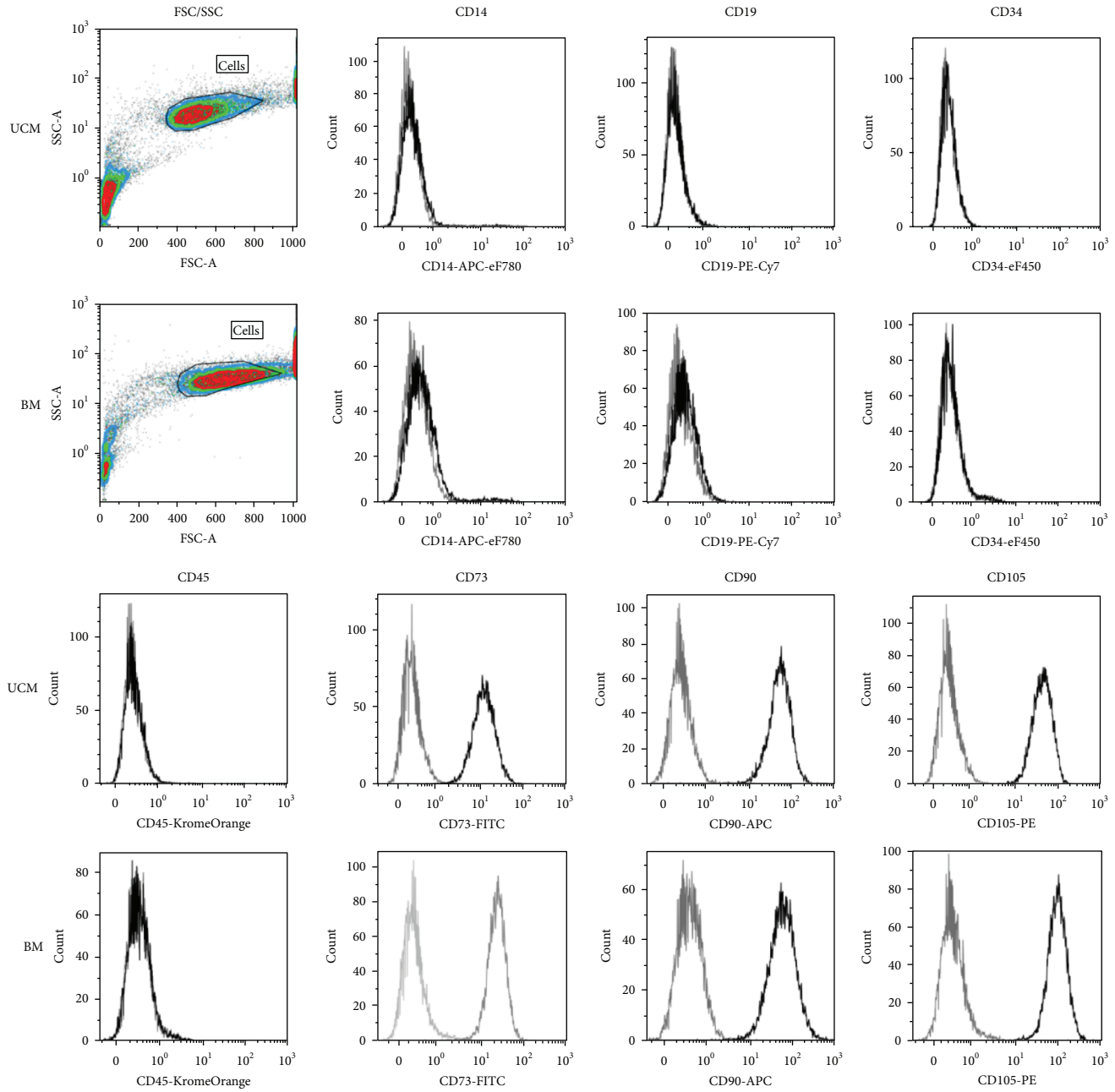

Figure 1: Human UCM and BM MSCs single stained with antibodies against surface markers. MSCs were CD14-CD19-CD34-CD45-CD73+CD90+ and CD105+, correlating with an MSC phenotype defined by ISCT. Grey: unstained; black: stained.

differentiation. Organoids can result in increased cell numbers compared to the cell suspension method [24], and the hydroxyapatite layer on CHACC should accelerate the differentiation of cells and consequently mineralisation [24–26].

Although both BM and UCM MSCs were able to attach to CHACC microparticles, form organoids, proliferate, and differentiate down the osteogenic lineage, as expected, the BM MSCs showed higher levels of osteogenic differentiation than UCM MSCs. BM MSCs showed a dramatic increase in cell proliferation indicating that they entered into the first stage of osteogenic differentiation [27] before UCM MSCs. Increased osteogenic differentiation in BM MSCs was further evidenced by increased expression of runx2 and ALP and the labelling of osteocalcin in immunocytochemistry [25]. Other researchers have also found BM MSCs to have superior osteogenic potential compared to UCM MSCs [28]. Similar to our study, Schneider et al. found BM MSCs to express more ALP but less type I collagen than UCM MSCs [29]. Zhang et al. compared MSCs on 3D scaffolds derived from different sources and found BM MSCs to form more bone than UCM MSC [18]. Reduced osteogenic potential of UCM MSCs maybe explained by the anatomical origins that they

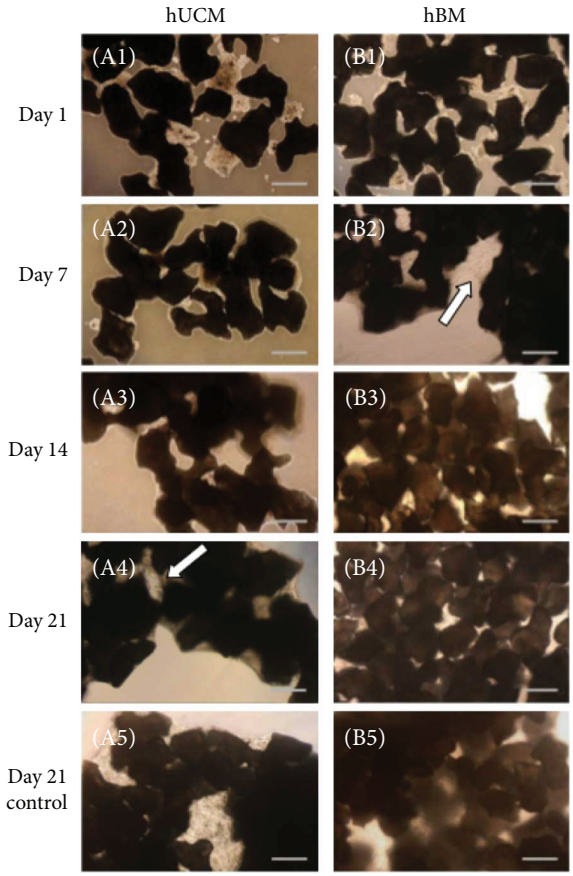

Figure 2: Bright field images of organoids with UCM (A) and BM (B) MSCs during the process of osteogenesis. Images were taken on days 1 (A1, B1), 7 (A2, B2), 14 (A3, B3), and 21 (A4, B4) of the differentiation process and compared to a control (α-MEM) image at day 21 (A5, B5). BM MSCs were observed to proliferate into the voids created by the numerous coral particles by day 7 and UCM MSCs by day 7 (white arrows). SP: scaffold particle. Scale bars: 250 μm.

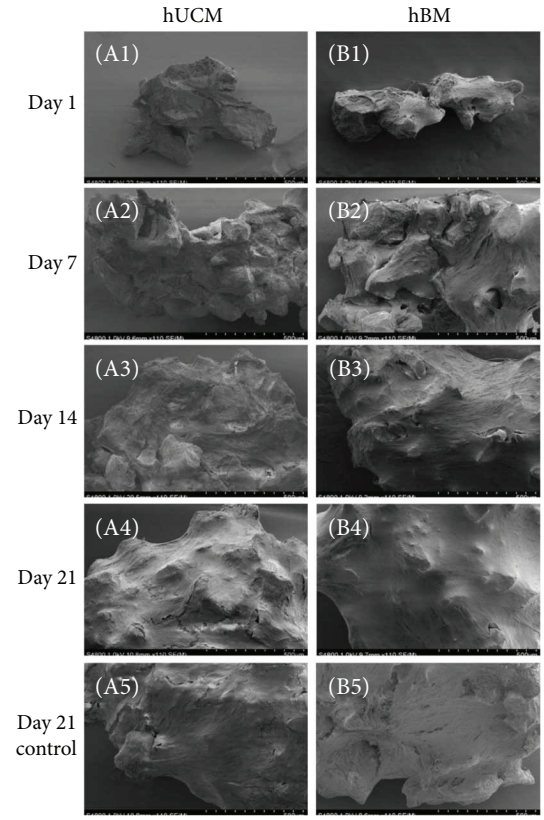

Figure 3: SEM images of organoids with UCM (A) and BM (B) MSCs during the process of osteogenesis. Images were taken on days 1 (A1, B1), 7 (A2, B2), 14 (A3, B3), and 21 (A4, B4) of the differentiation process and compared to a control (α-MEM) image at day 21 (A5, B5). Over time, the voids within the organoid were filled with MSCs and associated extracellular matrix which formed a smoother surface that covered CHACC surfaces. Significant coverage was exhibited using BM MSCs at day 14 (B3), whereas UCM MSCs did not cover surfaces until day 21 (A4). Scale bars: 500 μm.

were derived from. Panepucci et al. found higher levels of genes related to osteogenesis in BM MSCs compared to umbilical cord vein MSCs [30]. Umbilical cord vein MSCs expressed genes more related to matrix remodelling via metalloproteinases and angiogenesis. Consequently, UCM MSCs could be less committed to osteogenesis but instead committed to angiogenesis.

Interestingly, Zhang et al. also showed that UCM MSCs could differentiate down the osteogenic lineage better than BM MSCs if they were cultured in monolayer [18]. Based on this study, future work should investigate differentiating UCM MSCs in monolayer first and then seed these cells onto 3D scaffolds. Although ectopic bone formation using UCM MSCs has been proven to be inferior compared to BM MSCs in vivo, the angiogenic nature of UCMs has been utilised to improve bone regeneration. Todeschi et al. showed that UCM MSCs implanted orthotopically caused a similar amount of new bones to form compared to BM MSCs by recruiting host osteogenic cells [31]. Chen et al. also utilised the angiogenic nature of umbilical cord mesenchymal stem cells by coculturing them with human umbilical cord vein endothelial cells. They found that a similar amount of new bone formation could be achieved in vivo compared to coculturing human umbilical cord vein endothelial cells with BM MSCs [32].

There are a number of limitations to this study; immunocytochemistry and real-time PCR only assess a narrow spectrum of markers, meaning MSCs could be differentiating down a lineage not being specifically looked at. Furthermore, quantitative PCR only gives a snap shot of RNA expression at the day it is extracted and has a very short half-life of approximately 9 hours [33] meaning expression levels could be missed. Cell attachment and growth was limited to arbitrary qualitative assessment via bright field and SEM images.

Future work is expected to overcome the inferior osteogenic capacity of UCM MSCs, such as to initiate the osteogenic differentiation at 2D culture stage, and the osteogenic gene and protein expression will be assessed at more time points to show the full spectrum of differentiation over the three-week period or longer to assess the full potential of UCM MSCs. Also, to utilise the angiogenic nature of UCM, MSCs with CHACC should be explored as well.

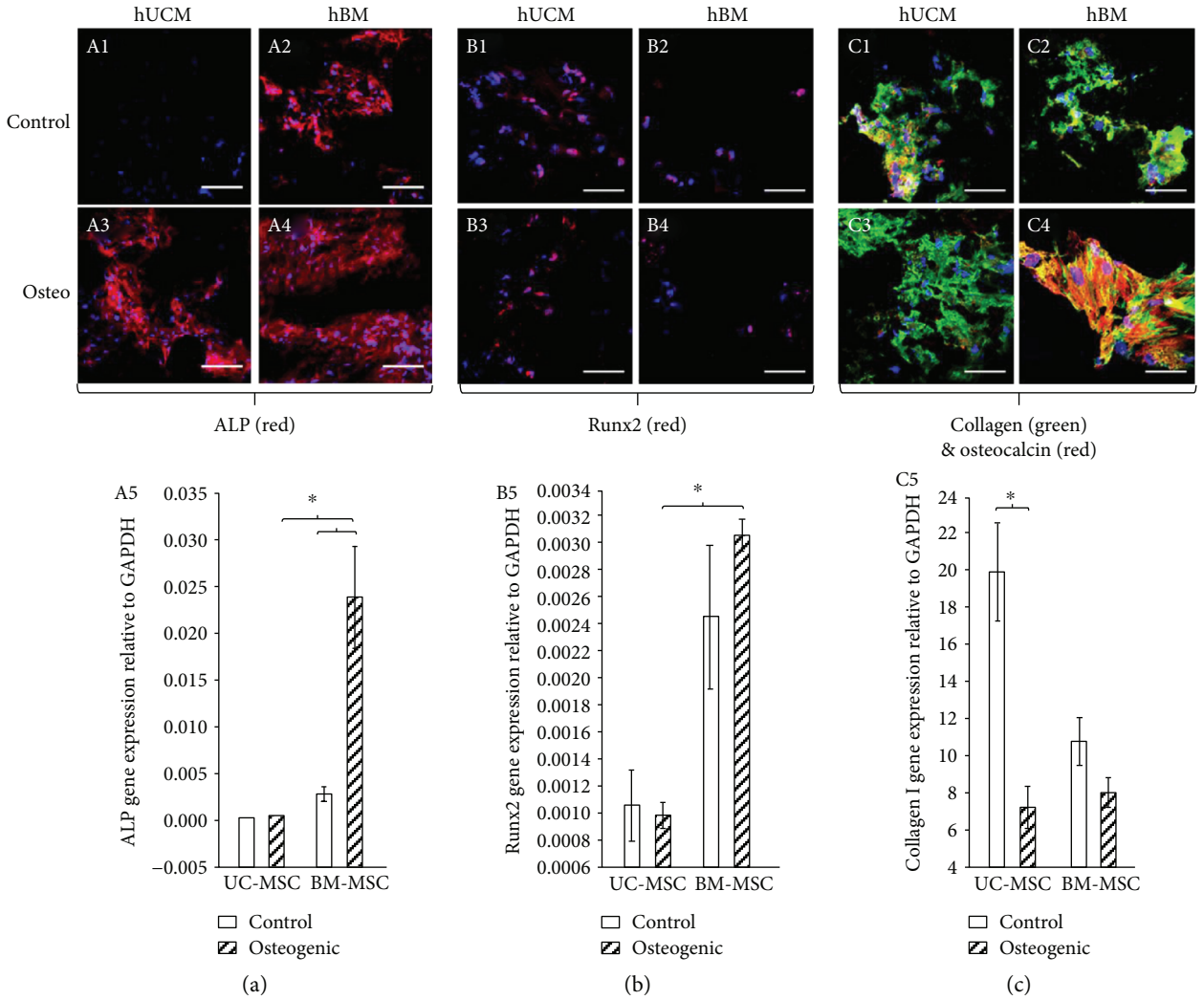

Figure 4: On day 21, control and osteogenically induced organoids were cryosectioned (10 μm) and stained for alkaline phosphatase (ALP) (a), Runx2 (b), collagen type I, and osteocalcin (c). Real-time PCR was used to assess mRNA levels of ALP (A5), Runx2 (B5), and collagen type I (C5) in UCM and BM MSCs lysed directly from the control and osteogenically induced scaffolds at 21 days. MSCs derived from UCM expressed good collagen I mRNA and protein production but poor ALP and Runx2 in relation to MSCs derived from BM. $n = 4$ ($^*p < 0.05$).

5. Conclusion

This study has shown that 200–300 μm CHACC granules can be a suitable carrier for human MSC proliferation and differentiation *in vitro*, for the purpose of injectable delivery opening up the use of CHACC for new applications within maxillofacial surgery and dentistry. In addition, UCM MSCs show inferior osteogenic capacity when cultured as CHACC organoids compared to BM MSCs. Therefore, further research is required to optimise the osteogenicity of UCM MSCs to release their full potential as a readily available, accessible, and abundant tissue source for bone tissue engineering.

Data Availability

Data are available from Swansea University; requests for access should be made to Dr. Zhidao Xia (z.xia@swansea.ac.uk).

Conflicts of Interest

All authors state that they have no conflicts of interest.

Acknowledgments

The authors would like to thank the Newborn Immunity Group for providing antibodies and umbilical cord collections and Professor Ian Pallister and the Dept. of Trauma and Orthopaedics at Morriston Hospital, Swansea, for bone marrow collections. They thank Dr. David Guy, Dr. Chris Wright, Dr. Sam Webster, Dr. Jo Bishop, and Professor Cathy Thornton for their support and advice for this research project. This project was supported by the European Regional Development Fund (ERDF), Hainan International S&T Cooperation Project (GJXM201101), National Natural Science Foundation of China (NSFC 81260271), Osseo Regenerative Technologies (UK) LTD., and Knowledge Economy Skills Scholarships (KESS).

References

[1] G. E. Friedlaender, "Bone-Banking," *The Journal of Bone & Joint Surgery*, vol. 64, no. 2, pp. 307–311, 1982.

[2] P. D. Costantino and C. D. Friedman, "Synthetic bone graft substitutes," *Otolaryngologic Clinics of North America*, vol. 27, no. 5, pp. 1037–1074, 1994.

[3] N. Shibuya and D. C. Jupiter, "Bone graft substitute: allograft and xenograft," *Clinics in Podiatric Medicine and Surgery*, vol. 32, no. 1, pp. 21–34, 2015.

[4] D. J. Sartoris, R. E. Holmes, R. W. Bucholz, V. Mooney, and D. Resnick, "Coralline hydroxyapatite bone-graft substitutes in a canine diaphyseal defect model: radiographic-histometric correlation," *Investigative Radiology*, vol. 22, no. 7, pp. 590–596, 1987.

[5] S. Koëter, S. J. Tigchelaar, P. Farla, L. Driessen, A. van Kampen, and P. Buma, "Coralline hydroxyapatite is a suitable bone graft substitute in an intra-articular goat defect model," *Journal of Biomedical Materials Research Part B: Applied Biomaterials*, vol. 90B, no. 1, pp. 116–122, 2009.

[6] K. Fu, Q. Xu, J. Czernuszka, G. R. G. Russell, and J. T. Triffitt, "Characterisation, osteogenic potential and clinical performance of a South China Sea coralline hydroxyapatite/calcium carbonate," *Calcified Tissue International*, vol. 83, no. 1, pp. 20–20, 2008.

[7] R. Vago, D. Plotquin, A. Bunin, I. Sinelnikov, D. Atar, and D. Itzhak, "Hard tissue remodeling using biofabricated coralline biomaterials," *Journal of Biochemical and Biophysical Methods*, vol. 50, no. 2-3, pp. 253–259, 2002.

[8] J. S. Thalgott, Z. Klezl, M. Timlin, and J. M. Giuffre, "Anterior lumbar interbody fusion with processed sea coral (coralline hydroxyapatite) as part of a circumferential fusion," *Spine*, vol. 27, no. 24, pp. E518–E525, 2002.

[9] K. Fu, Q. Xu, J. Czernuszka, J. T. Triffitt, and Z. Xia, "Characterization of a biodegradable coralline hydroxyapatite/calcium carbonate composite and its clinical implementation," *Biomedical Materials*, vol. 8, no. 6, article 065007, 2013.

[10] K. Fu, Q. Xu, J. Czernuszka et al., "Prolonged osteogenesis from human mesenchymal stem cells implanted in immunodeficient mice by using coralline hydroxyapatite incorporating rhBMP2 microspheres," *Journal of Biomedical Materials Research. Part A*, vol. 92, no. 4, pp. 1256–1264, 2010.

[11] J. Michel, M. Penna, J. Kochen, and H. Cheung, "Recent advances in hydroxyapatite scaffolds containing mesenchymal stem cells," *Stem Cells International*, vol. 2015, Article ID 305217, 13 pages, 2015.

[12] Y. Sambuy and I. De Angelis, "Formation of organoid structures and extracellular matrix production in an intestinal epithelial cell line during long-term in vitro culture," *Cell Differentiation*, vol. 19, no. 2, pp. 139–147, 1986.

[13] A. Astashkina and D. W. Grainger, "Critical analysis of 3-D organoid in vitro cell culture models for high-throughput drug candidate toxicity assessments," *Advanced Drug Delivery Reviews*, vol. 69-70, pp. 1–18, 2014.

[14] N. Eliopoulos, A. al-Khaldi, M. Crosato, K. Lachapelle, and J. Galipeau, "A neovascularized organoid derived from retrovirally engineered bone marrow stroma leads to prolonged in vivo systemic delivery of erythropoietin in nonmyeloablated, immunocompetent mice," *Gene Therapy*, vol. 10, no. 6, pp. 478–489, 2003.

[15] A. Can and S. Karahuseyinoglu, "Concise review: human umbilical cord stroma with regard to the source of fetus-derived stem cells," *Stem Cells*, vol. 25, no. 11, pp. 2886–2895, 2007.

[16] Y. Diao, Q. Ma, F. Cui, and Y. Zhong, "Human umbilical cord mesenchymal stem cells: osteogenesis *in vivo* as seed cells for bone tissue engineering," *Journal of Biomedical Materials Research Part A*, vol. 91A, no. 1, pp. 123–131, 2009.

[17] S. Honsawek, D. Dhitiseith, and V. Phupong, "Effects of demineralized bone matrix on proliferation and osteogenic differentiation of mesenchymal stem cells from human umbilical cord," *Journal of the Medical Association of Thailand= Chotmaihet thangphaet*, vol. 89, Supplement 3, pp. S189–S195, 2006.

[18] Z.-Y. Zhang, S. H. Teoh, M. S. K. Chong et al., "Superior osteogenic capacity for bone tissue engineering of fetal compared with perinatal and adult mesenchymal stem cells," *Stem Cells*, vol. 27, no. 1, pp. 126–137, 2009.

[19] L. Wang, M. Singh, L. F. Bonewald, and M. S. Detamore, "Signalling strategies for osteogenic differentiation of human umbilical cord mesenchymal stromal cells for 3D bone tissue engineering," *Journal of Tissue Engineering and Regenerative Medicine*, vol. 3, no. 5, pp. 398–404, 2009.

[20] M. Dominici, K. le Blanc, I. Mueller et al., "Minimal criteria for defining multipotent mesenchymal stromal cells. The International Society for Cellular Therapy position statement," *Cytotherapy*, vol. 8, no. 4, pp. 315–317, 2006.

[21] H. T. Maecker and J. Trotter, "Flow cytometry controls, instrument setup, and the determination of positivity," *Cytometry Part A*, vol. 69A, no. 9, pp. 1037–1042, 2006.

[22] L. A. Herzenberg, J. Tung, W. A. Moore, L. A. Herzenberg, and D. R. Parks, "Interpreting flow cytometry data: a guide for the perplexed," *Nature Immunology*, vol. 7, no. 7, pp. 681–685, 2006.

[23] D. F. Alvarez, K. Helm, J. DeGregori, M. Roederer, and S. Majka, "Publishing flow cytometry data," *American Journal of Physiology. Lung Cellular and Molecular Physiology*, vol. 298, no. 2, pp. L127–L130, 2010.

[24] F. Langenbach, C. Naujoks, A. Laser et al., "Improvement of the cell-loading efficiency of biomaterials by inoculation with stem cell-based microspheres, in osteogenesis," *Journal of Biomaterials Applications*, vol. 26, no. 5, pp. 549–564, 2010.

[25] K. Jähn, R. G. Richards, C. W. Archer, and M. J. Stoddart, "Pellet culture model for human primary osteoblasts," *European Cells and Materials*, vol. 20, pp. 149–161, 2010.

[26] M. Kabiri, B. Kul, W. B. Lott et al., "3D mesenchymal stem/stromal cell osteogenesis and autocrine signalling," *Biochemical and Biophysical Research Communications*, vol. 419, no. 2, pp. 142–147, 2012.

[27] S. J. Roberts, Y. Chen, M. Moesen, J. Schrooten, and F. P. Luyten, "Enhancement of osteogenic gene expression for the differentiation of human periosteal derived cells," *Stem Cell Research*, vol. 7, no. 2, pp. 137–144, 2011.

[28] S. Kargozar, M. Mozafari, S. J. Hashemian et al., "Osteogenic potential of stem cells-seeded bioactive nanocomposite scaffolds: a comparative study between human mesenchymal stem cells derived from bone, umbilical cord Wharton's jelly, and adipose tissue," *Journal of Biomedical Materials Research Part B: Applied Biomaterials*, vol. 106, no. 1, pp. 61–72, 2016.

[29] R. K. Schneider, A. Puellen, R. Kramann et al., "The osteogenic differentiation of adult bone marrow and perinatal umbilical mesenchymal stem cells and matrix remodelling in three-

dimensional collagen scaffolds," *Biomaterials*, vol. 31, no. 3, pp. 467–480, 2010.

[30] R. A. Panepucci, J. L. C. Siufi, W. A. Silva Jr et al., "Comparison of gene expression of umbilical cord vein and bone marrow-derived mesenchymal stem cells," *Stem Cells*, vol. 22, no. 7, pp. 1263–1278, 2004.

[31] M. R. Todeschi, R. el Backly, C. Capelli et al., "Transplanted umbilical cord mesenchymal stem cells modify the in vivo microenvironment enhancing angiogenesis and leading to bone regeneration," *Stem Cells and Development*, vol. 24, no. 13, pp. 1570–1581, 2015.

[32] W. Chen, X. Liu, Q. Chen et al., "Angiogenic and osteogenic regeneration in rats via calcium phosphate scaffold and endothelial cell co-culture with human bone marrow mesenchymal stem cells (MSCs), human umbilical cord MSCs, human induced pluripotent stem cell-derived MSCs and human embryonic stem cell-derived MSCs," *Journal of Tissue Engineering and Regenerative Medicine*, vol. 12, no. 1, pp. 191–203, 2018.

[33] B. Schwanhäusser, D. Busse, N. Li et al., "Corrigendum: global quantification of mammalian gene expression control," *Nature*, vol. 495, no. 7439, pp. 126-127, 2013.

Hindawi
Stem Cells International
Volume 2018, Article ID 1943980, 8 pages
https://doi.org/10.1155/2018/1943980

Research Article

Very Small Embryonic-Like Stem Cells, Endothelial Progenitor Cells, and Different Monocyte Subsets Are Effectively Mobilized in Acute Lymphoblastic Leukemia Patients after G-CSF Treatment

Andrzej Eljaszewicz,[1] **Lukasz Bolkun**,[2] **Kamil Grubczak**,[1] **Malgorzata Rusak**,[3] **Tomasz Wasiluk**,[2] **Milena Dabrowska**,[3] **Piotr Radziwon**,[2,4] **Wojciech Marlicz**,[5] **Karol Kamiński**,[6,7] **Janusz Kloczko**,[2] **and Marcin Moniuszko**[1,8]

[1]*Department of Regenerative Medicine and Immune Regulation, Medical University of Bialystok, Ul. Waszyngtona 13, 15-269 Bialystok, Poland*
[2]*Department of Haematology, Medical University of Bialystok, Ul. Waszyngtona 13, 15-276 Bialystok, Poland*
[3]*Department of Hematological Diagnostics, Medical University of Bialystok, Ul. Waszyngtona 13, 15-276 Bialystok, Poland*
[4]*Regional Centre for Transfusion Medicine, Ul. M. Skłodowskiej-Curie 23, 15-950 Bialystok, Poland*
[5]*Department of Gastroenterology, Pomeranian Medical University, Ul. Unii Lubelskiej 1, 71-252 Szczecin, Poland*
[6]*Department of Cardiology, Medical University of Bialystok, Ul. Waszyngtona 13, 15-276 Bialystok, Poland*
[7]*Department of Population Medicine and Prevention of Civilization Diseases, Medical University of Bialystok, Ul. Waszyngtona 13, 15-276 Bialystok, Poland*
[8]*Department of Allergology and Internal Medicine, Medical University of Bialystok, Ul. Waszyngtona 13, 15-276 Bialystok, Poland*

Correspondence should be addressed to Andrzej Eljaszewicz; andrzej.eljaszewicz@umb.edu.pl
and Marcin Moniuszko; marcin.moniuszko@umb.edu.pl

Received 6 March 2018; Accepted 3 June 2018; Published 21 June 2018

Academic Editor: Zengwu Shao

Background. Acute lymphoblastic leukemia (ALL) is a malignant disease of lymphoid progenitor cells. ALL chemotherapy is associated with numerous side effects including neutropenia that is routinely prevented by the administration of growth factors such as granulocyte colony-stimulating factor (G-CSF). To date, the effects of G-CSF treatment on the level of mobilization of different stem and progenitor cells in ALL patients subjected to clinically effective chemotherapy have not been fully elucidated. Therefore, in this study we aimed to assess the effect of administration of G-CSF to ALL patients on mobilization of other than hematopoietic stem cell (HSCs) subsets, namely, very small embryonic-like stem cells (VSELs), endothelial progenitor cells (EPCs), and different monocyte subsets. *Methods.* We used multicolor flow cytometry to quantitate numbers of CD34+ cells, hematopoietic stem cells (HSCs), VSELs, EPCs, and different monocyte subsets in the peripheral blood of ALL patients and normal age-matched blood donors. *Results.* We showed that ALL patients following chemotherapy, when compared to healthy donors, presented with significantly lower numbers of CD34+ cells, HSCs, VSELs, and CD14+ monocytes, but not EPCs. Moreover, we found that G-CSF administration induced effective mobilization of all the abovementioned progenitor and stem cell subsets with high regenerative and proangiogenic potential. *Conclusion.* These findings contribute to better understanding the beneficial clinical effect of G-CSF administration in ALL patients following successful chemotherapy.

1. Background

Acute lymphoblastic leukemia (ALL) is a malignant disease of lymphoid progenitor cells, characterized by accumulation of lymphoblasts in the bone marrow. Standard therapeutic procedure involves use of chemotherapy to first induce remission and next reduce tumor burden and kill residual cells in the bone marrow [1]. Chemotherapy is associated

with numerous side effects including neutropenia, and therefore granulocyte colony-stimulating factor (G-CSF) is routinely used in order to improve neutrophil renewal [2]. However, chemotherapy causes considerable damage to many other cells, such as different progenitor and stem cells and tissues. Activation of regenerative processes requires involvement of stem and progenitor cells that could initiate mechanisms improving cell renewal, development of new vasculature, and tissue reconstruction. However, chemotherapy used in ALL depletes not only stem cells in the bone marrow but also stem cells in the vascular niche of the bone marrow [3, 4]. The bone marrow-associated vascular niche plays a key role in supporting such hematopoiesis processes as hematopoietic stem cell (HSC) maintenance, differentiation, and transendothelial migration. Multiple signaling and adhesion molecules are involved in vascular niche homeostasis, including Jag-1, Notch, c-kit, SCF, angiopoietin-1 (Ang-1), and Tie-2. Importantly, recent reports indicated a role of Ang-1/Tie2 signaling in vascular niche regulation and regeneration [5].

The bone marrow is a reservoir of numerous stem and progenitor cells, both hematopoietic and nonhematopoietic (non-HSCs). Adult HSCs were the first identified and thoroughly characterized group of stem cells in humans [6]. To date, HSCs are the ones of few stem cell subtypes that are used routinely in clinical practice worldwide [7]. On the other side, non-HSCs are comprised of several different populations of stem and progenitor cells including endothelial progenitor cells (EPCs) and very small embryonic-like stem cells (VSELs) [8–10]. It has been hypothesized that adult EPCs are delivered from HSCs, while VSELs represent distinct population of adult pluripotent stem cells [9, 11]. Although bone marrow-delivered VSELs do not exhibit direct hematopoietic activity, they can acquire hematopoietic potential under specific conditions, and thereby they may support bone marrow renewal [12]. Similarly, release of VSELs to the circulation can contribute to supporting regenerative processes in distal tissues. In contrast to VSELs, EPCs are primarily involved in supporting vascularization processes [13, 14]. The role of EPCs in the promotion of angiogenesis and revascularization is usually supported by other cell types including pericytes and proangiogenic subsets of monocytes. In addition, proangiogenic monocytes, similarly to EPCs, were shown to support local stem and progenitor cell differentiation in the bone marrow [15, 16].

Granulocyte colony-stimulating factor (G-CSF) was the first cytokine identified and introduced into medical practice in order to treat neutropenia and to induce mobilization of hematopoietic stem cells (HSC) in donors before transplantation. Physiological plasma levels of G-CSF are either very low or undetectable; however, G-CSF can be produced locally by many tissues in response to proinflammatory signaling mediated by IL-1b, TNF, and IFN-β, among others [2, 17]. Moreover, locally produced G-CSF affects neutrophil function by increasing their survival in inflamed/infected tissue by apoptosis inhibition. Furthermore, release of G-CSF into the circulation stimulates neutrophil production and their release from the bone marrow [18]. On the other hand, the recent report of our group indicated that repetitive G-CSF administration to pediatric patients effectively induced significant mobilization of EPCs and putative proangiogenic monocytes [19]. Similarly, other reports showed that G-CSF may be used to improve outcome of patients with cardiovascular events [20]. However, to date, the effect of G-CSF treatment on VSELs and EPCs mobilization in immunocompromised patients has not been evaluated. Therefore, we hypothesized that the use of G-CSF in the prevention of chemotherapy-induced neutropenia in ALL patients may support regeneration of damaged tissues by mobilization of stem and progenitor cells. In this report, we aimed to assess the effect of G-CSF administration on the mobilization of VSELs, EPCs, and proangiogenic monocyte subsets in ALL patients with complete remission after chemotherapy. Furthermore, we set out to analyze the effects of G-CSF administration on chemotactic factors for VSELs, EPCs, and proangiogenic monocytes, namely, SDF-1 and angiopoietins.

2. Methods

2.1. Patients. 21 patients with diagnosed acute lymphoblastic leukemia B linage and 12 age-matched normal donors were enrolled in the study. Patients' median age at the time of sample collection was 39 (21–58). Diagnoses were established according to the 2008 WHO recommendation [21]. Blood counts, flow cytometry, molecular study, FISH, and cytogenetic analysis were performed, reviewed, and classified. Patients were treated at the Department of Haematology, Medical University of Bialystok from 2013 to 2016, with induction and 2 consolidation chemotherapy regimens corresponding to the standard therapy based on the Polish Adult Leukemia Group [22]. All included patients were in complete remission and had no minimal residual disease after the induction $< 0.1\%$ and consolidation $< 0.01\%$ [22]. After induction, the response was evaluated in accordance with the recommendation by NCCN Guidelines. G-CSF (Neupogen) was given s.c. at the dose of 5 μg/kg, for 7 days, as a prophylaxis of neutropenia. The samples were collected before stimulation and at the 8th day following treatment. All samples were collected upon the approval of the Ethics Committee of the Medical University of Bialystok.

2.2. Flow Cytometry. Freshly obtained EDTA-anticoagulated whole blood specimens were stained by using panel of mouse anti-human monoclonal antibodies (Table 1), according to stain-and-then-lyse-and-wash protocol as previously described [19, 23]. Briefly, 100 μL (for monocytes) and 175 μL (for EPC and VSELs) of whole blood were stained with monoclonal antibodies (Table 1) and incubated for 30 min at room temperature, in the dark. Thereafter, 2 mL of FACS lysing solution (Becton Dickinson Bioscience) was added for erythrocyte lysis, followed by 15 min incubation in the dark. Next, cells were washed twice with cold PBS (phosphate-buffered saline, Corning) and fixed with CellFix (BD Biosciences). For all stainings, appropriate fluorescence-minus-one (FMO) controls were used for setting compensation and to assure correct gating. Samples were analyzed with FACSCalibur flow cytometer (BD

Table 1: Characteristic of used monoclonal antibodies.

Marker	Fluorochrome	Host	Clone	Manufacturer
CD14	PE	Mouse anti-human	MφP9	Becton Dickinson Bioscience
CD16	FITC	Mouse anti-human	B73.1	Becton Dickinson Bioscience
CD34	FITC	Mouse anti-human	581	Becton Dickinson Bioscience
CD45	PE	Mouse anti-human	HI30	Becton Dickinson Bioscience
CD133	APC	Mouse anti-human	AC133	Miltenyi Biotec
CD235a	FITC	Mouse anti-human	GA-R2 (HIR2)	Becton Dickinson Bioscience
CD309	PE	Mouse anti-human	89,106	Becton Dickinson Bioscience

PE: phycoerythrin; FITC: fluorescein isothiocyanate; APC: allophycocyanin.

Biosciences). Obtained data were analyzed using FlowJo ver. 7.6.5 software (Tree Star) as previously described [19, 23].

2.3. Cytokine Assay. SDF-1, angiopoietin-,1 and angiopoietin-2 plasma levels were quantified by means of commercially available enzyme-linked immunosorbent assays (ELISA, DuoSet, R&D) in 96-well plates. Samples were directly assayed according to manufacturer's instructions. Protein levels in the specimens were calculated from a reference curve generated using appropriate protein standards. Finally, the plates were analyzed with automated light absorbance reader (LEDETEC 96 system). The results were calculated by MicroWin 2000 software.

2.4. Statistics. Statistical analysis was performed by using GraphPad Prism 6 (GraphPad software). Mann–Whitney U test was used to compare differences among groups, while Wilcoxon test was used to compare changes in course of G-CSF treatment. Additionally, Spearman correlation coefficient was used to determine correlations between plasma protein levels and analyzed cell subsets. The differences were considered statistically significant at $p < 0.05$. The results are presented as medians and interquartile range.

3. Results

First, we analyzed the numbers of all progenitor and stem cells identified as CD34+ cells as well as HSCs, VSELs, EPCs, and frequencies of monocyte subsets in ALL patients after chemotherapy before G-CSF administration, and we compared these values with age-matched control subjects. We found decreased numbers of CD34+ progenitor cells (Figure 1(a)), VSELs (Figure 1(b)), and HSCs (Figure 1(c)) in ALL patients as compared to healthy donors. Interestingly, we found no differences in the numbers of EPCs delineated by CD34+CD133+CD309+ phenotype (Figure 1(d)) between ALL patients and healthy subjects. Importantly, CD14+ cells could not be detected in the peripheral blood of 19 ALL patients after chemotherapy (Figure 1(e)).

Having found decreased numbers of analyzed stem and progenitor cells in immunocompromised patients, we next aimed to investigate effects of G-CSF treatment on hematopoietic stem cell mobilization in ALL patients. It should be noted that mobilization of hematopoietic/progenitor cells after G-CSF administration is usually delayed, with peak levels observed within 5–7 days [19]. As expected, we found significant increase in the numbers of CD34+ precursors and HSCs (from 122.5 (105.3–725.8) to 713.8 (270.9–3829), Figure 2(a), and from 7.843 (2.22–15.67) to 63.73 (18.21–117.5), Figure 2(b), resp.) in all analyzed individuals 7 days after initial treatment. Next, we evaluated the numbers of VSELs and EPCs (determined by linage-CD235a-CD45-CD133+ and CD34+CD133+CD309+ phenotype, resp.). Interestingly, we observed substantial increase of VSEL numbers after G-CSF administration from 2 (0.683–9.706) to 11.96 (2.85–61.37) (Figure 2(c)). Similarly, the numbers of EPCs increased from 2 (1.419–13) to 13.75 (4.257–42.63) (Figure 2(d)). Moreover, we observed substantial increase in CD14+ cell numbers after G-CSF treatment in all individuals (data not shown). Therefore, we next analyzed the composition of monocyte subsets after G-CSF therapy. We observed significantly higher frequencies of putative proangiogenic intermediate monocytes (delineated by CD14++ CD16+ phenotype, Figure 3(a)), but not nonclassical CD14+CD16++ monocytes (Figure 3(b)) in G-CSF-treated ALL patients as compared to normal donors (16.10 (11.90–22.10) versus 5.86 (4.54–9.35)). Consequently, frequencies of classical monocytes were lower in ALL patients following G-CSF therapy in comparison to healthy subjects (72.30 (64.90–79.90) versus 84.35 (81.43–86.68), Figure 3(c)).

In parallel, we evaluated levels of SDF-1 and two major angiopoietins, namely, Ang-1 and Ang-2. We observed that G-CSF administration increased SDF-1 (Figure 4(a)) and Ang-2 (Figure 4(b)), but not Ang-1 (Figure 4(c)) plasma levels in all analyzed individuals. Finally, we investigated whether plasma SGF-1, Ang-1, and Ang-2 levels were correlated to numbers of CD34+ cells, HSC, VSELs, EPCs, and different monocyte subsets. Interestingly, we found that CD34+ cell numbers correlated positively with Ang-1 and SDF-1 levels ($p = 0.0372$, $r = 0.5110$, and $p = 0.0383$, $r = 0.5545$, resp.). Surprisingly, HSC and VSEL numbers correlated positively only with Ang-1 ($p = 0.0257$, $r = 0.5297$) and Ang-2 ($p = 0.0208$, $r = 0.5944$) plasma levels, respectively. Furthermore, we found positive correlation between absolute numbers of CD14++CD16+, but not CD14+CD16+ monocytes and SDF-1 levels ($p = 0.0187$, $r = 0.1000$).

4. Discussion

Here, we demonstrated that chemotherapy regimens that are routinely used in ALL patients decreased the numbers of circulating CD34+ cells and, more specifically, HSCs, and

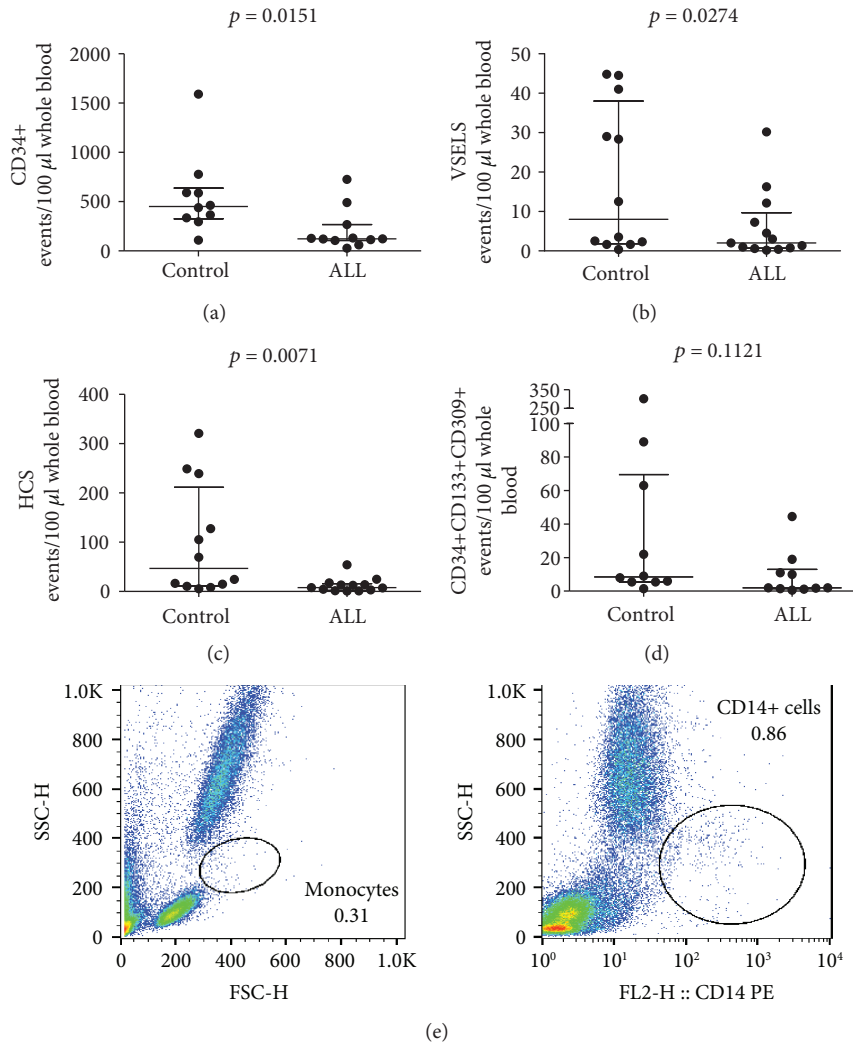

Figure 1: Summary of flow cytometry analyses of (a) CD34+ progenitor cells (CD34+ cells), (b) very small embryonic-like stem cells (VSELs, lin-CD235a-CD45-CD133+), (c) hematopoietic stem cells (HSC, VSELs, lin-CD235a-CD45+CD133+), and (d) endothelial progenitor cell (EPCs, CD34+CD133+CD309+ cells) numbers in normal donors (control) and ALL patients after successful chemotherapy before G-CSF treatment; Mann–Whitney U test was used; (e) representative flow cytometry dot plots of ALL patients after successful chemotherapy before G-CSF treatment.

VSELs, but did not affect EPC numbers. Thus, we found that the administration of G-CSF to immunocompromised adult patients is capable of inducing mobilization of progenitor and stem cells with high regenerative potential into the periphery. Moreover, we showed that G-CSF administration caused significant increases in plasma levels of SDF-1 and Ang-2, but not Ang-1.

Within the bone marrow, all progenitor cells reside in separated microenvironmental niches, which control their proliferation, differentiation, and release to the circulation [24]. High-dose chemotherapy used in ALL treatment directly induces regression of the bone marrow and destroys its ability to produce and release blood cells, namely, leukocytes, red blood cells, and platelets, as well as different subsets of progenitor cells involved in regeneration process, including EPCs and VSELs. This is also the main cause of neutropenia [25]. It is well established that progenitor cell recovery is highly dependent on the number of chemotherapy cycles. Interestingly, peak levels of these cells after chemotherapy correlated with the rate and extent of platelet recovery [26]. On the other hand, it is believed that regeneration of the bone marrow vascular niche is crucial for proper reconstruction of hematopoiesis after chemotherapy. Notably, bone marrow endothelial cells were shown to support differentiation of hematopoietic progenitors and their mobilization to the periphery [27, 28]. Therefore, EPCs may be one of the first subsets involved in the regeneration of the bone marrow, and their release into the circulation may improve vascularization of distal tissues damaged by chemotherapy. Similarly, decreased numbers of VSELs in the peripheral blood of immunocompromised patients may be a consequence of their contribution to the restoration of hematopoiesis in the bone marrow. More importantly, as presented in this study, the process may be further supported by G-CSF application.

Notably, acquisition of hematopoietic function by VSELs was reflected by changes in the expression of certain

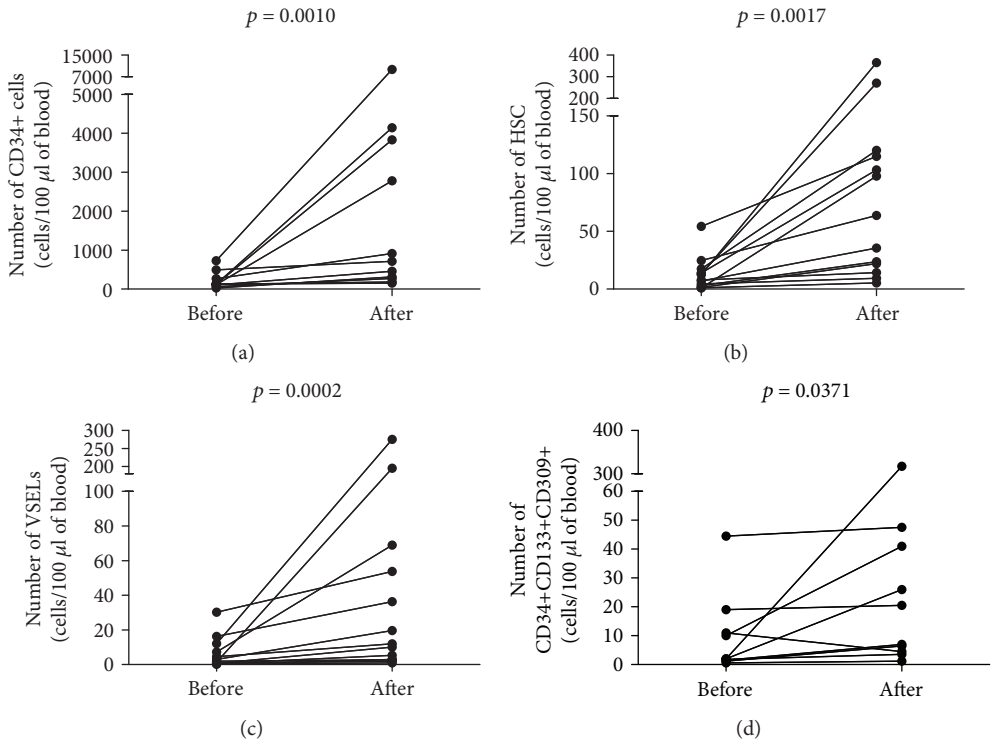

Figure 2: Changes in (a) CD34+ progenitor cells (CD34+ cells), (b) very small embryonic-like stem cells (VSELs, lin-CD235a-CD45-CD133+), (c) hematopoietic stem cells (HSC, lin-CD235a-CD45+CD133+), and (d) endothelial progenitor cell (EPCs, CD34+CD133+CD309+ cells) numbers in ALL patients after successful chemotherapy before and after G-CSF treatment; Wilcoxon test was used.

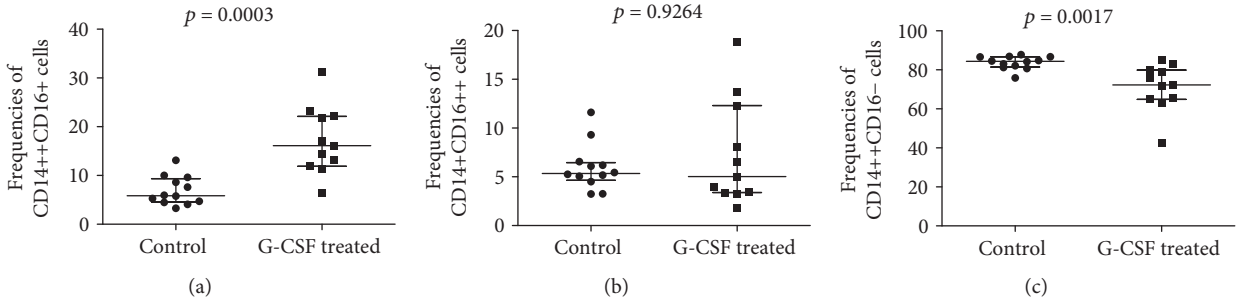

Figure 3: Summary of flow cytometry analyses of (a) intermediate (CD14++CD16+), (b) nonclassical (CD14+CD16++), and (c) classical (CD14++CD16−) monocyte frequencies in normal donors (control) and ALL patients after successful chemotherapy and G-CSF treatment; Mann–Whitney U test was used.

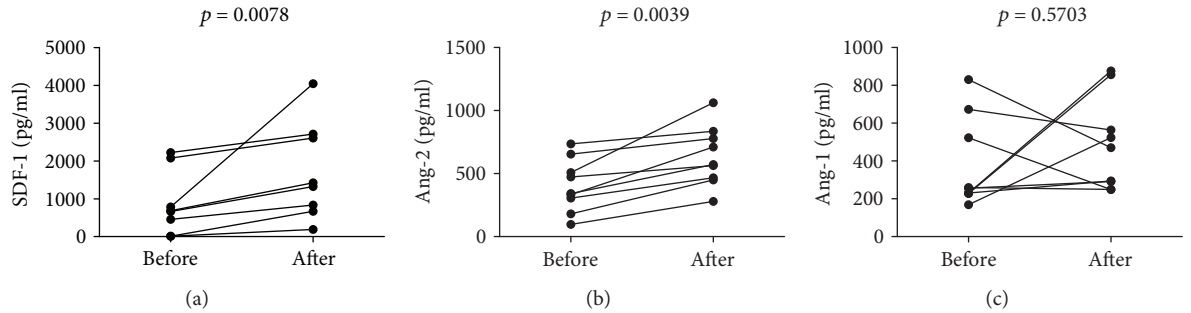

Figure 4: Changes in (a) SDF-1, (b) angiopoietin 2, and (c) angiopoietin 1 levels in ALL patients after successful chemotherapy before and after G-CSF treatment; Wilcoxon test was used.

genes that regulate hematopoietic processes, including PU-1, c-myb, LMO2, and Ikaros. In a consequence, VSELs differentiated into CD45+ hematopoietic cells. However, normal bone marrow-delivered VSELs express numerous markers characteristic for pluripotent cells, including SSEA-1, Rexo-1, Rif-1, Nanog, and Oct-4, and can be differentiated *in vitro* into cells of all three germ layers, namely, ectoderm, endoderm, and mesoderm [9, 29]. Importantly, VSELs are mobilized from the bone marrow into the circulation in response to tissue injury, including myocardial infraction and ischemia [30, 31]. Therefore, they are believed to support regeneration process in many degenerative conditions. Similarly to our results, in experimental mouse model, the administration of exogenous G-CSF resulted in increased mobilization and release of VSELs from the bone marrow. This might be a result of SDF-1 signaling, since VSELs were shown to express CXCR4 [32]. Surprisingly, in this study we found no significant correlation between the number of VSELs and SDF-1 plasma levels. Interestingly, previous observations in inflammatory bowel disease showed that VSELs and EPCs mobilization can occur in SDF-1-independent manner [33]. Furthermore, we showed that increased Ang-2 levels are, somehow, related to increased VSEL mobilization. However, further studies are needed to explain this phenomenon.

It was previously reported that EPC mobilization from the bone marrow to the periphery depends on SDF-1 signaling [34]. Interestingly, however, we found no association between the SDF-1 levels and numbers of EPCs. Furthermore, all endothelial cells were shown to express angiopoietin receptor (Tie-2) that may be activated by both angiopoietin-1 (Ang-1) and angiopoietin-2 (Ang-2). Kopp and collaborators showed that Ang-1 stimulated Tie-2 expression in the bone marrow vasculature, and thus they may play a role in the promotion of hematopoiesis. Of the four already described angiopoietins, Ang-1 and Ang-2 are to date the best characterized ones [35]. Ang-1 was recognized as principal activator of Tie-2, while Ang-2 acted as Tie-2 inhibitor that causes destabilization of blood vessels, what constituted the initial stage of vascularization process [36]. Notably, Tie-2 is expressed not only on EPCs but also on HSCs and small subset of CD16+ monocytes, namely, Tie-2-expressing monocytes (TEMs). In fact, intermediate CD14++CD16+ monocytes represent the predominant population of peripheral blood Tie-2-expressing cells [37]. Furthermore, reparative monocytes with proangiogenic potential were found to express SDF-1 receptor, namely, CXCR4 [38]. Importantly, Capoccia and collaborators showed that G-CSF-mobilized monocytes were able to induce vascularization at sites of ischemia [17]. In some contrast to our results, Murdoch and collaborators indicated that Ang-2 may serve as chemotactic factor for monocytes with proangiogenic potential [39]. Further studies supported these findings showing that Ang-2 signaling markedly enhanced proangiogenic activity of TEMs [40]. Thus, we hypothesized that G-CSF treatment in ALL patients after successful chemotherapy can increase numbers of reparative and proangiogenic monocytes in SDF-1-dependent manner; however, their activity may be controlled by increased Ang-2 signaling. However, further studies are still warranted in order to assess this mechanisms in more detail.

5. Conclusions

In summary, we showed that G-CSF treatment in immunocompromised patients induced efficient mobilization of stem and progenitor cells with high regenerative and proangiogenic potential. These findings could help to better understand beneficial clinical effects of G-CSF therapy in immunocompromised patients. Our findings suggest that G-CSF treatment can be considered as additional tool used in patients after chemotherapy in order to support recovery process. However, further studies are still needed to assess safety of such therapeutic approach in different clinical settings.

Data Availability

The datasets used and/or analyzed during the current study are available from the corresponding author on reasonable request.

Conflicts of Interest

Authors declare that there is no conflict of interests regarding publication of this paper.

Authors' Contributions

Andrzej Eljaszewicz, Lukasz Bolkun, and Marcin Moniuszko designed the study. Lukasz Bolkun, Tomasz Wasiluk, Janusz Kloczko, and Karol Kamiński provided patient and control samples and analyzed the clinical data. Andrzej Eljaszewicz, Kamil Grubczak, Malgorzata Rusak, and Milena Dabrowska performed the experiments. Andrzej Eljaszewicz analyzed the flow cytometry data, performed the statistical analysis, and prepared the figures. Lukasz Bolkun, Karol Kamiński, Piotr Radziwon, and Wojciech Marlicz helped in drafting the manuscript. Andrzej Eljaszewicz and Marcin Moniuszko wrote the manuscript.

Acknowledgments

The authors wish to thank Teresa Michno for the professional technical support. The study was supported by funds for statutory activities from the Medical University of Bialystok. Andrzej Eljaszewicz and Marcin Moniuszko were supported by funds from the Leading National Research Center (KNOW) of Medical University of Bialystok.

References

[1] H. Inaba, M. Greaves, and C. G. Mullighan, "Acute lymphoblastic leukaemia," *The Lancet*, vol. 381, no. 9881, pp. 1943–1955, 2013.

[2] K. Welte, "G-CSF: filgrastim, lenograstim and biosimilars," *Expert Opinion on Biological Therapy*, vol. 14, no. 7, pp. 983–993, 2014.

[3] A. T. Hooper, J. M. Butler, D. J. Nolan et al., "Engraftment and reconstitution of hematopoiesis is dependent on VEGFR2-mediated regeneration of sinusoidal endothelial cells," *Cell Stem Cell*, vol. 4, no. 3, pp. 263–274, 2009.

[4] H. G. Kopp, A. T. Hooper, S. T. Avecilla, and S. Rafii, "Functional heterogeneity of the bone marrow vascular niche," *Annals of the New York Academy of Sciences*, vol. 1176, no. 1, pp. 47–54, 2009.

[5] B. O. Zhou, L. Ding, and S. J. Morrison, "Hematopoietic stem and progenitor cells regulate the regeneration of their niche by secreting angiopoietin-1," *eLife*, vol. 4, article e05521, 2015.

[6] S. J. Morrison and D. T. Scadden, "The bone marrow niche for haematopoietic stem cells," *Nature*, vol. 505, no. 7483, pp. 327–334, 2014.

[7] E. C. Forsberg, D. Bhattacharya, and I. L. Weissman, "Hematopoietic stem cells: expression profiling and beyond," *Stem Cell Reviews*, vol. 2, no. 1, pp. 23–30, 2006.

[8] M. Ii, "Bone marrow-derived endothelial progenitor cells: isolation and characterization for myocardial repair," *Methods in Molecular Biology*, vol. 660, pp. 9–27, 2010.

[9] M. Z. Ratajczak, K. Marycz, A. Poniewierska-Baran, K. Fiedorowicz, M. Zbucka-Kretowska, and M. Moniuszko, "Very small embryonic-like stem cells as a novel developmental concept and the hierarchy of the stem cell compartment," *Advances in Medical Sciences*, vol. 59, no. 2, pp. 273–280, 2014.

[10] A. Shaikh, D. Bhartiya, S. Kapoor, and H. Nimkar, "Delineating the effects of 5-fluorouracil and follicle-stimulating hormone on mouse bone marrow stem/progenitor cells," *Stem Cell Research & Therapy*, vol. 7, no. 1, p. 59, 2016.

[11] M. Qin, X. Guan, H. Wang et al., "An effective ex-vivo approach for inducing endothelial progenitor cells from umbilical cord blood CD34(+) cells," *Stem Cell Research & Therapy*, vol. 8, no. 1, p. 25, 2017.

[12] M. Z. Ratajczak, "Why are hematopoietic stem cells so 'sexy'? On a search for developmental explanation," *Leukemia*, vol. 31, no. 8, pp. 1671–1677, 2017.

[13] E. B. Peters, "Endothelial progenitor cells for the vascularization of engineered tissues," *Tissue Engineering. Part B, Reviews*, vol. 24, no. 1, pp. 1–24, 2018.

[14] M. Zhang, A. B. Malik, and J. Rehman, "Endothelial progenitor cells and vascular repair," *Current Opinion in Hematology*, vol. 21, no. 3, pp. 224–228, 2014.

[15] R. Tamma and D. Ribatti, "Bone niches, hematopoietic stem cells, and vessel formation," *International Journal of Molecular Sciences*, vol. 18, no. 1, 2017.

[16] A. S. Patel, A. Smith, S. Nucera et al., "TIE2-expressing monocytes/macrophages regulate revascularization of the ischemic limb," *EMBO Molecular Medicine*, vol. 5, no. 6, pp. 858–869, 2013.

[17] B. J. Capoccia, R. M. Shepherd, and D. C. Link, "G-CSF and AMD3100 mobilize monocytes into the blood that stimulate angiogenesis in vivo through a paracrine mechanism," *Blood*, vol. 108, no. 7, pp. 2438–2445, 2006.

[18] A. W. Roberts, "G-CSF: a key regulator of neutrophil production, but that's not all!," *Growth Factors*, vol. 23, no. 1, pp. 33–41, 2005.

[19] A. Eljaszewicz, D. Sienkiewicz, K. Grubczak et al., "Effect of periodic granulocyte Colony-stimulating factor administration on endothelial progenitor cells and different monocyte subsets in pediatric patients with muscular dystrophies," *Stem Cells International*, vol. 2016, Article ID 2650849, 9 pages, 2016.

[20] R. Klocke, M. T. Kuhlmann, S. Scobioala, W. R. Schäbitz, and S. Nikol, "Granulocyte colony-stimulating factor (G-CSF) for cardio- and cerebrovascular regenerative applications," *Current Medicinal Chemistry*, vol. 15, no. 10, pp. 968–977, 2008.

[21] E. S. Jaffe, "The 2008 WHO classification of lymphomas: implications for clinical practice and translational research," *Hematology*, vol. 2009, no. 1, pp. 523–531, 2009.

[22] J. Holowiecki, M. Krawczyk-Kulis, S. Giebel et al., "Status of minimal residual disease after induction predicts outcome in both standard and high-risk Ph-negative adult acute lymphoblastic leukaemia. The Polish Adult Leukemia Group ALL 4-2002 MRD Study," *British Journal of Haematology*, vol. 142, no. 2, pp. 227–237, 2008.

[23] M. Zbucka-Kretowska, A. Eljaszewicz, D. Lipinska et al., "Effective mobilization of very small embryonic-like stem cells and hematopoietic stem/progenitor cells but not endothelial progenitor cells by follicle-stimulating hormone therapy," *Stem Cells International*, vol. 2016, Article ID 8530207, 8 pages, 2016.

[24] A. Ehninger and A. Trumpp, "The bone marrow stem cell niche grows up: mesenchymal stem cells and macrophages move in," *The Journal of Experimental Medicine*, vol. 208, no. 3, pp. 421–428, 2011.

[25] H. Ozer, "Chemotherapy-induced neutropenia: new approaches to an old problem," *Seminars in Oncology*, vol. 30, Supplement 13, pp. 1-2, 2003.

[26] L. J. Bendall and K. F. Bradstock, "G-CSF: from granulopoietic stimulant to bone marrow stem cell mobilizing agent," *Cytokine & Growth Factor Reviews*, vol. 25, no. 4, pp. 355–367, 2014.

[27] S. T. Avecilla, K. Hattori, B. Heissig et al., "Chemokine-mediated interaction of hematopoietic progenitors with the bone marrow vascular niche is required for thrombopoiesis," *Nature Medicine*, vol. 10, no. 1, pp. 64–71, 2004.

[28] S. Rafii, R. Mohle, F. Shapiro, B. M. Frey, and M. A. S. Moore, "Regulation of hematopoiesis by microvascular endothelium," *Leukemia & Lymphoma*, vol. 27, no. 5-6, pp. 375–386, 1997.

[29] J. Ratajczak, E. Zuba-Surma, I. Klich et al., "Hematopoietic differentiation of umbilical cord blood-derived very small embryonic/epiblast-like stem cells," *Leukemia*, vol. 25, no. 8, pp. 1278–1285, 2011.

[30] W. Wojakowski, M. Tendera, M. Kucia et al., "Mobilization of bone marrow-derived Oct-4^+ SSEA-4^+ very small embryonic-like stem cells in patients with acute myocardial infarction," *Journal of the American College of Cardiology*, vol. 53, no. 1, pp. 1–9, 2009.

[31] C. L. Guerin, X. Loyer, J. Vilar et al., "Bone-marrow-derived very small embryonic-like stem cells in patients with critical leg ischaemia: evidence of vasculogenic potential," *Thrombosis and Haemostasis*, vol. 113, no. 5, pp. 1084–1094, 2015.

[32] M. J. Kucia, M. Wysoczynski, W. Wu, E. K. Zuba-Surma, J. Ratajczak, and M. Z. Ratajczak, "Evidence that very small embryonic-like stem cells are mobilized into peripheral blood," *Stem Cells*, vol. 26, no. 8, pp. 2083–2092, 2008.

[33] W. Marlicz, E. Zuba-Surma, M. Kucia, W. Blogowski, T. Starzynska, and M. Z. Ratajczak, "Various types of stem cells, including a population of very small embryonic-like stem cells, are mobilized into peripheral blood in patients with

Crohn's disease," *Inflammatory Bowel Diseases*, vol. 18, no. 9, pp. 1711–1722, 2012.

[34] L. Shen, Y. Gao, J. Qian, A. Sun, and J. Ge, "A novel mechanism for endothelial progenitor cells homing: the SDF-1/CXCR4-Rac pathway may regulate endothelial progenitor cells homing through cellular polarization," *Medical Hypotheses*, vol. 76, no. 2, pp. 256–258, 2011.

[35] H. G. Kopp, S. T. Avecilla, A. T. Hooper et al., "Tie2 activation contributes to hemangiogenic regeneration after myelosuppression," *Blood*, vol. 106, no. 2, pp. 505–513, 2005.

[36] E. Fagiani and G. Christofori, "Angiopoietins in angiogenesis," *Cancer Letters*, vol. 328, no. 1, pp. 18–26, 2013.

[37] M. de Palma, M. A. Venneri, R. Galli et al., "Tie2 identifies a hematopoietic lineage of proangiogenic monocytes required for tumor vessel formation and a mesenchymal population of pericyte progenitors," *Cancer Cell*, vol. 8, no. 3, pp. 211–226, 2005.

[38] E. Shantsila, L. D. Tapp, B. J. Wrigley, S. Montoro-García, and G. Y. Lip, "CXCR4 positive and angiogenic monocytes in myocardial infarction," *Thrombosis and Haemostasis*, vol. 109, no. 2, pp. 255–262, 2013.

[39] C. Murdoch, S. Tazzyman, S. Webster, and C. E. Lewis, "Expression of Tie-2 by human monocytes and their responses to angiopoietin-2," *Journal of Immunology*, vol. 178, no. 11, pp. 7405–7411, 2007.

[40] S. B. Coffelt, A. O. Tal, A. Scholz et al., "Angiopoietin-2 regulates gene expression in TIE2-expressing monocytes and augments their inherent proangiogenic functions," *Cancer Research*, vol. 70, no. 13, pp. 5270–5280, 2010.